ANATOMY OF CEREBELLAR NUCLEO-BULBAR PROJECTIONS IN THE RAT

Anatomie van cerebellaire nucleo-bulbaire projecties in de rat

PROEFSCHRIFT

ter verkrijging van de graad van doctor
aan de Erasmus Universteit Rotterdam
op gezag van de rector magnificus
Prof. Dr. P.W.C. Akkermans MA
en volgens besluit van het College voor Promoties
De openbare verdediging zal plaats vinden op
Woensdag 29 September 1999 om 15.45 uur

door Thea MariekeTeune
geboren te Rijswijk

Promotiecommissie:

Promotor:	Prof. Dr. J. Voogd
Copromotor:	Dr. T. J. H. Ruigrok
Overige leden:	Prof. Dr. H. Collewijn
	Prof. Dr. H. J. Groenewegen
	Dr. J. L. van der Want

"Healing,"
Papa would tell me
"is not a science,
but the intuitive art
of wooing Nature."
W.H. Auden
The Art of Healing

Drukwerk: Ridderprint Offset Drukkerij, te Ridderkerk

Dit proefschrift is tot stand gekomen binnen de afdeling Anatomie van de Erasmus Universiteit Rotterdam, en mogelijk gemaakt door N.W.O. grant 903-47-005.

ISBN 90-90129-83-9

Contents

Chapter 1	General introduction	6
Chapter 2	Topography of cerebellar nuclear projections to the brain stem and diencephalon in the rat	43
Chapter 3	A retrograde double labeling technique for light microscopy. A combination of axonal transport of cholera toxin B subunit and a gold-lectin conjugate	112
Chapter 4	Cerebellar projections to the red nucleus and inferior olive originate from separate populations of neurons in the rat: a non-fluorescent double labeling study	129
Chapter 5	Cerebellar collateralization to prerubral, rubral, pontine tegmental reticular and inferior olivary nuclei. A non-fluorescent double labeling retrograde tracing study in the rat	140
Chapter 6	Preservation of the cerebellar modular organization in nucleo-bulbar projections. A non-fluorescent anterograde double labeling study in the rat	186
Chapter 7	Single Purkinje cell can innervate multiple classes of projection neurons in the cerebellar nuclei of the rat: a light microscopic and ultrastructural triple-tracer study	212
Chapter 8	Summary and general discussion	237
Literature cited		243
Abbreviations		196
List of publications		266
Curriculum vitae		287
Dankwoord / Acknowledgements		268
Color Figures		272

CHAPTER 1:
GENERAL INTRODUCTION

1. The cerebellum and the brain

The cerebellum is located caudal to the cerebral hemispheres and is connected to the rest of the brain by way of three "peduncles", that convey its afferent and efferent information. The cerebellum is functionally related to spinal, bulbar and cerebral motor systems. Its role in the correct and harmonious execution of movements was already suggested early in the 19th century (Flourens, 1823; Hammond, 1869; Magendie, 1824; Rolando, 1809), and was substantiated in the first decades of the 20th century (Babinski, 1902; Holmes and Stewart, 1904). A schematic representation of the cerebello-cerebral relationships is depicted in Fig. 1.1.

The cerebellum receives its input through two different pathways: the mossy fiber system and the climbing fiber system (for a review see Voogd, 1995). Mossy fibers originate from various brain stem nuclei, exemplified in Fig. 1.1 by the nucleus reticularis tegmenti pontis (NRTP: Gerrits and Voogd, 1981). The climbing fibers stem from a single source, the inferior olive (IO: Desclin, 1974). Both types of fibers terminate directly within the cerebellar cortex, and both provide the cerebellar nuclei (CN) with collaterals. Mossy fibers and climbing fibers convey information from the cerebral cortex and the brain stem, together with input from the spinal cord, to the cerebellum. Apart from the mossy and climbing fiber collaterals, the CN receive their main input from the cerebellar cortex. Figure 1.2 gives a scheme of these pathways and structures.

The CN provide the output of the cerebellum. The medial cerebellar nucleus (MCN), the target nucleus of the vermis, is connected to the brain stem through bilateral pathways. The uncinate tract decussates within the cerebellum; the ipsilateral pathway enters the brain stem in the lateral wall of the 4th ventricle. The output of the nuclei of the hemisphere is directed via the superior cerebellar peduncle (scp), to a variety of brain stem and diencephalic nuclei.

Basically three, functionally different, groups of nuclei may be recognized to receive cerebellar input: the premotor nuclei, the precerebellar nuclei that give rise to mossy and climbing fibers (thus establishing direct recurrent circuits), and the pre-olivary nuclei. For example, the red nucleus (RN) and the ventrolateral nucleus of the thalamus, both of which receive a crossed projection from the scp, can be considered as premotor nuclei. The RN as well as the motor cortex gives rise to descending motor systems. The RN is the source of the rubrospinal tract and the thalamus innervates the motor cortex, which is the main origin of the pyramidal tract. Precerebellar nuclei include several reticular nuclei that give rise to mossy fibers (NRTP, nucleus reticularis paramedianus, and nucleus reticularis lateralis) and the only climbing fiber source, the IO. Several pre-olivary nuclei that give rise to substantial projections onto the IO are located at the mesodiencephalic junction (MDJ). As can be appreciated from Fig. 1.1, the connections of the cerebellum with the IO and the NRTP

are part of recurrent cerebellar circuits. Other (premotor) nuclei are also reciprocally connected to the cerebellum, but these loops are more elaborate.

The diagram of Fig. 1.1 is a general scheme, which applies to all CN. However, the cerebellum is not a uniform structure, but is subdivided into modules (Voogd and Bigaré, 1980). The modular organization of the cerebellum concerns the output of the cortex to the CN and the arrangement of the climbing fiber innervation of the cortex and the CN. A module consists of a discrete strip of cortex with the cerebellar or vestibular target nucleus of the Purkinje cells contained in this strip. The Purkinje cells of the module receive a specific climbing fiber input from a particular subnucleus of the IO, with a collateral projection to their target nucleus. This thesis will focus on the relation between the cerebellar modules and their connections with the brain stem.

2. Cerebellar nucleo-bulbar connections

It is generally assumed that the CN contain two kinds of relay cells, i.e. small, GABAergic neurons and non-GABAergic neurons, which are medium- to large-sized (Batini *et al.*, 1992; Tolbert *et al.*, 1976) The presence of interneurons in the CN is still disputed (Chen and Hillman, 1993). The small GABAergic neurons were found to project to the IO (nucleo-olivary pathway: De Zeeuw *et al.*, 1989b; Graybiel *et al.*, 1973; Mugnaini and Oertel, 1981). Available evidence suggests that this projection is reciprocally organized, with each cerebellar nucleus projecting to the subdivision of the IO from which it receives a collateral projection. The organization of the nucleoolivary system has been studied with various anatomical and physiological methods, in different species (Angaut and Cicirata, 1982; Asanuma *et al.*, 1983a; Beitz, 1976; Billard *et al.*, 1989; Buisseret-Delmas and Angaut, 1993; Dietrichs and Walberg, 1985; 1986; 1989; Dietrichs *et al.*, 1985; Dom *et al.*, 1973; Faull, 1978; Fredette and Mugnaini, 1991; Haroian, 1982; Kalil, 1979; Legendre and Courville, 1987; Ruigrok and Voogd, 1990; 1995a; Tolbert *et al.*, 1976; Van der Want *et al.*, 1994). Various studies differ with respect to the collateralization of nucleoolivary projections to other bulbar structures (e.g. Legendre and Courville, 1987; Tolbert *et al.*, 1976).

The projections from the non-GABAergic relay cells of the CN to the brain stem, the thalamus and the spinal cord have been studied repeatedly. Two schools of thought have emerged from these studies. One group of authors maintains that the target nucleus of each module projects to a discrete set of structures and thus influences a particular aspect of motor behavior. Others attach more importance to the overlap in the projections of the CN to these target nuclei.

The modular organization of the flocculus and the nodulus with their projections to the oculomotor nuclei (Ito and Nagao, 1991; Tan *et al.*, 1995; Wylie *et al.*, 1994) is the most studied example of the first paradigm. Each module of the vestibulocerebellum monitors eye movements in a

particular plane and receives information about this movement by its climbing fiber afferents (van der Steen *et al.*, 1991; 1994). The idea that each cerebellar module influences a particular aspect of motor behavior has been generalized by Oscarsson (1979) and Bloedel (1992). This generalization implies the existence of a highly differentiated projection of the cerebellum, with the cerebellar target nucleus of each module projecting to a different region in the brain stem, the thalamus or the spinal cord. The differential projection of the CN to different nuclei in the brain stem, the thalamus and the cord, has only been partially confirmed in most studies of the output of the cerebellum. The differential projections of the target nuclei of the vermis (via medial cerebellar nucleus and vestibular nuclei to the vestibular nuclei, the bulbar reticular formation and the spinal cord), and of the target nuclei of the cerebellar hemisphere (via lateral or dentate and interposed nuclei to the RN and the ventrolateral nucleus of the thalamus) are not disputed. At a more detailed level, however, overlap, rather than discrete zones of projections, appears to be the rule. Overlap of the projections of the different CN has been described in the projections to the premotor nuclei (i.e. the RN, the colliculus superior, and the thalamus), to the precerebellar mossy fiber nuclei (i.e. the NRTP) and to the pre-olivary nuclei (i.e. the nuclei of the MDJ).

Systematic overlap of their projections may be a general property of the CN. Overlap at the level of the RN is an essential element in Kennedy's hypothesis (Kennedy, 1990), claiming that motor learning occurs through the dentate-rubral-olivary loop, but that movements, once learning is complete, are monitored through the interposito-rubral pathway.

3. Aim of this thesis

From the above, it may be obvious that presently, despite a wealth of anatomical studies, the implementation of the cerebellar modular organization in the brain stem circuitry is still far from clear. Obviously, technical limitations will have played a role in the failure to provide definite answers to e.g. questions of divergence and convergence of cerebellar nucleo-bulbar projections. In anterograde tracing studies the placement of discrete injections in a single cerebellar nucleus without overlap with neighboring nuclei is the crucial factor. On the other hand, the interpretation of retrograde labeling studies of the projections of the CN depends, apart from the size and the extension of the injection sites, on the presence of uptake and transport of the tracer by passing fibers. Moreover, the possibility that certain CN are characterized by the pattern of collateralization of their efferent fibers to different brain stem nuclei, rather than by their projection to a single nucleus, should be taken in account. Ideally, anterograde tracing experiments should be combined with retrograde tracing of the same system with multiple tracers. This approach, which has only been rarely used to study the output of the CN (Nakano *et al.*, 1980; Noda, 1991), will be adopted in this thesis to study questions of

overlap and collateralization in the nucleobulbar connections of the rat.

In doing so, we have selected and used modern or even new combinations of tracers that enabled small, discrete injection sites. This newly developed non-fluorescent retrograde double labeling technique will be described in Chapter 3. It is important to stress that all tracing experiments on which this thesis is based, be it with single, dual or multiple tracers, were executed using non-fluorescent labels, thus enabling analysis with light microscopy in counterstained sections. For analysis of the sections a semiautomatic, computerized plotting system was used (Neurolucida™). Hence, by computerized plotting of non-fading labels directly in sections in which sufficient cytoarchitectonic detail can be recognized, an, in our view, exceptionally high level of analysis could be obtained.

Nevertheless, despite the technological aids and appliances, it was not possible to describe in sufficient detail the con- and divergence properties of all nucleobulbar projections. Therefore, especially as far as the retrograde and anterograde double labeling studies were concerned, we had to limit ourselves to only a few brain stem target areas. These areas were selected as type specific examples of the different classes of brain stem groups that receive cerebellar information: i.e. premotor nuclei, precerebellar nuclei, and preolivary nuclei. The RN was selected as a premotor nucleus, the IO (source of climbing fibers) and the NRTP (source of mossy fibers) were selected as type specific constituents of precerebellar nuclei, and the medial mesodiencephalic junction (prerubral area) was chosen as a recipient of cerebellar information with connections to the IO. Chapters 4 to 6 will deal with detailed descriptions of these studies.

As mentioned earlier, basically two types of neurons are found in the CN. As will be clear from Chapters 4 and 5, both types of cells are more or less intermingled throughout the CN (Batini *et al.*, 1992; Chan-Palay, 1977; Tolbert *et al.*, 1976). Hence, especially when examining the impact of the cerebellar modular organization by way of the different (parts of the) CN, it became a point of interest whether or not both cell types receive the same information from the cerebellar cortex, or whether they may be contacted by different subgroups of Purkinje cells that belong to the same cortical strip. Part of this question is examined in a combined lightmicroscopic and ultrastructural study that is described in Chapter 7.

In the course of this thesis study it was felt that we should put some effort into providing a comprehensive survey of the projections of the individual CN of the rat. Such a description, to the best of our knowledge, was not yet available. The only concise report on ascending and descending cerebellofugal projections in the rat to date was based on lesions of the scp (Faull, 1978; Faull and Carman, 1978). Although these studies are informative, both the method (lesioning induces a pathological state, and has an impact on the surrounding tissue as well) and the indirect approach (the scp carries fibers arising from all CN)

make it impossible to discriminate accurately between projections from (parts of) individual CN. All other studies are mainly concerned with describing cerebellar projections to a selected part of the brain stem or diencephalon or describing the nucleo-bulbar projections of a single cerebellar nucleus (e.g. Chan-Palay, 1977). Therefore, Chapter 2 of this thesis will present such a comprehensive description of nucleobulbar projections, based on detailed analysis of nineteen cases with small anterograde tracers in selected parts of the CN.

In order to be able to place the results of these studies, some of the, mostly anatomical, characteristics of the main constituents of this thesis, i.e. the cerebellum, the NRTP, the IO and the area of the RN will be reviewed below. This will be followed by a short discussion on views of function of the cerebello-bulbar circuitry.

4. The cerebellum

The cerebellum is situated dorsal to the medulla oblongata and pons. It consists of a midline portion, the vermis, and two lateral lobes or hemispheres; this separation is more evident on the inferior side than on the superior side of the cerebellum. The surface of the cerebellum is divided into lobes and lobules by transverse fissures (for a recent review see Voogd, 1995), enumerated I through X (Larsell, 1970), Fig. 1.3.

4A: The cerebellar nuclei

Structure

The CN are located in the roof of the fourth ventricle. Traditionally, they are divided into two groups of interconnected nuclei, that are separated by myelinated fibers (for a review, see Voogd, 1995). The two caudally located nuclei are the posterior interposed nucleus (PIN) and the MCN, and the two slightly more rostrally located nuclei are the anterior interposed nucleus (AIN) and the lateral cerebellar nucleus (LCN). In the rat, the terminology introduced by Goodman and Welch (Goodman *et al.*, 1963, see also Korneliussen, 1968), who distinguished several subnuclei peculiar to the rat, is generally used. (Fig. 1.4)

The MCN (or fastigial nucleus), the medialmost nucleus, is characterized by the prominent dorsolateral protuberance (DLP) of Goodman (1963). Korneliussen divided the MCN into three parts: the middle part, the caudomedial subdivision, and the dorsolateral protuberance. The caudomedial subdivision contains predominantly small cells (Beitz and Chan-Palay, 1979). The DLP contains mainly large cells. Large neurons are also present rostrally and ventromedially in the middle part of the nucleus, they are absent centrally and ventrolaterally. The middle part of the MCN stands out because of its large content of myelinated fibers. These fibers belong to the uncinate tract and to the so-called "perforating fibers", a fiber system that originates from vermal Purkinje cells and that perforates the CN on their way to the vestibular nuclei (Voogd, 1964).

The PIN is the smallest of the CN, but it has the highest cell count (Voogd, 1995). It contains rather large cells, small cells are found at its ventral and medial borders. The border region of the MCN and the PIN was distinguished by Buisseret-Delmas and Angaut (1993) as a separate subnucleus (the interstitial cell groups, ICG). Some of the cells in this region are fairly large.

The AIN, situated dorsal, rostral and lateral to the PIN, protrudes medially and laterally as the dorsomedial crest (DMC) and the dorsolateral hump (DLH), respectively. The cells in the dorsomedial crest and the medial part of the AIN are smaller than the neurons of the lateral part of the AIN. The dorsolateral hump is situated on top of the rostrolateral and dorsal surface of the nucleus, and contains large cells.

The LCN (or dentate nucleus), the lateralmost nucleus, consists of a dorsolateral magnocellular portion and a ventromedial parvicellular portion (Chan-Palay *et al.*, 1977; Korneliussen, 1968). Ventrally, located within the floccular peduncle, a cluster of cells representing group y can be distinguished (Highstein and Reisine, 1979; Sato *et al.*, 1982).

Neuronal population

The neuronal population of the CN follows a binomial size distribution (Chan-Palay, 1977; Courville and Cooper, 1970; Palkovits *et al.*, 1977). All CN contain randomly distributed small-sized neurons (Chan-Palay, 1977; Korneliussen, 1968). These small neurons predominantly project to the IO, and are GABAergic (De Zeeuw *et al.*, 1989a; Fredette and Mugnaini, 1991; Mugnaini and Oertel, 1981; Nelson and Mugnaini, 1989; Ruigrok and Voogd, 1990; Sotelo *et al.*, 1986). It has been speculated whether these small neurons give rise to recurrent collaterals terminating in the CN, thus establishing an extra inhibitory drive, in addition to the GABAergic Purkinje cell input (Kitzman and Bishop, 1997; Nelson and Mugnaini, 1984). The larger neurons are mainly excitatory and contain aspartate and/or glutamate as a neurotransmitter (Batini *et al.*, 1992; Chen and Hillman, 1993) and provide other targets than the IO with an input (Tolbert *et al.*, 1980). Some of these neurons presumably give rise to collaterals, which terminate as mossy fibers in the cerebellar cortex (Angaut *et al.*, 1997; Buisseret-Delmas, 1988a; 1988b; Tolbert *et al.*, 1980). Another population of the CN consists of interneurons, which are small, and present throughout all CN. The main distinctive feature of these small cells, of which many were found to be GABAergic, is that they are also glycine immunoreactive (Chen and Hillman, 1993); glycine has not been found in nucleoolivary neurons (De Zeeuw and Berrebi, 1995a; 1995b).

Efferents

The cerebellum communicates with the other parts of the central nervous system through the CN. Apart from the Purkinje cell axons from the anterior vermis and the vestibulocerebellum, terminating in the vestibular nuclei, the CN provide the only route to convey cerebellar cortical information to other parts of the nervous system (Voogd *et al.*, 1996b). The cerebellar nuclear efferents terminate throughout the brain stem, the spinal cord and the

forebrain. The efferent connections of the CN were reviewed by Voogd (1990; 1995), Ruigrok and Cella, (1995), and Glickstein and Voogd (1995).

The MCN projects through the crossed uncinate tract and the uncrossed fastigiobulbar tract to the vestibular nuclei, the pontine and medullar reticular formations; a small uncrossed ascending tract is directed to the central gray, the mesencephalic tegmentum and the thalamus (Angaut, 1969; Angaut and Bowsher, 1970). The uncinate tract decussates within the cerebellum, in the caudal part of the cerebellar commissure, rostral to the interfastigial area. The crossed fibers pass rostrally to and through the contralateral MCN. The tract arches dorsal to the scp, which contains the efferent fibers from the lateral and interposed nuclei, immediately rostral to the AIN and joins the inferior cerebellar peduncle in its course lateral to the vestibular nuclei. Some fibers of the uncinate tract join the medial part of the scp as the crossed ascending limb of the uncinate tract (Haroian *et al.*, 1981). An uncrossed fastigiobulbar tract appears to be present in the rat, however, less distinct than in the cat (Voogd, 1964). Fibers from both the crossed and uncrossed fastigiobulbar tracts originate from neurons in all parts of the MCN (Batton *et al.*, 1977; Carpenter and Batton III, 1982). The precise trajectory of the nucleoolivary fibers from the MCN is not known (Ruigrok and Voogd, 1990; Voogd, 1995).

The thin nucleoolivary efferents from the lateral and interposed nuclei run from the lateral angle of the 4th ventricle in a separate bundle ventral to the scp to ascend to the decussation (Cholley *et al.*, 1989; Legendre and Courville, 1987). The nucleoolivary tract crosses the midline below the scp, and then runs lateral and below to the latter tract. The non-GABAergic projection neurons of the interposed nuclei and the LCN give rise to the scp.

In the scp, the cerebellofugal fibers run in an organized pattern: the fibers arising from the LCN run in the ventrolateral part of the scp, the AIN fibers in the dorsomedial part, the PIN fibers in the ventromedial section and (some of) the fibers that arise from the MCN occupy the dorsomedial section of the peduncle (Haroian *et al.*, 1981).

The scp decussates at the border of metencephalon and mesencephalon. At its decussation the scp separates into ascending and descending limbs. The descending limb terminates in the nuclei of the pons and the medulla. Its main target is the NRTP (Carpenter and Stevens, 1957; Chan-Palay, 1977; Faull, 1978; Legendre and Courville, 1987). The region of the dorsolateral hump of the AIN gives rise to an uncrossed descending branch of the scp, which detaches from the peduncle before its decussation and which courses through the lateral reticular formation (Bentivoglio and Molinari, 1986; Cajal, 1911). This uncrossed descending branch has only been observed in rodents (Cajal, 1911). The ascending branch projects heavily onto the RN, the tectum and the pretectum, the pre-olivary nuclei in the MDJ including the nucleus of Darkschewitsch and finally terminates in the thalamus. Extensive ipsilateral ascending and descending

projections of the LCN were described in an autoradiographic study using [^{3}H] methionine (Chan-Palay, 1977), but these ipsilateral projections were not confirmed in later studies.

Not all nuclei contribute equally to each projection. The differential projection of the MCN to the vestibular nuclei and pontine and medullary reticular formation was referred to above. Both the LCN and AIN project to the NRTP (Angaut *et al.*, 1985a; Asanuma *et al.*, 1983a; Faull and Carman, 1978; Faull, 1987) and the RN. The distribution of terminals in the RN demonstrates a preferential projection (Angaut, 1970; Angaut *et al.*, 1986; Angaut and Cicirata, 1988; Daniel *et al.*, 1988; 1987; Flumerfelt, 1978; Flumerfelt *et al.*, 1973). The PIN does not participate in a projection to the NRTP and only provides a minor projection to the RN (Martin *et al.*, 1974; Torigoe *et al.*, 1986a; 1986b; Yuen *et al.*, 1974). Its fibers mainly terminate in the nuclei of the MDJ, the tectum and the thalamus.

Double labeling experiments in cat and rat (Bentivoglio and Kuypers, 1982; Bharos *et al.*, 1981; Gonzalo-Ruiz and Leichnetz, 1987; McCrea *et al.*, 1978; Tolbert *et al.*, 1978a) and electrophysiological studies (Ban and Ohno, 1977; Tsukahara *et al.*, 1971) demonstrated that the non-GABAergic projection neurons collateralize to functionally different target areas. Some of the nucleoolivary neurons collateralize to other targets than the IO. However, using anatomical techniques, a collateral projection from the olivary projecting neurons to the thalamus or RN has been denied (Legendre and Courville, 1987). Evidence indicating that an inhibitory collateral projection, however very small, to the pontine nuclei might exist (Aas and Brodal, 1990; Berretta *et al.*, 1991a), is controversial, since recent evidence does not support such a GABAergic input originating from the CN (Verveer *et al.*, 1997).

Afferents

Input to the CN occurs through Purkinje cell axons, and mossy and climbing fiber collaterals. A small input is obtained from monoaminergic systems (Bishop and Ho, 1985; Kitzman and Bishop, 1994). The Purkinje cell projection upon the cerebellar nuclear neurons is strongly convergent (Purkinje cells outnumber cerebellar nuclear neurons in a ratio of 260 : 1; see Eccles, 1973; Ito, 1984). Purkinje cells use GABA as a neurotransmitter and therefore inhibit their target cells. The CN receive an excitatory (non-GABAergic) drive from mossy fibers and climbing fiber collaterals; however, it is debated whether all cerebellar nuclear neurons receive such a collateral input (see section on IO, Borsello *et al.*, 1994; Eccles, 1973; Van der Want *et al.*, 1994).

4B: The cerebellar cortex

Structure

Structurally the cerebellum consists of an outer layer, the cortex, and of centrally located white matter, in which the CN are located. The cerebellum is connected with the brain stem through the three pairs of the already mentioned cerebellar peduncles (the inferior, middle and superior cerebellar peduncle).

The structure of the cerebellar cortex is highly stereotyped. It consists of three layers. The outermost layer is the molecular layer, with few cells and many transversely oriented axons of the granule cells (the parallel fibers). The second layer is a single layer of Purkinje cells, whose flattened dendritic tree extends in the molecular layer where they are contacted by parallel and climbing fibers, while their axon descends towards the CN. The third layer, the granular layer, contains the granule cells (Cajal, 1911). This organization is depicted in Figs. 1.2 and 1.5.

Information is directed to the cerebellar cortex via two main systems: the climbing fiber system and the mossy fiber system. The climbing fibers arise from the IO (Desclin, 1974), a medullary nucleus, and course through the inferior and along the middle cerebellar peduncles, and through the granular and Purkinje cell layer and climb in the Purkinje cell dendritic tree, where they terminate on the proximal, smooth branches (Szentágothai and Rajkovits, 1959). The mossy fibers originate from many different brain stem and spinal cord sources (Anderson, 1943; Voogd *et al.*, 1969). The mossy fiber terminals contact, in the granular layer, the granule cells, which give off the transversely oriented parallel fibers that run in the molecular layer and make synaptic contact with the distal, spiny branchlets of the Purkinje cell dendrites (Figs. 1.2 and 1.5).

The cerebellar cortical output is directed to the cerebellar and vestibular nuclei; from here, it is directed to other parts of the brain (brain stem, the thalamus and the spinal cord) through the inferior and superior cerebellar peduncles.

Modular organization

Although the cerebellar cortex, as outlined above, appears to be uniform, it conceals a complex longitudinal zonal organization (Ito, 1984; Ito, 1990; Jansen and Brodal, 1940; Oscarsson, 1979; Voogd, 1964; Voogd and Bigaré, 1980, Fig. 1.6). This organization is not revealed by cytoarchitectonic characteristics, but is related to differences in efferent and afferent connections. On the basis of the longitudinal zonal organization the cerebellar cortex can be subdivided into regions with different functional characteristics of the cerebellar modules. Modules consist of a Purkinje cell zone with its efferent fibers, its cerebellar target nucleus and its afferent olivary climbing fiber input. Unlike other arrangements of similarly constructed modules (e.g. striatum, ocular dominance columns in the visual cortex), the cerebellar modules are aligned as a series of parallel, parasagittal strips. The longitudinal zones transgress the borders between the lobules, and often extend over the entire surface of the cerebellum. The anatomical demarcation of these zones rests on their cortico-nuclear projection. Three main zones can be distinguished: a vermal, a paravermal and a hemispherical zone corresponding with the MCN, the interposed nuclei and the LCN, respectively (Chambers and Sprague, 1955a; 1955b; Jansen and Brodal, 1940). Each of the three main zones can be further subdivided into two or more smaller zones each with its own target nucleus. This zonal pattern was

first described in the ferret and the cat (Voogd and Bigaré, 1980) and later confirmed in the rat with some modifications by Buisseret-Delmas, (1988a; 1988b; Buisseret-Delmas and Angaut, 1988; 1989a), see (Buisseret-Delmas and Angaut, 1993) for a review.

The vermis can be subdivided into the A zone (with the MCN as its target nucleus), the X zone (corresponding with the interstitial cell groups of Buisseret-Delmas (1988a; 1988b) and the B zone (targeting the lateral vestibular nucleus). The paravermal zone includes the C1, C2 and C3 zones, with the anterior and posterior interposed nuclei as their target nuclei. In the rat an additional zone, the lateral extension of the A zone, which projects to the dorsolateral protuberance of the MCN, is present in the medial hemisphere of the lobules VI and VII (Buisseret-Delmas, 1988a). A narrow Cx zone, with a projection to the interstitial cell groups, is present between the C1 and C2 zones (Buisseret-Delmas *et al.*, 1993). The hemispheres can be subdivided into the D1 and D2 zones, with the LCN as their target nucleus. In the rat an extra zone is present, between the C3 and the D1 zone, known as the D0 zone. D0 projects to the dorsolateral hump (Buisseret-Delmas, 1988a; Buisseret-Delmas and Angaut, 1993). The Purkinje cells from each of these zones receive input from climbing fibers originating from specific inferior olivary subnuclei (Buisseret-Delmas and Angaut, 1993; Furber and Watson, 1983; Voogd, 1964; Voogd and Bigaré, 1980).

Several zones, or the medial and lateral halves of these zones, are innervated by transversely branching climbing fibers from the same olivary subnucleus (Ekerot and Larson, 1982). Systematic transverse branching of climbing fibers has been observed in the cat between the X and Cx zones, the C1 and the medial half of C3 zone, and the lateral half of the C3 zone and the "y" zone, a zone located in the cerebellar hemisphere of the cat. A similar pattern of transverse branching of climbing fibers, and a medio-lateral subdivision of the C3 zone, may be present in the rat. The cerebellar nuclear neurons, receiving the Purkinje cell input from a zone, project back to the same inferior olivary subnuclei that provide the corresponding Purkinje cell zones with input. The inferior olivary subnuclei, in turn, supply the matching cerebellar nuclear sections with a collateral projection.

Each olivo-cerebello-nuclear pathway is thought to constitute a functional unit of the cerebellum and is presumed to control a particular motor mechanism (Ito, 1984). In the rat, the olivo-cerebellar modular pattern has been outlined by Buisseret-Delmas and Angaut in 1993 (Fig. 1.6).

Some mossy fibers also terminate in discrete longitudinal strips. Mossy fiber systems displaying this feature include the spinocerebellar tracts (Ji and Hawkes, 1994; Tolbert *et al.*, 1993), the fibers originating from the lateral reticular nucleus (Chan-Palay *et al.*, 1977; Künzle, 1975) and the cuneocerebellar tract (Ekerot and Larson, 1980; Ji and Hawkes, 1994), whereas others distribute fibers in a more diffuse fashion (e.g. the pontocerebellar system, including the NRTP, Gerrits and Voogd, 1981) or

even in a patchy pattern (tactile information (Bower and Woolston, 1983; Welker, 1987).

The functional anatomy of the cerebellum is, despite the wealth of information present, not well understood. Its input is derived from the periphery but, in addition, includes efferent copies of motor signals of various kinds. Its output is directed at motor centers, but is also fed back along mossy and climbing fiber systems into the cerebellum. Although its role in motor functions has been described extensively, and its position as a side path to the cerebral motor system has been acknowledged, it has been suggested that the cerebellum (and the IO) may also be involved in visceral functions and affective behavior (Bradley *et al.*, 1987; Haines *et al.*, 1990; Nisimaru *et al.*, 1991; Waldrop and Iwamoto, 1991), as well as in certain cognitive functions (Fiez, 1996; Fiez *et al.*, 1992; Ito, 1990; Ito, 1991; Leiner *et al.*, 1993; Leiner *et al.*, 1986; Schmahmann, 1991). Detailed knowledge on the efferent connections of the cerebellum may assist in gaining insight into the position of the cerebellum obtains within the organization of the nervous system, and the processes it is involved in.

5. The precerebellar nuclei

The brain stem nuclei that supply the CN with input are collectively known as precerebellar nuclei (Altman and Bayer, 1987a; 1987b; Flumerfelt and Hrycyshyn, 1985; Ruigrok and Cella, 1995), which suggests a certain degree of similarity. However, these cerebellar afferents belong to a great many morphologically and functionally different systems.

A division in two large groups already has been introduced: the largest and most heterogeneous group comprises the mossy fiber sources, and the second group of cerebellar afferents consists of the climbing fiber sources. Origins of mossy fibers are found in the spinal cord, the basilar pontine nuclei, various precerebellar reticular nuclei (e.g. the lateral reticular nucleus, the NRTP and the paramedian reticular nucleus), the vestibular and perihypoglossal nuclei, the dorsal column nuclei and the trigeminal nuclei. The sole origin of climbing fibers is the IO (Desclin, 1974).

A third group of cerebellar afferents is derived from monoaminergic and cholinergic nuclei of the brain stem. These fibers most likely participate as modulators in the functioning of the cerebellum (André *et al.*, 1991; Bishop and Ho, 1985; Jaarsma *et al.*, 1997; Kitzman and Bishop, 1994; Strahlendorf *et al.*, 1991). They include serotonergic fibers, terminating diffusely in the granular layer and in the CN (Bishop and Ho, 1985; Kitzman and Bishop, 1994), and noradrenergic fibers, that terminate on all cerebellar cortical layers and within the CN (Chan-Palay, 1977; Hökfelt and Fuxe, 1969; Olson and Fuxe, 1971).

Since the cerebellar projections to the NRTP and the IO form major constituents of this thesis, anatomical and functional characteristics of both areas will be discussed below.

5A: The nucleus reticularis tegmenti pontis: a mossy fiber source

Structure

The NRTP of Bechterew (1885) derived its name from its location in the ventromedial tegmentum of the pons. It is located close to the midline, and is situated dorsal to the medial lemniscus, which separates it from the basal pontine nuclei, rostral to the trapezoid body, ventral and lateral to the abducens nucleus, and caudal to the decussation of the scp (for a review, see Ruigrok and Cella, 1995; Fig. 1.7).

In the rat, two parts can be distinguished (Torigoe *et al.*, 1986a; 1986b) which have not been described in such detail in other species: a central region (NRTPc) which is built of tightly packed neurons, flanked ventrally at caudal levels by a peripheral part (NRTPp), which contains scattered small neurons. At rostral levels, the NRTPp is located dorsal and lateral to the central part. The lateral extension of the NRTP corresponds to the processus tegmentalis lateralis in cat (Brodal and Brodal, 1971; Kawamura and Hashikawa, 1981b) and monkey (Brodal, 1980a), and is known to contain larger cells. The NRTPc consists of both large and small neurons, while in the NRTPp small neurons always dominate (Torigoe *et al.*, 1986b).

Afferents

The afferents of the NRTP have been subject to many studies, related to its role as a relay nucleus in the (pre)tecto-ponto-cerebellar and cortico-ponto-cerebellar pathways. In the rat, a diffuse projection from the cerebral cortex has been reported to terminate in the NRTP (motor cortex, premotor cortex, sensorimotor cortex, visual cortex, Torigoe *et al.*, 1986a; 1986b). In the cat and monkey, a rather restricted cortical projection was found, mainly from visuo-motor related areas (motor, premotor, frontal eye fields, Brodal and Brodal, 1971; Brodal, 1980a); e.g. a cingulate cortex projection, as demonstrated in the rat (Torigoe *et al.*, 1986a), was not found in the monkey (Brodal, 1980a) or in the cat (Brodal and Brodal, 1971). However, since the frontal eye field in the primate is thought to be equivalent with the cingulate gyrus in the rat (Leichnetz and Gonzalo-Ruiz, 1987), the cortical projections in both species can be considered to be consistent (Künzle and Akert, 1977).

The tectum, i.e. the superior colliculus (Graham, 1977; Harting, 1977; Sefton and Dreher, 1995), but not the inferior colliculus (Burne *et al.*, 1981), and the ventral lateral geniculate nucleus (Graybiel, 1974), project massively to the NRTP. The superior colliculus projects ipsilaterally to the processus tegmentalis lateralis, and contralaterally to the dorsomedial NRTP at middle rostrocaudal levels of the NRTP. A projection from the nucleus of the optic tract is still controversial. Terasawa (1979) demonstrated a direct input from the nucleus of the optic tract to the NRTP, which was denied by others (rabbit: Holstege and Collewijn, 1982; tree shrew: Weber and Harting, 1980; cat: Itoh, 1977). Optokinetic system related nuclei that project to the NRTP are the reticular formation of the

mesencephalon, the pons and the medulla, the nucleus of the posterior commissure, the supra-oculomotor periaquaeductal gray, the interstitial nucleus of Cajal, the fields of Forel, the zona incerta and the ventral tegmentum (Burne *et al.*, 1981; Torigoe *et al.*, 1986a; 1986b). Additionally, some afferents arise from the limbic system, such as the habenula, the mammillary nuclei, the hypothalamus, the preoptic nucleus and the nucleus of the diagonal band of Broca (Allen and Hopkins, 1990; Cruce, 1977; Terasawa *et al.*, 1979). The input of the vestibular nuclei (the superior and lateral vestibular nucleus) to the NRTP is restricted to a small dorsomedial portion (Balaban, 1983; Gerrits and Voogd, 1981; Hosoya and Matsushita, 1981).

A major source of afferents arises from the contralateral CN. In the rat and in other species, all CN, except for the PIN, were found to project to the NRTP (rat: Torigoe *et al.*, 1986b; cat: Angaut *et al.*, 1985a; Brodal and Szikla, 1972; Gerrits and Voogd, 1981; Voogd, 1964; opossum: Martin *et al.*, 1974; monkey: Asanuma *et al.*, 1983a; Chan-Palay, 1977). Despite the massive input, not all of the NRTP is reported to receive cerebellar afferents. Each cerebellar nucleus has its preferred area of termination within the NRTP. The LCN projects to all of the NRTP but the medial parvicellular part (Angaut *et al.*, 1985a; Mihailoff *et al.*, 1981a); the medial part of the NRTP receives almost exclusively input from the MCN (Angaut *et al.*, 1985a; Cicirata *et al.*, 1982), and the interposed nuclei (without distinguishing between anterior or posterior divisions) were found to project to the ventral parts of the nucleus (Angaut *et al.*, 1985a). The areas of termination within the NRTP were found to overlap considerably (Asanuma *et al.*, 1983a; Brodal and Brodal, 1971), also with terminal areas from other afferents (Lee and Mihailoff, 1990), their Fig. 4B6; (Schmahmann and Pandya, 1995). It has been demonstrated that part of the GABAergic neurons in the CN, which find their main projection in the IO, collateralize to the NRTP (Aas and Brodal, 1990), and that part of the non-GABAergic neurons project to the RN as well (Bernays *et al.*, 1988). The organization of the cerebellar nuclear projection to the NRTP has been described in different species (monkey: Asanuma *et al.*, 1983a; cat: Brodal *et al.*, 1972a; rat: Cicirata *et al.*, 1982; Faull, 1978; opossum; Martin *et al.*, 1974). However, the columnar organization of this projection, as presented by Faull (1978) in analogy with Brodal's observations in the cat, has been denied in the rat by Cicirata (1982) and Angaut (1985a) and in the cat by Gerrits (1984b). Gerrits (1984b) demonstrated in his reconstructions of the NRTP that labeled terminals were distributed in dense patches, which did not form a continuous column. Part of the present study therefore will concern the investigation of the distribution of the cerebellar nuclear projection onto the NRTP.

The cerebral, the tectal, and the cerebellar projections upon the NRTP are topically arranged in a medio-lateral order (Asanuma *et al.*, 1983b; Blanks, 1988; Brodal, 1980a); the medial part of the NRTP is related to the allocortex, and the lateral part is related to the neocortex (Brodal,

1980a). The dorsal and medial parts of the NRTP receive very little cortical input (Brodal, 1980a).

Mossy fibers predominantly utilize glutamate for neurotransmission (Ji *et al.*, 1991; Ottersen, 1993; Somogyi *et al.*, 1986), but other neuropeptides and neurotransmitters haven been found in certain systems (cat: acetylcholine, Barmack *et al.*, 1992a; Barmack *et al.*, 1992b; Ikeda *et al.*, 1991, and calcitonin gene-related peptide, Bishop, 1992; opossum: cholecystokinin, King and Bishop, 1990; enkephalins, Schulman *et al.*, 1981) which underlines the heterology of the mossy fibers origins. The rat NRTP is highly immunoreactive for glutamate (Moffett *et al.*, 1994). Compared with other brain stem areas, the NRTP contains very little GABA. Most GABA and GAD-immunoreactivity was found within axonal structures and terminals in this nucleus (Border and Mihailoff, 1985; Brodal *et al.*, 1988). The input to the NRTP is mainly excitatory (Allen and Tsukahara, 1974; Kitai *et al.*, 1976; Tsukahara, 1972), although some inhibitory afferents have been demonstrated (Aas and Brodal, 1990; Berretta *et al.*, 1991a; Verveer *et al.*, 1997).

Efferents

The NRTP projects exclusively to the cerebellar cortex, the CN and, possibly, group y (Azizi *et al.*, 1981; Brodal, 1980b; Gerrits, 1987; Gerrits and Voogd, 1987; Hoddevik, 1978; Mihailoff *et al.*, 1981a). It terminates bilaterally, but with a slight contralateral predominance, especially in the visual vermal lobes VI, VII and VIII, the flocculus and the ventral paraflocculus (Blanks *et al.*, 1983; Gerrits *et al.*, 1984a; Gerrits and Voogd, 1981; Yamada and Noda, 1987), areas related to visuo-motor functions. Mossy fiber collaterals were reported to terminate in the LCN in different species (rat: Angaut *et al.*, 1985a; cat: Brodal *et al.*, 1986; Gerrits, 1987; opossum: Martin *et al.*, 1974), but the distribution of terminals to the AIN and PIN, as well as to the MCN has been debated. Gerrits and Voogd (1987) observed terminals in the lateral parts of the PIN, as well as in the caudal part of the MCN, and a few in the AIN, whereas Brodal (1986) denied a projection both to the MCN and the AIN. A projection to the vestibular nuclei, as suggested by electrophysiological experiments (Precht, 1981; Precht and Strata, 1980) could not be substantiated in the cat and rabbit (Gerrits and Voogd, 1986) and has been denied in the rat (Torigoe *et al.*, 1986b).

Function

A role for the NRTP as a relay nucleus of visuo-motor related information in the cortico-cerebellar pathway is debated (Büttner-Ennever and Büttner, 1988), since direct input from the nucleus of the optic tract is questioned in anatomical (Holstege and Collewijn, 1982) and physiological studies (Crandall and Keller, 1985). The NRTP has been suggested to be involved in a cerebello-cerebellar loop, in which the cortico-tegmentoreticular projection provides a background or a modulatory influence, and in which the cerebellar input provides a major driving force (Allen and Tsukahara, 1974).

Recently, it has been implied that the NRTP and CN are involved in both an inhibitory and an excitatory feedback control mechanisms (Berretta *et al.*, 1991a), enabling the transmission of high-frequency information in the cerebro-cerebellar pathway. Perhaps the most distinctive property of the NRTP is its collateral projection to the CN. It shares this property with another precerebellar reticular nucleus, the nucleus reticularis lateralis, and certain nuclei in the spinal cord (Qvist, 1989). Hence, the resulting self-sustaining reverberating loops of activity may be modulated by the cerebellar cortex.

5B: The inferior olivary complex: the source of the climbing fibers

Structure

The IO is located ventromedially in the caudal part of the medulla oblongata. Three main subdivisions are recognized: the principal olive (PO), the medial accessory olive (MAO) and the dorsal accessory olive (DAO), Fig. 1.10. The PO is located between the MAO and the DAO and consists of a dorsal and ventral lamellae of gray matter. Caudal extensions of the PO are the ventrolateral outgrowth (VLO) and the dorsal cap of Kooy (DC, Kooy, 1916). The MAO consists of several subdivisions, including the mediocaudally situated nuclei a and b, the medial and caudal subnucleus c, the group ß (ß) and the medially located dorsomedial cell column (DMCC). The MAO is found ventromedial to the PO. The DAO is boomerang-shaped and generally is subdivided in a caudomedial handle and a large, oval body. In the rat, these two subdivisions correspond to the dorsal and ventral fold respectively (Azizi and Woodward, 1987; De Zeeuw, 1990; Ruigrok and Voogd, 1990).. The IO can be described as a single, semi-continuous folded sheet. This configuration of the IO can be appreciated from Fig. 1.8, adapted from Ruigrok and Voogd (1990), and Fig. 1.9, after Ruigrok (1997).

Afferents

The afferents to the IO can be categorized according to the neurotransmitters involved (GABAergic versus non-GABAergic), or according to their source (cerebral cortex, mesencephalon, caudal brain stem and spinal cord). GABAergic afferents to the IO predominantly arise from the small-sized neurons within all CN, and also from smaller neurons in the vestibular nuclei (medial vestibular nucleus, lateral vestibular nucleus; Andersson *et al.*, 1988; Angaut and Sotelo, 1989; Buisseret-Delmas *et al.*, 1989; De Zeeuw *et al.*, 1994; 1988; 1989a; 1989b; 1993; Fredette and Mugnaini, 1991; Nelson and Mugnaini, 1988; 1989). This projection is mainly contralateral, but a small ipsilateral projection has been acknowledged. The nucleoolivary and olivocerebellar projections are arranged according to a reciprocal schedule (Beitz, 1976; Dietrichs and Walberg, 1985; 1986; 1989; Dietrichs *et al.*, 1985; Ruigrok and Voogd, 1990; 1995b); for a review, see (Brodal and Kawamura, 1980; Ruigrok and Cella, 1995). Additional GABAergic inputs have been demonstrated to arise from the nucleus parasolitarius, which projects ipsilaterally to the caudal parts of the

IO, and from the contralateral nucleus cuneatus (Nelson and Mugnaini, 1989).

Non-GABAergic, presumably glutaminergic / aspartergic, afferents, predominantly terminating in the DAO and caudally in the MAO originate from the spinal cord, the dorsal column nuclei and the spinal trigeminal nucleus. The nucleus cuneatus efferents and the nucleus gracilis efferents overlap with cervical and lumbosacral spinal cord terminals, in the rostral ventromedial bend of the DAO and in the lateral DAO, respectively (Berkley and Worden, 1978; Boesten and Voogd, 1975; Martin *et al.*, 1975). The PO and rostral half of the MAO are mainly provided with input from descending systems that originate from nuclei at the mesencephalic junction and eye movement related mesencephalic areas. The nucleus of the tractus opticus and the accessory optic nuclei project to the dorsal cap and to the ventrolateral outgrowth, respectively (Gerrits *et al.*, 1985; Swenson and Castro, 1983a; 1983b). The nuclei at the mesencephalic junction, or rather, the area prerubralis parafascicularis (Carlton *et al.*, 1982; Ruigrok and Cella, 1995), project to the rostral MAO and the remainder of the PO. The area prerubralis parafascicularis includes the nucleus of Darkschewitsch, the prerubral area and the rostral part of the parvicellular RN, the medial accessory oculomotor nucleus and the rostral interstitial nucleus of the medial longitudinal fasciculus (Bentivoglio and Molinari, 1984; Brown *et al.*, 1977; De Zeeuw *et al.*, 1989b; 1990; Onodera, 1984; Swenson and Castro, 1983a; 1983b). Whether the rostral part of the RN, i.e. the parvicellular part, also projects to the IO in the rat, is still controversial (Brown *et al.*, 1977; Carlton *et al.*, 1982; Kennedy and Humphrey, 1987; Ruigrok *et al.*, 1993). The terminal areas within the inferior olivary subnuclei of the ascending and descending brain stem and spinal cord afferents may overlap with the descending projections from the superior colliculus and pretectum, the vestibulo-olivary projections and the trigemino-olivary projections. E.g. subnucleus ß is a recipient of fibers arising in the medullary reticular formation, the vestibular nuclei, the nucleus prepositus hypoglossi and the lateral part of the deep mesencephalic nuclei; the vestibular nuclei, the nucleus prepositus hypoglossi, the prerubral area, and the mesodiencephalic junction innervate the dorsomedial cell column. Within the caudal MAO, efferents from the vestibular nuclei, the spinal trigeminal nucleus, the medullary reticular formation, the lateral reticular nucleus, the nucleus prepositus hypoglossi, the lateral and medial parts of the deep mesencephalic nuclei and the mesodiencephalic junction overlap (Berkley and Hand, 1978; Berkley and Worden, 1978; Bull *et al.*, 1990; Swenson and Castro, 1983a; 1983b).

A direct projection from the cerebral cortex to the IO, although small, also overlaps with other terminal fields: fibers arising from the frontal cortex, which is reported most consistently to project to the IO, terminate in the medial DAO, the dorsomedial cell column and the caudomedial MAO. Most cortico-olivary connections, however, are

relayed via mesodiencephalic nuclei (Nakamura *et al.*, 1983; Oka *et al.*, 1979; Saint-Cyr, 1987; Sousa-Pinto, 1970). The afferents from the dorsal column nuclei and the spinal cord to the DAO overlap considerably and are clearly separated from cortical and other descending inputs with the possible exception of the afferents from the pretectum (Berkley and Hand, 1978; Berkley and Worden, 1978).

The IO transmits a number of sensory (visual, auditory, and sensorimotor) modalities, of which the "motor" and "sensory" modalities are partially segregated (Berkley and Hand, 1978; Berkley and Worden, 1978; Walberg, 1956): most of the principal nucleus and the rostral half of the MAO receive a (descending) motor input, whereas the two accessory nuclei receive a somatosensory (ascending) input (Edwards, 1972; Sousa-Pinto, 1969; Walberg, 1956). These different modalities are reflected in the functional organization of the IO and the cerebellum (Azizi, 1989): a caudal somatosensory zone, which receives ascending somatosensory input, includes the DAO and the caudal MAO; a medial visuo-vestibular zone, relaying mesencephalic visuo-vestibular input to the vestibulo-cerebellum (the posterior vermis and the flocculus), includes the subnuclei c, β, the ventrolateral outgrowth, the dorsomedial cell column and the dorsal cap, and finally the diencephalic and telencephalic motor input, covers the principal and rostral MAO. Some of the mesodiencephalic areas that project to the IO receive a cerebellar nuclear input and, therefore, constitute excitatory cerebello-mesencephalo-olivary loops, superimposed on the GABAergic nucleoolivary projection (Bull and Berkley, 1991; Kawamura *et al.*, 1982; Sugimoto *et al.*, 1982).

Cholinergic and serotonergic afferents have been found to terminate in the IO (Bishop and Ho, 1984; Bishop and King, 1986; Wiklund *et al.*, 1977); the presence of neuropeptide containing terminals within the IO has been demonstrated as well (opossum: King *et al.*, 1989; rat: Bishop and Ho, 1984). Dopaminergic projections from the prerubral parafascicular region to the ventrolateral outgrowth of the IO have recently been described (Toonen *et al.*, 1998).

Efferents

The IO is the only source of climbing fibers (Desclin, 1974). The climbing fibers terminate in the molecular layer of the cerebellar cortex where they climb into and terminate on the Purkinje cell dendritic tree (Eccles *et al.*, 1966; Szentágothai and Rajkovits, 1959): also see Figs. 1.1, 1.2, 1.5, 1.6. They use glutamate and aspartate for neurotransmission (Moffett *et al.*, 1994; Wiklund *et al.*, 1984). Climbing fiber collaterals are directed to the CN (Kitai *et al.*, 1977; van der Want *et al.*, 1989). The organization of the projection of the climbing fiber collaterals (Fig. 1.9) corresponds with the sagittal arrangement of the inferior olivary projections to the cerebellar cortex, the Purkinje cell projection to the cerebellar subnuclei and the nucleoolivary projection (Buisseret-Delmas and Angaut, 1993), for a review see (Voogd, 1995). The olivocerebellar projections are all topographically arranged, as has been

demonstrated in physiological and anatomical studies. Their organization appears to be highly consistent amongst different species.

Anatomical (Brodal *et al.*, 1980; Hrycyshyn *et al.*, 1989; Wharton and Payne, 1985; Wiklund *et al.*, 1984) and electrophysiological (Apps *et al.*, 1991; Armstrong *et al.*, 1971; Ekerot and Larson, 1982; Faber and Murphy, 1969) studies have demonstrated in various species that some climbing fibers branch in the parasagittal plane, terminating on Purkinje cells in different lobules (e.g. anterior lobe and ipsilateral paramedian lobe), and in the mediolateral plane, (Campbell and Armstrong, 1985; Ekerot and Larson, 1982; Takeda and Maekawa, 1984); recently, a combined electrophysiological and tracing technique confirmed that branches of climbing fibers terminate in individual cortical zones (Apps *et al.*, 1991). These cross-links between functionally different units may tune their respective activities (Apps *et al.*, 1991). The extent of the branching of climbing fibers remains to be determined and varies from few (Ekerot and Larson, 1982) to a fairly high numbers of collaterals (Apps *et al.*, 1991; Campbell and Armstrong, 1985).

Since the nucleoolivary projections have been studied extensively (Ruigrok, 1997; Ruigrok and Voogd, 1990), their topography will not be further investigated in this thesis; the reports on the nucleoolivary projection will be used as a reference for cases with cerebellar nuclear injection sites. The debated collateralization of nucleoolivary fibers, however, will be studied in this thesis.

6. The red nucleus: a premotor nucleus

Structure

The RN is located in the tegmentum mesencephali of the vertebrate brain. It is not present in the brain of limbless vertebrates. It supposedly derived its name from its appearance in fresh human brain sections; its reddish/pinkish color has been attributed to an increased vascularisation of this nucleus in regard to the surrounding tissue, but illustrations of brain stem vascularisation do not seem to agree with this hypothesis (Massion, 1988). A high iron concentration and a high mitochondrial cytochrome oxidase activity, plus a rich blood supply might be related to its reddish appearance (Ralston, 1994).

Caudally the RN of the rat can be distinguished from the neighboring reticular formation as an area of rather large neurons encapsulated by the brachium conjunctivum. Its caudal pole is found at the level of the oculomotor nucleus, rostral to the decussation of the scp (Fig. 1.10). The rostral boundary of the RN is rather difficult to establish, but conventionally, is defined just caudal to the level of the fasciculus retroflexus. At rostral levels, the neurons tend to be smaller and more dispersed and the nucleus cannot be distinguished from surrounding structures (Padel *et al.*, 1981).

In the rat, up to four different cell types have been identified in the RN (Reid *et al.*, 1975a; 1975b; Strominger *et al.*, 1987; Tucker and Kennedy, 1990); the consensus is that the caudal pole contains the largest

neurons. Within this large-celled part, a ventrolateral, compact part and a dorsolateral, loosely arranged part are distinguished (Reid *et al.*, 1975b). The ventrolateral part is continuous with the so-called lateral horn of the rat RN (Reid *et al.*, 1975b), which separates from its dorsomedial part. The dorsomedial part is divided into a dorsomedial and a dorsal group of neurons. Ruigrok and Cella (1995) used the distribution of lateral cerebellar nuclear input to define the rostral pole of the RN, and proposed to include the "nucleus minimus" or rather the nucleus pararubralis, a cell cluster lateral to the parvicellular RN (rabbit: Von Monakow, 1909; cat: Brodal and Gogstad, 1954; Taber, 1961) in the pararubral area, which is located adjacent to the lateral horn and blends rostrally with the parvicellular RN, within the definition of the RN complex.

Apart from the neurons from which the descending tracts arise, the RN also contains small-sized GABAergic interneurons (André *et al.*, 1987; Elekes *et al.*, 1986; Vuillon-Cacciuttolo *et al.*, 1984), which, in the magnocellular part, terminate on rubrospinal neurons (Matsumoto and Walker, 1991; Ralston and Milroy, 1992; Sakaguchi *et al.*, 1984; Schmied *et al.*, 1991).

Neuronal size has been used in mammals to separate a caudal magnocellular part from a rostral parvicellular part (Hatschek, 1907), an important functional distinction since the magnocellular part of the primate RN gives rise to the rubrospinal tract, and the parvicellular part gives rise to the ipsilateral rubro-olivary projecting fibers in the central tegmental tract (Hinman and Carpenter, 1959; Pompeiano and Brodal, 1957; Walberg, 1956). However, the degree of delineation, as the distribution of cell sizes (Tucker *et al.*, 1989), varies between species, being most obvious in primates (Flumerfelt *et al.*, 1973), and least clear in the cat (Brodal and Gogstad, 1954; Taber, 1961) and opossum (King *et al.*, 1971). An involution of the magnocellular, caudal part parallels the evolution of the parvicellular, rostral part from lower species through opossum, cat, and primate to man (ten Donkelaar, 1988). The rat falls somewhere between the extremes (Reid *et al.*, 1975b). Therefore, the efferent connections of the RN may give insight into the subdivisions. However, information from the literature on the red nuclear efferents is confusing.

Efferents

In rat and cat, the origin of the rubrospinal tract is not restricted to the large cells in the caudal part of the nucleus (Flumerfelt and Gwyn, 1974; Gwyn, 1971; Murray and Gurule, 1979), but also includes some of the smaller cells in the rostral, parvicellular pole of the RN (cat: Brodal and Gogstad, 1954; Pompeiano and Brodal, 1957; rat: Huisman *et al.*, 1983; 1981; Kennedy, 1990; Shieh *et al.*, 1983; Tucker *et al.*, 1989; Waldron and Gwyn, 1969).

The rostral, parvicellular part of the RN in primates (Poirier and Bouvier, 1966), opossum (Linauts and Martin, 1978; Martin *et al.*, 1975) and in the cat (Edwards, 1972; Hinman and Carpenter, 1959; Walberg, 1956; Walberg, 1958) gives rise to a projection to the ipsilateral IO, typically

to the dorsal leaf of the principal olive. In the rat, however, the existence of such a projection has been disputed. Such a rubro-olivary projection has been demonstrated with anterograde and retrograde techniques (Swenson and Castro, 1983a; 1983b), but these observations could not be confirmed in other studies (Carlton *et al.*, 1982; Rutherford *et al.*, 1984), which attributed this projection to another cell population next to the RN. Rubro-olivary projecting fibers have been suggested to be collaterals of the rubrospinal tract (Kennedy, 1990; Tucker and Kennedy, 1990; Tucker *et al.*, 1989).

Carlton (1982) suggested that the olivary projecting area includes a rather wide region surrounding the fasciculus retroflexus, and should be referred to as area prerubralis parafascicularis. This region should be distinguished from the RN proper. In their view, the area parafascicularis prerubralis includes the rostral part of the nucleus of Darkschewitsch and the medial accessory oculomotor nucleus (Carlton *et al.*, 1982); for a review, see (Ruigrok and Cella, 1995). Kennedy (1990) proposed that the area prerubralis parafascicularis should be redefined as a part of the parvicellular RN, in line with the definition in the monkey. However, in the rat the parvicellular part of the RN holds significantly less olivary projecting neurons than the area parafascicularis prerubralis, which undermines this notion. Recently, an appeal was made to include the pararubral area in the rubral complex (Ruigrok and Cella, 1995).

In addition to the rubrospinal tract a crossed rubrobulbar projection exists. In the rat, the rubrobulbar tract arises as collaterals from the rubrospinal tract. In humans, however, parts of it, such as the rubrofacial tract (Nieuwenhuys *et al.*, 1998) are considered as separate entities. The rubrobulbar tract terminates in various brain stem centers such as the lateral part of the facial nucleus, the rostral part of the lateral reticular nucleus, the oral part of the spinal trigeminal nucleus, the principal sensory trigeminal nucleus, the spinal vestibular nucleus and the dorsal column nuclei (Flumerfelt and Gwyn, 1974; Hinrichsen and Watson, 1983).

Finally, the RN also gives rise to a recurrent projection to the cerebellum (rat: Yu *et al.*, 1991; cat: Brodal and Gogstad, 1954; Courville and Brodal, 1966). This projection arises as a collateral pathway from rubrospinal and/or rubrobulbar fibers (Huisman *et al.*, 1983). Projections of the RN to the diencephalon (the posterior thalamic nuclear group in the rat, Roger and Cadusseau, 1987) and to the ventrolateral thalamic nucleus in the cat (Condé and Condé, 1980), have been repeatedly mentioned and denied in the literature.

Afferents

The RN receives an input from the CN and from the cerebral cortex. Other sources of input in the rat are reported to arise from the posterior thalamic nucleus (Roger and Cadusseau, 1987), the zona incerta (Ricardo, 1981), the hypothalamic areas, the central pontine gray, the nuclei raphe dorsalis and magnus, the gigantoreticular nucleus, the parvicellular reticular nucleus, the parabrachial nuclei, and the locus

coeruleus (Bernays *et al.*, 1988); in the cat, projections from the dorsal column nuclei have been demonstrated to terminate within the RN (Boivie, 1988).

The CN give rise to a major input to the contralateral RN, as has been demonstrated with anterograde and retrograde tracing techniques in the rat (Angaut *et al.*, 1986; 1987; Angaut and Cicirata, 1988; Caughell and Flumerfelt, 1977; Daniel *et al.*, 1988; 1987). These projections are somatotopically organized. The AIN provides the larger part of input to the caudal, magnocellular RN; the lateral part of the AIN projects to the dorsomedial part, the medial part of the AIN provides the ventrolateral part and the lateral horn of the caudal RN with input. Only the medial part of the PIN was found to project to the RN. It terminates as a shell surrounding the caudal, magnocellular portion of the RN (Daniel *et al.*, 1987). In addition, projections of the PIN to the medial part of the area parafascicularis prerubralis and to the medial accessory oculomotor area have been documented.

The LCN projects predominantly to the parvicellular pole of the RN. The rostral part of the LCN projects to the ventromedial rostral RN, and the caudal LCN projects to the dorsolateral areas of the rostral RN (Angaut and Cicirata, 1988). The parvicellular part of the LCN was found to project specifically to the area pararubralis (Daniel *et al.*, 1987; Ruigrok *et al.*, 1993; Ruigrok and Cella, 1995). A projection from the LCN to the magnocellular part of the RN could be derived from (Robinson *et al.*, 1987; Voogd, 1964) in the cat and from (Ostrowska *et al.*, 1993) in the rabbit, but has not been substantiated in the rat or monkey. The MCN has been found to project to the medial part of the base of the lateral horn (Ruigrok and Cella, 1995).

The cerebello-rubral projection is presumed to be excitatory (Oka, 1988; Toyama *et al.*, 1968) and mainly occurs through collaterals of fibers on their way to the thalamus (Shinoda *et al.*, 1988). From physiological experiments, it has been concluded that at least some of the GABAergic nucleoolivary projection neurons in the cat (De Zeeuw, 1990; De Zeeuw *et al.*, 1989a; Fredette and Mugnaini, 1991) collateralize to the RN and/or the thalamus (Andersson and Hesslow, 1987b; McCrea *et al.*, 1978), although in agreement with double labeling studies in the rat (Bentivoglio and Kuypers, 1982) and cat (Bharos *et al.*, 1981), their number presumably is very low.

Information on cerebral cortical input to the RN is rather sparse; in the rat, Cajal (1911) already described a cortical input, which was derived from the sensorimotor cortex; in the rat, this projection has been found to terminate in the parvicellular part of the RN (Brown, 1974; Gwyn and Flumerfelt, 1974), and in the pararubral area (Brown, 1974), areas receiving cerebellar nuclear input from the LCN and the PIN. A (pre-)motor input to the magnocellular division, which converges upon the same cells as the cerebellar nuclear input has been described by several authors (Giuffrida *et al.*, 1988a; 1988b; Gwyn and Flumerfelt, 1974). Cortical input and cerebellar input have been demonstrated to converge on RN

neurons in the monkey (Ralston, 1991).

Summarizing, as proposed by Ten Donkelaar (ten Donkelaar, 1988), the RN in non-primates is best defined according to its relative position in the tegmentum mesencephali, by its contralateral rubrospinal or rubrobulbar projections, and by crossed cerebellar afferents. In primates its magnocellular and parvicellular parts are best identified according to their target sites, either electrophysiologically or anatomically (Robinson *et al.*, 1987). In non-primates the term "parvocellular RN" should be used with specific qualifications, because it gives rise to rubrospinal and bulbar fibers and does not qualify as one of the major pre-olivary nuclei.

7. Function of cerebello-bulbar circuitry

The electrophysiological principles of the cerebellar circuit were established by Eccles (1967). Two circuits are distinguished, the mossy fiber afferent system, and the climbing fiber afferent system. The main circuit encompasses the mossy fiber / parallel fiber afferents. The mossy fibers terminate on the granule cells in the granular layer, and the granular cell axon ascends into the molecular layer where it bifurcates and, running in a transverse direction, terminates on the dendritic trees of multiple Purkinje cells. Purkinje cell axons leave the cerebellar cortex and terminate in the cerebellar and vestibular nuclei. The CN distribute efferents to different sources of mossy fibers. Each Purkinje cell dendritic tree is individually innervated by a climbing fiber, although climbing fibers have been demonstrated to branch and to innervate multiple Purkinje cells, located in different lobuli (Apps *et al.*, 1991; Brodal *et al.*, 1980; Campbell and Armstrong, 1985; Ekerot and Larson, 1982; Faber and Murphy, 1969; Rosina and Provini, 1983a; 1983b; 1987; Wharton and Payne, 1985). Purkinje cells project to the CN that harbor the nucleoolivary neurons that project to the contralateral IO, from which the climbing fibers originate (Desclin, 1974). A feed back / feed forward signal on the Purkinje cells is derived via parallel fiber input to stellate and basket cells that excite, and to Golgi cells that inhibit the Purkinje cells.

Climbing fibers, mossy fibers and parallel fibers are excitatory, and thus excite their postsynaptic structure (i.e. Purkinje cells, cerebellar nuclear cells, interneurons). Purkinje cells contain GABA and are inhibitory. Since cerebellar cortical output occurs through the Purkinje cell axons, the cerebellar cortical output is inhibitory.

The mossy fiber - granule cell system was found to dictate the rate at which Purkinje cells fire; the frequency at which Purkinje cells are triggered by climbing fibers supposedly is too low to contribute significantly to the output. This on itself is remarkable, since climbing fibers and Purkinje cells appear to be optimally tuned, both morphologically and electrophysiologically.

From these data it follows that the simple spikes of a Purkinje cell would inhibit its target cerebellar nuclear neuron, and thus inhibit the cerebellar

output (Eccles, 1973). The CN are disinhibited and their activity is stimulated or allowed during a pause in Purkinje cell activity, caused by the removal of simple spikes through the activation of Golgi cells (Murphy and Sabah, 1971a), inhibition of the Purkinje cells by basket or stellate cells or by the tonic depression of climbing fibers of simple spike discharge. Both acute and chronic effects of climbing fibers on simple spikes have been found. The acute effect includes the pause in simple spike firing, following the complex spike (Colin *et al.*, 1980). Chronic effects are caused by long term depression (LTD) of the parallel fiber - Purkinje cell synapses, and, similarly, will lead to the suppression of simple spikes.

In rats (Ruigrok, 1997; Ruigrok *et al.*, 1994), and cats (Armstrong *et al.*, 1973; Eccles *et al.*, 1974a; Kitai *et al.*, 1977) cerebellar nuclear cells were found to respond to climbing fiber stimulation with a short latency activation of 4 - 5 msec, followed by a silent period of several tenths of msecs which varies in length ,and an enhancement of the activation (or excitatory rebound, Armstrong *et al.*, 1973; Ruigrok *et al.*, 1994). The early activation corresponds with a monosynaptic climbing fiber collateral excitation and the triggered complex spikes, blocking cerebellar nuclear activity would cause the silent period.

Similar responses of nuclear cells were described in rat cerebellar slices, co-cultured with extracts of the IO by (Audinat *et al.*, 1992). The early, fast-rising excitatory postsynaptic potentials –EPSP- and the inhibitory postsynaptic potentials –IPSP- in the nuclear cells could be blocked by 6-cuano-7-nitroquinoxaline-2,3-dione, an AMPA receptor blocker presumably at the level of the climbing fiber - nuclear and the climbing fiber - Purkinje cell synapse respectively. The late, slow rising, EPSP could be blocked by D-2-amino-5-phosphonovalerate, suggesting an effect of climbing fiber collateral, NMDA receptor mediated activity at the level of the CN. Therefore, both the inhibition of simple spike firing by the complex spike as demonstrated in barbiturate-anesthetized animals (Bloedel and Roberts, 1971; Sato *et al.*, 1993) and the NMDA-mediated excitation by climbing fiber collaterals could contribute to the production of the excitatory rebound. However, a direct temporal relation between the peristimulus simple spike frequency and the cerebellar nuclear response could not be established in ketamine-sedated rats (Ruigrok, 1997; Ruigrok *et al.*, 1994).

Short latency activation (i.e. climbing fiber collateral input) proved not to be a prerequisite. Nevertheless, the relationship between the Purkinje cell activity and neurons in the cerebellar nuclei is still not clear. E.g. in contrast to what may be expected, recordings from Purkinje cell - nuclear neuron pairs only rarely demonstrated the expected reciprocity at climbing fiber activation of Purkinje cell and cerebellar nuclear cells. In stead, an increased response of cerebellar nuclear cells usually was found (Armstrong and Edgley, 1984; 1988; McDevitt *et al.*, 1987a; 1987b).

Part of the output of the CN is directed at the contralateral IO. This nucleoolivary pathway parallels the

nucleo-mesodiencephalic-olivary pathway. The nucleoolivary pathway is GABAergic and inhibitory (Angaut and Sotelo, 1989; De Zeeuw *et al.*, 1989a; Fredette and Mugnaini, 1991). The Purkinje cells inhibit the nucleoolivary neurons, which, on their turn, disinhibit the inferior olivary neurons and facilitate olivary neuronal discharge (Andersson *et al.*, 1988; Andersson and Hesslow, 1987a; 1987b). As a result, the climbing fibers continue to excite the Purkinje cells (Eccles *et al.*, 1974b; Kitai *et al.*, 1977). The nucleo-mesodiencephalic projection onto the pre-olivary nuclei (see introduction), the nucleus of Darkschewitsch, the interstitial nucleus of Cajal, the prerubral area, the parvicellular RN (De Zeeuw and Ruigrok, 1994; Oka, 1988; Onodera, 1984) is non-GABAergic and excitatory (Berretta *et al.*, 1993; De Zeeuw and Ruigrok, 1994; Toyama *et al.*, 1968). The pre-olivary nuclei provide the IO with an excitatory input, which also increases the climbing fiber discharge. Basically, therefore, the excitatory nucleo-mesodiencephalo-olivary circuit is operating in conjunction with a GABAergic nucleoolivary pathway. In a study on the effect of mesodiencephalic and cerebellar nuclear electrical stimulation on the excitability of inferior olivary neurons in the cat (Ruigrok and Voogd, 1995b) it was observed that a reduction of the GABAergic influence on the IO (by lesioning the nucleoolivary path) resulted in a decrease of likelihood of olivary neurons to be triggered by the nucleo-mesodiencephalic-olivary path. This may be explained by the regulatory role of the nucleoolivary pathway on the electrotonic coupling of the inferior olivary neurons (Angaut and Sotelo, 1989; De Zeeuw, 1990; De Zeeuw *et al.*, 1989a; Llinás *et al.*, 1974; Sotelo *et al.*, 1986). Lesioning the nucleoolivary pathway induces a strong and permanent coupling of parts of the IO, which heightens the threshold for excitation of these cells, but, simultaneously, induces a powerful oscillation of their membrane potential (Yarom, 1989; 1991). Thus, removal of the nucleoolivary GABAergic projection results in increased coupling and synchronicity of olivary neurons, whereas nucleo-olivary pathway stimulation appears to decrease the coupling of olivary neurons (Ruigrok, 1997).

Legends to figures

Fig. 1.1. Diagram of the projections of the dentate and interposed cerebellar nuclei (CN) and the mossy fiber and climbing fiber recurrent circuits. The non-GABAergic projections (1) of the nuclei divided in ascending (A and C) and descending (B) branches. The descending branch terminates in the nucleus reticularis tegmenti pontis (NRTP), one of the main sources of the mossy fiber collateral projection to the nuclei. The ascending branch terminates in the red nucleus (RN), the nuclei of the mesodiencephalic junction (MDJ), a relay in the recurrent cerebello-mesencephalo-olivary loop, and in the ventral tier nuclei of the thalamus (VA/VL). The GABAergic nucleoolivary projection (2) terminates in the inferior olive (IO). Reproduced with permission of Dr.T.J.H.Ruigrok.

Fig. 1.2. Diagram of the cerebellar circuit. Inhibitory neurons are indicated in black. Abbreviations: cf: climbing fiber; GR; granule cell; IO: inferior olive; mf: mossy fibers; no: nucleoolivary axons; Pcell: Purkinje cell; PCN: precerebellar nuclei; pf: parallel fibers. Reproduced with permission of Prof.Dr.J.Voogd.

Fig. 1.3. Subdivision and nomenclature of the cerebellum. Left: numbering of cerebellar lobules according to Larsell (1952) and comparative anatomical nomenclature of Bolk (1906). Right: nomenclature of the human cerebellum. Reproduced with permission of Prof.Dr.J.Voogd.

Fig. 1.4. Standardized sections of the (right side) cerebellar and vestibular nuclear complex of the rat. The individual subnuclei are indicated with different shadings as explained at bottom of figure. **A.** Transverse sections, from caudal (1) to rostral (11) at 160 μm intervals. **B,C.** Flattened and semi-stretched-out display of cerebellar nuclei, according to right hand panel in B. Abbreviations: AIN: anterior interposed nucleus; DLH: dorsolateral hump; DLP: dorsolateral protuberance; drLCN: dorsorostral part of lateral cerebellar nucleus; ICG: interstitial cell group; LVN: lateral vestibular nucleus; MCN: medial cerebellar nucleus; PIN: posterior interposed nucleus; SVN: superior vestibular nucleus; vcLCN: ventrocaudal part of LCN. Reproduced with permission of Dr. T.J.H. Ruigrok.

Fig. 1.5. Semidiagrammatic 3D parasagittal section through a folium of the mammalian cerebellum. Abbreviations: B: basket cells; Ba: basket cell axon; Cl: climbing fibers; Coll: recurrent Purkinje cell axon collateral; G: Golgi cells; Gr: granule cell; Mf: mossy fibers; P: Purkinje cell layer; Pd: Purkinje cell dendrites; Pf: parallel fibers; S: stellate cells. After Ramon y Cajal, 1911.

Fig. 1.6. Schematic drawings summarizing the topographical relationships of the inferior olive, the cerebellar cortex and the cerebellar and lateral vestibular nuclei in the rat. **A.** Location of the retrogradely labeled neurons in the contralateral inferior olive projecting to the different zones. **B.** Parasagittal zones A, B, C1, C2,

C3 demarcated by small injections of WGA-HRP in the cerebellar cortex. **C.** Location of anterogradely labeled corticonuclear projections of the A zone to the fastigial nucleus (horizontal hatching), the B zone to the lateral vestibular nucleus (black), the C1 and C3 zones to the interposed nuclei (stippled), the C2 zone to the middle part of the interposed nucleus (vertical hatching), the D0 zone to the dorsolateral protuberance (coarse stippling), and the D1 and D2 zones to the dorsal and ventral parts of the lateral cerebellar nucleus (filled dots and dots with asterisk, respectively). The X zone, located between A and B in the anterior lobe and lobule VI is not indicated. After Buisseret-Delmas and Angaut, 1993.

Fig. 1.7. Schematic drawing of transverse sections through the pons in the rat, spaced 160 μm apart. Abbreviations: BPN: basilar pontine nuclei; lfp: longitudinal pontine fascicle; ml: median lemniscus; NRTP: nucleus reticularis tegmenti pontis; py: pyramidal tract; Tzb: trapezoid body.

Fig. 1.8. Diagrams depicting the standardized (left side) inferior olivary complex in the rat. **A.** The various olivary subnuclei, in different shades as explained at the bottom of the figure. Levels spaces 160 μm apart, from caudal (1) to rostral (16). **B.** The left hand panel shows a dorsal view of the whole olivary complex, based on the transverse sections in A. The right hand panel shows the unfolding of the olivary complex and the reconstruction to establish the flattened and unfolded diagram as depicted in **C.** Abbreviations: DAO: dorsal accessory olive; DC: dorsal cap; DMCC: dorsomedial cell column; DMPO: dorsomedial group of the PO; MAO: medial accessory olive; PO: principal olive; VLO: ventrolateral outgrowth. Reproduced with permission of Dr. T.J.H. Ruigrok.

Fig. 1.9. Schematic representation of the relation between the inferior olive and the cerebellar nuclei as observed for the nucleoolivary and olivo-nuclear projections. Both the inferior olive and cerebellar nuclei are represented as unfolded and more or less continuous sheets of cells. Basic folding places of both sheets are indicated by large (approximately 180 °) and small (approximately 90 °) arrowheads. After Ruigrok, 1997, with permission.

Fig. 1.10. Schematic standardized transverse sections through the mesencephalon, spaced 160 μm apart. Abbreviations: APT: anterior pretectal nucleus; cc: corpus callosum; cp: cerebral peduncle; Dk: nucleus of Darkschewitsch; DpG: deep gray layer colliculus superior; f: fornix; FF: nucleus of fields of Forel; fr: fasciculus retroflexus; ic: internal capsule; InG: intermediate gray layer colliculus superior; ml: median lemniscus; mlf: medial longitudinal fascicle; mp: mammilothalamic peduncles; pag: periaquaeductal gray; PF: nucleus parafascicularis; RNm: magnocellular part of red nucleus; RNp: parvicellular part of red nucleus; SN: substantia nigra; SuG: superficial gray layer colliculus superior; ZI: zona incerta

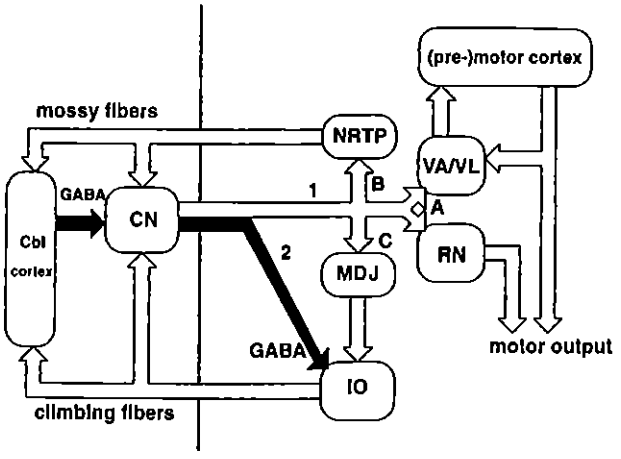
(pre-)motor cortex
mossy fibers
NRTP
VA/VL
GABA
1
B
A
CN
Cbl
cortex
C
RN
2
MDJ
motor output
GABA
IO
climbing fibers

Fig. 1.1

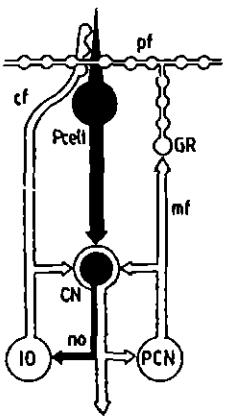

Fig. 1.2

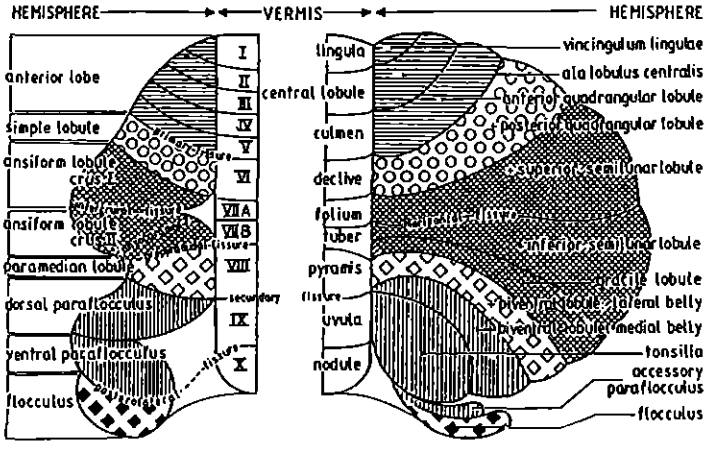
HEMISPHERE
VERMIS
HEMISPHERE
anterior lobe
simple lobule
ansiform lobule
crus I
ansiform lobule
crus II
paramedian lobule
dorsal paraflocculus
ventral paraflocculus
flocculus
I
II
III
IV
V
VI
VIIA
VIIB
VIII
IX
X
secondary fissure
lingula
central lobule
culmen
declive
folium
tuber
pyramis
fissure
uvula
nodule
vincingulum lingulae
ala lobulus centralis
anterior quadrangular lobule
posterior quadrangular lobule
superior semilunar lobule
inferior semilunar lobule
gracile lobule
biventral lobule, lateral belly
biventral lobule, medial belly
tonsilla
accessory paraflocculus
flocculus

Fig. 1.3

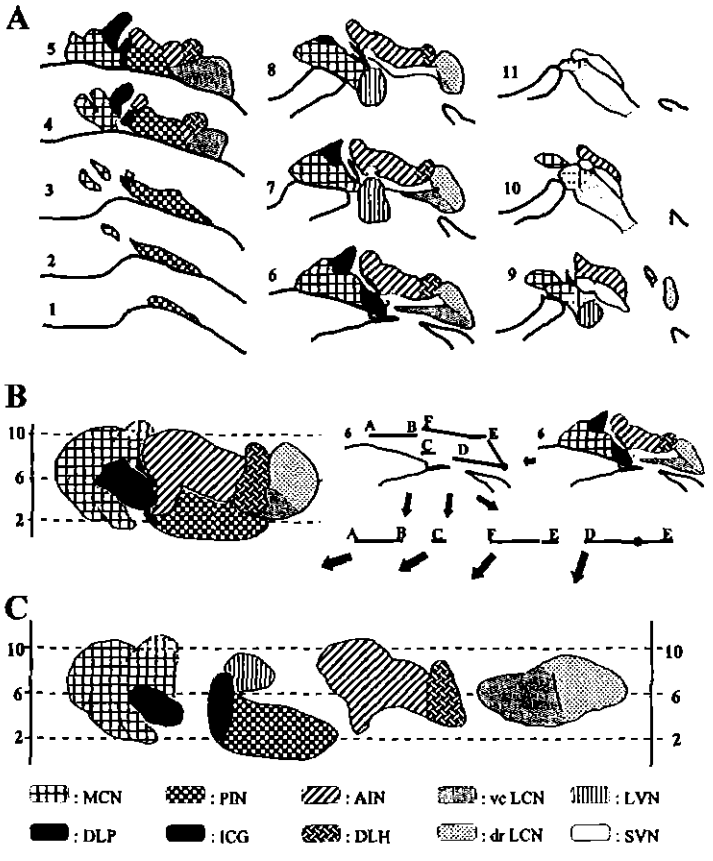
A
5
4
3
2
1
8
7
6
11
10
9
B
10
6
2
A
B
C
D
E
C
: MCN
: PIN
: AIN
: vc LCN
: LVN
: DLP
: ICG
: DLH
: dr LCN
: SVN

Fig. 1.4

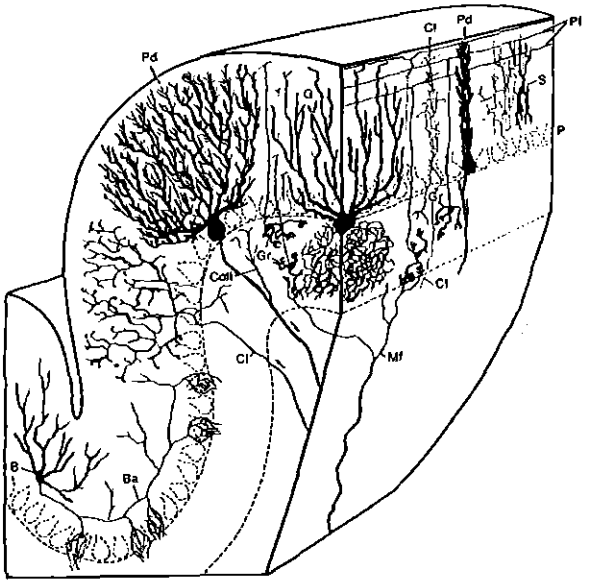

Fig. 1.5

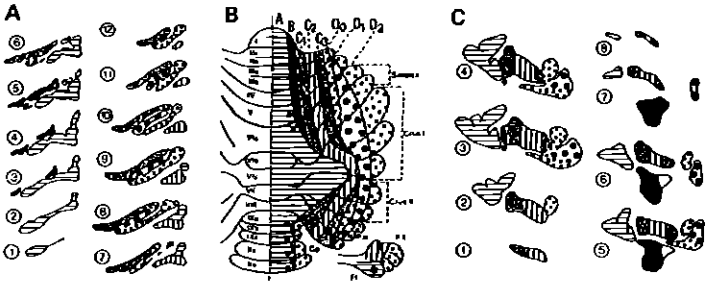

Fig. 1.6

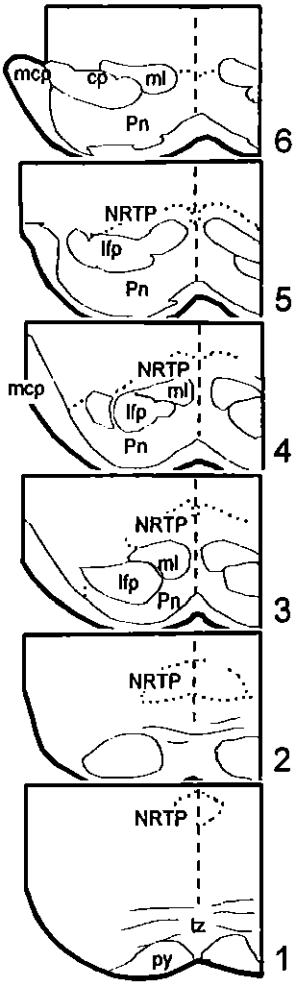
mcp
cp
ml
Pn
6
NRTP
lfp
Pn
5
mcp
NRTP
ml
lfp
Pn
4
NRTP
ml
lfp
Pn
3
NRTP
2
NRTP
tz
py
1

Fig. 1.7

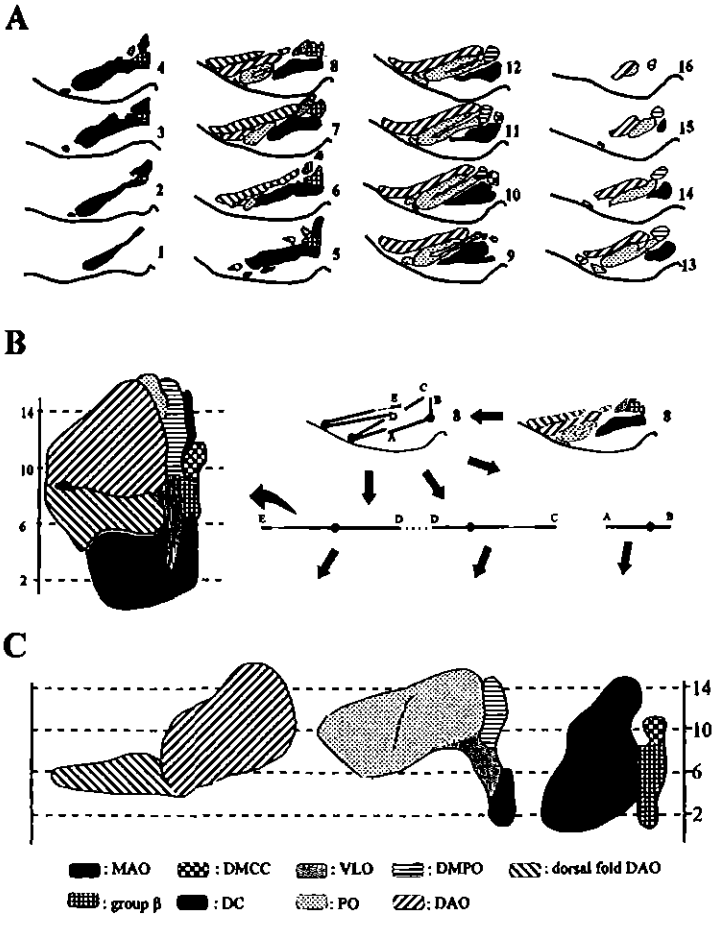

Fig. 1.8

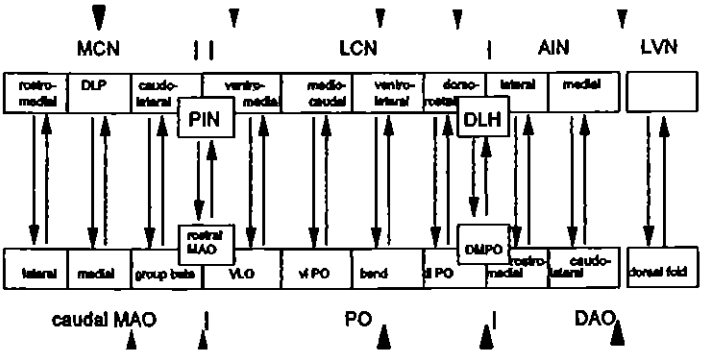
MCN
LCN
AIN
LVN
rostro-medial
DLP
caudo-lateral
ventro-medial
medio-caudal
ventro-lateral
dorso-rostral
lateral
medial
PIN
DLH
rostral MAO
DMPO
lateral
medial
group beta
VLO
vl PO
bend
dl PO
rostro-medial
caudo-lateral
dorsal fold
caudal MAO
PO
DAO

Fig. 1.9

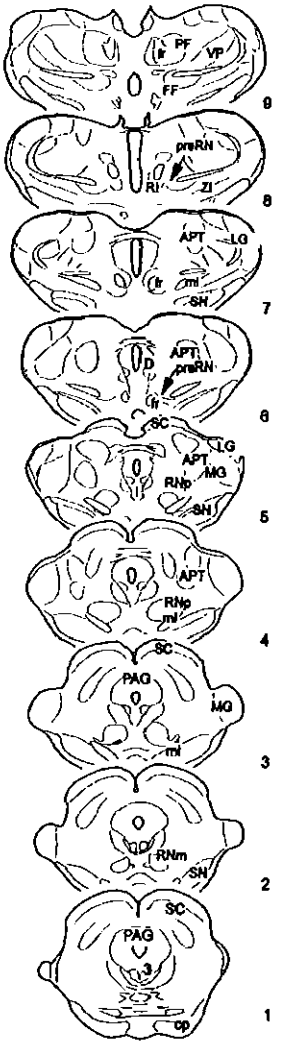
PF
VP
fr
FF
9
preRN
RI
ZI
8
APT
LG
fr
ml
SH
7
APT
D
preRN
fr
6
SC
LG
APT
MG
RNp
SH
5
APT
RNp
ml
4
SC
PAG
MG
ml
3
RNm
SH
2
SC
PAG
3
op
1

Fig. 1.10

CHAPTER 2:
TOPOGRAPHY OF CEREBELLAR NUCLEAR PROJECTIONS TO THE BRAIN STEM AND DIENCEPHALON IN THE RAT

T.M.Teune, J. van der Burg, J. van der Moer, J. Voogd and T.J.H. Ruigrok

Abstract

The organization of the cerebellum is characterized by a number of parallel and parasagittally ordered olivocorticonuclear modules. As such, the cerebellar nuclei basically function as output system of these modules. The present study aims to provide a comprehensive and detailed description of the organization of the connections from the cerebellar nuclei to the brain stem in the rat. Nineteen small injections with the anterograde tracer *Phaseolus vulgaris* leucoagglutinin or biotinylated dextran amine which were centered on various aspects of the cerebellar nuclear complex are described and are illustrated with serial plots detailing the distribution of labeled varicosities throughout the brain stem and diencephalon. In every case at least 1,000 and up to 36,000 varicosities were plotted.

All injections resulted in some or heavy labeling concentrated within specific regions of the contralateral inferior olivary complex and, usually, in some labeling of the contralateral ventrolateral thalamus. However, apart from these two areas it is shown that the cerebellar projections are generally very widespread and may be found throughout the entire brain stem and diencephalon. Below, only a survey of main projection areas will be given. Terminal arborizations originating from the rostral part of the medial cerebellar nucleus are mostly found in the caudal half of the brain stem with emphasis on the vestibular nuclear complex, whereas its caudal part rather connects to midbrain areas. Terminals that originate from the dorsolateral protuberance of the medial cerebellar nucleus are distributed more evenly throughout the brain stem and are mostly confined to reticular areas. The interstitial cell groups, interspersed between the medial and both interposed cerebellar nuclei, provide major projections to the ipsilateral vestibular nuclear complex and contralateral mesodiencephalic regions. However, reticular areas are also targeted over a large rostrocaudal range. The medial part of the posterior interposed nucleus sends most projections to the caudomedial red nucleus, prerubral regions and parvicellular reticular formation, all contralateral to the injection site. Projections that originate from more laterally placed injections are directed, apart from the inferior olivary complex, to the rostral half of the contralateral brain stem, where most labeled varicosities are found in the superior colliculus and zona incerta. The anterior interposed nucleus specifically targets the inferior olive, the red nucleus, the pontine reticulotegmental nucleus, the pretectum and the ventrolateral thalamic nucleus. More laterally placed injections also project to the ipsilateral parvicellular reticular formation and deep layers of the spinal trigeminal complex. The latter areas are more specifically targeted by the dorsolateral hump. In addition, its projections are found in the red nucleus and pretectum but do not seem to reach the ventrolateral thalamus. Projections from the lateral cerebellar nucleus are all characterized by a widespread distribution of terminals. Especially, the caudal aspect of the nucleus sends, apart from projections to the

deep mesencephalic nucleus, red nucleus, periaquaeductal grey, pretectum, prerubral area, and several thalamic regions, prominent projections to the caudal brain stem which terminate in the inferior olive and gigantocellular reticular formation. Projections from the ventral, parvicellular part of the nucleus are mostly, but not exclusively, directed to the rostral half of the brain stem and mainly terminate in the pararubral area, accessory oculomotor nuclei, pretectal areas, zona incerta, parafascicular thalamic nucleus and ventrolateral thalamic nucleus.

We conclude that the impact of the cerebellar nuclei on brain stem and diencephalon is widespread. Projections from different regions of the same cerebellar nucleus may show important differences in distribution of labeled terminals. On the other hand, injections placed in different cerebellar nuclei may result in a similar distribution of at least part of their terminal fields. Hence, complex divergence and convergence between and within the projections of individual cerebellar nuclei appear to be an essential characteristic of the cerebellar nucleobulbar organization.

Introduction

The cerebellum, a highly organized structure with a relatively simple architecture, is involved in motor control (Bloedel, 1992; Ito, 1984), cognition (Leiner *et al.*, 1986; Schmahmann, 1996; Thach, 1996), affection and visceral functions (Bradley *et al.*, 1987; Haines *et al.*, 1990; Nisimaru *et al.*, 1991; Waldrop and Iwamoto, 1991). To exert these different functions, the cerebellar cortical output is directed, via the cerebellar nuclei (CN), onto a large number of different brain stem nuclei (see Voogd, 1995) as has been studied in different species (rat: Chan-Palay, 1977; Faull, 1978; Faull and Carman, 1978; Voogd, 1995; cat: Voogd, 1964; monkey: Asanuma *et al.*, 1983a).

The output profile of the cerebellum is organized according to a modular pattern (Buisseret-Delmas and Angaut, 1993; Oscarsson, 1969; Tolbert *et al.*, 1978b; Voogd, 1964). A module consists of one or more parasagittally arranged strips of Purkinje cells that project onto a specific subdivision of the CN, both of which receive information from a specific part of the contralateral inferior olive (IO). These olivo-cortico-nuclear modules have been suggested to represent functional cerebellar units (Ekerot *et al.*, 1995; Oscarsson, 1979). In this way, different modules are thought to be involved in different tasks (Godschalk *et al.*, 1994; van der Steen *et al.*, 1994). As such, it would be expected that the output of these modules will reflect this functional heterogeneity.

However, to our knowledge, a detailed and comprehensive anterograde tracer study of the nucleobulbar projections in the rat is not available. Reports by Faull (1978) and Faull and Carman (1978) provide profiles of the distribution of nucleo-fugal projections, based on lesions and subsequent degeneration of the axons of the superior cerebellar peduncle (scp). Other investigations into the cerebellar nuclear efferents

only concerned parts of these projections, such as the projections of the CN to the IO (Ruigrok and Voogd, 1990), the red nucleus (Angaut and Cicirata, 1988; Daniel *et al.*, 1988), the nucleus reticularis tegmenti pontis (Angaut *et al.*, 1985a; Cicirata *et al.*, 1982) or the thalamus (Angaut *et al.*, 1985b; Haroian *et al.*, 1981). Only for the output of the lateral cerebellar nucleus an overview of all brain stem projections based on radioactive methionine tracing has been provided by Chan-Palay (1977). A survey of some of the main brain stem targets of the interface between the medial and interposed cerebellar nuclei was recently given by Buisseret-Delmas and colleagues (Buisseret-Delmas *et al.*, 1998).

This report aims to provide a comprehensive oversight of the nucleo-fugal projections in the rat, resulting from anterograde tracer deposits in different parts of the CN, thereby verifying and complementing results from the previously mentioned studies.

Materials and methods

Surgical techniques

Adult male purpose-bred Wistar rats were used in the present study, which was approved by the institute's animal experiments committee and adhered to the National Institutes of Health guidelines. In all, 85 animals, including animals that had been part of other studies (e.g. Ruigrok and Voogd, 1990; Teune *et al.*, 1999) were used to investigate the nucleobulbar projections.

Animals were anesthetized with a cocktail of ketamine (100 mg / kg i.p.) and thiazine-hydrochloride (3 mg / kg i.p.), which was supplemented with additional doses of ketamine when needed. The anesthetized animals were positioned in a Kopf stereotact according to guidelines by Paxinos and Watson (1986). A vertical, nuchal midline incision, with lateral spreading of the covering soft tissues, whereby the occipital bone was exposed and partially removed and followed by careful midincision and spreading of the covering dura, allowed access to the cerebellum. Guided by coordinates from Paxinos' atlas, and under continuous monitoring of the spontaneous electrical activity of the nervous tissue (see Ruigrok *et al.*, 1995b), a single barrel pulled glass pipette (tip diameter 10 - 14 μm) was advanced onto the CN, in caudorostral direction. Table 2.1 summarizes the location of the injection sites as well as the tracer used. In experiments labeled with "R", the pipette contained the plant lectin *Phaseolus vulgaris leucoagglutinin* (PhaL). In "T" labeled cases the pipette contained either biotinylated dextran amine (BDA) or PhaL. In some cases, both tracers had been injected in different parts of the CN of the same animal. PhaL (Sigma) had been dissolved in Tris-buffered saline (2.5%, in 0.05 M TBS, pH 8.4). BDA (List Laboratories, mol. weight 10.000) was used as a 10% solution in phosphate-buffered saline (10% in 0.05 M phosphate buffered saline, PBS, pH 7.2). Both tracers were applied iontophoretically (15 - 30 min., +2 - 8 μA, 7 sec. on/off cycle); specific data for each experiment are given in Table 2.1.

After depositing the tracer, the dura was reapposed, the soft tissues were sutured and the skin was closed with stainless steel surgical staples. Animals were allowed to recover from surgery for 6 to 7 days, during which they were monitored twice daily for any signs of discomfort or distress. Hereafter, they were deeply anesthetized with sodium pentobarbital (120 mg/kg i.p.) and transcardially perfused to fixate the brains. First, through an intra-aortic catheter, the cardiovascular system was cleared with 250 ml of a solution containing 0.8% NaCl, 0.8% sucrose and 0.5% d-glucose, dissolved in 0.05 M PBS, pH 7.2, which was followed by 1000 ml of a freshly prepared fixative, containing 2.5% glutaraldehyde, 0.5% paraformaldehyde and 4% sucrose in 0.05 M PBS, pH 7.2.

The brains were removed from the calvarinae, blocked, and kept in the fixative for postfixation for 2 hours at room temperature. To safeguard the tissue from cryoartefacts, the brains were submerged in 10% sucrose in 0.05 M PBS, pH 7.2, in the cold, over night. Next, the brains were embedded in gelatin (10-12% gelatin, dissolved in distilled water with 10% sucrose), which was allowed to set at room temperature and was hardened in 10% formaline with 30% sucrose, dissolved in 0.05 M PBS, pH 7.2, for 2 hours at room temperature. Finally, the embedded brains were stored at 4 °C in 30% sucrose in 0.05 M PBS, pH 7.2, until sectioning.

Immunohistochemical procedures.

Serial, transverse sections were cut at 40 μm thickness on a freezing microtome, and collected in 0.1 M PBS, pH 7.2 vials. To visualize PhaL containing structures, sections were incubated with a goat-anti-PhaL-antibody (1:4000, in 0.05 M Tris-buffered saline -TBST-, pH 8.4, with 0.1% Triton X-100; Vector) for 48 to 72 hours, in the cold under constant agitation. After several rinses with 0.05 M TBST, pH 8.4, sections were incubated with a rabbit-anti-goat antibody (1:200 in 0.05 M TBST, pH 8.4; Sigma) for 2 hours at room temperature. After several rinses with 0.05 M TBST, pH 8.4, sections were incubated with peroxide-anti-peroxidase (PAP, 1:400 in 0.05 M TBST, pH 8.4; Sigma). After a final series of rinses with 0.05 M PB, pH 7.2, sections were DAB-reacted to render a brown stained reaction product (37.5 mg DAB in 150 ml 0.05 M PB, pH 7.2, with 25 μl 30% for 30 to 45 minutes. The reaction was stopped with several rinses with 0.05 M PB, pH 7.2.

BDA processing consisted of overnight incubation of the sections in avidine-biotine-complex (1:100 in 0.05 M TBST, pH 8.4; ABC Elite Kit, Vector) at 4 °C under constant agitation. After several rinses with 0.05 M PB, pH 7.2, sections were reacted with DAB with cobalt chloride, to obtain a black stained product (75 mg DAB, in 150 ml 0.05 PB, pH 7.2, with 3 ml 1% $CoCl_2$, and 25 μl 30% H_2O_2) for 15 minutes at room temperature. With several rinses in 0.05 M PB, pH 7.2, this process was stopped.

All sections were mounted, air dried, counterstained with thionin, dehydrated through graded ethanol and xylene baths, and coverslipped with Permount.

Analysis and reconstructions

Sections were analysed with an Olympus microscope, equipped with a Lucivid™ miniature monitor, and using Neurolucida™ software. Experiments in which the tracer was confined to a subregion of the CN nuclei, without apparent spread to adjacent structures, were selected for reconstruction. At low magnification, the contours and delineation of main brain stem nuclei and fiber tracts were plotted of equally spaced sections (spacing 320 μm of levels rostral to the decussation of the scp and 640 μm of levels caudal to this point). Subsequently, at high magnification (objective 20x), the sections were systematically scanned and the position of all individual varicosities was digitized by mouse clicks. Varicosities in both PhaL and BDA labeled fibers have been implicated to reflect synaptic boutons (Wouterlood and Groenewegen, 1985; Wouterlood and Jorritsma-Byham, 1993) and thus represent the most likely sites where information is transmitted to postsynaptic structures. In this way, for every plotted section, both the positions and number of plotted terminals was determined with reasonable accuracy. Only in areas with a very dense labeling such as occurring in the CN projections to the inferior olive or red nucleus is it likely that the number of plotted terminals represents an underestimate of the actual number of labeled varicosities. The number of plotted varicosities and the analysed surface area of the analysed section were used to design a bulbar projection profile of a particular case. This profile indicates the relative amount of labeling along the rostrocaudal axis of the brain stem (e.g. see Fig. 2.8). Table 2.2, representing a survey of the results of all analyzed cases, was based on the computerized plots as well as on a supplement of the actual sections.

Nomenclature of most brain stem structures is mostly based on Paxinos and Watson (1986). For the nomenclature and the subdivision of the red nucleus and the medial region of the mesodiencephalic junction we have followed Ruigrok and Cella (1995). The nomenclature will be further considered in the discussion. Delineation of the rat CN was modified after Korneliussen (1968), also see Voogd (1995) and Ruigrok (Ruigrok *et al.*, 1995b; Ruigrok and Voogd, 1990).

Results

To warrant a comprehensive survey of the nucleobulbar projection that covers all parts of the CN, a selection of 19 experiments was made (out of 85 cases). Selection was based on the rostrocaudal or mediolateral position of the injection site within a specific part of the CN nuclei, whilst regarding the confinement of the tracer to this specific nucleus. The location of the injection sites was indicated in standardized transverse drawings of the CN (Fig. 2.2), and characteristics of the injections are listed in Table 2.1. The location of the injection sites was verified according to the inferior olivary labeling pattern (Ruigrok and Voogd, 1990).

Both BDA and PhaL injection sites appeared as rounded, well-defined deposits of tracer substance from

which labeled fiber bundles emerged. Within the brain stem these fiber bundles collateralized and showed terminal arborizations which carried many varicosities. The location of the varicosities was indicated in the plots. In accordance with a report on the similarity of BDA and PhaL-tracing (Wouterlood and Jorritsma-Byham, 1993), we noted no obvious differences in staining characteristics. However, based on the amount of labeled varicosities, BDA usually resulted in a smaller number of labeled terminal structures (Fig. 2.1), which most likely is related to the somewhat smaller appearance of the injection site. The results presented below will be illustrated with serial plots of actual sections and with the projection profiles which indicate the rostrocaudal levels of the brain stem that receive most prominent projections. An overview of the bulbar projections of all analysed cases is shown in Table 2.2.

Projections from the medial cerebellar nucleus

Five cases were selected with injections that were confined to various parts of the medial cerebellar nucleus (MCN: Fig. 2.2). Two of these cases, T199 and T195, were restricted to its rostral half. The injection in T199 was centered slightly medioventrally to that of case T195 which was rather centered at the juxtaventricular part of the nucleus. Two additional cases were placed in the dorsolateral protuberance (DLP): the injection of case R127 covered the lateral aspect of this conspicuous group of cells whereas in R128 the injection was placed in its medial part. Finally, the injection in case R100 covered the caudal aspects of the MCN. Together, they provide an impression of the targets of the entire nucleus.

T199

In this case a small BDA injection was centered on the ventrorostral part of the MCN. Serial plots indicating the brain stem areas with varicosities are shown in Fig. 2.3. A profile indicating the relative density of plotted varicosities in these analysed sections is shown in Fig. 2.8 and indicates that most labeling is found in the caudal half of the brain stem.

Within the contralateral inferior olivary complex some labeled terminal arborizations were found in the lateral aspect of the caudal-most part of the medial accessory olive (MAO). Sparse labeling was found in the lateral reticular nucleus (LRN). In this case, most conspicuous labeling was observed in the contralateral gigantocellular reticular nuclei (Gi), with a few varicosities extending into the medullary reticular nuclei and rostrally well into the lateral paragigantocellular nuclei of the medullary reticular formation, but terminal fields extended well into both the caudal (PnC) and oral (PnO) parts of the pontine reticular nuclei. Furthermore, both the ipsi- and contralateral superior (SVN), medial (MVN) and spinal vestibular nuclei (SpVN), as well as the ipsilateral lateral vestibular nucleus (LVN) contained labeled terminals. Within the vestibular complex most conspicuous labeling was observed bilaterally in the rostral ventral (magnocellular) MVN

and in the contralateral SpVN. Caudally, this labeling extended into the parasolitary nucleus.

The distribution of terminals to the mesodiencephalon was rather sparse. The deep mesencephalic nuclei (DpMe) and the lateral horn of the magnocellular red nucleus (RNm) contained a few labeled terminals. Within the ventromedial (VM), ventrolateral (VL) as well as the parafascicular nucleus (PF) some sparse thalamic projections were found.

T195

Here, the BDA injection was centered in the rostral juxtaventricular part of the MCN (Fig. 2.2) and resulting labeling is shown in Fig. 2.4. From these plots as well as from the projection profile shown in Fig. 2.8, it is obvious that most labeling was found in the caudal part of the brain stem.

The caudolateral MAO (not indicated) and subnucleus β contained a few labeled terminals. Main brain stem targets were the vestibular nuclei. In particular, the SVN, LVN and SpVN, and the rostral, magnocellular parts of the MVN were heavily labeled. Within the SVN, MVN and LVN, most labeling was found at the ipsilateral side, whereas the labeling in the SpVN was predominantly observed contralateral to the injected side. The latter labeling extended caudalwards into the parasolitary region. Within the reticular formation, both the ipsilateral and contralateral medullary reticular nuclei and the Gi showed some bilateral terminal labeling. However, within the pontine reticular formation labeling was restricted to the contralateral side. Some labeling was noted within and directly below the locus coeruleus of both sides (Fig. 2.4: level 10). As in case T199, the mesencephalon contained little labeling; some labeled terminals were found in the lateral horn of the magnocellular red nucleus.

Within the medial mesodiencephalic region varicosities were noted in the interstitial nucleus of Cajal (INC), and in the area surrounding the fasciculus retroflexus, such as the prerubral field, the rostral interstitial nucleus, the subparafascicular nucleus, and which have been collectively termed the area parafascicularis prerubralis by Carlton et al. (1982). Within the diencephalon, some labeling was noted ventrally in the VM and medially in the VL.

R127

In case R127, PhaL had been injected into the lateral aspect of the DLP region of the MCN (Fig. 2.2). Plots, shown in Fig. 2.5, as well as the projection profile (Fig. 2.8) indicate that a considerable part of the projection from this area is directed to more rostral brain stem areas.

In the IO, terminal labeling was found medially in the caudal MAO, but not in the adjacent subnucleus β. Although some labeling was observed in the caudal part of the contralateral reticular formation, most labeling was noted at more rostral levels. Labeling was especially dense in the parvicellular reticular nucleus (PCRt) but was also distributed to the dorsolateral Gi, as well as to dorsal and lateral part of the PnC and PnO extending into the pedunculopontine tegmental nucleus. Relatively few terminals were found in the vestibular

complex; only the SVN and the SpVN contained some labeled terminals. The ipsilateral projection to the SVN predominated over the contralateral projection. The deeper parts of the contralateral spinal trigeminal nucleus (the pars caudalis, the pars interpolaris and, to a lesser extent, the pars oralis) also were provided with input. Some labeling was also found in the nucleus reticularis tegmenti pontis (NRTP).

A small but significant projection to the parabrachial nuclei (PB) was found, ipsi- as well as contralateral to the injection site, with the contralateral projection predominating. In the midbrain, the DpMe received a strong projection from the DLP injection site, however, the red nucleus (RN) remained devoid of labeling. Heavy labeling was observed in the INC. Several additional regions such as the medial accessory oculomotor nucleus (MA3), the nucleus of the posterior commissure, and the prerubral region contained labeled terminals. In addition, varicosities were noted in the deep layers of the superior colliculus (SC).

In the diencephalon, terminals filled with PhaL were found in several nuclei such as the parafascicular nucleus, the central medial nucleus (CM) as well as in the VM, VL and posterior thalamic nuclear group (Po).

R128

This case also contained a PhaL injection that was centered on the DLP. However, compared to R127, the injection site was smaller, and rather covered the medial aspect of the cellgroup (Fig. 2.2). Nevertheless, the overall impression of the projection pattern was rather similar to that in case R127, although the relative amount of varicosities found in the midbrain is clearly less compared to case R128 (Fig. 2.8).

Although not shown in Fig. 2.6, some labeled terminals were found in the medial part of the caudal MAO. As in case R127, most obvious labeling was noted in the contralateral PCRt and Gi, but tended to be located more ventrally into the lateral paragigantocellular nucleus and extending more caudally in the medullary reticular nuclei compared to the former case. Also, the vestibular nuclei were only poorly provided with terminal arborizations, which mostly reached the contralateral SpVN. The contralateral parasolitary nucleus, however, contained a conspicuous amount of varicosities. In accordance with case R127 labeling was noted in the deep layers of the spinal trigeminal nucleus. Within the PB labeling was specifically noted contralateral to the injection site. In the pontine reticular formation the density of terminals was somewhat less compared to case R127. In the mesencephalic region, labeling was noted in the INC, in the DpMe and within several places in the periaquaeductal grey (PAG), however, not in the MA3. A few labeled terminals were found in the intermediate and deep layers of the superior colliculus.

The posterior thalamic group, the intralaminar thalamic nuclei, and the VM and VL showed labeled terminals resembling the distribution of varicosities in case R127.

R100

In this case, the injection of PhaL was centered on the caudal aspect of

the MCN, but ventral to the DLP. This particular case demonstrated a large yield of labeled varicosities which was distributed over the entire length of the investigated part of the brain stem (Figs. 2.7,2.8).

Within the contralateral IO labeled terminals were observed in the lateral-most aspect of the caudal MAO as well as in the ventromedial part of subnucleus β and possibly converging on the medial aspect of subnucleus c (Akaike, 1992). From Fig. 2.7 it is obvious that most prominent labeling was found in the medial part of the contralateral reticular formation at the rostral medullar and pontine levels. In the medullary reticular formation, labeling was mostly restricted to the dorsal part of the Gi where it appeared to be continuous with labeling in the nucleus prepositus hypoglossi (PrH). Labeling within the PnC was continuous with dense projections to the pontine central grey. Some ipsilateral projections to these areas were also noted. Labeling was virtually absent in the PCRt and spinal trigeminal complex. Relatively sparse labeling was observed in the vestibular complex on both sides of the brain. A more conspicuous projection to the contralateral parasolitary nucleus was in accordance with other cases of this series. The PB and pedunculopontine tegmental nucleus received a mostly bilateral projection. Furthermore, labeled fibers carrying varicosities reached dorsal and medial aspects of the NRTP and basal pontine nuclei (BPN).

The mesencephalon also contained numerous labeled terminals, mainly distributed to the contralateral DpMe, MA3 and PAG. Both the magnocellular and the parvicellular RN contained only a few labeled terminals. More dense terminal labeling was observed in the pararubral and prerubral regions, including the nucleus of Darkschewitsch, the area surrounding the fasciculus retroflexus, and the nucleus of the posterior commissure. In addition, labeling was noted in the deep and intermediate layers of the SC and extending into the pretectal regions. Ventral to the RN, some terminals reached into the ventral tegmental area (VTA).

The thalamus contained terminals in the VM, and in the intralaminar nuclei, with most abundant labeling in the PF. Additional labeling was observed in the fields of Forel (FF) which extended into the dorsomedial part of the zona incerta (ZI). In this series of MCN injections, this was the only case that demonstrated terminal labeling that reached the dorsal aspects of the hypothalamus.

Summary

From the plots shown in Figs. 2.3-2.7, also reflected in Table 2.2, and combined with the overview of the rostrocaudal projection profiles shown in Fig. 2.8, the following main conclusions may be drawn. The DLP (R127, R128) predominantly provides the lateral parts of the contralateral reticular formation (PCRt and lateral Gi) with input, and projects only sparsely to the vestibular nuclei. The caudal MCN (R100) sends projections to the medial reticular formation (Gi) including the PrH. Bilateral vestibular projections are at best characterized as moderate. In contrast, the rostral MCN (T195 and T199) project more impressively onto the vestibular nuclei;

more moderate projections were directed to the intermediate (mediolateral) levels of the reticular formation and to the lateral paragigantocellular nucleus. In addition, all MCN cases, supply afferents to brain stem areas at the meso- and diencephalic levels. However, these projections become increasingly more numerous when shifting from rostral MCN to DLP to caudal MCN, respectively (Fig. 2.8, Table 2.2).

Projections from the posterior interposed nucleus and the interstitial cell groups

Four injections were selected to characterize the projections from the posterior interposed nucleus (PIN). Selection of these cases was mainly based on differences in the mediolateral position of the injection site. The most medially placed injection (T82) involved the so-called interstitial cell groups that are interspersed between the MCN and both interposed nuclei (Buisseret-Delmas *et al.*, 1993). The injections in cases T79, T109 and T108 were placed at progressively more lateral levels but remained confined within the boundaries of the PIN.

T82

The BDA injection in this case was centered on the ICG, without any obvious involvement of either the MCN or the AIN (Fig. 2.2). This could be ascertained by the fact that virtually no terminal labeling was observed in the DAO, indicating that the medial AIN was not involved in the injection site (Buisseret-Delmas *et al.*, 1998; Ruigrok and Voogd, 1990). As shown in the plots of Fig. 2.9 and in the projection profile of Fig. 2.13, the projection pattern was more or less equally dispersed over virtually the whole length of brain stem. The only clear concentration of terminals was found in the lateral half of the central MAO. Further medullary labeling was noted in the contralateral Gi and paragigantocellular nucleus and in the ipsilateral vestibular nuclei which did not extend into the parasolitary nuclei. Some labeling was also noted in the NRTP and pontine reticular formation. In the mesencephalon projections were noted to the DpMe, the INC and the prerubral region. In the RN, especially its magnocellular and to a lesser extent its parvicellular part, displayed labeled varicosities that were mostly concentrated along the ventromedial contour of the nucleus. The ventral part of the zona incerta displayed several labeled terminals as did the PF. More pronounced labeling was noted in the FF, the VM, the Po, and scattered throughout the VL.

Projections originating from the ICG and terminating in the caudoventral RN, the dorsal NRTP, the INC, the VN (especially ipsilaterally) and the IO have recently been described by Buisseret-Delmas *et al.* (1998). Since the spinal cord was not investigated in this study, the potentially important projections from this area to the cervical cord could not be verified (Horn *et al.*, 1995).

T79

BDA had been injected medially in the more rostral parts of the PIN

without obvious involvement of either the ICG or AIN. When compared to the former case, the resulting projections may be characterized by the relative lack of labeling in the caudal brain stem (Figs. 2.10, 2.13). Olivary labeling was noted caudally in the rostral half of the MAO, at a level somewhat more rostral than in case T82. As can be observed from Fig. 2.10, only a relatively small amount of labeling was observed. In the medulla, besides the olivary labeling, only some varicosities were distributed to the contralateral PCRt. A more pronounced labeling was noted in the medial margin of the magnocellular RN. Additional projections were noted to the DpMe, the visual tegmental relay zone (VTRZ) and to part of the nucleus parafascicularis prerubralis located just dorsal to the fasciculus retroflexus (level 16 of Fig. 2.10). Unfortunately, rostral thalamic levels were not available for analysis.

T109

The tracer (BDA) had been injected into the central part of the caudal PIN (Fig. 2.2). The projections emanating from this injection were characterized by the virtual absence of labeling to the medulla (Figs. 2.11, 2.13). Only within the IO, a small, but dense patch of labeling was found within the rostral MAO. However, rostral sections of the brain displayed numerous labeled terminals. Abundant terminal labeling was specifically found in the DpMe, in the deep and intermediate layers of the SC, and in the dorsal part of the ZI. Furthermore, projections were noted to the VTRZ, the nucleus of the optic tract (level 17, Fig. 2.11), the PAG, the nucleus of Darkschewitsch (Dk), the FF, and the area surrounding the fasciculus retroflexus. Thalamic projections were mostly directed to the ventral lateral geniculate nucleus, the VM and to the VL.

T108

The injection site (BDA) in T108 was centered on the lateral aspect of the PIN (Fig. 2.2). In the IO, a dense patch of terminal labeling was found medially in the rostral-most tip of the MAO. As in case T109, other medullar areas remained devoid of labeling (Figs. 2.12, 2.13). A large part of the projections were directed to the SC where especially the deep and intermediate levels contained many labeled varicosities. Compared to the SC labeling observed in case T109, the lateral PIN project to distinctively more medial and rostral levels. Projections also reached the DpMe, the INC, the PAG, the nucleus of the posterior commissure, the Dk and, more sparsely, to the prerubral area surrounding the fasciculus retroflexus. The RN was virtually devoid of labeled varicosities. As in case T109, the ZI received a considerable projection, which extended into the ventral lateral geniculate nucleus. However, the terminal field was located slightly dorsal to that in case T109 (compare level 19 of Fig. 2.12 with level 20 of Fig. 2.11). In the thalamus, further terminal labeling was found in the VM and in the dorsomedial part of the VL.

Summary

The cases displayed in Figs. 2.9-2.12 and in the profiles of Fig. 2.13 demonstrate the effect of a shift in the mediolateral position of the injection site in the PIN. All four cases result in

terminal labeling in the IO, however, the mediolateral position in the PIN is transformed to an axis positioned from caudolateral to rostromedial in the rostral part of the MAO. Descending projections were only noted to originate from the ICG (to the contralateral reticular formation and ipsilateral vestibular nuclei). This case was furthermore unique in its projections to the NRTP. All cases showed contralaterally ascending projections. The medial part of the PIN projects specifically to the medial part of the RN whereas the central and lateral part of the PIN mostly project to the SC, DpMe and ZI. Only relatively small projections were noted to the prerubral regions and to the thalamic nuclei.

Projections from the anterior interposed nucleus

Two cases with a medially (R89 and T83) and one with a more laterally (R98) placed injection in the AIN were selected to illustrate the pattern of labeling arising from this part of the CN.

R89.

Here, the medial part of the rostral half of the AIN had been injected with PhaL (Figs. 2.2, 2.14). Although most fibers were directed to the contralateral ascending pathway, some scattered labeled varicosities were found in the ipsilateral vestibular nuclei, particularly within the SpVN, in the PCRt and, sparsely, within the spinal trigeminal complex. An abundant projection, however, was noted to the lateral part of the caudal DAO. At pontine levels, the contralateral NRTP and BPN contained labeled terminals. More distributed varicosities were noted in the PnO and pedunculopontine tegmental nucleus. The ventral part of the contralateral magnocellular RN contained a dense cluster of labeled terminals which extended somewhat into the parvicellular part of the nucleus. Projections were furthermore noted to the DpMe, the SC, the prerubral area, and the PAG. the labeling to the DpMe extended into the ventral part of the anterior pretectal nucleus (APT) where a significant projection was observed. In addition, labeling was noted in the posterior pretectal nucleus. In the diencephalon, both the dorsal and ventral parts of the ZI contained a fair amount of terminals. Furthermore, terminal labeling was observed in the PF, VM, VL, and laterodorsal thalamic cell groups (LD). Within the VL most labeling was found at the periphery of the nucleus.

T83.

In this case, a small BDA injection was also centered medially in the rostral AIN, but slightly lateral to that of R89 (Fig. 2.2). In the IO, terminal labeling was found laterally in the caudal DAO. In the rest of the brain stem only a single other cluster of dense labeling was noted (Figs. 2.15,2.19), which was specifically centered on the ventrolateral part of the magnocellular RN. Otherwise, the medulla, pons and mesencephalon were virtually devoid of any labeled varicosities, although some terminals were found in the NRTP and BPN (not present in the levels shown in the plots

of Fig. 2.15). Some varicosities were noted in the APT. At diencephalic levels, a small patch of labeling was noted in the ventrolateral ZI. In the thalamus, projections were mostly directed to the lateral and rostral margins of the VL.

R98

Case R98 was characterized by a PhaL injection that was centered on the lateral part of the AIN, however without involvement of the DLH (Fig. 2.2, also see below). Plots and projection profile are shown in Figs. 2.16 and 2.19, respectively. In contrast to T89 and T83, now an impressive number of labeled terminals was located in the medial part of the rostral DAO.

The ipsilateral medulla oblongata, in particular the PCRt and the deep layers of the entire spinal trigeminal nucleus, received a substantial projection from the lateral AIN. Some labeling extended into the subtrigeminal part of the LRN. Also, varicosities were noted ventrally in the LVN. At pontine levels, more abundant projections were noted to especially the contralateral NRTP and, to a lesser extent, the BPN. Also, some terminals were observed in the approximate location of the ipsilateral A5 noradrenergic group (Fig. 2.16, level 10). More rostrally, the dorsal half of the magnocellular RN contained a dense cluster of labeled terminals, which extended to the parvicellular part of this nucleus. The DpMe, intermediate layers of the SC, and the prerubral area only received a minor projection. A very prominent projection, however, was noted to the pretectal area, especially to the APT. A mediolateral band of labeled varicosities was furthermore found in the ventral ZI. Most labeling in the thalamus was found in the VL and PF, although some varicosities were noted in the PO, LD, and VM.

Summary

All injections centered on the AIN are characterized by major projections to the magnocellular part of the RN and to the DAO of the IO, which both obey a strict topography. The medial AIN connects to the ventrolateral RN and caudolateral DAO, whereas the lateral AIN projects to the dorsomedial RN and rostromedial DAO. Furthermore, the NRTP, APT and VL appear to be main targets of this cerebellar nucleus. Ipsilaterally descending projections to the ventrolateral reticular formation and adjacent deep layers of the spinal trigeminal nucleus specifically arise from the lateral AIN.

Projections from the dorsolateral hump

The dorsolateral hump (DLH) consists of a conspicuous cellular mass, which protrudes somewhat between the lateral parts of the interposed nuclei and the dorsomedial part of the lateral cerebellar nucleus. Two cases, T94-BDA and R138, were selected whose injections involved the DLH.

T94-BDA

In this case, the BDA injection was centered on the medial part of the DLH, incorporating the lateral-most part of the AIN (Fig. 2.2). Plots of this case are shown in Fig. 2.17. Within the

IO, dense terminal labeling was found bilaterally in the dorsomedial group (DM), which is usually considered a part of the principal olive (PO), e.g. (Buisseret-Delmas and Angaut, 1993), however, see (Ruigrok and Voogd, 1990). In addition, labeling was observed in the medial-most aspect of the DAO. As indicated in the projection profile a major part of the bulbar projection is directed to the caudal brain stem. Most of these terminal arborizations were found ipsilateral to the injection site within the PCRt and deeper parts of the trigeminal nuclei. However, a small contralateral projection was noted as well. Caudalwards, the ipsilateral projections at least reached the level of the pyramidal decussation. At pontine levels, many labeled varicosities were found interspersed between the principal and motor nuclei of the trigeminal complex (Fig. 2.17, level 11). Ventralwards these fibers appeared to reach the A5 noradrenergic cell group. Furthermore, pontine projections were noted contralaterally to the NRTP, bilaterally to the BPN and ipsilaterally to the PB.

Both the magnocellular and the parvicellular parts of the RN contained a few labeled terminals, predominantly in their dorsal and dorsomedial aspects. Dorsal to the red nucleus, terminal labeling was found in the DpMe which extended into the APT. Some terminals were noted in the VTRZ and in the prerubral area. In this case, the ZI was virtually devoid of varicosity-like labeling. In the thalamus, sparse labeling was observed in the VM, VL, and CM.

R138

The injection site in this experiment was located in the rostral part of the DLH, without obvious involvement of either the interposed or lateral cerebellar nuclei. The IO showed labeling which was mostly confined to the DM of the PO. From the projection profile (Fig. 2.19) it is obvious that in this case only a fraction of its connections was directed to levels rostral to the pons. In accordance with the pattern of labeling displayed in T94, several structures in the medulla oblongata and metencephalon, ipsilateral to the injection site, contained numerous labeled terminals. The medullary reticular nuclei (both ventral and dorsal subdivisions), the PCRt, and along the whole length of the spinal trigeminal nucleus, contained a prominent focus of labeled varicosities was noted. The projection to the PCRt also contained a small contralateral component. In this case, the distribution of labeled terminals at the pontine and mesencephalic levels was very similar to that noted in case T94-BDA. However, projections appeared to be more focussed on the VTRZ compared to the former case. Also, and in contrast with case T94-BDA, almost no labeling was noted in pretectal regions. At thalamic levels only sparse labeling was noted, medially in the Po and extending somewhat into the intralaminar nuclei (CM). No projection to the VL was observed.

Summary

The DLH is characterized by impressive ipsilaterally descending projections which are mainly directed to the lateral parts of the reticular

formation and adjacent spinal trigeminal nuclei. The corresponding subnucleus in the IO is found in the DM group which is targeted bilaterally (although with a contralateral preponderance). At mesencephalic levels, it appears that the DLH proper is directed to the dorsomedial-most regions of the RN, to the VTRZ and DpMe just ventral to the APT. Relatively sparse thalamic projections terminate medially within the Po and intralaminar nuclei without reaching the VL.

Projections from the lateral cerebellar nucleus

Five cases were selected to analyse the bulbar projections that originate from the lateral cerebellar nucleus (LCN). One injection covered the dorsal tip of the rostral LCN (T77), whereas others were centered on the ventral (T98, R178) and caudal (T94-PhaL, R133) aspects of the nucleus.

T77

In this case, a relatively small injection with PhaL was centered at the dorsal margin of the rostral half of the LCN, however, without involvement of the DLH (Fig. 2.2). This was corroborated by the observation that the olivary projection was restricted to the dorsal lamellae of the PO, without any labeling of the DM group (Fig. 2.20).

In the medulla oblongata, terminal labeling was distributed bilaterally. Apart from the olivary labeling, the most prominent projections were observed in the ipsilateral PCRt, which appeared reminiscent to the projections arising from lateral AIN and DLH, although they did not extend as far caudally. Labeled varicosities were also noted within the confines of the spinal trigeminal nucleus, especially within its oral part. At the pontine level a conspicuous input to the ipsilateral noradrenergic A5 area was also noted. Dense patches with varicosities were furthermore located within the contralateral NRTP. Some varicosities were noted in the dorsal raphe nucleus (Fig. 2.20, level 14).

In the mesencephalon, input was specifically noted to the DpMe and extending into the nucleus of the optic tract and caudal part of the APT. In the RN, most terminals were distributed within the dorsomedial aspect of its parvicellular part, extending somewhat into the VTRZ but more prominently into the prerubral region and FF. Within the ZI, only a few scattered varicosities were noted. Thalamic labeling was noted in the VM and caudomedial VL. More rostral levels, however, were not available for analysis.

T98

Here, the injection (BDA) was centered on the ventral aspect of the rostral LCN (Fig. 2.2). Within the IO, most prominent labeling was confined to the caudal-most aspect of the dorsal lamellae of the PO (Fig. 2.21). From the projection profile (Fig. 2.25) it can be seen that the major part of the projection is directed to the mesodiencephalic transition area (level 18-22 of Fig. 2.21). Within the medulla oblongata, only a few labeled terminals were found, mainly ipsilateral to the injection site, in the contralateral Gi and paragigantocellular reticular

nucleus. Some scattered varicosities were located in the ipsilateral SVN and MVN and extending into the PB. A more noticeable projection was directed to the contralateral NRTP and BPN.

In the mesodiencephalon, the ventral part of the parvicellular part of the red nucleus was densely labeled. In addition, many terminals were noted in a region covering the rostral parts of the MA3, and extending into the prerubral field and adjacent area surrounding the fasciculus retroflexus and incorporating FF. Terminal arborizations were furthermore noted in a band aligning the ventrolateral margin of the APT. Additional labeling was noted in the posterior pretectal nucleus. A major projection was observed in the dorsal part of the ZI. Within the thalamus the most prominent labeling was observed in the medial parts of the VL, but, in addition, also within the PF, VM and Po.

R178

In this case, a PhaL injection was also centered on the ventral part of the LCN, however at distinctively more caudal levels compared to case T98 (Fig. 2.2). In fact, the injection appeared to be completely confined to the parvicellular part of the nucleus. In the PO, the ventral part of the lateral bend of the PO was densely labeled in the contralateral IO. The ipsilateral IO also displayed a few corresponding labeled terminals. As can be discerned from Fig. 2.22 and the projection profile displayed in Fig. 2.25, the medulla oblongata showed no further labeling. The pons contained several structures with labeling contralateral to the injection site. Here, most distinct labeling was found in the caudal and dorsal boundaries of the NRTP, several patches in the lateral and medial parts of the BPN as well as a more scattered projection to the PnO and pedunculopontine tegmental nucleus.

Most terminals were directed to the mesodiencephalic region (Fig. 2.25). In contrast with former cases, virtually all projections also displayed a small ipsilateral component. Particularly abundant projections were noted to reach all layers of the SC, the DpMe, the dorsal part of the APT, the nucleus of the posterior commissure, the MA3 and the PAG. A conspicuous aggregate of labeling was noted directly lateral to the magnocellular part of the RN, which, more rostrally converged with projections to the lateral part of the parvicellular part of the nucleus. For this reason, the area directly lateral to the magnocellular RN has been designated as the pararubral area (Ruigrok and Cella, 1995). Labeling to the parvicellular RN extended into the prerubral region and FF, where a prominent projection was noted. Dense terminal fields were also observed in the dorsal part of the ZI, with some patches extending into its ventral part. At the lateral margin of the ZI, some labeled fibers entered the confines of the ventral lateral geniculate nucleus. The ZI projections were especially abundant at the more rostral levels of this area where, medially, the terminal fields included the VM. A very dense and salient patch of labeling was noted within the dorsal part of the PF. This terminal field extended into the medial parts of the LD group. More laterally within this

group some additional labeling was noted. Unfortunately, more rostral thalamic levels were not available for analysis.

Case R178 also displayed a definite projection to dorsal and lateral hypothalamic regions. A few labeled varicosities were observed in the mammillary nuclei (Fig. 2.22, level 15).

T94-PhaL

In this case, which also contained a BDA injection into the lateral AIN (described earlier as case T94-BDA), a PhaL injection was made dorsally in the caudal LCN bordering, but not involving, the DLH (Fig. 2.2). In the IO, the corresponding labeling remained confined to the ventral lamellae of the rostral PO without involvement of the DM group. Plots and the projection profile of this case are shown in Figs. 2.23 and 2.25, respectively.

At the medullary levels, this case was characterized by a strong projection to the contralateral Gi and paragigantocellular nucleus, extending ventrally into the region immediately dorsal to the inferior olive (into the ventral gigantocellular nucleus and nucleus gigantocellularis pars alpha of Jones, (1995), and medially to include the raphe nuclei. Some labeling was present in the ipsilateral PCRt and adjacent spinal trigeminal nucleus especially within its ventral margin. Projection patterns to the PnO, pedunculopontine tegmental nucleus, NRTP and BPN were very similar to those observed in case R178, however, projections were also noted in the PnC which appeared as a rostral continuation of the medullar Gi labeling. Patches with labeled varicosities were also seen laterally within the central grey of the pons. Also, some labeling was found in the ipsilateral noradrenergic A5 region.

As in the former case, a large contingent of labeled varicosities was observed at the mesodiencephalic transition area. Major projections were noted to the MA3, PAG, pararubral area, DpMe, and APT. Also, the prerubral region and area surrounding the fasciculus retroflexus were studded with labeled varicosities, extending into the FF, ZI, and nucleus of the posterior commissure. As such the terminal arborizations within these areas appeared to be of a more or less continuous nature. In the thalamus, labeling was found in the PF (both dorsally and medially), within the VM, LD, and, most prominently, within the caudomedial regions of the VL. Finally, as in case R178, the lateral and dorsal hypothalamic area received a projection.

R133

The last case to be described here received a PhaL injection that was located medially within the caudal LCN (Fig. 2.2). Plots and projection profiles are shown in Figs. 2.24 and 2.25. This injection resulted in labeling that, like case T94-PhaL, was confined to the ventral lamellae of the rostral-most part of the PO. The general pattern of other labeling in the medulla also was very similar to the former case, however, especially the labeling within the ventral Gi appeared less dense. Again, the labeled terminal fields were continuous with labeling in the PnC and PnO. Projections to the contralateral NRTP and BPN were also present. However, virtually no terminals were discerned within the A5

territory. At the mesencephalic level, considerable projections were noted to the MA3, DpMe, pararubral region, dorsolateral part of the parvicellular RN, deep and intermediate layers of the SC, APT, nucleus of the posterior commissure, and within the PAG. Rubral projections extended into the prerubral region and FF. Projections to the ZI mostly reached its ventral part. Within the thalamus, projections were observed to the PF, with extensions to labeled terminal arborizations in the CM, dorsal PO and LD groups. Furthermore, labeling was found in the VM, and medial VL. Some labeled fibers descended ventrally to provide some terminal arborizations to dorsal hypothalamic regions.

Summary

All injections that were confined to the LCN resulted in terminal labeling within the contralateral PO. Rostrodorsal parts of the LCN connect to the caudal aspect of the dorsal lamellae of the PO, whereas caudal and ventral LCN parts rather relate to the rostral area of its ventral lamellae. Medullary projections that originate from the LCN are mainly derived from its caudal parts and are specifically distributed to the ventral part of the Gi. All LCN levels provide projections to the NRTP, BPN and DpMe. Contrary to the other LCN cases, its dorsal part (T77) does not contribute to projections to the MA3, PAG, APT and SC. The parvicellular RN, as well as the prerubral region were targets in all LCN cases. However, the pararubral region only receives a prominent projection when the ventral or caudal LCN is involved in the injection site. These cases also provided a major output to the PF, LD and ZI and displayed terminals that reached hypothalamic areas. Labeling to VM and VL was observed in all cases. The number of plotted terminals within the VL, however, never exceeded 10% of the total number of plotted varicosities.

Discussion

Aim of this study

The cerebellar organization is characterized by the modular connectivity pattern between longitudinal strips of Purkinje cells, the cerebellar nuclei, and the inferior olive (Ruigrok, 1997; Ruigrok and Voogd, 1990; Voogd *et al.*, 1996b; Voogd and Ruigrok, 1997). Since the cerebellum appears to be involved in a large number of different functions, such as motor coordination, cognition, affective and visceral functions (e.g. see (Bloedel, 1992; Bradley *et al.*, 1987; Haines *et al.*, 1990; Schmahmann, 1996), it is to be expected that these different functions will be reflected in the projections of the target nuclei of the cerebellar modules. Presently, this view has been substantiated mainly in electrophysiological studies on the modulation of the oculomotor system by modules in the vestibulocerebellum and the visual vermis (Ekerot *et al.*, 1997; Godschalk *et al.*, 1994; van der Steen *et al.*, 1994), the adaptation of limb movements by the C1 and C3 zones of the anterior lobe (Ekerot *et al.*, 1997; Gibson *et al.*, 1987) and on the eyeblink conditioning of the C3 zone of the simple lobule (Steinmetz and Sengelaub, 1992). A detailed map of the brain stem and diencephalon

projections that originate from (parts of) the individual CN, which serve as the output stations of the modules, should be able to corroborate such a view. However, a comprehensive overview of cerebellar nuclear projections to the brain stem does not appear to be available. Here, we present such a overview of the output patterns of the individual CN in the rat as studied with modern anterograde tracing techniques that allow the application of minute amounts of tracer in well circumscribed parts of the CN.

Classically, cerebellar output is known to reach the brain stem through either the scp or via the uncinate or direct fastigiobulbar tracts which specifically originate from parts of the MCN (Voogd, 1995). An earlier comprehensive report on the terminations of (parts of) the scp, using lesion induced degeneration, was provided by Faull (1978) and by Faull and Carman (1978). They showed that the scp basically distributes fibers to three different pathways, i.e. a contralateral ascending path, and two descending pathways, one ipsilateral and one contralateral. The contralateral ascending tract moves rostrally from the decussation of the scp up to the diencephalon. Its terminal fields were found to involve the red nucleus, the oculomotor nucleus and the accessory oculomotor nuclei, the superior colliculus, the periaquaeductal grey, the mesencephalic reticular formation (deep mesencephalic nucleus), and various parts of the thalamus. The ipsilateral descending pathway runs ventrally from the scp at the level of the trigeminal motor nucleus, turns caudally and terminates within the parvicellular reticular nucleus. The contralateral descending tract proceeds caudally from the scp decussation and runs in the ventromedial region of the magnocellular reticular formation of the pons and medulla. Terminals arising from its fibers were found to terminate in the NRTP, the BPN, the IO, and throughout the pontine and medullar reticular formation (Faull, 1978). The, crossed, uncinate and, uncrossed, direct fastigiobulbar tracts provide projections to the vestibular and reticular nuclei.

Since, in the present study, varicosities rather than the axons were plotted, we charted the presumed sites of synaptic transmission (Wouterlood and Groenewegen, 1985) and did not attempt to provide new information on the fiber trajectories.

Below, we will briefly discuss our results in relation to existing literature on CN projections to the brain stem and diencephalon in the rat.

Cerebellar projections to the rat brain stem

Medulla oblongata

Projections to the inferior olive

The inferior olive (IO), located in the ventromedial medulla oblongata, is the only source of climbing fibers (Desclin, 1974), and, apart from afferents from the CN, receives input from many different sources in the brain stem and spinal cord (see (Ruigrok and Cella, 1995) for details).

The topography of the nucleo-olivary projection adheres closely to

the modular organization of the cerebellum, as has been pointed out in several species, and also in the rat (Angaut and Cicirata, 1982; Angaut and Sotelo, 1987; Buisseret-Delmas and Angaut, 1993; Haroian *et al.*, 1981; Ruigrok, 1997; Ruigrok and Cella, 1995; Ruigrok and Voogd, 1990). Our results are in accordance with the pattern established by Ruigrok and Voogd (1990). In fact, this pattern often could be used to verify the exact boundaries of the injection sites. Basically, the LCN projects onto the PO, the AIN onto the DAO, the PIN onto the rostral MAO, the MCN connects with the caudal MAO, and the DLH projects to the dorsomedial group of the PO (see Ruigrok and Voogd, 1990). In addition, the latter study also established that distinct topographical relations can be established between parts of the individual CN and the related IO subnuclei. These relations could be verified by the present study (e.g. compare the projections from the medial AIN to the caudolateral DAO in cases T83 and R89 and the projections from the lateral AIN to the rostromedial DAO in cases R98). Involvement of more than a single subnucleus in the injection site revealed itself as additional labeling in several of the IO subnuclei. A clear example is case T94-BDA where the injection covered the lateral-most aspects of the AIN but also involved the DLH. Within the IO dense terminal labeling was observed in the medial-most aspect of the DAO as well as of the DM group of the PO.

Projections to the lateral reticular nucleus

The lateral reticular nucleus (LRN) is an important source of cerebellar mossy fibers. It is suggested to be involved in the control and coordination of motor activity (Arshavsky *et al.*, 1978; Ekerot, 1990; Koekkoek and Ruigrok, 1995). Its efferents project both to the cerebellar cortex and provide collaterals to certain parts of the CN (Chan-Palay, 1977; Hrycyshyn *et al.*, 1982; Ruigrok *et al.*, 1995a; van der Want *et al.*, 1987). The LRN receives its input from the spinal cord (Cella *et al.*, 1991; Flumerfelt *et al.*, 1982; Hrycyshyn and Flumerfelt, 1981), but also from several supraspinal centers such as the contralateral red nucleus (Corvaja *et al.*, 1977; Hinman and Carpenter, 1959; Qvist *et al.*, 1984) and the MCN (Walberg and Pompeiano, 1960); for a review, see (Ruigrok and Cella, 1995).

Our material only contained one case (T199), with an injection of the juxtaventricular part of the MCN, which displayed terminal labeling in the rostral part of the contralateral LRN, including the subtrigeminal part. The latter projection appears to be rather small, which contrasts with data in the cat (Walberg and Pompeiano, 1960), in which a rather impressive projection was demonstrated to originate from the rostral third of the nucleus. Presently, it is not clear whether this difference may be method-related (i.e. degeneration study or anterograde tracing) or represents a species difference. In addition, one other area was found that supplied sparse but definite projections to the LRN. Case R98, with an injection centered on the

lateral AIN, showed projections to the subtrigeminal region of the ipsilateral LRN. In the same area, a very scant projection was noted after an injection in the medial AIN (case R89). Nevertheless, it would appear that in the rat, the role of the LRN as an integrator or relay nucleus of spinal and supraspinal input does not critically depend on a major direct feedback from the CN.

Projections to the trigeminal nuclear complex

Although the trigeminal complex is not restricted to the medulla, it will be regarded here as a whole. It basically consists of a motor part and of a sensory part. The motor trigeminal nucleus is involved in mastication and control of jaw movement (Travers, 1995). The sensory trigeminal nucleus is subdivided in three main groups: the mesencephalic nucleus, the principal sensory nucleus which is located at the metencephalic level, and a spinal trigeminal nucleus which itself consists of an oral, interpolar and caudal part which all receive their main input from the trigeminal nerve. Efferents of the sensory parts of the trigeminal nucleus are directed to various parts of the brain stem, such as the reticular formation of the pons and mesencephalon, and the thalamus but also reach the cerebellum either directly by way of trigemino-cerebellar projections or indirectly by way of e.g. trigemino-olivo-cerebellar pathways (Huerta *et al.*, 1983; Jacquin *et al.*, 1989; Van Ham and Yeo, 1992).

Here, we show that parts of the CN project to the deeper regions of all divisions of the ipsilateral sensory trigeminal nucleus, including the principal nucleus. In particular, the dorsal and caudal aspects of the LCN (T77, R133, T94-PhaL), the DLH (R138) and the lateral AIN (T94-BDA and R98) display terminal fields that, though mainly covering the adjacent parvicellular reticular formation, extend into the adjacent region of the trigeminal nuclei. The DLP (R128, R127) projects to the deeper parts of the contralateral trigeminal nuclei. The PIN does not project to this nuclear complex. Projections from the LCN to the ipsilateral trigeminal complex were already described by Chan-Palay (1977) and Woodson and Angaut (1984), however, the projections to its motor nucleus could not be confirmed in our study. The projections of the CN to the sensory trigeminal complex evidently may present a pathway influencing the processing of sensory information from the face.

Projections to the vestibular, prepositus hypoglossal, and parasolitary nuclei

The vestibular nuclei (VN) are composed of four main parts, the lateral, the medial, the superior and the spinal vestibular nuclei (Rubertone *et al.*, 1995b; Voogd *et al.*, 1996b). The VN are involved in maintaining equilibrium and balance, and in the control of eye movements. Input, apart from the vestibular nerve, arises from the spinal cord, the CN and vestibulocerebellum and areas in the mesodiencephalon and cerebral cortex (Rubertone *et al.*, 1995b).

Our data demonstrate conspicuous and essentially bilateral projections from the MCN to most of the vestibular

nuclear complex. Most prominent vestibular projections arise from the rostral MCN (T195), and are distributed symmetrically. The caudal aspect of the MVN only receives a very minor projection. The vestibular projections from the DLP are essentially restricted to the contralateral SpVN (cases R127 and R128). These data agree well with a recent study on the fastigiovestibular projection in the rat by Omori and colleagues (Omori *et al.*, 1997) and confirm and elaborate on reports based on various animal species as reviewed by Rubertone *et al.* (1995b). The ICG was found to project to all components of the ipsilateral VN. Only some occasional varicosities were found in the ipsilateral VN after injections in the AIN, DLH or, in some cases, the LCN (e.g. R89, R98, T83, R138, T98). Projections from the interposed nuclei to the ipsi- as well as to the contralateral VN complex of the rat were recently described by Compoint *et al.* (1997).

The caudal MCN provides a major projection to the contralateral nucleus prepositus hypoglossi (R100), which is known to be intimately linked with the oculomotor and vestibular system but also provides a mossy fiber input to the cerebellum (for review see Rubertone *et al.*, 1995b). MCN projections to this nucleus have been described earlier in the cat by Walberg *et al.* (1962). More recently, modest bilateral prepositus projections from the caudomedial part of the MCN have been described in the rat by Omori *et al.* (1997). In addition to the MCN afferents, occasional varicosities in this nucleus were also noted in case T94-PhaL (injection in caudal LCN).

All MCN injections but in particular case R100, resulted in a very dense and conspicuous patch of labeling in the contralateral parasolitary nucleus, which is consistent with data in the monkey (Batton *et al.*, 1977) and the cat (Walberg *et al.*, 1962). The parasolitary nucleus provides the subnucleus β and the DMCC with an inhibitory vestibulo-olivary projection (Barmack *et al.*, 1993).

We conclude that cerebellar nuclear projections to the VN complex and prepositus hypoglossi originate from several subdivisions of not only the MCN but, more sparsely, also from other nuclei. Projections to the parasolitary nucleus only originate from the contralateral MCN.

Projections to the medullar reticular formation

Although the reticular formation refers to the netlike structure of cells and fibers that extends throughout the medulla, pons, and mesencephalon of the brain stem (Cajal, 1911; Jones, 1995), we will first focus on the projections to its medullar part. In the present study, a medial gigantocellular cell field (Gi) that includes the paramedian reticular nucleus, the ventral gigantocellular nucleus and the gigantocellular nucleus pars alpha, and a laterally located parvicellular cell field (PCRt) including the intermediate reticular field were delineated, as well as a lateral paragigantocellular reticular field (LPGi) which is located directly dorsolateral to the IO and rostral to the LRN. The reticular neurons give rise to long descending projections to the spinal cord, and to ascending projections to the mid- and

forebrain. They tend to collateralize extensively (for review see Jones, 1995).

Labeling in Gi was noted in all cases with injections centered on the MCN (R100, R127, R128, T195, T199), ICG (T82), and caudal LCN (T94-PhaL, R133). Efferents from the caudal aspects of the MCN (R100) were noted in its dorsal aspects, whereas the DLP (R127, R128) and rostral MCN (T195, T199) rather supplied fibers to progressively more ventral regions of the Gi. DLP projections tend to terminate more lateral compared to the projections from the rest of the MCN. Reticular projection from the DLP were more numerous in the rostral part of the medulla (and continuing into the pontine regions), whereas the rostral MCN mostly reached rather more caudal medullary levels. Dense projections from the caudal LCN were mostly found in the medial and ventral aspects of the Gi. Here, overlap with the projections from the MCN is likely to occur. All projections to the Gi were essentially contralateral with at best only a very sparse ipsilateral component (with the exception of case T195, in which a considerable projection to the ventral part of the ipsilateral Gi was noted). Labeling from the LCN (especially from its caudal part), and to a lesser degree from the ICG and MCN, to the ventral Gi usually extended somewhat into the LPGi. Although the projections to the Gi are mostly contralateral, the CN terminations in the PCRt were found to be mostly ipsilateral. They belong to the projection area of the uncrossed descending limb of the scp, which was already described by (Cajal, 1911). Especially the caudal and dorsal LCN (T94-PhaL, R133, T77), the DLH (T194-BDA, R138) and lateral AIN (R98) provide input to the PCRt with a clear ipsilateral preponderance. Most labeling is usually found at the transition area with the sensory trigeminal nucleus (see above). These data confirm earlier studies on the origin of the uncrossed descending limb in the rat (Achenbach and Goodman, 1968; Bentivoglio and Molinari, 1986; Chan-Palay, 1977; Mehler, 1967; Rubertone *et al.*, 1990; Woodson and Angaut, 1984). Contralateral PCRt projections without an ipsilateral component were noted after injections in the DLP (R127, R128) and medial PIN (T79) as mentioned earlier by Bentivoglio and Kuypers (1982), Rubertone *et al.* (1990) and Shammah-Lagnado *et al.* (1992).

We conclude that the various subdivisions from the medullar part of the reticular formation may receive input from multiple sources of the CN.

Metencephalon

Projections to the reticulotegmental and basilar pontine nuclei

The nucleus reticularis tegmenti pontis (NRTP) and the basilar pontine nuclei (BPN) are major sources of cerebellar mossy fiber afferents (for review see Ruigrok and Cella, 1995). The NRTP receives input from the CN, from the cerebral cortex, and from a number of brain stem areas such as the superior colliculus, the VTRZ, and the reticular formation (Angaut *et al.*, 1985a; Ruigrok and Cella, 1995; Torigoe *et al.*, 1986a; 1986b).

In accordance with earlier studies it was noted that most cerebellar nuclear regions project to the contralateral NRTP. Only when the injections were centered on the rostral MCN (T199, T195) or PIN, none or only very few varicosities were noted in this area. This observation is in accordance with earlier studies in various species (opossum: Yuen *et al.*, 1974, cat: Brodal *et al.*, 1972b, rat: Torigoe *et al.*, 1986a; 1986b; Watt and Mihailoff, 1983a, monkey: Asanuma *et al.*, 1983a). The ipsilateral NRTP only receives a small projection in several cases with injections centered on the LCN (R133, T94-PhaL). Most abundant projections are found after injections in the caudal MCN (T100), lateral AIN (R98) and LCN. (e.g. T94-PhaL). AIN/DLH projections tend to be located centrally to the LCN derived labeling. Projections from the caudal MCN or DLP appear to terminate in more medial and caudal aspects. In general, the basic organization of the cerebellar projection to the NRTP is in accordance with earlier descriptions that were based on autoradiographic tracing (Angaut *et al.*, 1985a; Cicirata *et al.*, 1982). In support of findings in the cat by Gerrits *et al.* (1984b), we found no support of the zonal or columnar organization as proclaimed by Brodal and collaborators (Brodal *et al.*, 1972b).

Most LCN centered injections supply multiple patches of terminal arborizations to the BPN. These patches, usually elongated in the rostrocaudal direction, are noted in medial and lateral parts of the BPN (T94-PhaL, R178, R133). Patches derived from injections centered on the lateral AIN and DLH (R98, T94-BDA, R138) were located at intermediate positions. As far as the MCN is concerned, only case R100 resulted in some labeling in the rostromedial part of the BPN which extended from labeled patches in the overlying NRTP. All projections are essentially contralateral with no or only a very small ipsilateral component. Basically, these results are in line with earlier reports (Angaut *et al.*, 1985a; Ho and Leong, 1977; Watt and Mihailoff, 1983a), however, a zonal organization, as suggested by Ho (Ho and Leong, 1977), was not noted.

In conclusion, it can be stated that, apart from the PIN, all CN supply afferents to the NRTP. However, within each cerebellar nucleus large variations may occur with respect to the actual contribution to these projections (e.g. caudal versus rostral MCN, lateral versus medial AIN).

Projections to the pontine reticular formation

The pontine reticular formation is usually divided in a caudal part (PnC), located directly dorsal to the level of the superior olive and trapezoid body, and in an oral part (PnO), located directly dorsal to the BPN. Interspersed between the PnC and PnO medially and the motor nucleus of the trigeminal complex caudally and the nuclei of the lateral lemniscus rostrally, the subcoeruleus has been identified as a rostral continuation of the intermediate reticular field of the medulla (Jones, 1995). The cerebellar connections to these reticular areas do not appear to strictly adhere to these boundaries. Injections centered on the MCN and LCN usually demonstrate

sparse to moderately dense labeling mainly in the contralateral pontine reticular formation. Terminal arborizations from the caudal part of the MCN (R100) extend rostral to the abducens nucleus along the midline (thus incorporating the pontine raphe nuclei). Projections from the DLP (R127, R128) are located more laterally. Projections from the LCN (R178, R133, T94-PhaL) show some overlap with the caudal MCN projection but terminate preferentially in the lateral aspects of the PnC and PnO, and in the subcoerulear area. These observations are in accordance with retrograde tracing studies by Gonzalo-Ruiz and collaborators (Gonzalo-Ruiz and Leichnetz, 1987; Gonzalo-Ruiz *et al.*, 1988).

The medial and intermediate parts of the pontine tegmental fields (i.e. PnC, PnO and subcoeruleus) are involved in postural and level setting functions and in premotor functions, respectively (Holstege, 1995). The pontine raphe nuclei and the adjacent medial pontine paramedian reticular formation serve as premotor centers for saccades. The projection of the caudal MCN to these areas strongly resembles the projection of the oculomotor region of the fastigial nucleus in the macaque monkey as described by Noda (1991).

Projections to the pontine central grey matter

Both the caudal MCN (R100) and the caudal LCN (T94-PhaL) supply terminals to the contralateral pontine central grey matter. The LCN projections take up a position somewhat lateral to those originating from the MCN. Sparse ipsi- or bilateral projections were noted in case R178, and in some cases that involve the PIN (T79, T109) or ICG (T82).

Projections to the parabrachial nuclei

The parabrachial nuclei relay visceral information from the nucleus of the solitary tract to the forebrain and as such are thought to function as an interface between reflexes executed at the medullary level and forebrain behavioral and integrative regulation of the autonomic system (Saper, 1995). Most prominent cerebellar projections were noted in the contralateral parabrachial nuclei and originated from the caudal MCN (R100) and DLP (R127, R128). Sparse projections from the ipsilateral dorsal LCN and/or DLH were noted in cases T94-PhaL, T77 and R138.

Apart from the projections to the parabrachial nuclei, it was noted that in the same cases a conspicuous afferent projection was noted to the areas located between the motor and principal sensory nucleus of the trigeminal complex (intertrigeminal nucleus: Paxinos and Watson, 1986) on the same side, especially to cells located between the efferent fibers of the motor nucleus of the trigeminal nerve. In this region the noradrenergic cells of the A5 group are located, which have been suggested to provide a descending input to the preganglionic sympathetic cells groups (Saper, 1995).

Hence, these results suggest that not only the MCN but also the LCN and/or DLH may be involved in cerebellar control of autonomic

processes (Tong *et al.*, 1993; Waldrop and Iwamoto, 1991).

Mesencephalon

Projections to the red nucleus

The red nucleus (RN), generally considered as a premotor structure, forms an outstanding globular cell mass, bilaterally located in the mesencephalon. In the rat, like in most mammals, it can be divided into a caudal, magnocellular part (RNm) and a rostral, parvicellular part (RNp); (Reid *et al.*, 1975b; Ruigrok and Cella, 1995; ten Donkelaar, 1988). In this species, however, the rostral pole of the RNp is difficult to identify and the nomenclature of this region has given rise to much confusion. Usually, it is located at a level where the fasciculus retroflexus enters the interpeduncular nucleus (Paxinos and Watson, 1986; Ruigrok and Cella, 1995). In primates, the RNp extends more rostrally, where it is traversed by the fasciculus retroflexus. Moreover, the origin of the rubrospinal and -bulbar tracts in this group of animals appears to be mostly restricted to the caudal magnocellular division of the nucleus, whereas the RNp gives rise to an uncrossed projection to the IO (Huisman *et al.*, 1982; Kennedy, 1990; Kennedy *et al.*, 1986; Kneisley *et al.*, 1978; Kuypers and Lawrence, 1967). A similar situation exists in the cat, where a relatively small, parvicellular division of the red nucleus, traversed by the fasciculus retroflexus was found to project to the olive, whereas the major, caudal portion of the red nucleus gives rise to the rubrobulbar and -spinal tracts (Huisman *et al.*, 1982; Onodera, 1984). In the rat, the entire RN gives rise to the crossed projection to the brain stem and spinal cord via the crossed rubrobulbar and rubrospinal tracts, respectively. and the region surrounding the fasciculus retroflexus, which gives rise to descending projections to the IO usually is not included in the red nucleus (Carlton *et al.*, 1982; Huisman *et al.*, 1981; Ruigrok and Cella, 1995; Rutherford *et al.*, 1984). Authors who described such projections of the rat RNp to the olive probably included this region in the RNp (Swenson and Castro, 1983a; 1983b). In the rat, the rubrospinal tract has been shown to emit collaterals to the cerebellum (Huisman *et al.*, 1983). A rubrothalamic projection has furthermore been described by Condé and Condé (1980) in the cat and by Roger and Cadusseau (1987) in the rat.

The cerebellar input to the RN in the rat has been extensively studied using autoradiographic anterograde and WGA-HRP retrograde tracing by Angaut and collaborators (Angaut *et al.*, 1986; Angaut and Cicirata, 1988; Angaut *et al.*, 1987; Daniel *et al.*, 1988; 1987). Our results are in general agreement with their observations. Basically, the AIN projects to the RNm, the LCN to the RNp. Within these projections a topographic arrangement is noted such that the medial AIN projects to the ventrocaudal-most part of the RNm, whereas the lateral AIN supplies afferents to more dorsal and rostral parts (e.g. compare cases T89 and R98). It should be noted, however, that the terminal fields that arise from injections centered on the AIN also invade the RNp. This agrees with the idea that the distinction between the

RNm and RNp is not very strict in the rat and in any case may not reflect the distinction between both RN parts made in primates (for review see: Ruigrok and Cella, 1995). The DLH projects to the dorsomedial part of the RN (T94-BDA and R138). According to Angaut and Cicirata (1988), the rostral part of the LCN connects to the ventromedial part of the RNp and the caudal LCN to more lateral regions. Although the present results generally agree with this scheme, our injections are separated in a more dorsoventral direction: dorsal LCN projecting to medial RNp and ventral LCN to lateral RNp (e.g. T77 and R178, respectively). In addition, it was noted that the RNp projections that originated from the ventral and caudal areas of the LCN (cases R133, R178 and T94-PhaL) extended caudalwards to the area located just lateral to the RNm. This region, which is generally incorporated in the DpMe, was designated as the pararubral region by Ruigrok and Cella (1995). Projections to roughly the same area were also noted in case R100 with an injection centered on the caudal MCN. In addition to the RN projections from the AIN, DLH and LCN, projections from the medial PIN to the medio-ventral margin of the RN (T79) were observed (Daniel *et al.*, 1987). Furthermore, a small but distinct projection from the MCN was noted to the lateral horn of the RN (T199, T195).

It can be provisionally concluded that both the AIN and all parts of the LCN have access to rubrospinal and rubrobulbar neurons in the RNm and the RNp. Rubrospinal and rubrobulbar neurons in RNp differ from the RNm in their afferent connections. In the rat, they receive projections from the cerebral cortex, the zona incerta and the posterior nucleus of the thalamus. These connections are lacking in the RNm. It is not known, however, whether the rubrospinal and rubrobulbar projections from the two divisions of the RN also differ in other properties. Similarly, it has not been established whether the target neurons of the PIN, located along the medial border of the RN and the target neurons of the MCN in the lateral horn of the RN, share the same properties with the rest of the RN neurons. Finally, the connections of the pararubral area, which is one of the main targets of the ventral LCN and PIN, remain largely unknown (Newman, 1985b).

Projections to the superior colliculus

The superior colliculus (SC) integrates input derived from a large variety of sources (e.g. see Cadusseau and Roger, 1985). The superficial layers are involved in relaying visual input, whereas input concentrated in the deep layers is polymodal and involves sensory, limbic and motor information (Cadusseau and Roger, 1985). As noted by others, all CN send projections to mostly the intermediate and deep layers of the SC (Gonzalo-Ruiz and Leichnetz, 1987; Kurimoto *et al.*, 1995). A difference in participation of the different subnuclei is noted in the literature: both the MCN (Gonzalo-Ruiz and Leichnetz, 1987; Gonzalo-Ruiz *et al.*, 1990), PIN and LCN (Kurimoto *et al.*, 1995) are claimed as suppliers of the majority of terminals. In our series, the deep layers of the

SC received the most prominent cerebellar input, but the terminal ramifications usually extended into more intermediate layers. These projections originated from injections centered on the caudal MCN and DLP (cases R100, R127, R128), on the lateral PIN (T108, T109), on the lateral AIN (R98) and on the caudal and ventral LCN (R133, T94-PhaL, R178). Projections from the AIN and particularly from the LCN may advance into more superficial levels (e.g. R178). These results agree well with the retrograde labeling in the CN from the SC by Bentivoglio and Kuypers (1982), Gonzalo-Ruiz and Leichnetz (1987), Lee *et al.* (1989) and with a recent study by Kurimoto *et al.* (1995). Although a specific topographical arrangement could not be discerned in our material, the latter authors showed that parts of different CN may supply afferents to the same general region of the SC.

Projections to the deep mesencephalic nucleus

The deep mesencephalic nucleus (DpMe) forms the rostral extension of the medullar and pontine reticular formation. It is generally located between the RN medially and the medial geniculate body laterally, and the SC and substantia nigra dorsally, respectively ventrally. As such, it incorporates the pararubral area mentioned above. Virtually all cases showed labeled terminals within the DpMe, but most prominent projections originated from the caudal MCN, lateral PIN and LCN.

Projections to the periaquaeductal grey

The periaquaeductal grey (PAG) receives input from the MCN, from the lateral PIN, and from the ventral and caudal LCN. Projections are mostly found in the contralateral supraoculomotor central grey but may also extend to more lateral areas of the PAG. Frequently, two more or less separated patches of terminals are observed (e.g. R100, level 14,15; T94-PhaL, level 11,12). Essentially similar results have been reported earlier in both the rat (Gonzalo-Ruiz and Leichnetz, 1987; Gonzalo-Ruiz *et al.*, 1990) and the monkey (Gonzalo-Ruiz *et al.*, 1988; May *et al.*, 1992). However, the notion observed in these studies that the MCN projections contain a prominent ipsilateral component could not be verified in the present study. Cerebellar projections to the supraoculomotor and Edinger-Westphal nuclei have been implicated in the control of the 'near-response': a set of eye adjustments executed by combined action of intra- and extraocular musculature upon shifting focus from a distant target to a near one (May *et al.*, 1992).

Projections to the pretectal region

The pretectum, although derived from the epithalamus, is found at the rostral border of the midbrain. Of the four subdivisions that are recognized, the anterior pretectal nucleus (APT) represents the largest entity and is found from the midrubral levels up to level where the fasciculus retroflexus reaches the habenula. Caudally, it is embedded between the DpMe and the

medial geniculate body. More rostrally, it is located between the parafascicular, posterior thalamic, and habenular cell groups (Paxinos and Watson, 1986). Like the SC, the pretectum is involved in visuosensory and visuomotor integration (Bull and Berkley, 1991; Kawamura *et al.*, 1982; Sefton and Dreher, 1995).

In the rat, projections from the CN to the pretectal area have not been reported (Sefton and Dreher, 1995), but they have been described in cat (e.g. Bull and Berkley, 1991; Kawamura *et al.*, 1982; Sugimoto *et al.*, 1982), where they may be involved in a somatosensory loop controlling input to the DAO from the dorsal column nuclei (Bull and Berkley, 1991; Bull *et al.*, 1990). Dorsal column nuclear and spinal projections to the anterior pretectal nucleus were described in the rat by Lund and Webster (1967a; 1967b). The pretecto-pontine projection rather overlaps with other visual afferents in the dorsomedial pontine nuclei and the NRTP. In this species, pretectal input was shown to originate from the caudal MCN, lateral and rostral parts of the interposed nuclei and LCN. Essentially similar results were obtained in the present study for the rat. Most prominent projections to the APT region of the pretectum were observed when the injection was centered on the lateral (case R98, T94-BDA) and rostromedial (case R89) AIN, caudal MCN (R100) and in all cases where the injection was centered on the LCN.

Projections to the medial mesodiencephalic junction

This area, located dorsomedial to RN and advancing rostralwards to incorporate the area surrounding the fasciculus retroflexus comprises several nuclei such as the nucleus of Darkschewitsch (Dk), medial accessory oculomotor nucleus (MA3), prerubral field (preR) and rostral interstitial nucleus of the medial longitudinal fascicle. These areas, sometimes collectively referred to as the nucleus parafascicularis (Carlton *et al.*, 1982; Ruigrok and Cella, 1995), have been implicated to be involved in oculomotor control (Berretta *et al.*, 1993), pain transmission and affective behaviour (Peschanski and Mantyh, 1983), but they also send afferents to the inferior olivary complex prerubralis (Bentivoglio and Molinari, 1984; Carlton *et al.*, 1982; Peschanski and Mantyh, 1983; Ruigrok and Voogd, 1995b; Rutherford *et al.*, 1984). In the rat, these neurons with projections to the IO form a compact shell surrounding the fasciculus retroflexus on its dorsal, medial and ventral sides, with scattered neurons located more laterally, which were positioned in the rostral interstitial nucleus of the medial longitudinal fascicle by Peschanski and Mantyh (1983) but indicated as prerubral field by Paxinos and Watson (1986) and in this chapter. The rat Darkschewitsch' nucleus was variously reported to be located outside this concentration of pre-olivary neurons (Carlton *et al.*, 1982; Ruigrok and Cella, 1995; Rutherford *et al.*, 1984) or within its confines (Bentivoglio and Molinari, 1984). The RN of the rat, as

argued above, does not participate in this projection to the IO.

The neurons surrounding the fasciculus retroflexus form the rostral part of a column of neurons with projections to the olive, which extends caudally in the ventral periaquaeductal grey, the medial accessory oculomotor nucleus and in the medial longitudinal fascicle, medial to the RN and Cajal's interstitial nucleus (Rutherford *et al.*, 1984). In our experiments the nuclei of the medial mesodiencephalic junction receive projections from the caudal MCN (case R100, focussed on the region ventromedial to the fasciculus retroflexus), the ICG (case T82), the PIN (cases T108/T109) and from the ventral and caudal LCN (cases T98, T94, R133, R178). The projections from the CN to these areas, which may be quite manifest in most cases, may be incorporated in cerebello-midbrain-olivary circuits as has been shown in the cat (De Zeeuw and Ruigrok, 1994; Ruigrok and Voogd, 1995a).

Diencephalon

Projections to the hypothalamus

Cerebellar projections to the hypothalamic areas have been described in cats and primates by Haines and collaborators (for review see Haines *et al.*, 1997). Basically, all four main cerebellar nuclei provide afferents to the posterior, lateral and dorsal hypothalamic regions as well as to the dorsomedial and paraventricular nuclei. In the rat, alleged direct projections to the paraventricular nucleus or directly surrounding areas could not be substantiated in a recent study by Rutherford (1995). In our material, only four cases showed a substantial projection to the hypothalamus. Injections centered on the caudal and ventral LCN (R133, R178 and T94-PhaL) mostly reached dorsal and lateral hypothalamic regions. Case R100, with an injection centered on the caudal MCN also displayed a conspicuous projection to hypothalamic areas directly surrounding the mammillothalamic tract. Projections to the paraventricular or other periventricular nuclei were not observed. It should be noted that the cases displaying projections to the hypothalamus only partly correspond to cases with projections to other areas involved in autonomic functions such as the parabrachial nuclei and lateral paragigantocellular nucleus (see Table 2.1; also see Rutherford, 1995). Hence, some parts of the CN appear to be involved at single, whereas others may be involved at multiple levels of autonomic system control.

Projections to the zona incerta and ventral part of the lateral geniculate nucleus

The zona incerta (ZI) spreads between the thalamus dorsally and the hypothalamus ventrally almost along the entire length of the diencephalon. Caudally, it is bordering the ventral part of the lateral geniculate nucleus, whereas more rostrally, it is continuous with the reticular thalamic nucleus. It is usually divided into a dorsal and a ventral part (Paxinos and Watson, 1986). The ZI appears to be a main integrative center with highly diversified connections. (Ricardo,

1981; Roger and Cadusseau, 1985; Shammah-Lagnado *et al.*, 1985). It has been suggested to be involved in somatosensory processing (Nicolelis *et al.*, 1992), in locomotor control (Supko *et al.*, 1991), in escape and/or nociceptive behavior (Shammah-Lagnado *et al.*, 1985), and in autonomic processes that are involved in sexual behavior (Dornan *et al.*, 1991; Edwards and Isaacs, 1991). Moderate or sparse projections from the interposed and lateral cerebellar nuclei to the ZI in the rat have been described earlier with anterograde (e.g. Aumann *et al.*, 1996; Chan-Palay, 1977; Faull and Carman, 1978; Roger and Cadusseau, 1985) and retrograde techniques (Shammah-Lagnado *et al.*, 1985). Here, we confirm that most injections in the LCN, injections in the rostral AIN (R98, R89, T83) and injections in the lateral PIN (R108, R109) result in terminal labeling in the contralateral ZI. Usually, one or more terminal fields are found that are elongated and positioned parallel to the cerebral peduncle. Also, in these cases, the projection to the ZI appears to be topographically arranged and may be classified as considerable. In addition, sparse projections originate from the medial PIN (T79), ICG (T82) and the DLP (T128). Contrary to findings by Shammah-Lagnado et al. (1985), we did not observe a ZI projection originating from the DLH.

In some cases, with injections centered on the caudal or ventral LCN (R178, R94-PhaL) and lateral PIN (R108, R109) the terminal fields in the ZI extended well into the ventral part of the lateral geniculate nucleus, as was described earlier for the lateral PIN by Vaudano and Legg (1992).

Projections to the intralaminar nuclei

The intralaminar nuclei consist of nuclei located within the internal medullary lamina of the thalamus. They comprise the central medial, paracentral and centrolateral as well as the centromedian and parafascicular nuclei (PF). Their functional role is complex and involves aspects of sensorimotor integration (Price, 1995). Projections from the caudal MCN, DLP as well as from the LCN are particularly prominent to the dorsal and lateral part of the PF. Projections from the caudal LCN and DLP, in addition, may extend to other parts of the intralaminar nuclei. Angaut and collaborators (Angaut *et al.*, 1985b), using the autoradiographic tracing technique, mention a projection from the caudal LCN to more rostral parts of the intralaminar nuclei, but did not report on the prominent projection to the PF, which was noted by others (Aumann *et al.*, 1994; Chan-Palay, 1977; Faull and Carman, 1978; Haroian *et al.*, 1981). Most connections were virtually exclusively contralateral. Only in cases R178 and T94-PhaL, with injections in the caudal and ventral LCN, some ipsilateral labeling was noted. Basically, these findings are in agreement with Haroian *et al.* (1981) but at variance with Angaut *et al.* (1985b).

Projections to principal thalamic nuclei

The principal thalamic nuclei can be subdivided into the anterior, medial, lateral and ventral tier nuclei. They

relay information from the sensory and motor systems to restricted areas of the cerebral cortex, from which they receive reciprocal connections (for review see Price, 1995). Of the four main subdivisions, the ventral tier nuclei are the main recipients of cerebellar nuclear input. Indeed, the cerebellar projections to the ventrolateral (VL) nucleus are often seen as the main output system of the cerebellum. However, as we show here, the rostral thalamus only receives a fraction of the total number of varicosities resulting from any injection. Obviously, in more 'consciously' behaving animals, such as primates, the relative importance of cerebellothalamic projections may increase (Chan-Palay, 1977).

In the rat, cerebellothalamic projections have been extensively studied by several groups (Angaut *et al.*, 1985b; Aumann *et al.*, 1994; 1996; Chan-Palay, 1977; Faull and Carman, 1978; Haroian *et al.*, 1981). Projections are usually found in parts of the ventromedial (VM), posterior (Po), ventral posterior (VP) and ventrolateral (VL) groups. Essentially, a medial to lateral topography may be discerned, when comparing projections from LCN, PIN and AIN, respectively. Overlap of the CL and paralaminar VL projections of the LCN occurs with the PIN and the MCN. However, PIN and LCN target different neurons in this region (Aumann *et al.*, 1994). The projection of the AIN to the dorsolateral VL appears to be completely segregated. Our data generally confirm the previous reports. All injections resulted in some labeling, mostly diffusely organized, within the confines of the VM. Usually, this labeling presented itself as a continuation of projections to the prerubral area and fields of Forel. Dense, patch-like terminal fields are found in combinations of the other ventral tier nuclei, most notably in the VL group. However, the DLH (cases R138, T94-BDA) does not appear to provide a conspicuous projection to the VL/VPL regions. In contrast with data by Angaut *et al.* (1985b) all our MCN injections, including the rostral-most one (case T199) resulted in some, sparse, thalamic labeling. However, we concur with these authors that the relative importance of the thalamic projections that originate from the LCN appears to be enhanced with respect to the projections from the other CN.

In addition to projections to the ventral tier nuclei, labeled varicosities are found in the lateral thalamic nuclei (in particular within the laterodorsal nucleus: LD) were noted when the injections were centered on the caudoventral part of the LCN, lateral PIN and AIN. It should be noted that the same injections also resulted in major projections to the SC and/or the pretectum, indicating the involvement of the lateral nuclei in the sensory-visual integration. Since at least part of the LD is connected to limbic cortical areas, cerebellar projections to this area may provide a pathway to control sensory input to the limbic system (for review see Price, 1995).

Functional implications

The results presented here clearly show that small injections placed into selected parts of the CN invariably

result in terminal projection patterns that are distributed over wide areas of the brain stem. It is likely that these output patterns relate to single cerebellar modules or submodules as based on intrinsic and olivocerebellar connections (Buisseret-Delmas and Angaut, 1993; Voogd *et al.*, 1996b). Moreover, the material shows that the projections to the IO usually are restricted to a single patch in one of its subdivisions indicating that in these cases the injection relates to a homogeneous olivocerebellar projection zone (Ruigrok, 1997; Voogd, 1995). Hence, we conclude that the modular output is distributed to and processed in parallel in many brain stem areas. E.g. projections from the ventral part of the LCN (such as case R 178), which serves as output of the D2 module (Buisseret-Delmas and Angaut, 1993) may simultaneously reach widely different regions such as IO, NRTP, pontine reticular formation, PAG, (para-)RN, several areas in the medial mesodiencephalon, SC, pretectum, ZI, dorsal hypothalamic areas and several thalamic regions. Some of these projections are bilateral. As a consequence, in order to fully understand cerebellar functioning, we suggest that the distributed nature of the modular output will have to be taken into account.

Cerebellar modules in the cat classically comprise the A, B, C1-C2-C3, D1 and D2 Purkinje cell zones (Voogd, 1964), which are connected to the MCN, lateral vestibular nucleus, AIN, PIN and dorsomedial and ventrolateral LCN, respectively. Additional zones were distinguished by Buisseret-Delmas and collaborators (Buisseret-Delmas, 1988a; 1988b; Buisseret-Delmas and Angaut, 1989b; 1993; Buisseret-Delmas *et al.*, 1993). The X-zone, with the ICG as its target nucleus, is located in the vermis between the A and B zones; the lateral extension of the A zone occupies the medial hemisphere of the lobules VI and VII, and projects to the DLP. Finally, an additional D0 zone is present in the hemisphere, lateral to the C3 zone and projects to the DLH. It appears from our results that it is difficult to clearly characterize the output of each cerebellar target nucleus unequivocally. Injections placed at various places in the same nucleus may show large differences in their terminal fields. E.g. compare terminal fields and termination profiles of two MCN injections (R100 and T195) and the two PIN injections (T79 and T108). On the other hand, injections in different nuclei (e.g. the LCN in case T94-PhaL and the MCN in case R100) may show a basically similar distribution of terminal fields.

Despite the great variety of brain stem structures that may be affected by the cerebellum, it would appear that most of them may be characterized as belonging to any of five basic groups. 1) The IO obviously functions as the source of cerebellar climbing fibers, with collaterals to all cerebellar target nuclei. The projections to different zones and their target nuclei do not seem to overlap and follow the patterns established previously (Ruigrok, 1997; Ruigrok and Voogd, 1990). 2) More diverse areas, such as the NRTP, BPN, LRN, etc. supply mossy fiber inputs. 3) In addition, as discussed above, several brain stem regions that receive a conspicuous

cerebellar input, such as the medial mesodiencephalic region, pretectum, and DpMe, may serve as a source of IO input (Bull and Berkley, 1991; De Zeeuw and Ruigrok, 1994). 4) Several areas may be classified as 'effector' areas, e.g. such as the RN and supraoculomotor nuclei. Some effector regions, such as the vestibular nuclei, the SC and the reticular formation and the trigeminal nuclei, also serve as sources of mossy fiber input and as pre-olivary relay nuclei. 5) Finally, the thalamic projections of the CN should be considered. Some of them can be classified as belonging to cortical effector systems, others are part of complicated loops, involving the basal ganglia and/or precerebellar or effector regions in the brain stem. Since in the present study varicosities were plotted and counted, we noted that, in the rat, only a relatively low percentage (< 10%) of terminals were observed in the VL of the thalamus, which, nevertheless, is known as one of the classic termination areas of the CN. In fact, in many cases, most diencephalic terminals were observed in the ZI and/or the parafascicular thalamic nucleus.

Because the cerebellar modules and/or micromodules have been implicated to act as functional units we will shortly review our main results again but this time from a modular point of view.

The A-module

The MCN serves as the target nucleus of the medial A zone of the vermis. The dorsolateral protuberance (DLP) of the rat MCN, however, is the target nucleus of a separate zone particular for rodents, the lateral extension of the A zone which is located in the medial hemisphere (Akaike, 1992; Buisseret-Delmas, 1988a). The caudal and rostral MCN and the DLP receive collaterals from different subnuclei of the caudal MAO. Rostral and caudal MCN receive collaterals from lateral subnucleus a, which relays somatosensory information from the cord and the dorsal column nuclei. The caudal MCN, in addition, receives collaterals from the group ß, a vestibular relay nucleus and from subnucleus c (Akaike, 1992). The DLP receives collaterals from a different population of cells in subnucleus c of the caudal MAO, which project to the lateral extension of the A zone, but which shares SC afferents with the cells projecting to the vermal visual area located in lobule VII (Akaike, 1992).

The MCN is characterized by bilateral, but mainly crossed projections to the medial medullary and pontine reticular formation. In the case of the rostral MCN these are combined with strong, bilateral projections to the vestibular nuclei. The DLP mostly lacks these vestibular projections. Its strong projections to the reticular formation involve the lateral parvicellular reticular field and extend rostrally into pons and mesencephalon, where they include the deep mesencephalic nucleus, the interstitial nucleus, the central grey and the deep layers of the SC. Vestibular projections of the caudal MCN, which receives Purkinje cell axons from the vermal visual area (lobule VII) and lobules IX and X, are mostly restricted to the SV. Its projections to brain stem includes several visual effector areas such as

the nucleus prepositus hypoglossi, the pontine paramedian reticular formation, the supraoculomotor region, the SC, the interstitial nucleus, the medial accessory oculomotor nucleus and the rostral interstitial nucleus of the medial longitudinal fascicle, here considered part of the area parafascicularis prerubralis. The caudal MCN and the DLP provide the major thalamic projections of the MCN, with the parafascicular and ventromedial nuclei as their main targets. Terminations in precerebellar nuclei providing mossy fibers, such as the NRTP and the NRL, are rather sparse. Some overlap occurs in the projections to the reticular formation of the rostral MCN with the DLP and the caudal MCN. All subdivisions of the MCN share a projection to the parasolitary nucleus, which is a preolivary nucleus projecting to the group β and the dorsomedial cell column (Barmack *et al.*, 1998).

Potential overlap in the projections of the MCN with other CN is present in the medullary reticular formation (for rostral MCN with LCN), in the pontine reticular formation (for DLP and caudal MCN with caudal LCN) and in the deep mesencephalic nucleus (for DLP and caudal MCN with all CN), and in several of the visual effector areas targeted by the caudal MCN (with lateral PIN and ventral and caudal LCN).

The X-module

The interstitial cell groups (ICG) receive Purkinje cell axons from the X zone, located between the A and B zones of the anterior vermis (Yatim *et al.*, 1995a; 1995b). Its bulbar connections recently were discussed by Buisseret-Delmas and collaborators (Buisseret-Delmas *et al.*, 1998). Their conclusion that this nucleus receives climbing fiber collaterals from the DAO, in addition to the MAO, could not be substantiated in our experiments. Its projections to the reticular formation, the vestibular nuclei, the area prerubralis parafascicularis, prerubral field and ventrolateral thalamic nucleus all overlap with those from other CN. A sparse projection to the caudal RN could be confirmed, and a small focus of termination was observed in the NRTP in our case T82. One of the main, and relatively exclusive, connections of the ICG with the contralateral spinal cord (Bentivoglio and Kuypers, 1982; Horn *et al.*, 1995) could not be studied in our material or that of Buisseret-Delmas *et al.* (1998). According to Bentivoglio and Kuypers (1982) these neurons collateralize both to the spinal cord and the thalamus.

The B-module

The lateral vestibular nucleus of Deiters (LVN), which serves as the target nucleus of the lateral B zone of the anterior vermis, has not been studied in this paper. Its Purkinje cells receive their climbing fiber input from the dorsal fold of the DAO which also provides a collateral projection to the LVN. The LVN gives rise to the lateral vestibulospinal tract (Rubertone *et al.*, 1995b).

The C2-module

The PIN is target nucleus of the C2 zone (Voogd and Bigaré, 1980). In the rat, however, the projection of the C1 zone includes the medial PIN. C2 projects to intermediate AIN and

lateral PIN (Buisseret-Delmas, 1988b). The PIN scarcely connects with the medulla and the pons, apart from its reciprocal connections with the rostral MAO. The rostral MAO is one of the main targets of the preolivary neurons in the area parafascicularis prerubralis. The RN receives a projection from the medial PIN, located along the medial border of the nucleus. It is not clear whether these terminals overlap with projections from other CN, such as the AIN or the LCN. A projection to the NRTP seems to be lacking. Several of its projections to mes- and diencephalon, especially those from lateral PIN, overlap with those from the ventral and caudal LCN, and less so, with the caudal MCN (SC, the central grey, the nucleus of the posterior commissure, the area parafascicularis prerubralis and the VL nucleus of the thalamus). Its projection to the zona incerta is shared by most CN, with the exception of the MCN. Most likely, the projections from the lateral PIN are related to coordination of eye movements which may explain the difference in projection between the medial and lateral part of this cerebellar nucleus (e.g. in their projection to the RN).

The C1- and C3-modules

The AIN is the target nucleus of the C1 and C3 zones. In the cat, however, as mentioned above, C2 may be connected to the intermediate AIN. It receives collaterals from the DAO, which is the most obvious somatosensory integration center of the IO. Its main projections include the RNm, the NRTP, the anterior pretectal nucleus, the zona incerta and the thalamus. In the VL nucleus of the thalamus its terminals are typically located laterally, segregated from the other CN. They presumably relay information of a sensorimotor nature to the motor cortex. The anterior pretectal nucleus, which is the recipient of a major part of the AIN efferents, gives rise to a projection to the ipsilateral IO, which, in the cat, terminates in the rostral DAO (Bull *et al.*, 1990).

The D0-module

The dorsolateral hump (DLH) is the target nucleus of the D0 zone (Buisseret-Delmas and Angaut, 1993). There is no clear equivalent of this zone in either cats or monkeys. The DLH is reciprocally connected with the dorsomedial group of the IO (Ruigrok, 1997; Ruigrok and Voogd, 1990). Afferents from the trigeminal nuclei and adjacent reticular formation terminate in this olivary subnucleus (see (Ruigrok and Cella, 1995) for a review). The rodent DLH is characterized by a unique ipsilateral projection to the lateral medullary parvicellular formation, the pontine reticular formation and the trigeminal nuclei (Woodson and Angaut, 1984). Neurons with similar projections are present in the adjacent lateral AIN and dorsomedial LCN, some of which also include a contralateral component (Bentivoglio and Kuypers, 1982). Crossed projections to RN, NRTP, deep mesencephalic nucleus and anterior pretectal nucleus are shared with the adjacent CN. The terminations in the thalamus are mostly restricted to the intralaminar nuclei.

The D1- and D2-modules

The LCN is the target nucleus of the D1 and the D2 zones. In the rat, Purkinje cells of these zones terminate in the rostral and dorsal, and the ventral and caudal parts of the LCN, respectively (Buisseret-Delmas and Angaut, 1993). The rostral and dorsal parts of the LCN receive collaterals from the dorsal leaf of the principal olive; the ventral and caudal part of the nucleus from the ventral leaf. The connections of the D1 and D2 zones in rodents and in carnivores appear to be reversed. In the cat, the ventral leaf of the principal olive provides climbing fibers to the medial D1 zone and collaterals to its target nucleus, the caudolateral LCN and the dorsal leaf innervates the lateral D2 zone and its target nucleus, the rostral, dorsomedial LCN (Voogd and Bigaré, 1980).

The rostral and dorsomedial and the caudal and ventral LCN display clear differences in their projection. Bilateral projections of the rostral LCN to the reticular formation and the trigeminal nuclei resemble the adjacent DLH. Strong projections to the ventromedial medullary reticular formation, which overlap with MCN projections, are characteristic of the caudal LCN. All subdivisions of the LCN give rise to projections to the deep mesencephalic nucleus, the RNp., the anterior pretectal nucleus, the prerubral field, the parafascicular prerubral area, the zona incerta and the ventromedial and ventrolateral thalamic nuclei. The terminal field of the rostral LCN in the RN includes the RNm, whereas the caudal LCN provides a strong projection to the pararubral area. The terminal field in the anterior pretectal nucleus extends into lateral and dorsal parts of the nucleus. Projections to visual effector areas mainly arise from the caudal LCN. These terminations in SC, the medial accessory oculomotor nucleus, the central grey, and the area parafascicularis prerubralis may partially overlap with the caudal MCN and the lateral PIN. In the paralaminar, medial VL nucleus of the thalamus, the caudal LCN projection overlaps with the PIN (Aumann *et al.*, 1994; 1996).

Conclusion

Complex patterns of divergence and convergence, established by the individual cerebellar nuclei or by different parts of the same nucleus, appear to be an essential characteristic of the cerebellar nucleobulbar organization. This complex organization can be further analysed using retrograde and anterograde double or multiple tracing techniques (e.g. see Aumann and Horne, 1996; Bentivoglio and Kuypers, 1982; Gonzalo-Ruiz and Leichnetz, 1987; Teune *et al.*, 1995). Such retrograde and anterograde double labeling tracing studies, focussed on certain combinations of the effector areas, the precerebellar and the preolivary nuclei, will be presented in the chapters 4-6 of this thesis.

Table 2.1. This table shows the injection sites together with the used tracer as well as the iontophoresis characteristics (current, and time of iontophoresis in minutes). BDA: biotinylated dextran amine; PhaL: Phaseolus vulgaris leucoagglutinin; MCN: medial cerebellar nucleus; AIN: anterior interposed nucleus; PIN: posterior interposed nucleus; LCN: lateral cerebellar nucleus.

	Experiment	Tracer	Current / time (minutes)
MCN	T199	BDA	+4 μA, 20'
	T195	BDA	+4 μA, 20'
	R127	PhaL	+4 μA, 40'
	R128	PhaL	+2 μA, 30'
	R100	PhaL	+4 μA, 30'
PIN	T82	BDA	+4 μA, 20'
	T79	BDA	+4 μA, 20'
	T109	BDA	+4 μA, 20'
	T108	BDA	+4 μA, 20'
AIN	R89	PhaL	+8 μA, 20'
	T83	BDA	+4 μA, 30'
	R98	PhaL	+4 μA, 30'
DLH	T94-BDA	BDA	+4 μA, 20'
	R138	PhaL	+5 μA, 30'
LCN	T77	PhaL	+4 μA, 20'
	T98	PhaL	+4 μA, 20'
	R178	PhaL	+6 μA, 30'
	T94-PhaL	PhaL	+4 μA, 30'
	R133	PhaL	+3 μA, 30'

Table 2.2

	MCN					PIN				AIN			DLH		LCN				
	T199	T195	R127	R128	R100	T82	T79	T109	T108	T89	R83	R98	T94	R136	T77	T98	R178	T94	R133
Medulla oblongata																			
Inferior olive	●	•	●	•	●	●	●	●	●	●	●	●	●/●|	●/●|	●	●/•|	●/•|	●/•|	●/•|
Lateral reticular nucl.	•				•	•				•|		•|							
Nucl. of the solitary tract										•|									
Parasolitary nucl.	•	●/•|	●	●	●															
Medullary reticular nucl.	•	●/●|	•	●	•	•						•|	●|	●|					
Paramedian nucl.						•														
Parvocell. retic. nucl.	•		•	•			•			•|		●|	•/●|	•/●|			●|	•/•|
Gigantocell. retic. nucl	●	●/●|	●	●	●	●									•	•			●/•|	●/•|
Lat. paragigantocell. nucl.	●	●				•													●/•|	•
Spinal trigem. nucl., oral part			•	•						•|		•|	●|	●/●|				•|	
Spinal trigem. nucl., interpolar part			•	•						•|		●|	●|	●|				-|	•/●|
Spinal trigem. nucl., caudal part				•								•|	●|	•|				•|	•|
Superior vestibular nucl.	•/•|	•/●|	•/●|	•	•/•|	•|													
Lateral vestibular nucl.	•/•|	•/●|			•/•|	•|				•|	•|	•|						
Medial vestibular nucl., rostral	●/•|	•/•|	•|	•	•/•|	•|				•|									
Medial vestibular nucl., caudal	•/•|	•/•|			•/•|	•|													
Spinal vestibular nucl.	●/•|	●/●|	•	•	•/•|	●|			•|				•|						
Nucl. prepositus hypoglossi					●/•|															
Metencephalon																				
Basal pontine nuclei					•					•	•	•	●/•|	●		●	●	●	•	
Nucl. retic. tegm. pontis			•	•	●	●	•			●	•	●	●	●	●	●	●	●	●	●/•|
A5 noradrenergic group (?)			•		•	●						•|	●|	●|	●|			•|	•|
Principal sens. trig. nucl.			•	•									•|	•						
Caud. pont retic. nucl.	●	●	●	●	●	●				•					•		•	●/•|	●/•|	
Oral pont. retic. nucl.	•	•	●	•	●	•				●					•	•	●/•|	●/•|	●/•|	
Central gray pons	•		•	•	●/•|		•	•									●	●		
Pedunculopontine tegm. nucl.			●	•	●		•			•					•|	•|	●	•		
Parabrachial nucl.			●/•|	●	•/•|								•/●|	-|	•|				
Mesencephalon																				
Red nucl., parvicellular		•			•	•	•			•		•	●	•	●	●	●	●	●	
Red nucl., magnocellular	•	•				•	●			●	●	●/•|	●	●	•	●				
Pararubral area			•		●															
Deep mesenceph. nucl.	•		●	●	●	●	•	●	●	•		●	●	●	●	•	●	●	●	
Superior colliculus, superficial																	●			
Superior colliculus, intermediate					•			•	●			•					●	•	•	
Superior colliculus, deep			●	●	●			●	●	•		•					●/•|	●	•	
Ventral tegmental area					•															
Dorsal raphe nucleus					•										•|			•		
Ventral tegm. relay zone					•		●	•					•	●	●	•	•	●		
Medial access. oculomot. nucl.			•		●											●	●/•|	●/•|	●	
Interstitial nucl. of Cajal	•	●	●	●	●	•	•	•	•							•	•	●/•|	●	
Nucl. of Darkschewitsch					●			•								•	●	•		
Nucl. parafascicularis prerubr.		●	•		●	●	●	•	●	●	•	•	•	•	●	●	●	●/•|	●	
Periaquaductal gray			●	•	●		•	•	•	•							●	●	●	
Nucl. of post. commissure					●			●	●			●					●	●/•|	●	
Anterior pretectal nucl.					•					●	•	●	●	•	●	●	●/•|	●	●	
Posterior pretectal nucl.										•		•			●	•	●/•|	•		

Table 2.2 (continued)

	MCN					PIN				AIN			DLH		LCN				
	T199	T195	R127	R128	R100	T82	T79	T109	T108	T89	R83	R98	T94	R138	T77	T98	R178	T94	R133
Diencephalon																			
Mammillary nuclei																	•		
Lateral hypothal. area					•												●/•i	•	
Dorsal hypothal. area					•												●/•i	•	
Zona incerta				•	•	•	•	●	●	●	•	●	•		•	●	●/•i	●/•i	●
Nucl. fields of Forel		•	•		●	●	•	•	•	•		•	•	•	●	●	●/•i	●/•i	●
Ventral lat. geniculate nucl.								•	•								•	•	
Parafascicular thalam. nucl.	•		●	●	●	•		•		●	•	•	•			•	●/•i	●	•
Central medial thalam. nucl.			•	•								•	●	•		•		•	●
Laterodorsal thalam. nucl.								•	•	•		•					●	•	•
Posterior thalamic nucl.			•	•		•			●	•	•	•	●	●	●	•		•	•
Ventroposterior thalam. group			•						•	•	•							•	
Ventromedial thalam. nucl.	•	•	●	●	●	•	•	•	•	•	•	•	•		•	•	●	●/•i	●
Ventrolateral thalam. nucl.	•	•	?		?	●	?	●	●	●	●	●			●?	●	?	●	●

Table 2.2 . Overview of all described cases and brain stem regions in which labeled varicosities were found. Large dot denotes dense labeling, small dot indicates only a minor projection, intermediate dot represents a fair projection. Question mark indicates that the area was not available for analysis; i indicates that the labeling was found ipsilateral to the injection site, otherwise the labeling was observed contralaterally.

Legends to figures

Fig. 2.1. This graph shows the mean number (± S.E.M.) of plotted varicosities per investigated mm^2 of all cases with PhaL injections and of all cases with BDA injections. It is obvious that PhaL usually results in a significantly higher ($p<0.05$) yield of labeled varicosities compared to BDA.

Fig. 2.2. Diagrams of the injection sites described in this paper. The injection sites are indicated in a standardized, equally spaced (160 μm), series of transverse sections displayed from caudal (1) to rostral (10).

Fig. 2.3. Serial plots indicating the distribution of labeled varicosities (dots) throughout the brain stem in case T199 with a BDA injection centered on the MCN. For details of the injection site, see Fig. 2.2. The boundaries of several brain stem nuclei (hatched lines) and fiber tracts (thin lines) are indicated. For abbreviations, see list.

Fig. 2.4. Serial plots showing the distribution of labeled varicosities in case T195 with a BDA injection centered on the MCN. Further as in Fig. 2.3.

Fig. 2.5. Serial plots showing the distribution of labeled varicosities in case R127 with a PhaL injection centered on the DLP. Further as in Fig. 2.3.

Fig. 2.6. Serial plots showing the distribution of labeled varicosities in case R128 with a PhaL injection centered on the DLP. Further as in Fig. 2.3.

Fig. 2.7. Serial plots showing the distribution of labeled varicosities in case R100 with a PhaL injection centered on the MCN. Further as in Fig. 2.3.

Fig. 2.8. Bar diagrams indicating rostrocaudal distribution of labeled varicosities of five cases with an injection centered on the MCN. The x-axis displays the section number of the corresponding plots (Figs. 2.3-2.7). The y-axis displays the percentage of plotted varicosities. The total number of plotted varicosities is indicated below the case number. The approximate rostrocaudal position of four brain stem areas (IO: inferior olive; BPN, basilar pontine nuclei; RN: red nucleus; and VL: ventrolateral thalamic nucleus) is indicated above each graph for easy reference. Note that cases R195 and R199 mostly projects to the caudal brain stem levels whereas cases that involve the DLP and especially the caudal MCN (R100) in addition or rather (R100) supply more rostral brain stem areas.

Fig. 2.9. Serial plots showing the distribution of labeled varicosities in case T82 with a BDA injection centered on the ICG. Further as in Fig. 2.3.

Fig. 2.10. Serial plots showing the distribution of labeled varicosities in case T79 with a PhaL injection centered on the PIN. Further as in Fig. 2.3.

Fig. 2.11. Serial plots showing the distribution of labeled varicosities in case T109 with a BDA injection centered on the PIN. Further as in Fig. 2.3.

Fig. 2.12. Serial plots showing the distribution of labeled varicosities in case T108 with a BDA injection centered on the PIN. Further as in Fig. 2.3.

Fig. 2.13. Bar diagrams indicating rostrocaudal distribution of labeled varicosities of four cases with an injection centered on the ICG (T82) or PIN (T79, T109, T108). Also see Figs. 2.9-2.12. For details see Fig. 2.8. Note that, contrary to cases T109 and T108, the cases with medially placed injections (T82, T79) send a fair percentage of terminals (> 10%) to the caudal brain stem even when excluding the projections to the IO.

Fig. 2.14. Serial plots showing the distribution of labeled varicosities in case R89 with a PhaL injection centered on the AIN. Further as Fig. 2.3.

Fig. 2.15. Serial plots showing the distribution of labeled varicosities in case T83 with a BDA injection centered on the AIN. Further as Fig. 2.3.

Fig. 2.16. Serial plots showing the distribution of labeled varicosities in case R98 with a PhaL injection centered on the AIN. Further as Fig. 2.3.

Fig. 2.17. Serial plots showing the distribution of labeled varicosities in case T94 with a BDA injection centered on the DLH. Further as Fig. 2.3.

Fig. 2.18. Serial plots showing the distribution of labeled varicosities in case R138 with a PhaL injection centered on the DLH. Further as Fig. 2.3.

Fig. 2.19. Bar diagrams indicating rostrocaudal distribution of labeled varicosities of five cases with an injection centered on the AIN (R89, T83, R98) or DLH (T94, R138). Also see Figs. 2.14-2.18. For details see Fig. 2.8. Note that the cases with injections in the DLH send a considerable part of their terminal fibers to the caudal brain stem.

Fig. 2.20. Serial plots showing the distribution of labeled varicosities in case T77 with a PhaL injection centered on the LCN. Further as Fig. 2.3.

Fig. 2.21. Serial plots showing the distribution of labeled varicosities in case T98 with a PhaL injection centered on the LCN. Further as Fig. 2.3.

Fig. 2.22. Serial plots showing the distribution of labeled varicosities in case T178 with a PhaL injection centered on the LCN. Further as Fig. 2.3.

Fig. 2.23. Serial plots showing the distribution of labeled varicosities in case T94 with a PhaL injection centered on the LCN. Further as Fig. 2.3.

Fig. 2.24. Serial plots showing the distribution of labeled varicosities in case R133 with a PhaL injection centered on the LCN. Further as Fig. 2.3.

Fig. 2.25. Bar diagrams indicating rostrocaudal distribution of labeled varicosities of five cases with an injection centered on the LCN. Also see Figs. 2.20-2.24. Note the generally wide rostrocaudal distribution of areas in which labeled varicosities were observed.

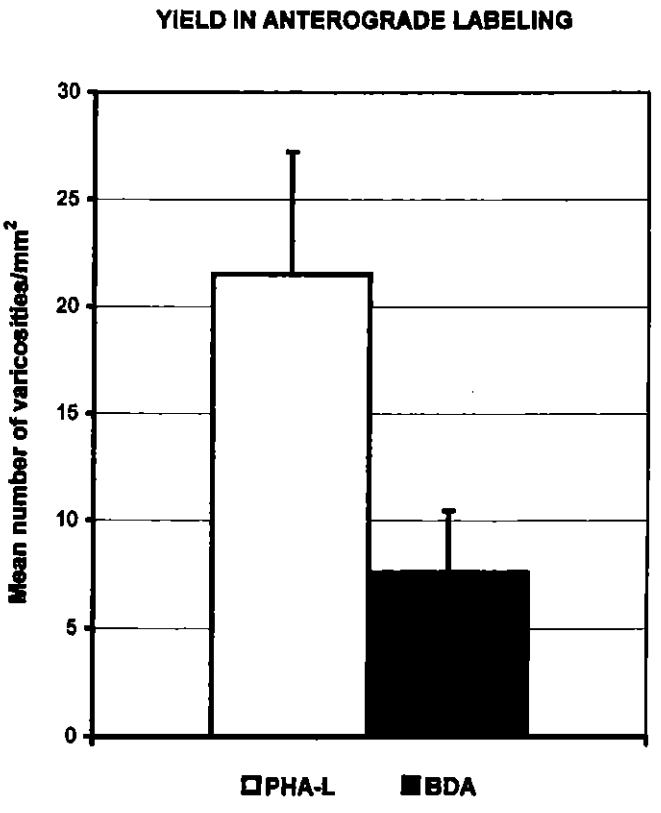
YIELD IN ANTEROGRADE LABELING
Mean number of varicosities/mm²
30
25
20
15
10
5
0
PHA-L
BDA

Fig. 2.1

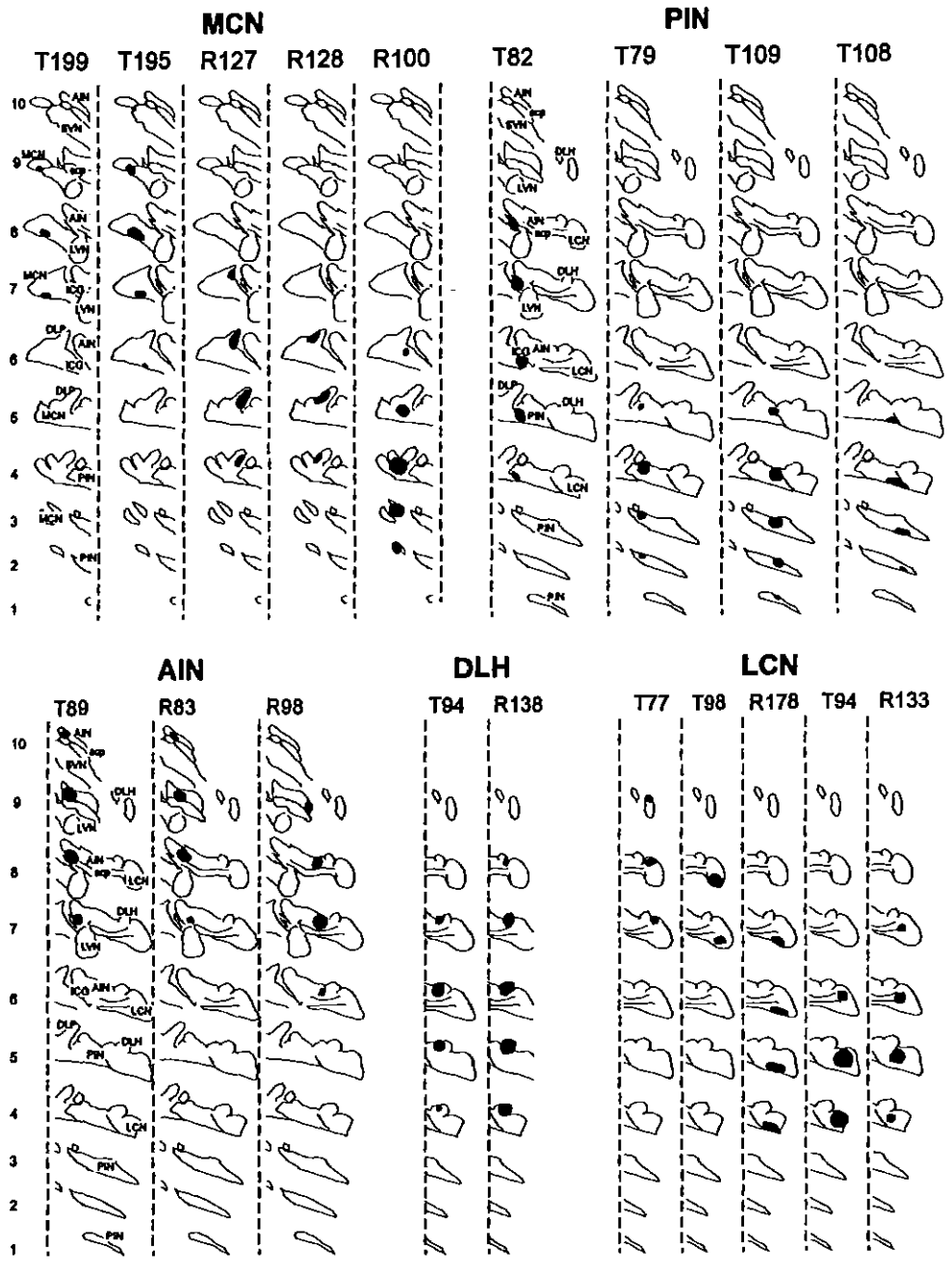
MCN
T199
T195
R127
R128
R100
PIN
T82
T79
T109
T108
AIN
T89
R83
R98
DLH
T94
R138
LCN
T77
T98
R178
T94
R133

Fig. 2.2

T 199

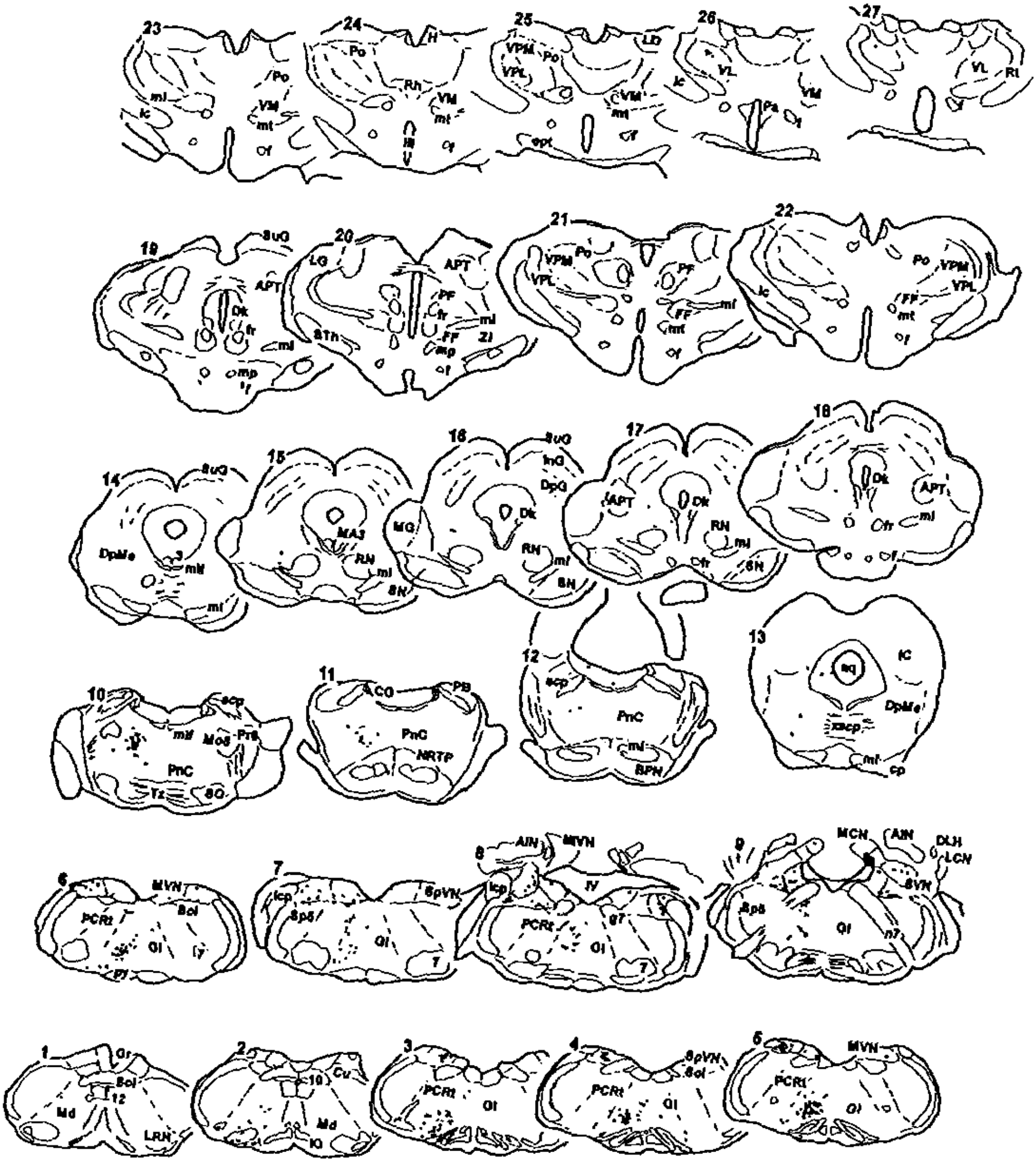

23
24
25
26
27
Po
VM
mt
ml
ic
f
H
Rh
VPM
VPL
LD
VL
Rt
opt
19
20
21
22
SuG
APT
Dk
fr
mp
LG
PF
FF
Zi
STh
14
15
16
17
18
DpMe
3
mlf
MA3
RN
SN
MG
InG
DpG
13
IC
aq
xscp
cp
10
11
12
scp
Mo5
Pr5
PnC
Tz
SO
CO
PB
NRTP
SPH
6
7
8
9
MVN
Sol
PCRt
OI
py
icp
Sp5
SpVN
AIN
g7
MCN
DLH
LCN
SVN
n7
1
2
3
4
5
Gr
Cu
Md
LRN
IO

Fig. 2.3

T195

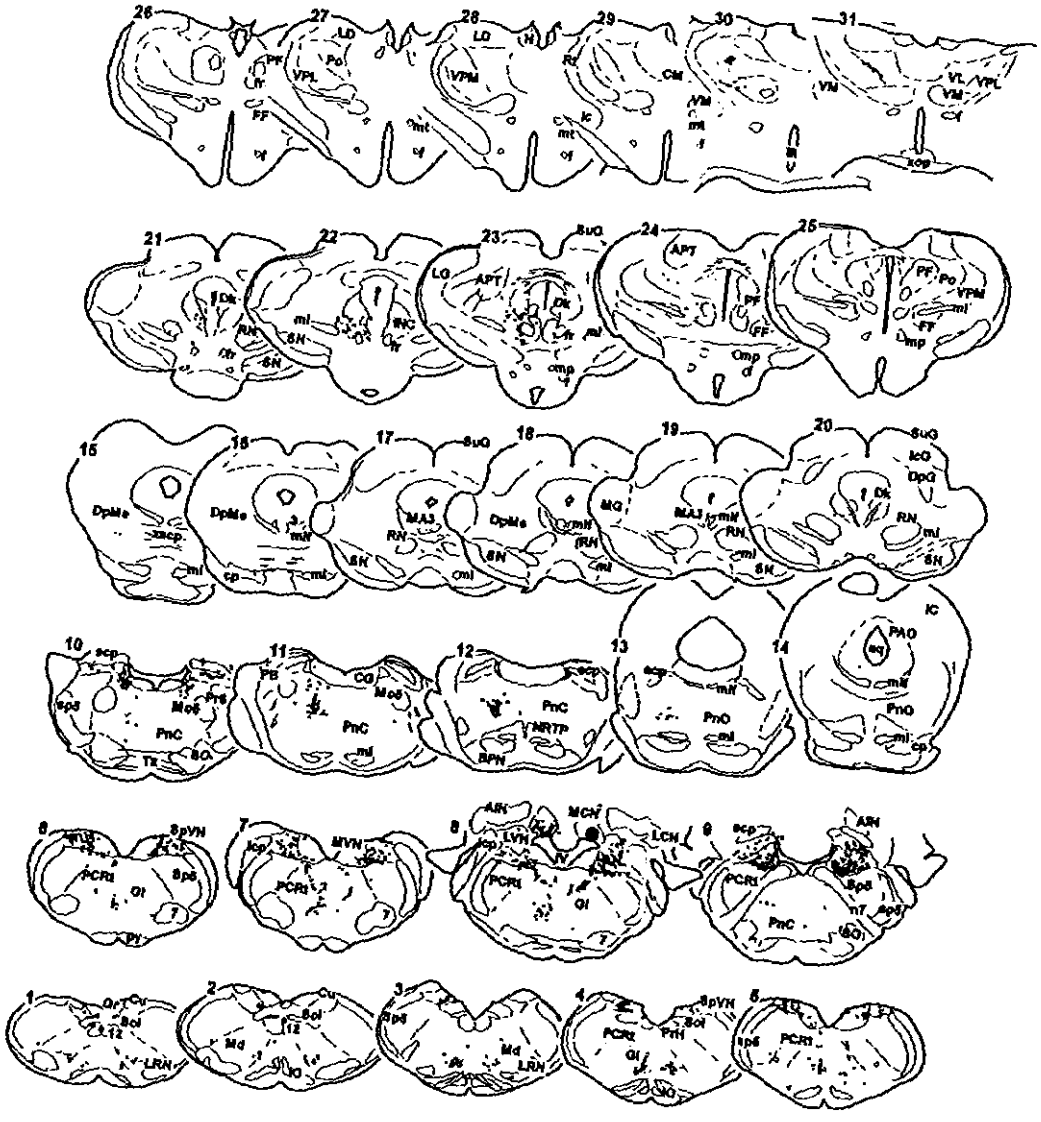

Fig. 2.4

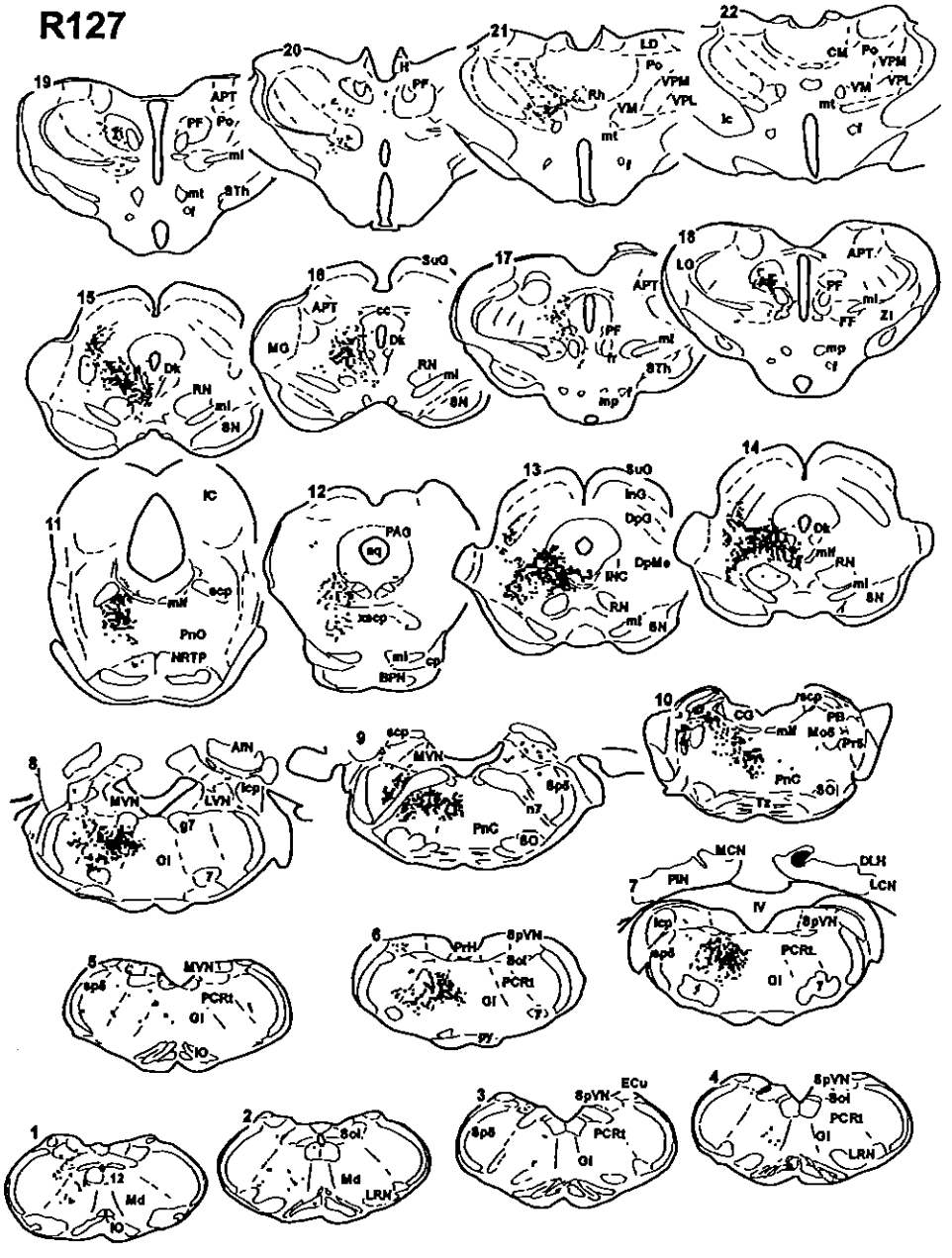
R127
19
APT
PF
Po
ml
mt
cf
STh
20
H
PF
21
LD
Po
VPM
VPL
Rh
VM
mt
cf
22
CM
Po
VPM
VPL
VM
mt
lc
cf
15
Dk
RN
ml
SN
16
SuG
APT
cc
MG
Dk
RN
ml
SN
17
APT
PF
ml
STh
mp
cf
18
LG
APT
PF
ml
ZI
mp
cf
11
IC
mlf
scp
PnO
NRTP
12
PAG
aq
xscp
ml
cp
BPN
13
SuG
InG
DpG
DpMe
INC
RN
ml
SN
14
Dk
mlf
RN
ml
SN
8
AIN
MVN
LVN
icp
97
GI
7
9
scp
MVN
Sp5
n7
PnC
SO
10
CG
scp
mlf
PB
MoS
Prs
PnC
SOl
Tz
7
MCN
DLH
PIN
LCN
IV
icp
sp5
SpVN
PCRt
GI
7
6
PrH
SpVN
Sol
PCRt
GI
7
py
5
MVN
sp5
PCRt
GI
IO
1
12
Md
IO
2
Sol
Md
LRN
3
SpVN
ECu
sp5
PCRt
GI
4
SpVN
Sol
PCRt
GI
LRN

Fig. 2.5

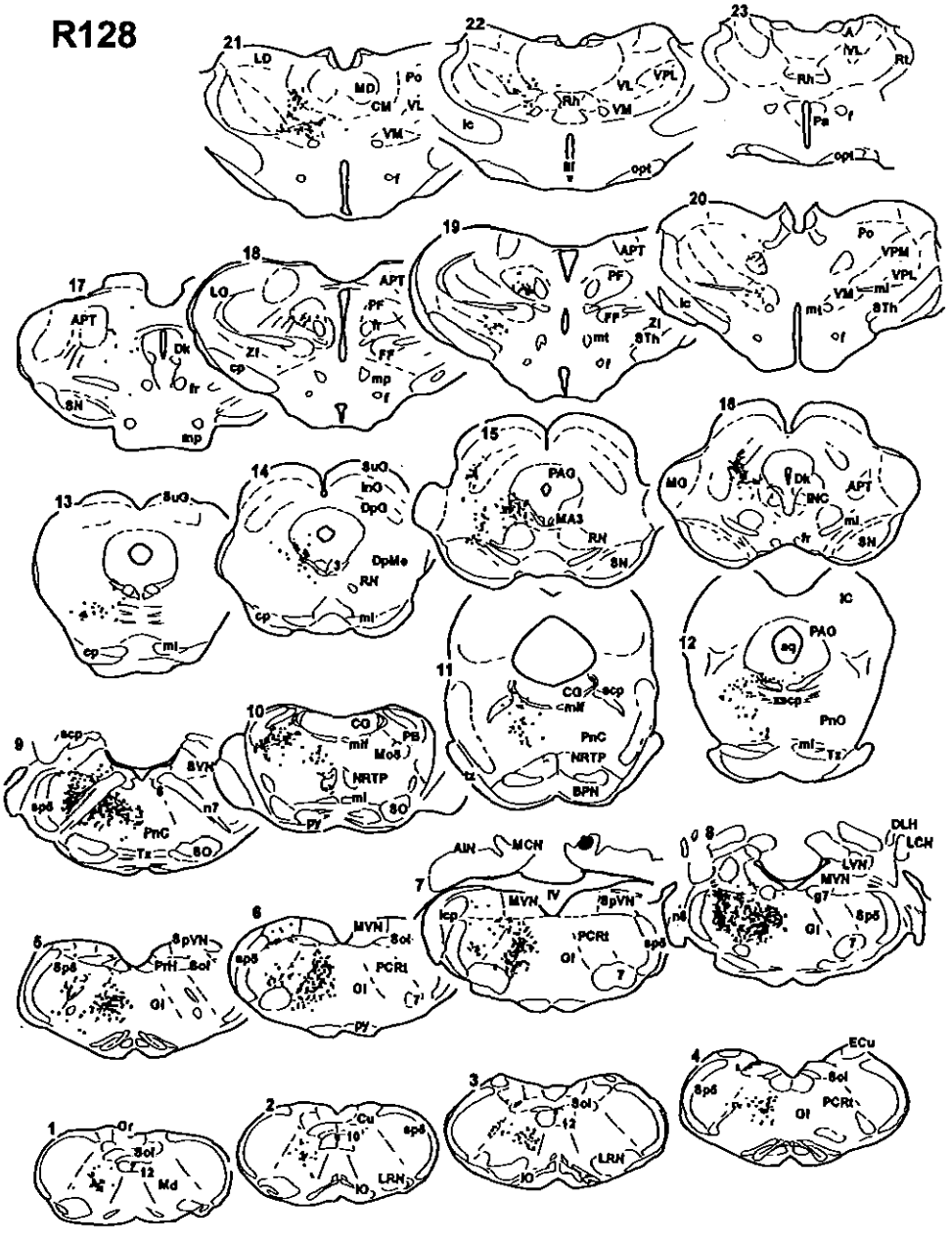
R128
21
LD
MD
CM
Po
VL
VM
of
22
Rh
VL
VPL
VM
lc
ml
opt
23
A
MVL
Rt
Rh
Pa
of
opt
17
APT
Dk
fr
SN
inp
18
LG
APT
PF
fr
FF
ZI
cp
mp
of
19
APT
PF
FF
ZI
STh
mt
of
20
Po
VPM
VPL
ml
VM
STh
lc
of
13
SuG
cp
ml
14
SuG
InG
DpG
DpMe
RN
cp
ml
15
PAG
MA3
RN
SN
16
MG
Dk
PAG
APT
ml
fr
SN
11
CG
scp
mlf
PnC
NRTP
BPN
12
lc
PAG
aq
scp
PnO
ml
Tz
9
scp
SVN
sp5
n7
PnC
Tz
SO
10
CG
mlf
PB
MoS
NRTP
ml
SO
PY
7
AIN
MCN
lcp
MVN
IV
SpVN
PCRt
sp5
Gl
8
DLH
LCH
LVN
MVN
g7
n8
Gl
sp5
6
SpVN
PrH
Sol
sp5
Gl
6
MVN
Sol
sp5
PCRt
Gl
PY
4
ECu
Sol
sp5
PCRt
Gl
3
Sol
12
IO
LRN
2
Cu
10
sp5
IO
LRN
1
Gr
Sol
12
Md

Fig. 2.6

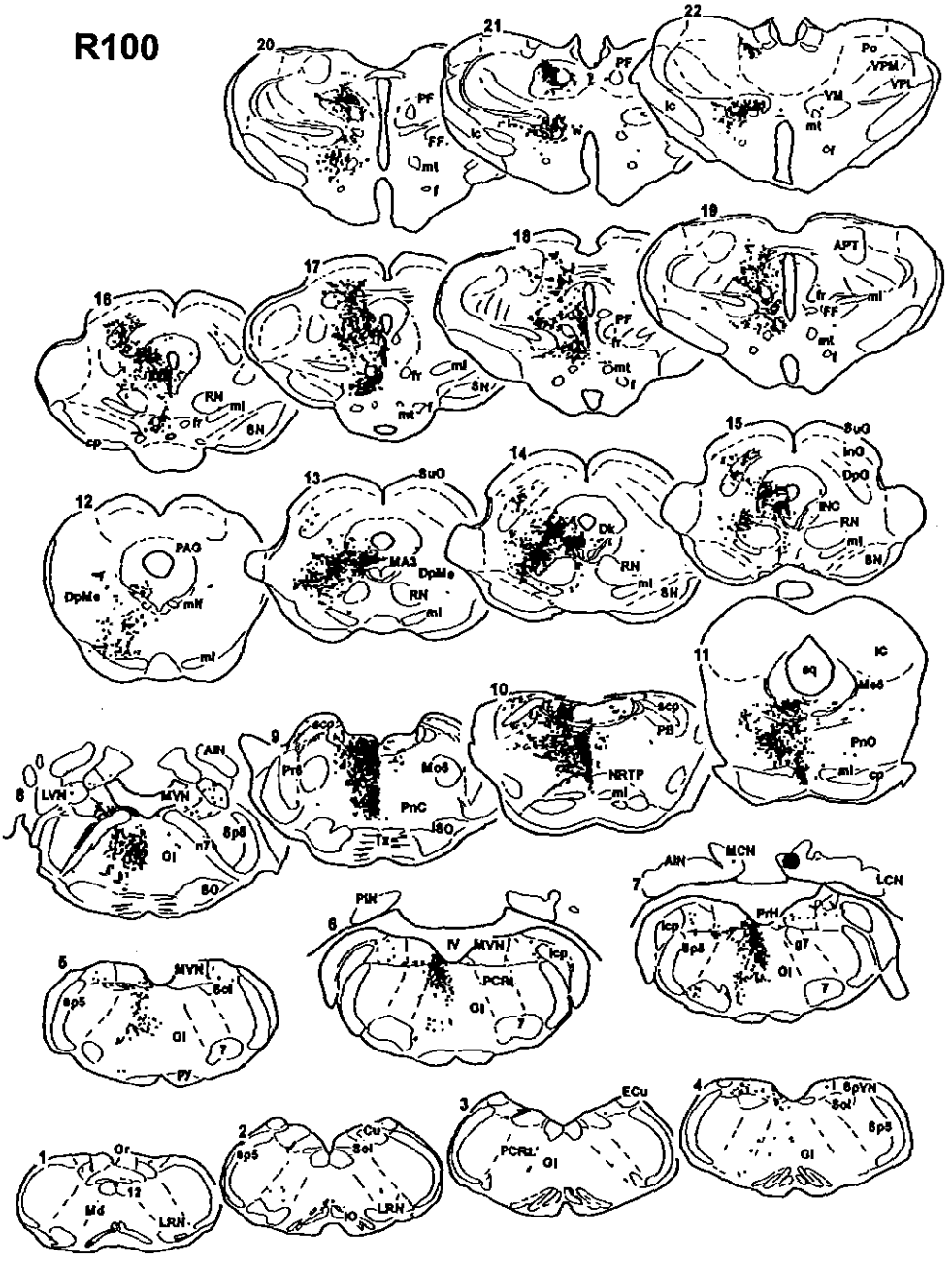
R100
20
21
22
PF
FF
mt
ic
Po
VPM
VPL
VM
ml
17
18
19
APT
fr
SN
RN
cp
12
PAG
DpMe
MA3
13
SuG
14
Dk
15
InG
DpG
INC
11
IC
eq
Me5
PnO
10
scp
PB
NRTP
9
Pr5
PnC
Tz
ISO
8
LVN
MVN
AIN
8ps
SO
7
MCN
LCN
PrH
6
PIH
IV
PCRt
5
Sol
PY
4
6pVN
3
ECu
PCRt
2
Cu
IO
LRN
1
Or
Md

Fig. 2.7

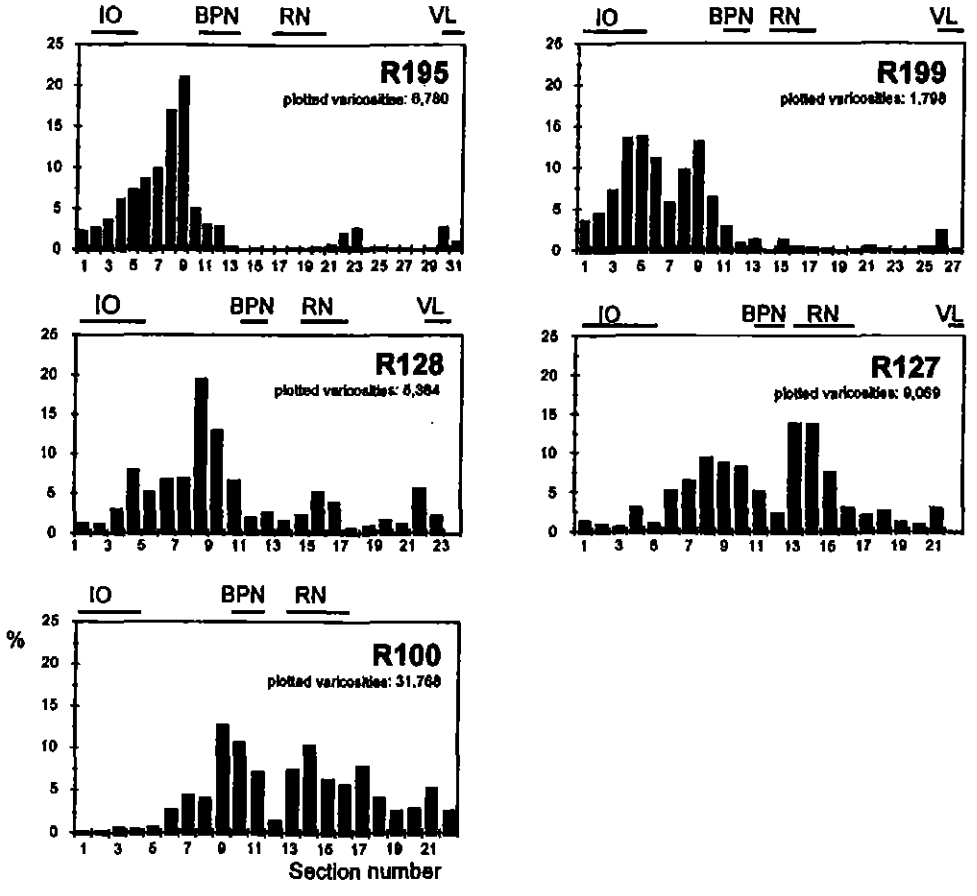
IO
BPN
RN
VL
R195
plotted varicosities: 6,780
R199
plotted varicosities: 1,798
R128
plotted varicosities: 8,384
R127
plotted varicosities: 9,069
R100
plotted varicosities: 31,768
%
Section number

Fig. 2.8

T82

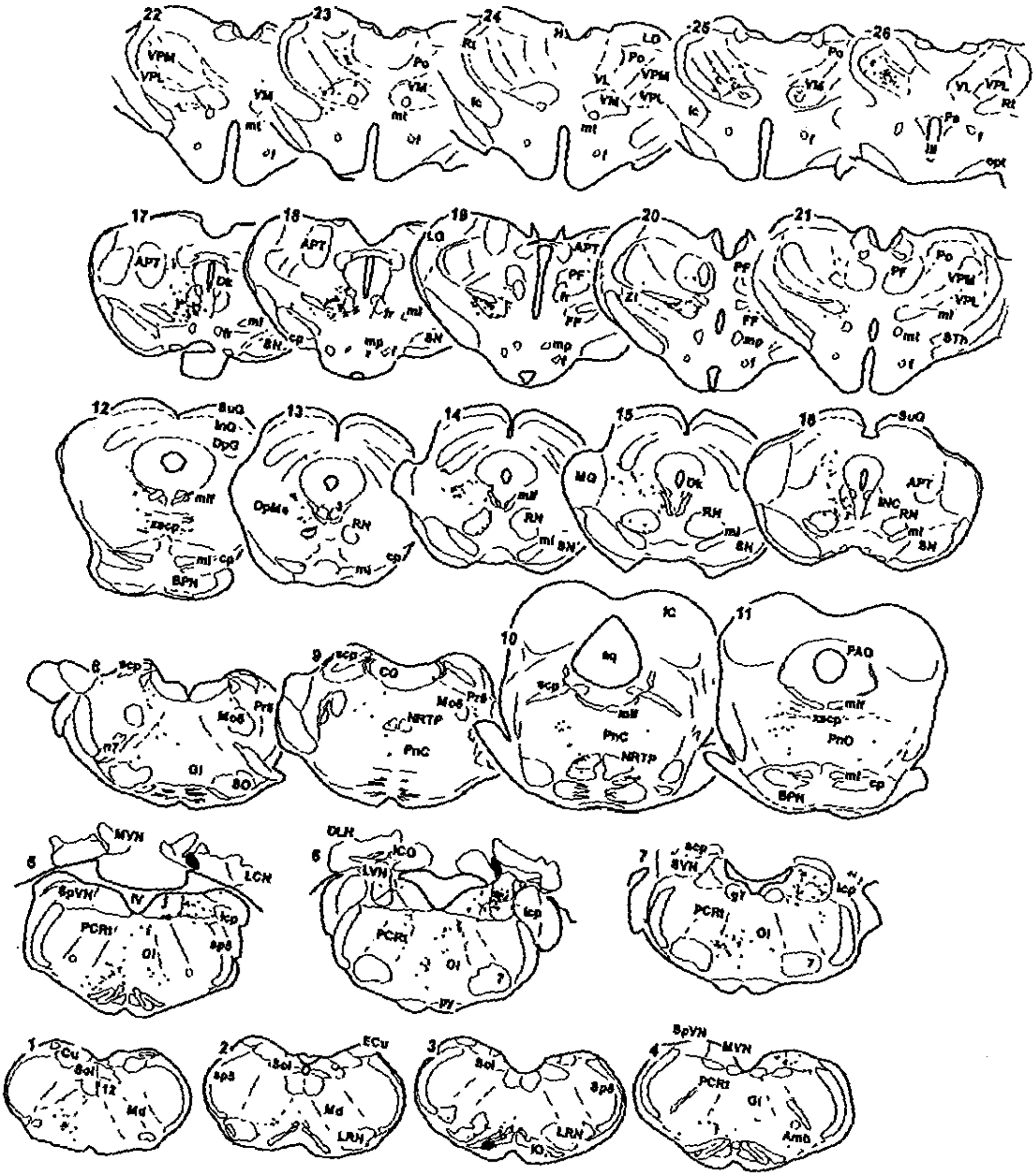
22
VPM
VPL
VM
mt
23
Po
VM
mt
24
Rt
LD
Po
VL
VPM
VM
VPL
ic
mt
25
Po
VM
ic
26
Po
VL
VPL
Rt
opt
17
APT
Dk
mt
SN
cp
18
APT
fr
ml
mp
SN
19
LG
APT
PF
fr
mp
20
PF
ZI
mp
21
PF
Po
VPM
VPL
ml
mt
STh
12
SuG
InG
DpG
mlf
xscp
ml
cp
BPN
13
OpMe
3
RN
ml
cp
14
mlf
RN
ml
SN
15
MG
Dk
RN
ml
SN
16
SuG
APT
INC
RN
ml
SN
8
scp
Pr5
Mo5
n7
Ol
SO
9
scp
CG
Mo5
Pr5
NRTP
PnC
10
IC
aq
scp
mlf
PnC
NRTP
11
PAG
mlf
xscp
PnO
ml
cp
BPN
5
MVN
LCN
SpVN
IV
icp
PCRt
Ol
sp5
6
DLN
ICO
LVN
icp
PCRt
Ol
7
py
7
scp
SVN
g7
icp
PCRt
Ol
7
1
Cu
Sol
12
Md
2
ECu
sp5
Sol
Md
LRN
3
Sol
sp5
LRN
IO
4
SpVN
MVN
PCRt
Ol
Amb

Fig. 2.9

T 79

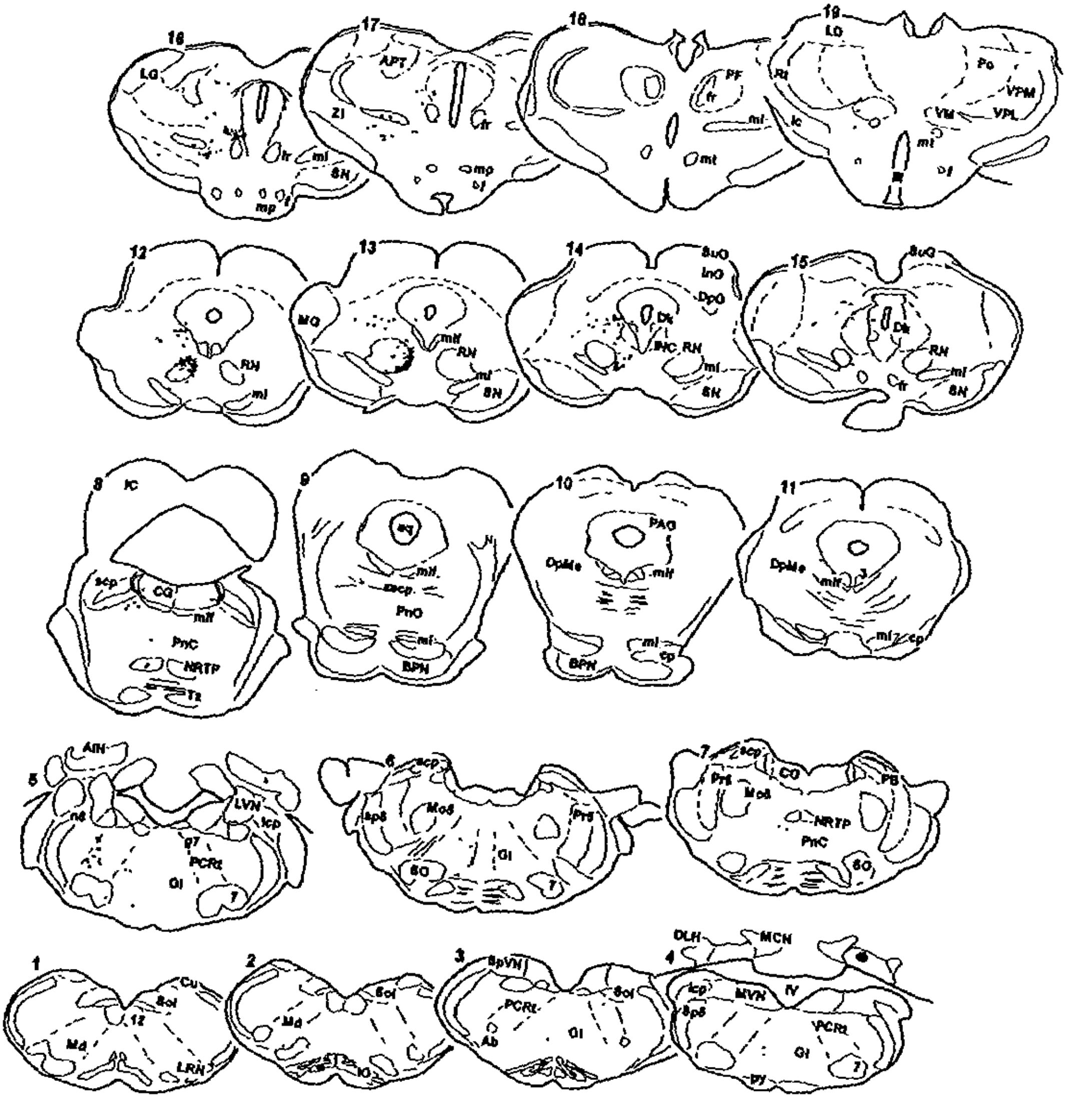
16
LG
fr
ml
SN
mp
17
APT
ZI
fr
mp
18
PF
fr
ml
19
LG
Rt
Po
VPM
VM
VPL
ic
ml
12
RN
ml
13
MG
mlf
RN
ml
SN
14
SuG
InG
DpG
Dk
INC
RN
ml
SN
15
SuG
Dk
RN
ml
fr
SN
8
IC
scp
CG
mlf
PnC
NRTP
Tz
9
aq
mlf
scp
PnO
ml
BPN
10
PAG
DpMe
mlf
ml
BPN
cp
11
DpMe
mlf
3
ml
cp
5
AIH
LVN
icp
g7
PCRt
Gi
7
6
scp
sp5
Mo5
Pr5
Gi
SO
7
7
scp
CG
Pr5
Mo5
PB
NRTP
PnC
SO
1
Cu
Sol
12
Md
LRN
2
Sol
Md
IO
3
SpVN
PCRt
Sol
Ab
Gi
4
DLH
MCN
icp
MVN
IV
Sp5
PCRt
Gi
7
py

Fig. 2.10


T109
23
Po
VPM
lc
mt
24
LD
H
VPL
VM
mt
25
VM
mt
10
26
mt
VL
cf
27
A
VL
Rt
lc
Cj
xopt
22
PF
Po
lp
VPM
VPL
ml
ZI
FF
mt
STh
cf
21
LG
Po
PF
FF
STh
mt
cf
20
APT
fr
FF
mp
cf
19
APT
fr
SN
mp
cf
18
ml
SN
fr
mp
17
SuG
NOT
APT
Dk
RN
ml
SN
16
MG
Dk
RN
ml
SN
15
mlf
RN
ml
SN
14
MA3
RN
ml
SN
13
SuG
InG
DpG
DpMe
3
mlf
ml
12
SuG
sp
DpMe
xscp
ml
BPN
11
IC
PAG
scp
PnO
ml
BPN
10
IC
scp
mlf
PnO
NRTP
9
scp
CG
PnC
Tz
SO
8
scp
Prs
MPB
Mo5
PnC
7
AIN
SVN
Bps
n7
6
MCN
AIN
LVN
icp
PCRt
Gl
7
5
AIN
MCN
LCN
icp
MVN
4V
SpVN
PCRt
Gl
7
py
4
MVN
SpVN
Sol
PCRt
Gl
3
ECu
Sol
Bps
Gl
2
ECu
Sol
DC
IO
1
12
Sol
Md
LRN

Fig. 2.11

T108

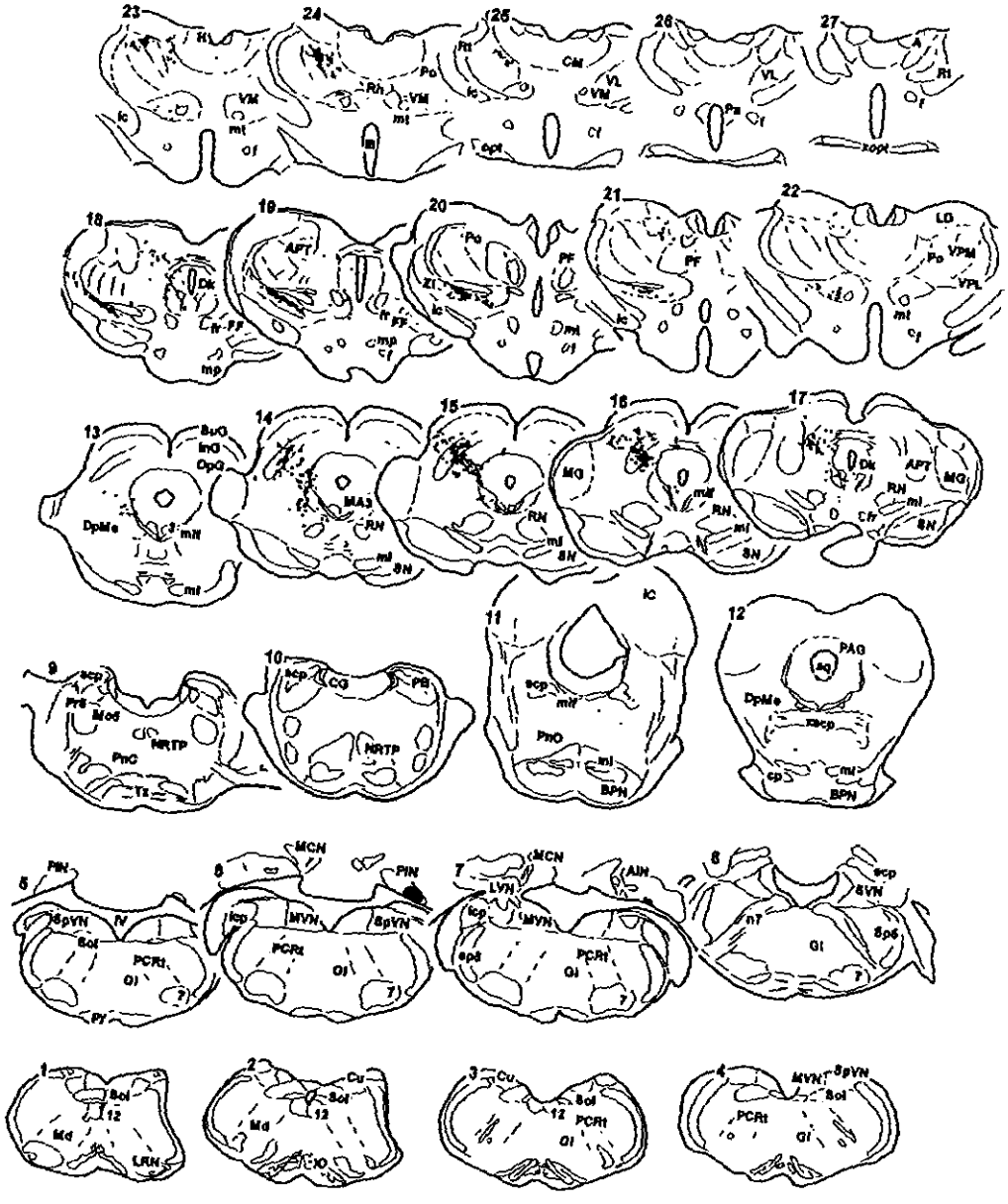

Fig. 2.12

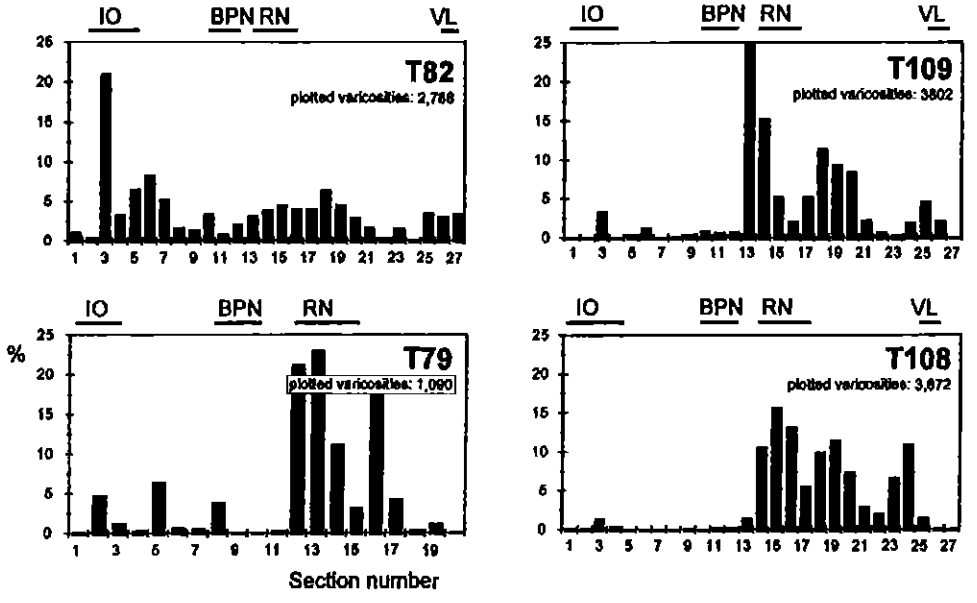
IO
BPN
RN
VL
T82
plotted varicosities: 2,766
T109
plotted varicosities: 3802
T79
plotted varicosities: 1,090
T108
plotted varicosities: 3,672
%
Section number

Fig. 2.13

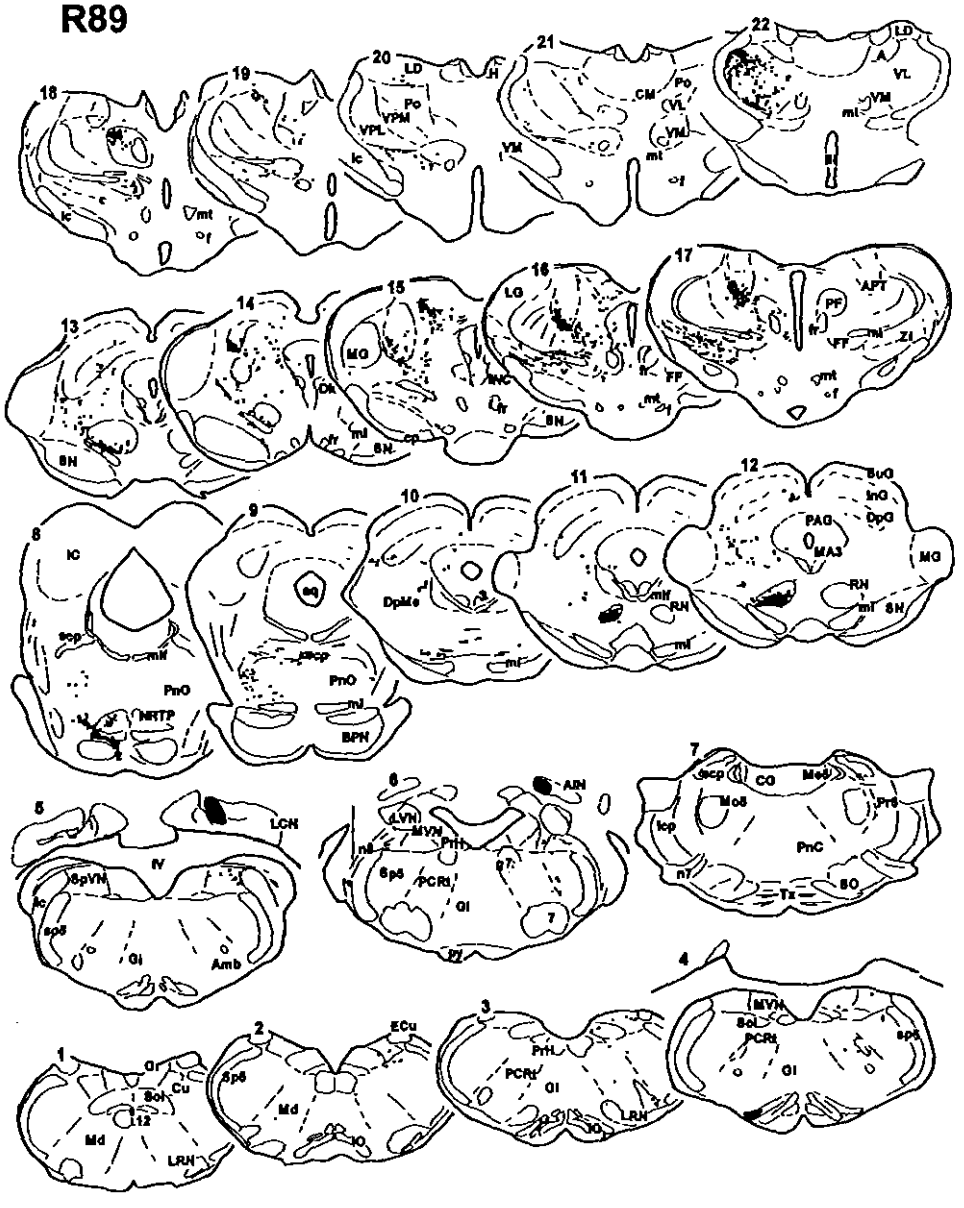
R89
18
19
20
21
22
LD
Po
VPM
VPL
VM
CM
VL
mt
ic
cp
13
14
15
16
17
MG
LG
APT
PF
Zi
SN
8
9
10
11
12
IC
scp
mlf
PnO
NRTP
BPN
DpMe
RN
PAG
MA3
SuG
InG
DpG
7
6
5
4
3
2
1
LCN
AIN
LVN
MVN
8pVN
8p8
PCRt
Gi
Amb
CG
Mo8
Pr8
PnC
Tz
SO
PrH
Sol
12
Md
LRN
IO
ECu
Cu

Fig. 2.14

T 83

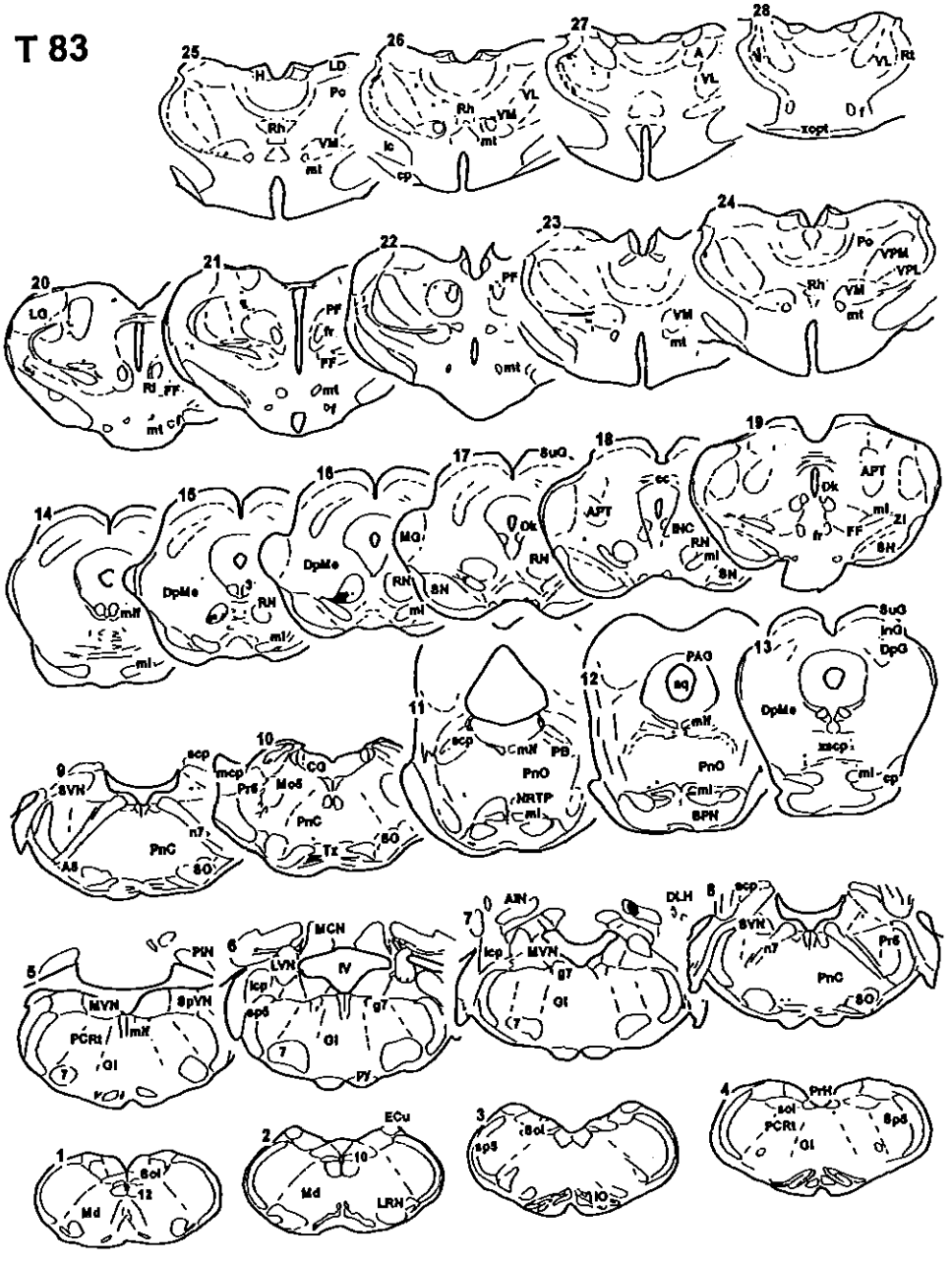
25
H
LD
Po
Rh
VM
mt
26
Rh
VL
VM
mt
lc
cp
27
A
VL
28
VL
Rt
Df
xopt
20
LG
Rt
FF
mt
cp
21
PF
fr
FF
mt
Dj
22
PF
mt
23
VM
mt
24
Po
VPM
VPL
Rh
VM
mt
14
mlf
ml
15
DpMe
RN
ml
16
DpMe
MG
RN
SN
ml
17
SuG
Ok
RN
18
ec
APT
BIC
RN
ml
SN
19
Ok
APT
ml
fr
FF
ZI
SN
9
scp
SVN
mcp
n7
PnC
AS
SO
10
CG
Pr5
MoS
PnC
Tz
SO
11
scp
cml
PB
PnO
NRTP
ml
12
PAG
sq
mlf
PnO
cml
BPN
13
SuG
inG
DpG
DpMe
xscp
cml
cp
5
PIN
MVN
SpVN
PCRt
mlf
7
GI
6
MCN
LVN
IV
lcp
sps
g7
7
PY
7
AIN
lcp
MVN
g7
GI
7
DLH
8
scp
SVN
n7
Pr5
PnC
SO
1
Sol
12
Md
2
ECu
10
Md
LRN
3
Sol
sps
IO
4
PrH
sol
PCRt
GI
Sps

Fig.2.15

R 98

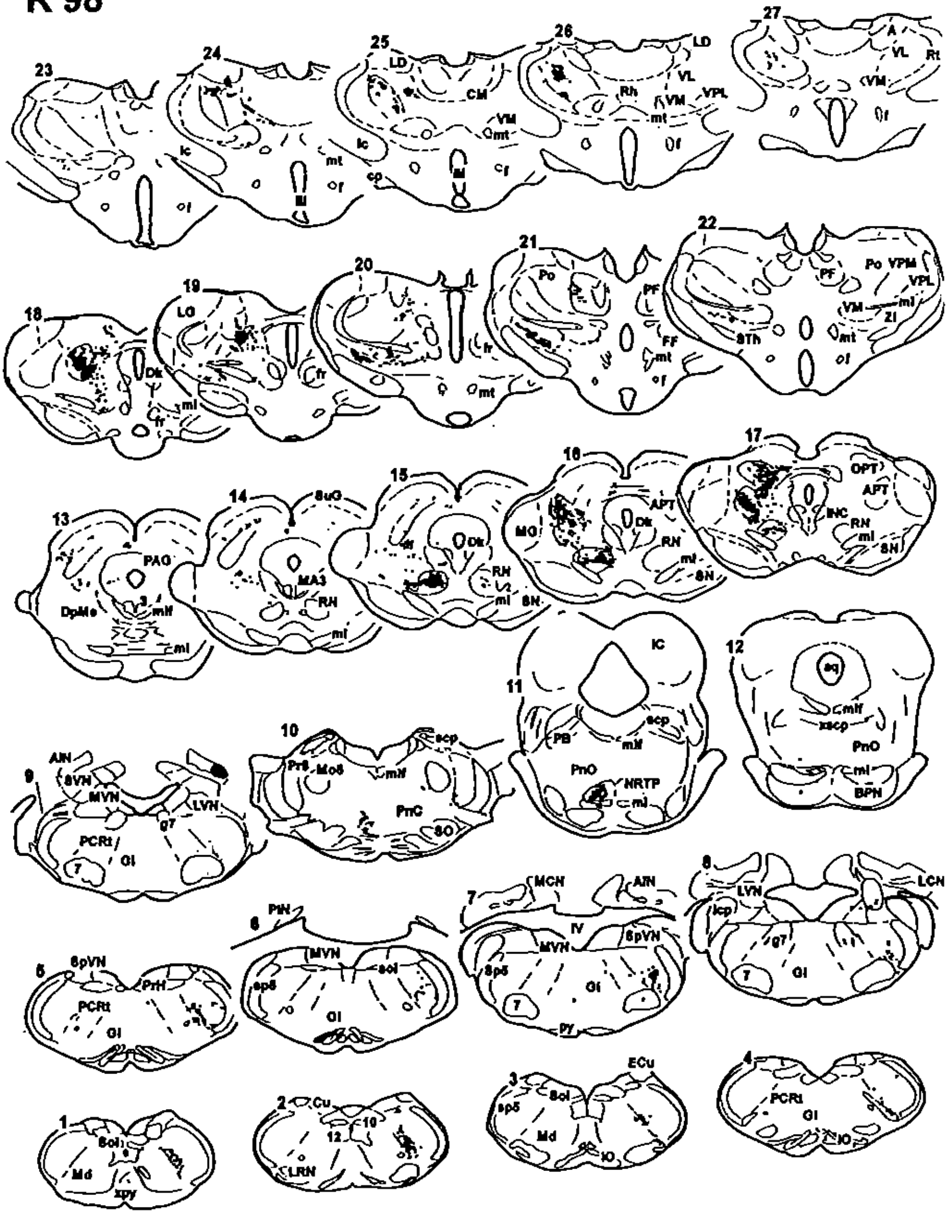

23
24
25
26
27
LD
CM
VM
mt
f
ic
cp
III
Rh
VL
VPL
A
Rt
18
19
20
21
22
LG
Dk
ml
fr
Po
PF
FF
VPM
ZI
STh
13
14
15
16
17
SuG
PAG
DpMe
mlf
MA3
RN
SN
MG
APT
OPT
INC
IC
11
12
aq
scp
xscp
PB
PnO
NRTP
BPN
9
10
AIN
SVN
MVN
LVN
g7
PCRt
Gi
7
Pr5
Mo5
PnC
SO
5
6
8
SpVN
PrH
PtN
sol
sp5
MCN
IV
Sp5
py
LCN
icp
1
2
3
4
Sol
Md
xpy
Cu
10
12
LRN
ECu
IO

Fig. 2.16

T 94-BDA

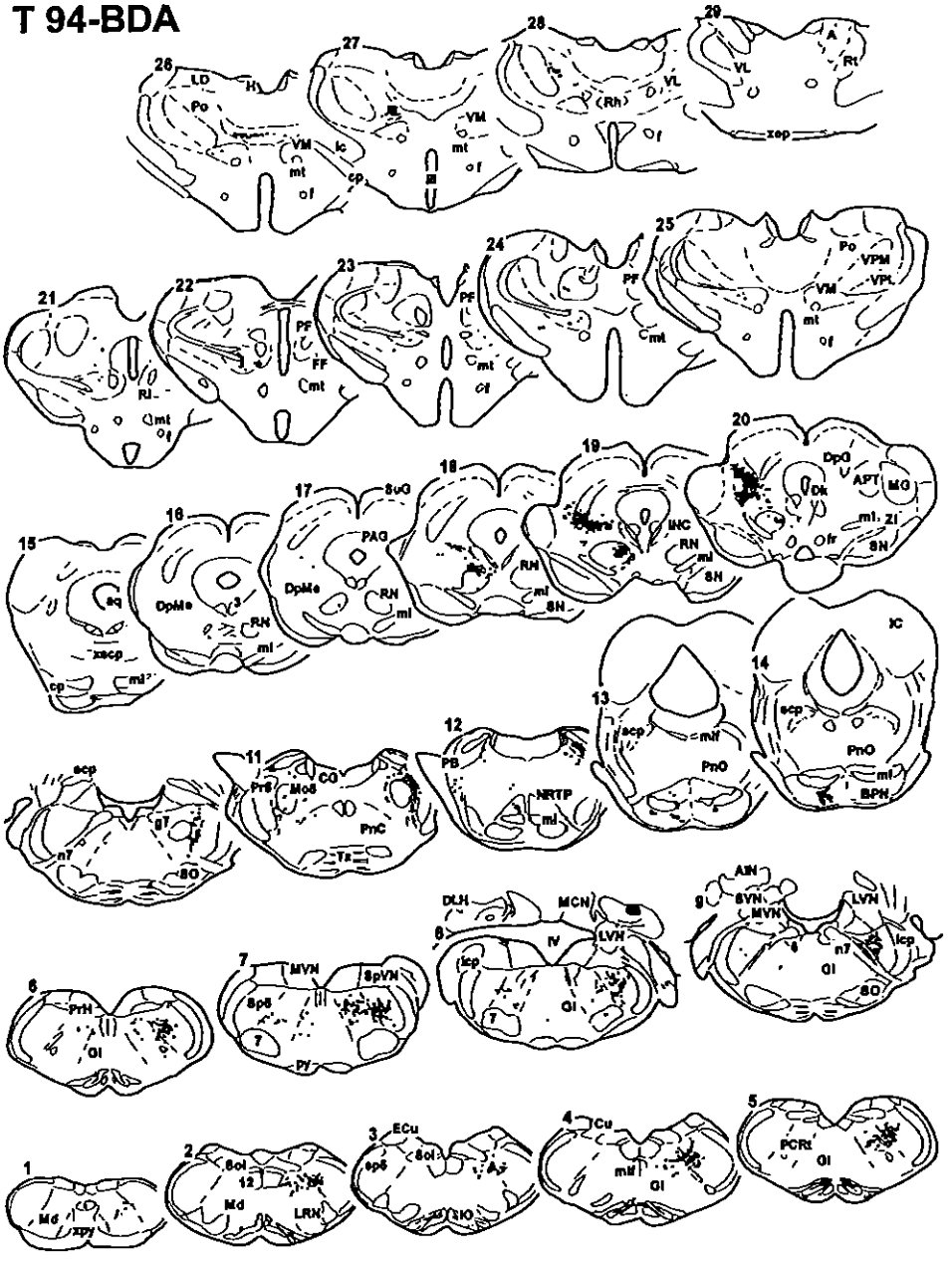

Fig. 2.17

R 138

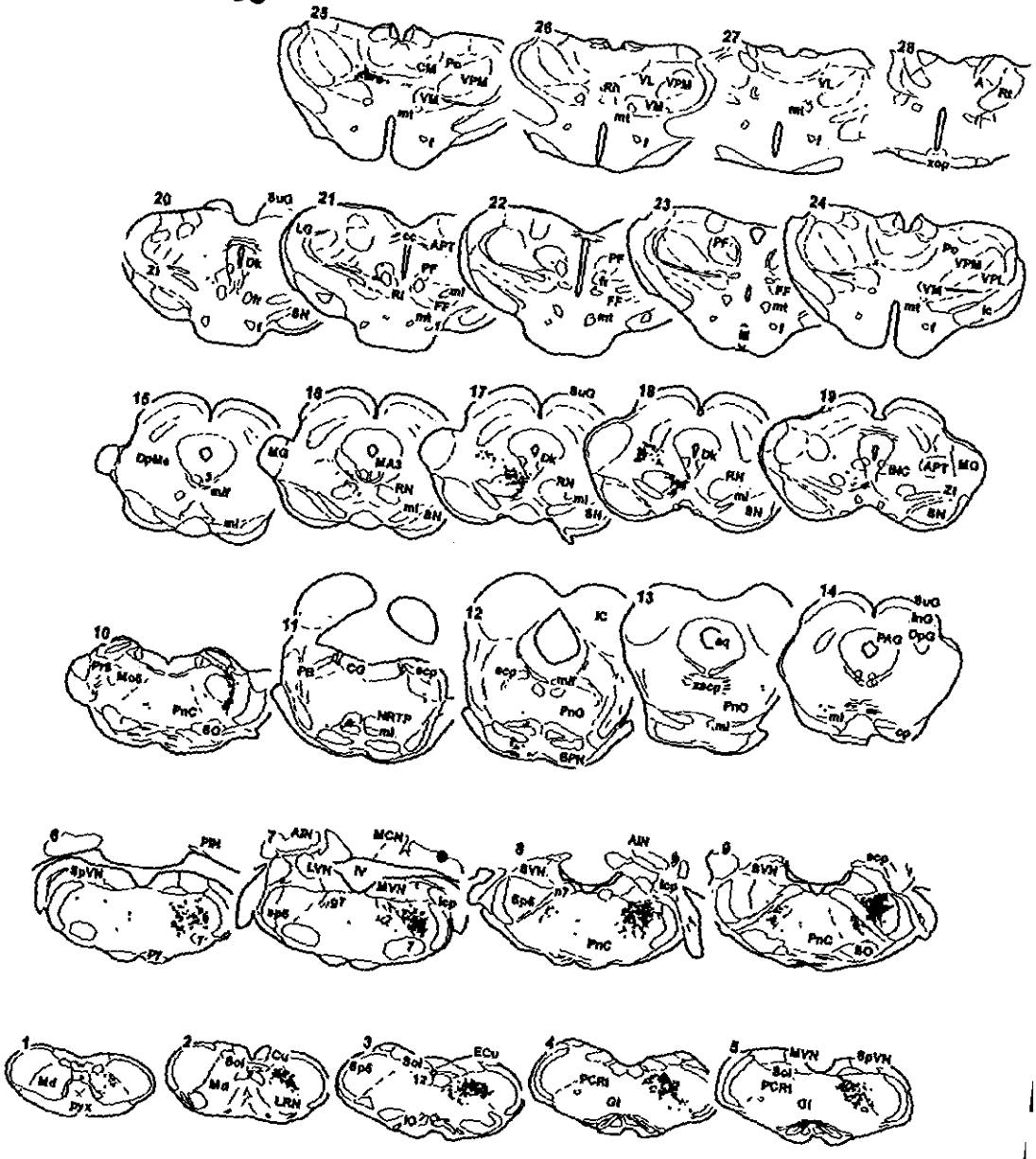

Fig. 2.18

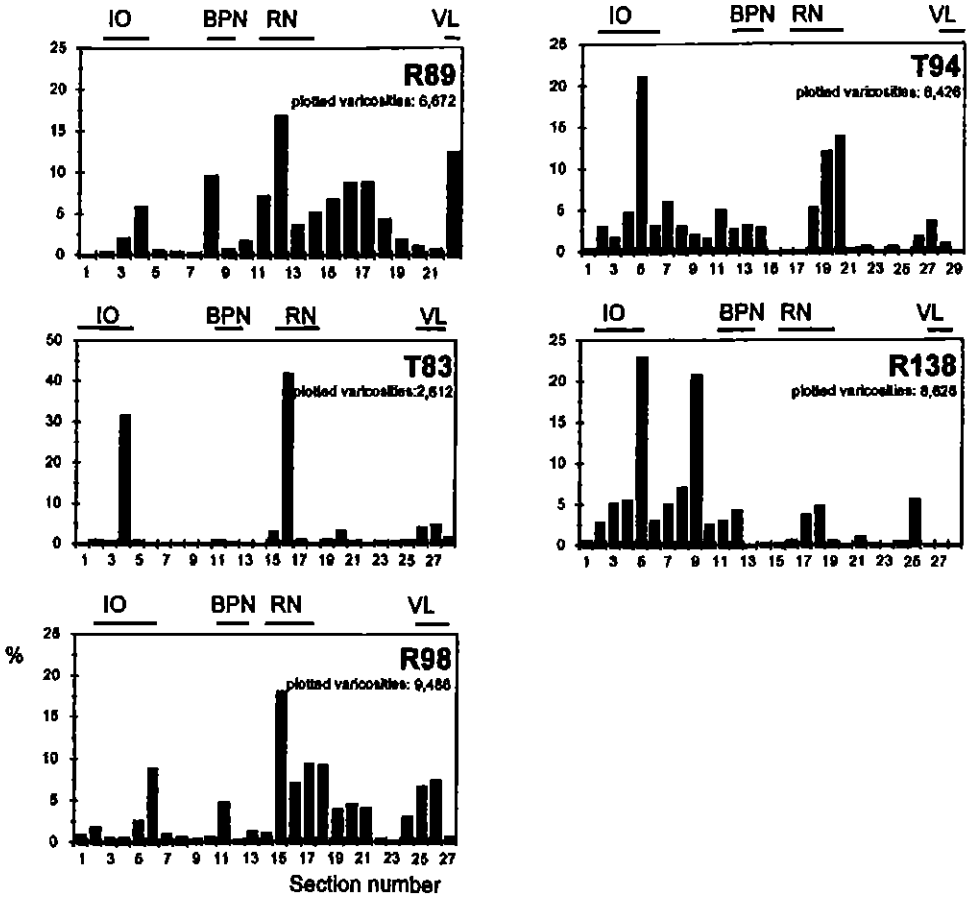
IO
BPN
RN
VL
R89
plotted varicosities: 6,672
T94
plotted varicosities: 8,426
T83
plotted varicosities:2,612
R138
plotted varicosities: 8,626
R98
plotted varicosities: 9,486
%
Section number

Fig. 2.19

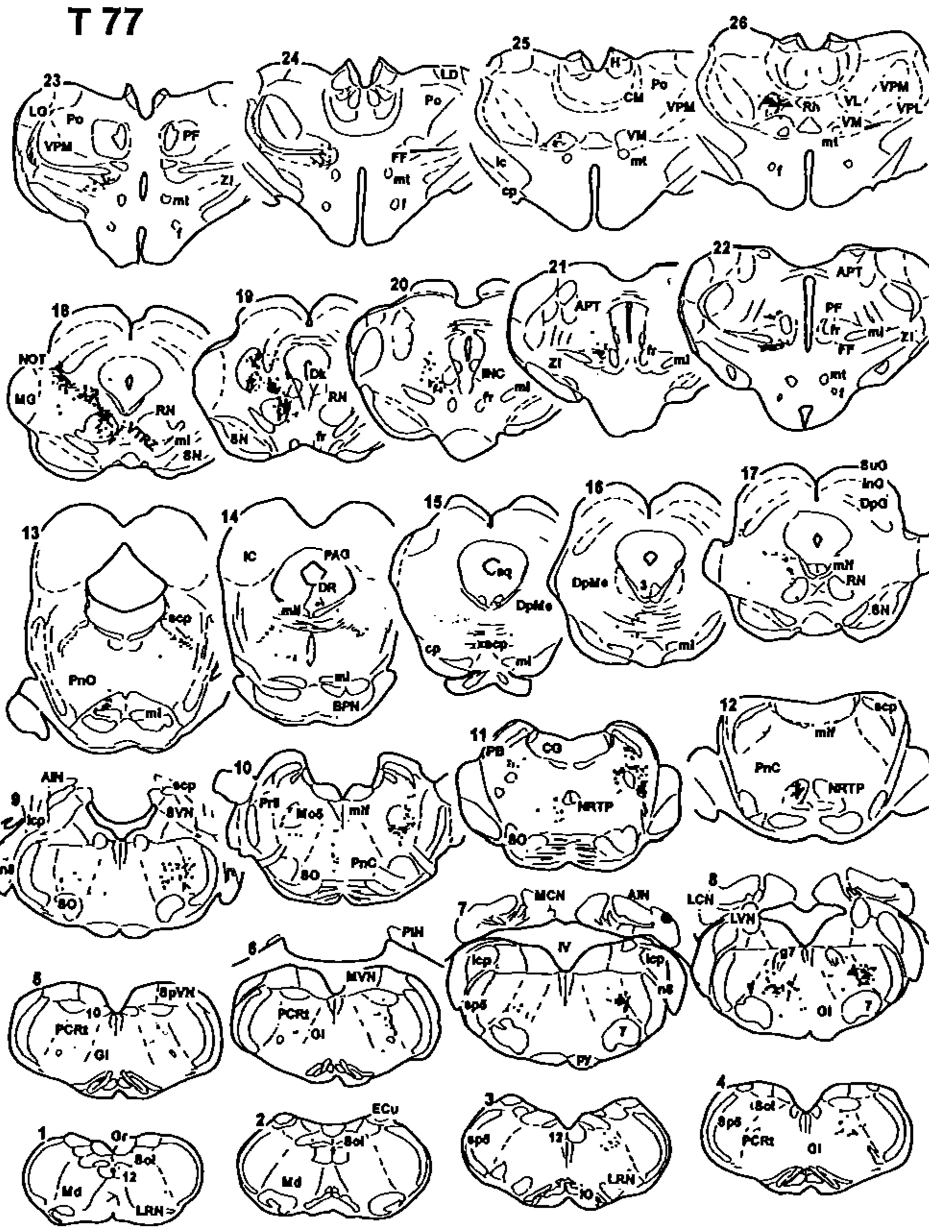
T 77
23
LG
Po
VPM
PF
ZI
mt
f
24
LD
Po
FF
mt
f
25
H
Po
CM
VPM
VM
mt
ic
cp
26
VPM
VPL
VL
VM
Rh
mt
f
18
NOT
MG
RN
VTRZ
ml
SN
19
Dk
RN
SN
fr
20
INC
ml
fr
21
APT
ZI
fr
ml
22
APT
PF
fr
ml
ZI
FF
mt
f
13
scp
PnO
ml
14
IC
PAG
DR
mlf
ml
BPN
15
aq
DpMe
cp
xscp
ml
16
DpMe
3
ml
17
SuG
InG
DpG
mlf
RN
SN
12
scp
mlf
PnC
NRTP
11
PB
CG
NRTP
SO
10
PrV
Mo5
mlf
SO
PnC
9
AIN
scp
SVN
icp
n8
SO
7
MCN
AIN
IV
icp
n8
sp5
7
py
8
LCN
LVN
g7
OI
7
6
PIN
MVN
PCRt
OI
5
SpVN
10
PCRt
OI
1
Gr
Sol
12
Md
LRN
2
ECu
Sol
Md
3
sp5
12
LRN
IO
4
Sol
Sp5
PCRt
OI

Fig. 2.20

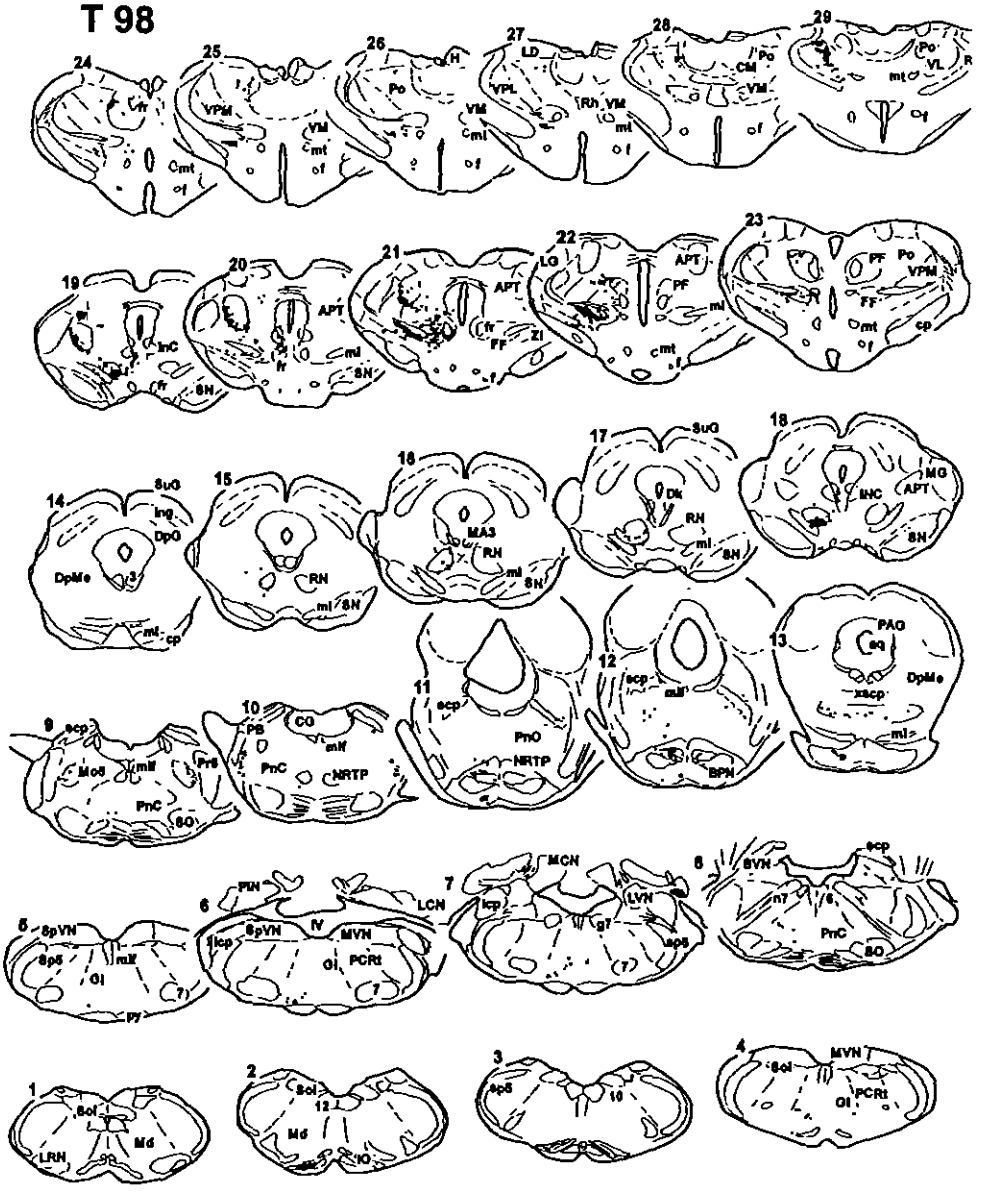
T 98
24
25
26
27
28
29
19
20
21
22
23
14
15
16
17
18
9
10
11
12
13
5
6
7
8
1
2
3
4
VPM
VM
Po
VPL
LD
CM
VL
APT
LG
PF
SuG
MG
DpMe
RN
MA3
RH
DK
PAG
PnC
NRTP
PnO
BPN
PB
CG
MCN
LCN
PTN
MVN
SpVN
LVN
SVN
PCRt
Sol
Md
LRN
IO
10
12

Fig. 2.21

R 178

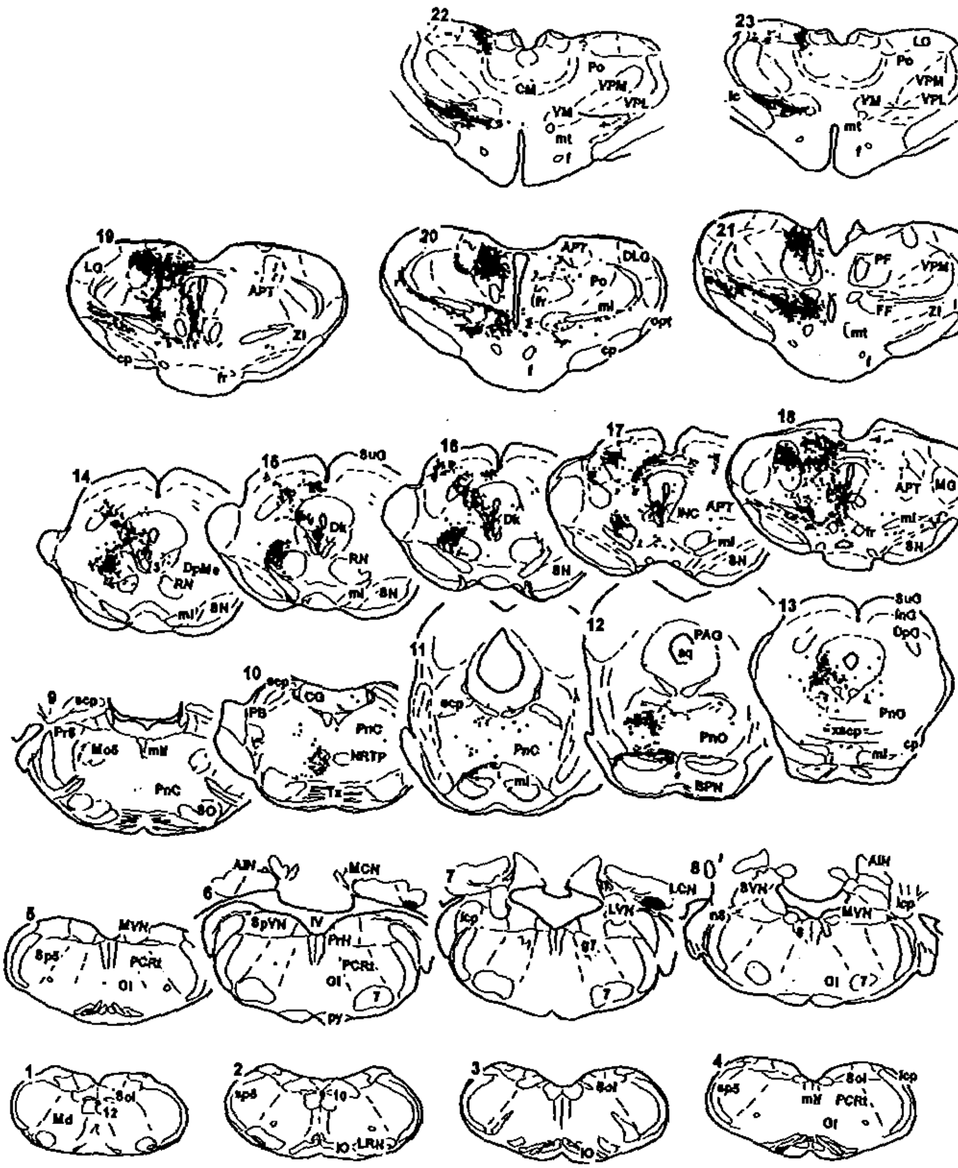
22
CM
Po
VPM
VPL
VM
mt
f
23
LG
lc
19
APT
ZI
cp
fr
20
DLG
ml
opt
21
PF
FF
14
DpMe
RN
SN
15
SuG
Dk
16
17
INC
18
MG
9
scp
Pr5
Mo5
mlf
PnC
SO
10
CG
PB
NRTP
Tz
11
12
PAG
aq
PnO
BPN
13
InG
DpG
xscp
5
MVN
Sp5
PCRt
GI
6
AIN
MCN
SpVN
IV
PrH
py
7
icp
g7
LVN
LCN
8
SVN
ns
1
Sol
Md
12
2
sp5
10
IO
LRN
3
4
mlf

Fig. 2.22

T 94-PhaL

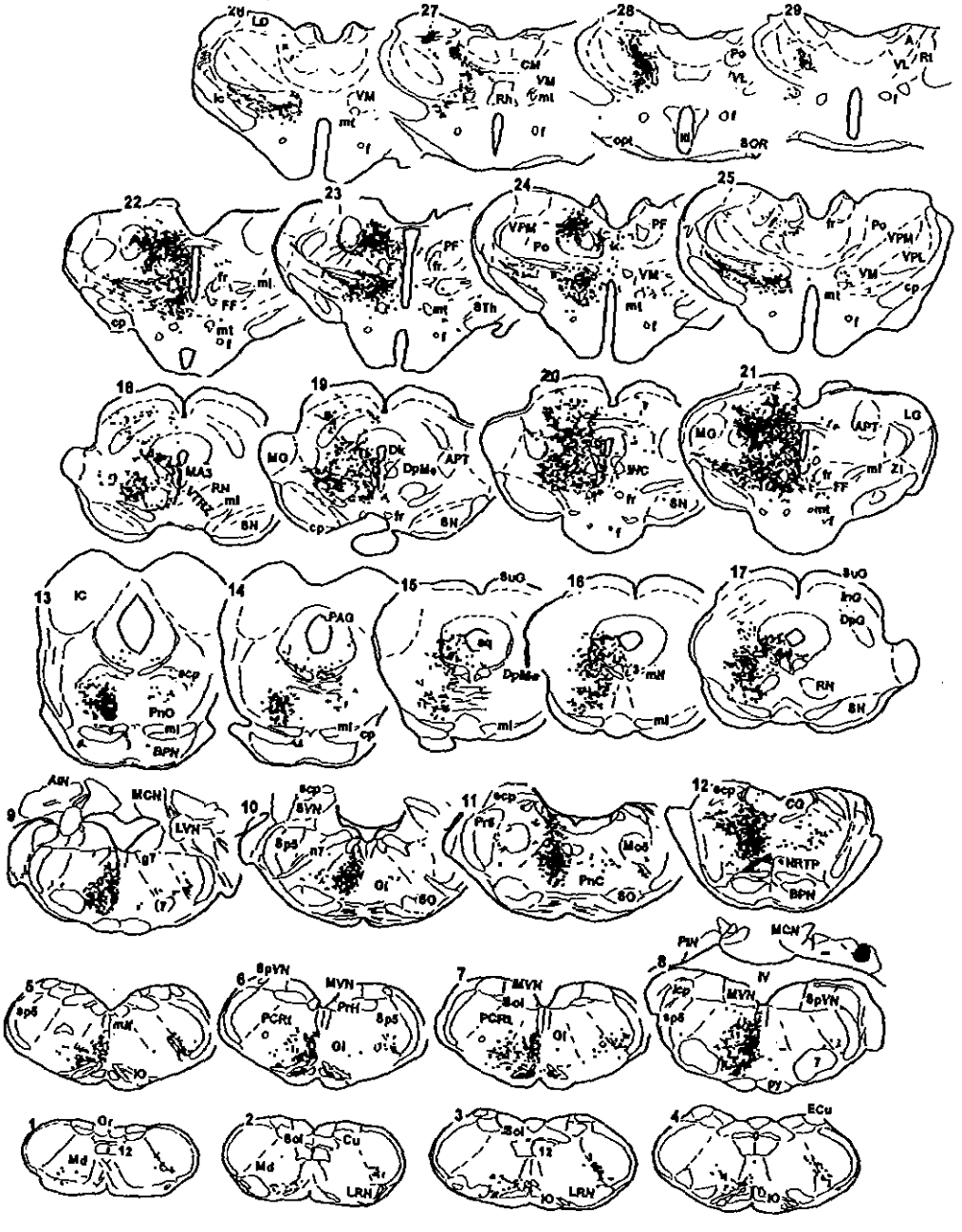

Fig. 2.23

R 133

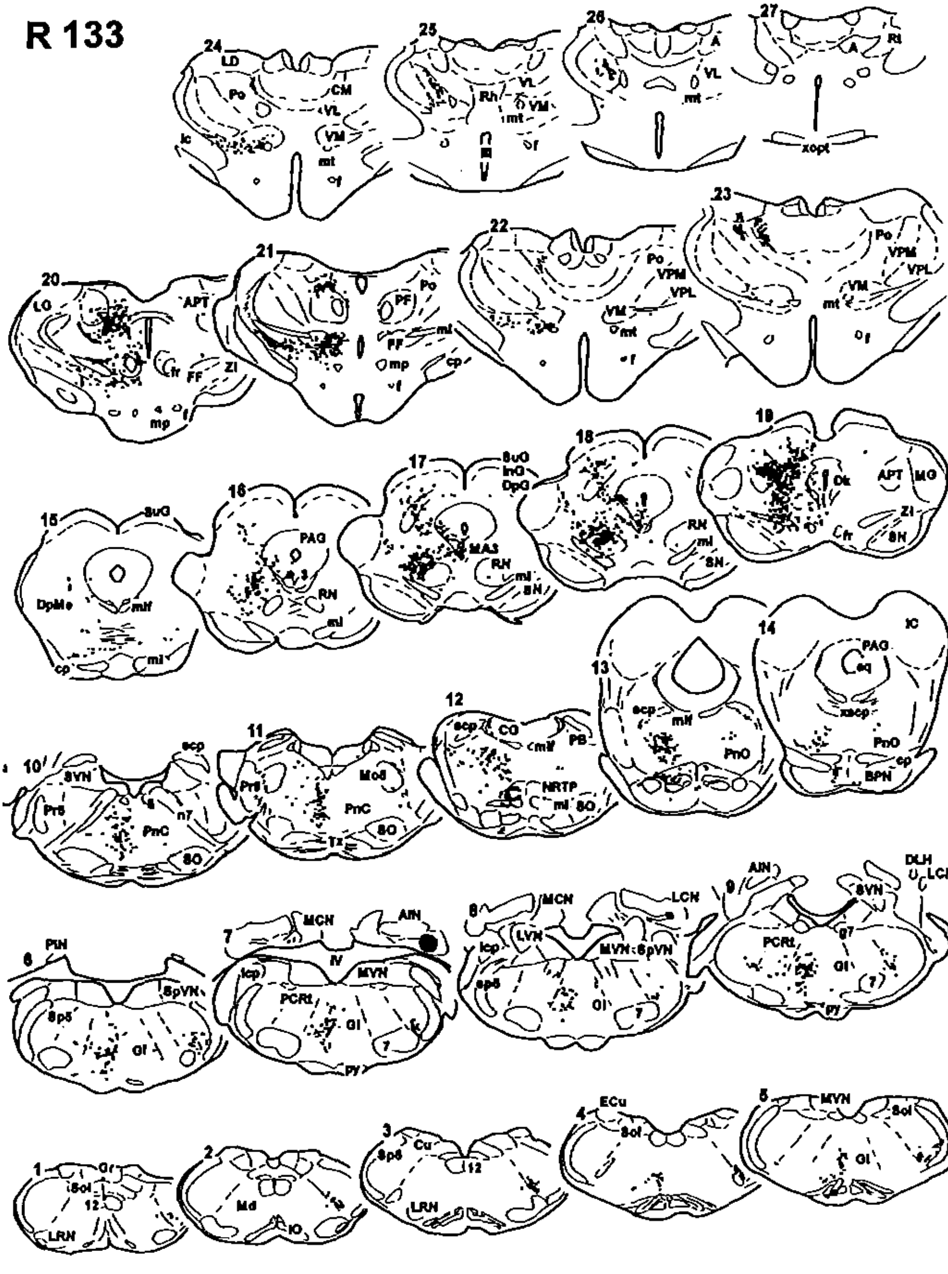

LD
Po
CM
VL
VM
mt
Rh
A
Rt
xopt
APT
PF
FF
ZI
mp
cp
VPM
VPL
SuG
InG
DpG
PAG
RN
ml
SN
MA3
APT
MG
DpMe
mlf
IC
aq
PnO
BPN
scp
CO
PB
NRTP
SO
SVN
Pr5
PnC
Mo5
Tz
PtN
SpVN
Sp5
Gi
MCN
AIN
IV
MVN
PCRt
py
LCN
LVN
icp
DLH
ECu
Sol
Cu
Gr
12
LRN
Md
IO

Fig. 2.24

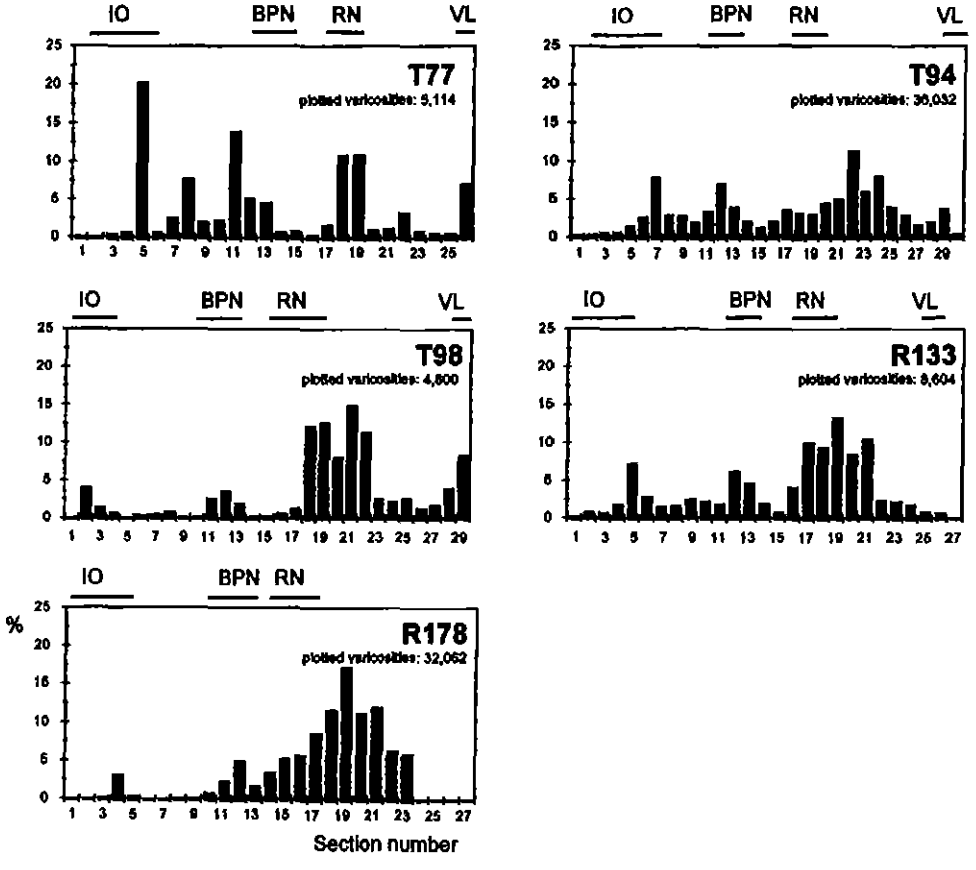
IO
BPN
RN
VL
T77
plotted varicosities: 9,114
T94
plotted varicosities: 36,032
T98
plotted varicosities: 4,800
R133
plotted varicosities: 8,604
R178
plotted varicosities: 32,052
%
Section number

Fig. 2.25

CHAPTER 3:
A RETROGRADE DOUBLE LABELING TECHNIQUE FOR LIGHT MICROSCOPY

A combination of axonal transport of cholera toxin B subunit and a gold lectin conjugate

T.J.H. Ruigrok , T.M. Teune, J. van der Burg, H. Sabel-Goedknegt

Journal of Neuroscience Methods 61 (1995) 127-138

Abstract

A light microscopical, non-fluorescent, retrograde double-labeling technique is described. Cholera toxin B subunit (CTb) and a conjugate of wheatgerm agglutinin and bovine serum albumin coupled to 10 nm gold particles (gold-lectin) are both excellent retrograde tracers and, when visualized by means of immunohistochemistry and silver intensification, respectively, may be readily identified within the same cell.

This light microscopical retrograde double-labeling technique is illustrated in rat with experiments designed to investigate the collateralisation (1) of vestibular neurons to the spinal cord and oculomotor complex, (2) of spinal neurons to the left and right lateral reticular nucleus, and (3) of inferior olivary neurons to the uvula of the cerebellum.

Advantages over fluorescent double-labeling experiments are found in the fact that the diaminobenzidine reaction product as well as the silver/gold deposits do not fade and can be examined in counterstained sections. Moreover, the injection sites can be kept quite small and may be guided by electrophysiological recording through the injection pipette.

Introduction

The introduction of the fluorescent retrograde double-labeling technique by Kuypers and collaborators (Bentivoglio *et al.*, 1980a; 1980b; Huisman *et al.*, 1983; Keizer *et al.*, 1983; Kuypers *et al.*, 1980; 1977) has aided neuroanatomical research enormously since it became possible to study the collateralisation of axons. More recently, the number of fluorescent tracers to choose from has increased dramatically and made triple or multiple retrograde labeling possible. Combinations of fluorescent tracers with wheatgerm agglutinated-horseradish peroxidase (WGA-HRP) have been employed also (Kitao *et al.*, 1989; Wigston and Kennedy, 1987). However, there are a number of disadvantages in employing fluorescent tracers. The analysis of the material is usually arduous since it has to be performed with the aid of fluorescence microscopy in which cytoarchitectural boundaries are difficult to identify. When tracers are used with different excitation wavelengths, filters may have to be changed. Moreover, fluorescence is prone to fading, especially after prolonged storage or illumination. In addition, fluorescent tracers are known to be rather toxic to both the animal (they may result in considerable tissue necrosis, see e.g. Keizer *et al.*, 1983) and the environment, and are, with some exceptions, difficult to dissolve. Because of this last property, injections with these fluorescent tracers (such as Fast Blue, Diamino Yellow and Nuclear Yellow) frequently result in large injection sites. Finally, it is usually not possible to record neuronal activity through the injection pipette to help establishing the optimal injection site.

For these reasons we searched for a combination of two retrogradely transported tracers that: (1) are both

easily detected with the light microscope; (2) are readily differentiated from one another even when present in the same neuron; (3) can be combined with counterstaining; (4) can be deposited in small-sized injection sites; (5) allow recording of neuronal activity through the injection pipettes.

We report here that the combination of cholera toxin B subunit (CTb) and a goldsol coupled to the lectin WGA that was conjugated to bovine serum albumin (BSA) fulfills these demands. The use of CTb as a retrograde tracer was introduced by Luppi (1990) and gold-lectin conjugates have first been used by Menétrey (1985; Menétrey and Lee, 1985).

Methods

Preparation and injection of tracers

1. Cholera toxin B subunit

Retrograde tracing with CTb results in the visualization of the soma and a large part of the dendritic tree of the labeled neurons (Luppi *et al.*, 1990; Shinonaga *et al.*, 1992). In addition, CTb is known to be transported in an anterograde fashion. We used iontophoretic injections of CTb as originally published by Luppi (Luppi *et al.*, 1990). However, since we predominantly made use of the low-salt variety of CTb (List Biological Lab Product #104, lot #CVXG-1SA), there was no need to desalt and exchange buffers. Thus, 0.5 mg of lyophilized CTb was dissolved in 50 µl of distilled water to a final concentration of 1% CTb in 0.2 M sodium phosphate (pH 7.5), which were aliquotted in 4 µl quantities and stored in the freezer.

Glass micropipettes containing an inner filament (outer diameter: 2 mm; Clark Electromedical Instruments) with tips broken at 12-15 µm were backfilled with the aliquotted CTb solution using a Hamilton syringe. The micropipette was connected to a 1.0 ml syringe with a Luer Lock adapter for catheters (Unimed, Geneva, Switzerland) and pressure was applied manually to the back of the micropipette to the point were CTb solution oozed out of the pipette tip. In this way, air bubbles trapped in the shank of the pipette were removed. A silver wire, insulated except for the tip, connected the solution with a Grass preamplifier.

Electrophysiological recordings were conventionally monitored and stored on tape (Fig. 3.1). After determination of the injection location, the pipette was connected to an iontophoresis device, capable of delivering constant positive current pulses (7 s on, 7 s off) of 4 µA for a period of 15-30 min. At the end of this period, the pipettes were left in situ for 5-10 min to minimize leakage of the tracer along the pipette track. In some types of experiments CTb was pressure-injected (e.g., in the spinal cord).

2. Goldsol coupled to WGA-BSA conjugate

Gold-lectin conjugates have been introduced as a neuroanatomical tracer by Menétrey and colleagues (Basbaum and Menétrey, 1987; Menétrey, 1985; Menétrey and Lee, 1985) and have been demonstrated to

be transported in a strictly retrograde direction (Llewellyn-Smith *et al.*, 1992). Initially, goldsol was coupled to WGA-HRP or WGA-apoHRP. Here, we report that 10 nm goldsol (Aurion) coupled to a conjugate of WGA and BSA also acts as an excellent, but much cheaper, retrograde tracer. The following steps (modified after Roth, 1983) were performed to prepare a tracer of a good, reproducible, quality.

Step I: preparation of the WGA-BSA conjugate. Dissolve 1 mg WGA (Sigma) and 4 mg BSA in 0.25 ml of 0.005 M NaCl. Adjust pH to 7.0 with either 0.2 M H_3PO_4 or 0.2 M K_2CO_3. Add 50 Al of 0.25% glutaraldehyde (E.M. grade) and stir for 2 h at room temperature. Finally, add 12.2 ml of 0.005 M NaCl and dialyze overnight in 0.005 M NaCl. Total volume of the protein solution is 12.5 ml and contains 5 mg of protein.

Step 2: preparation of the WGA-BSA-gold conjugate.

Prepare the following solutions in clear glass or plastic vials:

90 µl of protein + 10 µl of 0.005 M NaCl;
70 µl of protein + 30 µl of 0.005 M NaCl;
50 µl of protein + 50 µl of 0.005 M NaCl;
30 µl of protein + 70 µl of 0.005 M NaCl;
10 µl of protein + 90 µl of 0.005 M NaCl.

Adjust 10 nm colloidal gold solution (Aurion) to pH 9.9 (with 0.2 M K_2CO_3) and add 1 ml of goldsol to each vial. Vortex and wait for 2 min. Determine which vial remains just clear and use this combination of protein content and goldsol solution to prepare the definite WGA-BSA-gold conjugate. In this way, we usually found that 3.75 ml of the protein conjugate should be added to 85 ml of the pH-adjusted goldsol. Other protein/goldsol volume combinations also yielded qualitatively good tracers. Stir for 2 min and add 1% Carbowax (PEG 20M) to a final concentration of 0.05%.

Centrifuge at 45000 g for 30 minutes. Aspirate and discard supernatant, leaving approximately 10% of the initial volume. Add Carbowax 0.05% to original volume, resuspend loose part of sediment and centrifuge again at 45,000 x g for 30 min.

Carefully aspirate the supernatant, leaving in total approximately 50-100 µl of the WGA-BSA-gold conjugate, which can be used for injection. The conjugate can be stored for several months at 4 °C without losing its retrograde transport capabilities.

Gold-lectin conjugates are not suited to be delivered iontophoretically. Therefore, in order to be able to make restricted injections a pressure device was used (Gibson *et al.*, 1987). A small amount (about 1 µl) of the WGA-BSA-gold solution was sucked into a glass micropipette (tip diameter: 12-15 µm) by applying vacuum to the back of the pipette, which was Luer-locked to the pressure delivering device (Fig. 3.1). We empirically established that electrophysiological recordings through the WGA-BSA-gold solution could be made possible by introducing a thin (diameter: 75 µm) and except for the very tip, insulated silver wire into the pipette prior to filling (Fig. 3.1).

After establishing the optimal injection location, pressure pulses of varying intensity were applied to inject the tracer. The total injected volume (in nl) was estimated to be equal to $1/4\pi d^2h$, where d is the approximate diameter (in mm) of the gold-lectin meniscus in the shank of the injection pipette and h the displacement (in mm) of the meniscus during injection. In this way, volumes ranging between 10 and 1000 nl WGA-BSA-gold could be reliably injected.

Surgical procedure

Injections were made in male Wistar rats (200-250 g) which had been anesthetized with pentobarbital (120 mg/kg, i.p.) and were mounted in a stereotactic device. Injection sites were roughly determined with the aid of the stereotactic atlas of Paxinos and Watson (1986) but were verified by recording neuronal activity typical of region to be injected through the injection pipette. Target areas were combinations of inferior olivary nucleus, lateral reticular nucleus, cerebellar cortex, oculomotor area and cervical spinal cord. These areas were reached by drilling a hole in the parietal bone (oculomotor area) or by enlargement of the foramen magnum dorsalwards (after retraction of neck muscles from the squamosal part of the occipital bone) and opening of the dura mater and reflecting it laterally. The spinal cord was reached by performing a laminectomy at C4 or C5.

After both injections were made, the wounds were sutured, and the rats were allowed to recover from surgery. All rats were able to eat and drink at the first postoperative day and could move freely within their cages. Nevertheless, they were checked daily in order to be able to provide pain medications if behavior would indicate so. Depending on the length of the studied pathways, the rats survived for 3-8 days.

Perfusion

Prior to perfusion, the rats were given a lethal dose of sodium pentobarbital (200 mg/kg). The brain was perfusion-fixed by cannulation of the ascending aorta and by subsequent infusion of 200 ml of 0.05 M phosphate buffer (pH 7.4) containing 0.8% NaCl, 0.8% sucrose and 0.4% glucose followed by 1000 ml of fixative made up of 4% freshly prepared paraformaldehyde and 0.1% glutaraldehyde in 0.05% phosphate buffer containing 4% sucrose. After perfusion the brain and spinal cord were extracted and postfixed in the same fixative for 3-5 h. They were rinsed and stored overnight in 10% sucrose in phosphate buffer, embedded in gelatin (10%) which was hardened for 3 h in formaldehyde (4% and containing 30% sucrose) and again stored overnight in 30% sucrose in phosphate buffer.

Histology

Sections were serially cut at 40 µm on a freezing microtome and collected in glass vials containing 0.05 M phosphate buffer (pH 7.4). Due to the high density of the black gold particles, the location and size of the WGA-BSA-gold injection site could be easily evaluated during cutting. Cases with clearly misplaced WGA-BSA-gold

injections could be discarded already at this stage. Free-floating sections were incubated in anti-CTb (1:15,000; List Laboratories) in Tris buffer containing 0.5 M NaCl and 0.5% Triton X-100 (TBS +, pH 8.6) for 3 nights and days (at 4 °C). The sections were subsequently incubated in biotinylated donkey anti-goat (B-DAG, List Laboratories; 1:2000 in TBS +) for 2 h, rinsed and reacted with the avidine biotine complex (ABC Elite kit, Vector) for 2 h and, finally, reacted with diaminobenzidine (DAB: 37.5 mg in 150 ml of Tris-HCl, pH 7.6, with 25 µl 30% H_2O_2) for 30 min. Enhancement of the WGA-BSA-gold label was achieved with silver intensification (Aurion) which was performed on floating sections after the CTb immunohistochemistry. Sections were subsequently mounted serially on chrome-gelatinized glass slides, air dried, counterstained with thionin, cleared in xylene and coverslipped with Permount.

Results

Recording of neuronal activity through the injection pipette

One of the advantages of the currently used tracers is the possibility to make small injections. However, when doing so, the exact location of the injection is very important. Therefore, relying on stereotactic coordinates may result in wrong placements. Hence, recording of neuronal activity through the injection pipette may aid in determining the exact location of tracer injection. Multi-unit, but also single-unit, recordings may be obtained with CTb-filled as well as with WGA-BSA-gold-filled pipettes as is shown for recordings made within the cerebellar cortex and inferior olive (Fig. 3.2). Although the signal-to-noise ratio is better for the CTb pipette, the slow and irregular spontaneous firing of olivary action potentials (Ito, 1984) can also be registered and appreciated with the WGA-BSA-gold pipette. Using these recordings it was possible to make selective injections with one tracer in the rostral part of the medial accessory olive and place the other one in caudal part of the same olivary subdivision or to place one tracer in the dorsal accessory and the other one in the medial accessory olive at the same rostrocaudal level without making more than 1 or 2 injection tracks for each tracer. With the objective of studying the collateralization of olivocerebellar fibers it turned out to be useful to rely on recordings of complex spike activity, typical for Purkinje cells, in order to be able to deliver both tracers, directly adjacent to one another, in the uvula of the cerebellar cortex without the risk of injecting only the white matter or granule cell layer (Fig. 3.5).

Injection sites

Cholera toxin B subunit

CTb was routinely delivered iontophoretically. We used the low-salt CTb (List) although initially a number of iontophoretic injections were made with normal CTb that was desalted according to Luppi (1990). In both cases the injection site appeared similar and conformed to the

description given by Luppi et al. (Figs. 3.3A and 3.5A). From the small and circumscript injection site numerous axons could be traced either distally into their terminals or proximally unto their somata, indicating that CTb is transported in anterograde as well as retrograde direction. However, and in contrast to the observations by Luppi (1990), we are not convinced that passing, undamaged fibers do not take up and transport CTb, e.g., when CTb was injected into the inferior olive, especially after longer survival times, labeled neurons could be seen within the contralateral inferior olive as well as labeled climbing fibers within the ipsilateral cerebellar cortex. However, the staining intensity was always much lower compared to either the climbing fiber labeling in the contralateral cerebellar cortex or of retrograde labeling of neurons known to project to the inferior olive. Reducing the survival time to 3 or 4 days (when tracing connections within the brain stem) appears to minimize the problem of labeling passing fibers. Notwithstanding, this potential handicap, which may also occur with many other tracers, should be considered when designing a particular experiment.

In some experiments, CTb was pressure-injected. Injection of a total of 100-200 nl, divided over 2 or 3 tracks into either the right or left side of the spinal cord results in an injection site that covered most of the injected side but did not spread to the other half of the cord (Fig. 3.4A).

WGA-BSA-gold

All sections analyzed for gold-lectin tracer were routinely silver-intensified. Therefore, in the following account, gold-labeling actually refers to silver-intensified gold unless noted otherwise. As reported elsewhere (Basbaum and Menétrey, 1987; Llewellyn-Smith *et al.*, 1992) gold-labeled tracers result in small, well-defined injection sites (Figs. 3.3A and 3.4B), especially when compared to similar amounts of HRP-based tracers or CTb. However, we have noted that WGA- BSA-gold possesses an enhanced affinity for fiber bundles, e.g., it was frequently seen that large quantities of the gold-lectin tracer were predominantly located within the fiber bundles between the neuropil lamellae of the inferior olive. Nevertheless, undamaged, passing fibers do not appear to take up this tracer as was also concluded by Basbaum (1987).

Retrograde double-labeling

Retrograde labeling with CTb results in light- or dark brown-stained neuronal cell bodies from which frequently dendrites can be identified for considerable distances. Therefore, the neuropil surrounding the labeled somata may contain numerous thin labeled profiles which, depending upon the particular injection and analysis site, may result from retrograde labeling of distal dendrites, anterograde labeling of afferents, or anterograde labeling of recurrent axon collaterals from retrogradely labeled neurons. However, in all cases it is possible to identify the retrogradely labeled neuronal somata without difficulty (e.g. Figs. 3.3 and 3.4).

WGA-BSA-gold injections, contrary to the CTb injections, only result in retrogradely labeled neurons. Axonal labeling was never observed from the injection site, either in anterograde or retrograde direction. The retrogradely labeled cells were easily identified, although the degree of dendritic labeling was somewhat less compared to the CTb labeling (Figs. 3.3E and 3.4E). Darkfield illumination can be employed to search for labeling with low-power objectives (Fig. 3.3C).

Since both the color of the labeling as well as the labeling pattern is very different from one another, it is remarkably easy to determine whether a particular neuron contains both tracers (Figs. 3.3D,E and 3.4C,D,E). Only in some very small or very intensely CTb-stained neurons it may be difficult to identify small amounts of gold/silver particles. In these cases it is possible to rely on darkfield illumination in order to be able to determine whether a particular neuron is double-labeled.

In order to illustrate the possibilities, advantages and possible pitfalls of this double-labeling technique 3 types of experiments will be described; however, they will not be discussed in depth, since complete papers dealing with these specific topics are currently being prepared.

Labeling in the vestibular nuclei after injections in the spinal cord and oculomotor area

The vestibular nuclei contain the elements that link the sensory neurons of the vestibular ganglion to the motoneurons of the eye muscles as well as to the motoneurons of the spinal cord, in particular of the neck musculature. Many neurons in the vestibular nuclei can be related to eye as well as to head movements; however, anatomical data on collateralization are sparse. The present experiment was designed to provide data on collateralization of vestibular neurons in the rat. CTb was pressure-injected into the left half of the cervical spinal cord at C4 or C5. Three injection tracks were made and a total of 150 nl of CTb was injected, but the injection site did not appear to extend to the right side of the cord (Fig. 3.3A). The gold-lectin injection site was centered on the ipsilateral trochlear nucleus and surrounding area (Fig. 3.3B). As can be seen from Fig. 3.3C, showing a photomontage of the contralateral vestibular nuclei, areas containing numerous CTb and gold-labeled neurons can be clearly identified, even at low magnification. At higher magnification, double-labeled neurons, mostly on the left side and located within the large-celled part of the medial vestibular nucleus, can be clearly distinguished from single labeled neurons (Fig. 3.3D,E).

Labeling in spinal cord after bilateral injections into the lateral reticular nucleus

Various authors have shown that unilateral injections of retrograde tracers in the lateral reticular nucleus (LRN) result in bilateral labeling of neurons in the spinal cord. The question arises if, and to what extent, spinal neurons may project bilaterally to the LRN. Therefore, CTb was delivered iontophoretically (4 μA, 20 min) into the right LRN and

WGA-BSA-gold (200 nl) was pressure-injected into the left LRN. In this way, injection sites of a similar size and position could be obtained (Fig. 3.4A) and the resulting retrograde labeling in the spinal cord was analyzed.

It was an advantage to be able to analyze the spinal cord sections in counterstained sections with the light microscope. In this way, it was relatively easy to determine in which lamina labeled neurons were found. Both gold-labeled as well as CTb-labeled neurons were found in various laminae at either side of the spinal cord as illustrated in Fig. 3.4B. Occasionally, double-labeled neurons could also be identified (Fig. 3.4C,E). However, in 3 analyzed cases only 4 double-labeled neurons were encountered between 434 CTb-labeled and 454 gold-labeled neurons (10 sections/case were analyzed at various representative spinal cord levels). These data not only indicate that most spino-reticular neurons project either ipsi- or contralaterally but also that the sensitivity of both retrograde tracers are roughly comparable (i.e., a similar amount of CTb- and gold-labeled neurons was detected).

Labeling in the inferior olive after injections in the cerebellar cortex

The advantage of small-sized injection sites is especially clear when studying the organization of the projection from the inferior olive to the cerebellar Purkinje cells. It is well known that the climbing fibers, originating from particular olivary subdivisions, terminate on parasagittally organized strips of Purkinje cells as has been demonstrated by both anterograde and retrograde tracing techniques. However, especially with electrophysiological techniques, it was demonstrated that these strips may contain a number of functionally different subzones (Oscarsson, 1980). Therefore, it is worthwhile to study the olivocerebellar projection with increasing detail. In the experiment shown in Fig. 3.5, both the WGA-BSA-gold and CTb injection were made in lobule IXb of the rat cerebellum. The injection sites were both about 0.6 mm in diameter and appeared to touch each other. However, analysis (of every other section) indicated that only 2 double labeled inferior olivary cells were observed out of 74 gold-labeled and 67 CTb-labeled neurons. Further more, it can be observed that the labeling within the ß-subnucleus reveals a rostrolateral group of neurons labeled with CTb and a caudomedial one containing gold/silver particles. This indicates that the climbing fiber projection from the ß-subnucleus of the inferior olive to lobule IX may be subdivided into more, and potentially functionally different, zones. These observations in the rat are in line with (single) retrograde tracer studies in larger animals, such as rabbit and cat, that provide evidence that the caudal part of the ß-subnucleus projects onto a midline region, whereas its rostral part projects onto a more lateral zone of the uvula-nodulus (Kanda *et al.*, 1989; Sato and Barmack, 1985). Electrophysiological evidence that neurons in the rostral and caudal parts

of the ß-subnucleus in the rabbit are modulated differently by vestibular stimulation has recently been published (Barmack *et al.*, 1993).

Discussion

Injection, uptake, and transport characteristics

As demonstrated earlier by Menétrey and collaborators (Basbaum and Menétrey, 1987; Menétrey, 1985; Menétrey and Lee, 1985), the use of gold conjugates to trace connections in the central nervous system has many advantages over other tracers. It may be the only tracer known that is transported in retrograde direction only. It is actively taken up and transported by terminals, whereas uptake by damaged fibers appears to depend on diffusion only and consequently results in weak, if any, labeling of neurons. Passing, undamaged fibers do not appear to take up the tracer. Since it does not require a particular fixation protocol, it can be used with a variety of immunohistochemical procedures. Moreover, survival times may range from 2 days to several weeks. Silver-intensification of gold-labeled neurons results in a very characteristic labeling pattern that can be easily identified in both darkfield and brightfield microscopy.

Our gold-lectin conjugate consists of 10 nm gold particles conjugated to WGA that was glutaraldehyde-coupled to BSA. We have also prepared and used WGA-HRP-gold (prepared according to Basbaum, 1987) which, after silver intensification, results in retrograde labeling with similar sensitivity as compared to the WGA-BSA-gold conjugate or plain WGA-HRP (although the neuronal labeling is more intense in the latter case). The main advantage of the WGA-BSA-gold over the WGA-HRP-gold and especially over WGA-apoHRP-gold appears to be its relatively low price.

Neuronal recordings with gold-lectin-filled pipettes may not be optimal since the salt content of the solution is very low (0.005 M NaCl). Nevertheless, it appears possible to use recordings of neuronal activity to verify the location of the injection site. This may be especially important when small injections are required or when two different tracers are to be injected in adjacent areas.

The use of CTb as a neuronal tracer was discussed extensively by Luppi (1990). The recently available low-salt CTb does not require desalting and buffer-changing steps in order to be able to iontophorize the toxin. Despite the, relatively, low salt concentration, pipettes filled with CTb (tip diameter about 10-14 µm) are excellent for recording neuronal activity which, as mentioned above, may aid in determining the exact location of the injection. CTb is also a good anterograde tracer (Luppi *et al.*, 1990; Shinonaga *et al.*, 1992) which should be taken into account when designing double-labeling experiments, e.g., it may be difficult to locate small retrogradely labeled neurons within intensely labeled fields of terminal arborizations.

Although neurons retrogradely labeled with CTb display a superior dendritic uptake and staining intensity

compared to WGA-BSA-gold labeled neurons, we did not observe a difference in sensitivity of both tracers. When the injections were, subjectively, judged to be of a similar size and within similar areas (i.e. in the cases with bilateral injections in the LRN or within the cerebellar uvula), the number of labeled neurons containing either tracer was approximately similar.

A drawback of CTb may be the observation that passing, undamaged, axons may take up the tracer. This inadvertent retrograde labeling of neurons may be minimized by reducing the survival time (e.g. to 2-4 days for tracing brain stem connections) but should, nevertheless, be kept in mind when designing experiments.

Double retrograde labeling

Immunohistochemically detected and DAB-reacted CTb results in light to dark brown labeling of retrogradely labeled neurons. Labeling is not equally distributed but spot-like concentrations of reaction product are visible that may invade proximal and even distal dendrites. Silver/gold deposits are relatively small and intensely black, without even a shade of brown. Therefore, gold-labeling is instantly distinguishable from CTb labeling. Both labels can also be easily identified within a single neuron, especially when using 20x to 40x objectives. In cases of doubt, e.g., in densely CTb-labeled neurons, darkfield illumination may decide whether gold/silver particles are also present in these neurons.

Advantages over fluorescent double-labeling procedures

Fluorescent tracers have been widely employed in order to study the collateralization of neurons. Kuypers et al. were the first to use substances such as Fast Blue and True Blue in combination with Nuclear Yellow or Diamino Yellow in order to study axonal branching (Bentivoglio *et al.*, 1980a; Bentivoglio *et al.*, 1980b; Huisman *et al.*, 1983; Keizer *et al.*, 1983; Kuypers *et al.*, 1980; Kuypers *et al.*, 1977). More recently, fluorescent latex beads were introduced by Katz (Katz *et al.*, 1984; Katz and Iarovici, 1990) and simultaneously other excellent fluorescent tracers such as Fluoro-Gold became available (Schmued and Fallon, 1986). Since these tracers either labeled different neuronal structures or possessed different spectral characteristics, multiple retrograde labeling studies became possible (Campbell and Takada, 1989; Yu *et al.*, 1991). Also, combinations of fluorescent tracers and light microscopical tracers such as WGA-HRP (Kitao *et al.*, 1989; Wigston and Kennedy, 1987) and gold-lectin (Berrebi and Mugnaini, 1988; Berretta *et al.*, 1991a; 1991b; Van Bockstaele and Aston-Jones, 1992) have been used.

A major drawback of double or multiple labeling that involves one or more fluorescent tracers is the fact that fluorescence tends to fade, especially when excited by the proper wavelength. Although fading can be postponed when the sections are stored at 4 °C in the dark, reexamination of the sections may not be possible interminably. The

silver-intensified gold-lectin and DAB-incubated CTb immunohistochemistry do not fade for many years (at least eight), even when the sections are stored in daylight at room temperature. Another, rather important advantage of the gold-lectin/CTb double-labeling technique lies in the possibility of analyzing counterstained sections. Thus, the location of labeled neurons can be easily related to surrounding brain structures, especially since changing objectives is easy and large-powered fluorescence objectives requiring oil immersion are not necessary.

Injection sites of gold-lectin and CTb can be made at least as small as the injection sites with fluorescent latex beads and can be directed with the aid of electro-physiological recordings, which may be especially important in experiments requiring small injection sites. When designing double-labeling experiments one should be aware of the possibility that in addition to uptake by fiber terminals, inadvertent uptake by passing and/or damaged fibers (and their neuronal somata) may occur. Hence, in long survival experiments, we found evidence for uptake of CTb by passing olivo-cerebellar fibers (however, cf. Luppi *et al.*, 1990). Gold-lectin may be taken up by damaged fibers, so care should be taken to use fine-tipped pipettes (diameter 10-15 μm) and to inject larger quantities over a prolonged time. However, a similar, unintentional, retrograde labeling is also likely to occur using fluorescent tracers, especially since many of these substances may result in considerable necrosis at the injection site (Keizer *et al.*, 1983).

For these reasons, we feel that the combination of a gold-lectin conjugate, such as the relatively easily prepared and cheap WGA-BSA-gold, with CTb represents a good alternative for combinations of fluorescent tracers in order to tackle problems concerning the extent of collateralization of neurons in the nervous system.

Acknowledgements

We thank Dr. J.J.L. van der Want (University of Groningen, The Netherlands) and Monica Mentink (University of Leiden, The Netherlands) for their initial help in preparing the gold-lectin conjugate.

Legends to figures

Fig. 3.1. Schematic diagram of the experimental set-up. Note that electrical signals recorded at the pipette tip can be monitored after which ejection of the tracer may take place by either iontophoresis or pressure injection.

Fig. 3.2. Examples of electrophysiological recordings obtained with CTb-filled (**A** and **C**) and gold-lectin-filled (**B** and **D**) pipettes in the cerebellar cortex (**A** and **B**) and inferior olive (**C** and **D**). Note the most likely single-unit Purkinje cell recording in **B** displaying numerous simple spikes as well as a complex spike (star). **C** and **D** show the characteristic extracellular action potential of olivary neurons consisting of a negative-positive going spike followed by several spikelets. Horizontal bar equals 100 ms in A and B and 20 ms in C and D. Vertical bar equals 0.1 mV.

Fig. 3.3. Color microphotographs showing the CTb pressure injection into the left half of the cervical spinal cord (**A**) and the WGA-BSA-gold injection into the oculomotor area (**B**). Note that the injection is centered around the left trochlear nucleus. **C** shows a photomontage of the contralateral vestibular nuclei. Note the abundance of gold-labeled neurons in the medial vestibular nucleus (adjacent to the fourth ventricle: IV) as well as CTb-labeled neurons within the large-celled part of the medial vestibular nucleus. Some of these neurons also contain gold/silver particles (arrows). Note that, on this side of the brain, the lateral vestibular nucleus (dorsal to the magnocellular part of the medial vestibular nucleus) contains no labeled neurons. **D** and **E** show higher magnifications of single- and double-labeled neurons depicted in C. Bar equals I mm in A (B same magnification), 100 μm in C, and 25 μm in D (E same magnification). **See p. 273.**

Fig. 3.4. **A**: color microphotomontage showing the WGA-BSA-gold pressure and iontophoretic CTb injection site in the left and right LRN, respectively. Note that the injections are approximately the same size and are centered on similar parts of the LRN. **B** shows a color microphotograph of a section through the thoracic part of the spinal cord. Note several CTb-labeled neurons located ipsi- as well as contralaterally of the CTb injection site. At this magnification, gold-labeled neurons cannot be detected. **C** shows the same section with darkfield illumination. Note that now the gold/silver-labeled neurons can be easily spotted. **D** demonstrates that at higher magnification both CTb as well gold-labeled neurons may be readily detected as shown for these labeled neurons located directly dorsal to the central canal (and indicated in B by an open arrow). **E** shows a double-labeled neuron indicated by an arrow in B and C. Bar equals I mm in A and B (C same magnification as B), and 25 μm in D and E. **See p. 274.**

Fig. 3.5. Semidiagramatic representation of the distribution of retrogradely labeled neurons in the inferior olivary complex after small CTb (laterally) and WGA-BSA-gold (medially) injections in lobule IXb (uvula) of the contralateral side. Note that most gold-labeled neurons are located in the caudomedial part of the ß-subnucleus and within the lateral part of the caudal part of the MAO (MAO).

CTb neurons are located within the rostrolateral part of the b-subnucleus, the dorsomedial cell column (DMCC) and in the dorsomedial group (DM) of the principal olive (PO). Only 2 double-labeled neurons were encountered, in the rostral part of the ß-subnucleus (at 1440 μm from the caudal pole of the inferior olive). Bar equals 1 mm.

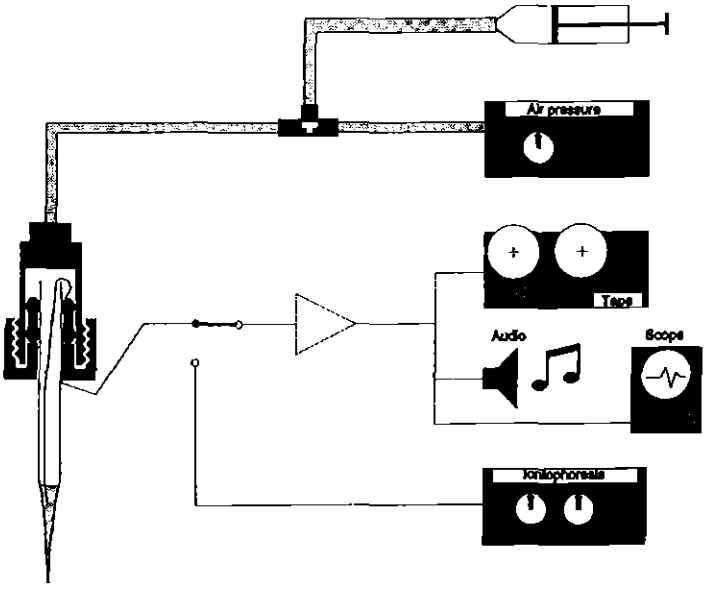

Fig. 3.1

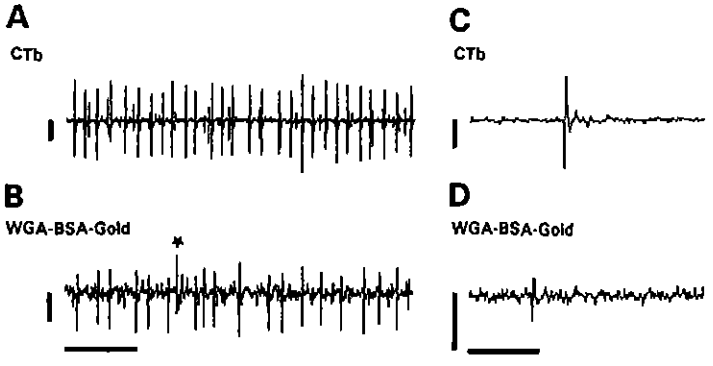

Fig. 3.4

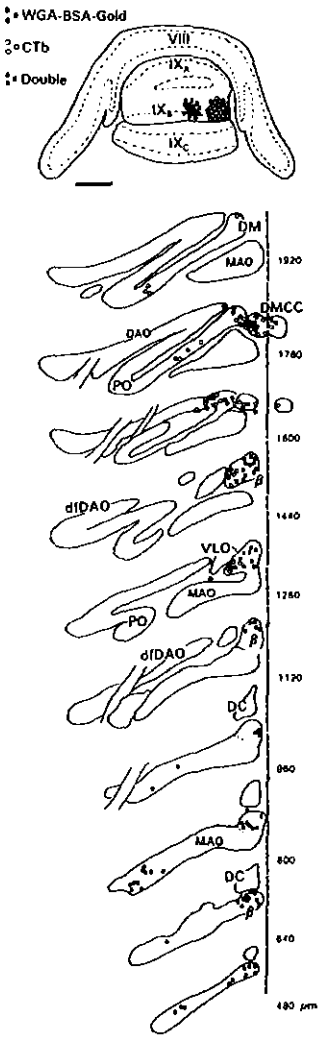
WGA-BSA-Gold
CTb
Double
VIII
IX
DM
MAO
1920
DMCC
DAO
PO
1780
1600
dlDAO
1440
VLO
MAO
1260
PO
dlDAO
1120
DC
980
MAO
800
DC
640
480 μm

Fig. 3.5

CHAPTER 4:
CEREBELLAR PROJECTIONS TO THE RED NUCLEUS AND INFERIOR OLIVE ORIGINATE FROM SEPARATE POPULATIONS OF NEURONS IN THE RAT:

A non-fluorescent double labeling study

T.M. Teune, J. van der Burg, and T.J.H. Ruigrok

Brain Research 673 (1995) 313-319

Abstract

In the rat, the extent of collateralization of projections from the cerebellar nuclei to the red nucleus and inferior olive was investigated using a retrograde double labeling technique. The combination of tracers selected, cholera toxin B subunit and WGA-BSA-gold, not only enabled the use of small injection sites but also resulted in clearly distinguishable and permanently stained neurons that could be analyzed in counterstained sections.

Light microscopic analysis of the contralateral cerebellar nuclei confirmed the generally held belief that neurons projecting to the magnocellular part of the red nucleus are mainly found in the interposed nuclei whereas those projecting to its parvicellular part are predominantly located in the lateral cerebellar nucleus. Small neurons, retrogradely labeled from the inferior olive, are scattered throughout all divisions of the cerebellar nuclei. In all cases, less than 0.5% of all labeled neurons contained both labels indicating that these cells may project to the red nucleus as well as to the inferior olive.

These findings support and strengthen the concept that the projection from the cerebellar nuclei to the red nucleus and inferior olive originates from different sets of neurons, which, consequently, may transmit different information.

Introduction

The cerebellar nuclei, together with the vestibular nuclei, are the targets of the Purkinje cells of the cerebellar cortex. The output of the cerebellar nuclei (CN) is directed, predominantly via the scp, to a variety of brain stem structures in thalamus, mesodiencephalon and medulla (Chan-Palay, 1977; Faull, 1978; Faull and Carman, 1978). Detailed projections have been described to the red nucleus (Angaut and Cicirata, 1988; Daniel *et al.*, 1988) and the inferior olive (Ruigrok and Voogd, 1990). It has been shown in the rat (Angaut and Sotelo, 1987; Fredette and Mugnaini, 1991; Nelson and Mugnaini, 1989) and the cat (De Zeeuw *et al.*, 1989b) that the nucleoolivary projection is likely to be completely derived from GABAergic neurons. The projections to the red nucleus appear to be excitatory as demonstrated with electrophysiological (Toyama *et al.*, 1968) and immunohistochemical (Bernays *et al.*, 1988; Monaghan *et al.*, 1986) techniques. GABA has been identified as a neurotransmitter in the red nucleus (André *et al.*, 1987; Vuillon-Cacciuttolo *et al.*, 1984). It has been attributed to interneurons (Katsumaru *et al.*, 1984; Murakami *et al.*, 1983), but a contribution of ascending collaterals of GABAergic nucleoolivary fibers has not been excluded.

The cells of origin of the nucleoolivary projections are small (see (Legendre and Courville, 1987) for references). Neurons projecting to the red nucleus have not been measured, but those projecting to the thalamus are estimated to be generally larger (cat: Legendre and Courville, 1987; Tolbert *et al.*, 1978a). Populations of small GABA-immunoreactive neurons (mean

diameter 10-22.5 μm, peak near 10 μm) and larger glutamate-immunoreactive neurons (mean diameter 10-35 μm, peak at about 20 μm) were distinguished by Batini *et al.*, (1992) in the cerebellar nuclei of the rat.

However, several electro-physiological studies in the cat (Andersson and Hesslow, 1987a; Ban and Ohno, 1977; McCrea *et al.*, 1978; Tolbert *et al.*, 1978a) indicate that a substantial contingent of nucleoolivary projections may have ascending collaterals. Fluorescent double retrograde tracing studies by Bentivoglio and colleagues in the rat (Bentivoglio and Kuypers, 1982; Bentivoglio and Molinari, 1986) and by Bharos (1981) in the cat with tracer combinations injected in thalamus and caudal medulla resulted in many single labeled small-sized nucleoolivary neurons but also in a contingent of double labeled larger neurons located in specific subdivisions of the cerebellar nuclei. No double labeled cells were observed by Legendre and Courville (1987) in their experiments with injections of fluorescent tracers in the inferior olive and the thalamus of the cat.

We decided to reinvestigate the collateralization of nucleoolivary fibers to the red nucleus of the rat, because no experiments with double labeling from injections delivered to the red nucleus and the inferior olive have been reported. A non-fluorescent double retrograde tracing technique (Ruigrok *et al.*, 1995b), making use of cholera toxin B subunit (CTb) and a gold-lectin conjugate, was used in this study. This combination ensures small injection sites, permanently and easily discriminated retrograde labeling of neurons, and the possibility to examine the resultant labeling in counterstained sections with the light microscope. Since the red nucleus (RN) is classically divided into a caudally positioned magnocellular part (RNm) and a parvicellular rostral pole (RNp) (Reid *et al.*, 1975b), injections were centered on either of these different parts in order to study potential differences in collateralization to these two areas and to the inferior olive (IO).

Materials and methods

Male Wistar rats (n = 12), weighing 200-250 g, were anesthetized with sodium-pentobarbital (120 mg/kg i.p.) and mounted in a stereotactic frame. Glass micropipettes (tip diam. 10-15 μm) were initially placed based on coordinates from the atlas by Paxinos and Watson (1986), and prior to injection the final site was verified by recording the characteristic firing of either rubral or olivary cells. CTb (low salt: List Biol. Lab., Campbell, CA) was applied iontophoretically to the red nucleus (4 μA positive current, for 30 min with a 7 s on, 7 s off cycle: Fig. 4.1A). The gold-lectin conjugate consisted of 10 nm gold sol (Aurion, Wageningen, the Netherlands) conjugated to wheatgerm agglutinin and bovine serum albumin (WGA-BSA), prepared according to Roth (1983), and was pressure injected through a glass micropipette (tip diameter 12-16 μm) into the inferior olivary complex, ipsilateral to the CTb injection. A total of 200-300 nl WGA-BSA-gold was injected using

multiple injection tracks in order to obtain a large injection site but to spare the reticular formation overlying the olive (Fig. 4.1B). After a survival time of 7-10 days, the animals were perfused with 300 ml of a 0.8% NaCl, 0.8% sucrose, 0.4% d-glucose solution in 0.05 M phosphate buffer (PB, pH 7.3), which was followed by 4% paraformaldehyde, 0.1% glutaraldehyde and 4% sucrose in PB. The brains were removed, blocked, embedded in gelatin and cryoprotected in 30% sucrose in 0.05 M PB. Transverse sections (40 µm) were cut on a freezing microtome and collected in 0.1 M PB. Free floating sections were incubated at 4 °C in the dark with constant agitation in anti-CTb (List Biol. Lab.), dilution 1:15,000 in Tris buffer containing 0.5 M NaCl and 0.5% Triton X-100 (TBS +, pH 8.6) for 72 hours. After rinsing, the sections were subsequently incubated at room temperature in biotinylated donkey anti-goat (List Biol. Lab., dilution 1: 2000 in TBS +) for 2 h, rinsed and reacted with the avidine-biotine-complex (ABC Elite kit, Vector, Burlingame CA) for 2 h and, finally, reacted with diaminobenzidine (DAB: 37,5 mg in 150 ml Tris-HCl, pH 7.6 with 25 µl 30% H_2O_2) for 30 min. Next, sections were silver intensified (Aurion), mounted, counterstained and coverslipped with Permount.

Results

Light microscopic examination showed numerous labeled neurons within the CN contralateral to the injection sites (Fig. 4.1C,D). Double labeled cells could be easily distinguished from unlabeled or single labeled cells since the characteristic small, black, gold-silver particles can be clearly distinguished from the brown DAB reaction product indicating CTb labeling.

Two representative experiments (R42 and R45) will be described. In R42, as shown in Fig. 4.2, the CTb injection was centered on the RNm (see also Fig. 4.1A), whereas the RNp was injected in case R45. In both animals, the WGA-BSA-gold injection covered approximately 80% of the ipsilateral IO (Fig. 4.1A, Fig. 4.2). For both cases, the resulting retrograde labeling in the contralateral CN is shown in Fig. 4.3. The location of CTb positive cells and gold-silver labeled cells are represented as one dot per 5 labeled cells. Each double labeled cell is indicated individually. The injection located in the RNm (R42) resulted in labeling of medium to large neurons, which were mainly found within the interposed nuclei and, occasionally, within the lateral cerebellar nucleus (LCN). Case R45 resulted in labeling of neurons predominantly located in the LCN. Labeling originating from the IO injection was observed in small cells throughout the CN. Double labeled cells (less than 0.5% of all labeled cells) were found only rarely in the interposed nuclei (R42) or in the LCN (R45) and are medium- to large-sized (Fig. 4.4). Fig. 4.5 shows a camera lucida drawing from part of the LCN of case R45 to give an impression of the distribution of the labeled neurons. In this particular area of the chosen section, both gold-silver labeled and CTb labeled neurons were abundantly present, leaving only a relatively small amount of non-labeled

neurons. However, here, not a single double labeled cell was observed (see also Fig. 4.1C). Note that all gold-labeled neurons fall within the small-sized category.

Discussion

Results from our experiments indicate that only a very small number of CN neurons may collateralize to the RN and IO, since less than 0.5% of all labeled cells were double labeled through the application of tracers in the RN and IO. This number is clearly less than may be concluded from the experiments of Bentivoglio (Bentivoglio and Kuypers, 1982) with large injections of fluorescent tracers in the caudal medulla and the thalamus (Bentivoglio and Molinari, 1986). However, as indicated by these authors, definite conclusions on the collateralization of nucleo-thalamic and nucleoolivary projections could not be drawn from this study, because the CN also project to extra-olivary areas in the caudal medulla and to the spinal cord (Buisseret-Delmas *et al.*, 1993; Chan-Palay, 1977; Faull, 1978). Although the injection sites in the present study were much smaller, inadvertent labeling of passing fibers destined for the spinal cord or extra-olivary medullary regions may be responsible for double labeling a few neurons with projections to the red nucleus in our experiments. Especially, since the diameters of these double labeled neurons exceed the diameters of single labeled nucleoolivary neurons but fit into the size distribution of single labeled nucleo-rubral neurons (Fig. 4.4). Consequently, we conclude that in the rat, most, if not all, nucleoolivary neurons do not posses ascending collaterals that terminate within the RN. This conclusion is identical to the conclusions of Legendre and Courville (1987) from their fluorescent double labeling study in the cat with injections of the inferior olive and the thalamus.

Nevertheless, electrophysiological observations in the cat, of collisions of antidromically evoked action potentials of individual neurons in the cerebellar nuclei after stimulation of the RN and IO (Andersson and Hesslow, 1987a; Ban and Ohno, 1977; Bharos *et al.*, 1981; McCrea *et al.*, 1978; Tolbert *et al.*, 1978a), suggest that such collateralization indeed may occur. However, these data must be interpreted with caution. Especially for projections from the lateral and anterior interposed nuclei, it is very difficult to follow the course of the nucleoolivary fibers directly after the decussation (Legendre and Courville, 1987) and it cannot be ruled out that some fibers may ascend to the level of the RN before descending to the IO and therefore may be stimulated by an electrode placed near the RN. Also, as mentioned above, collaterals of nucleo-rubral fibers may terminate in the vicinity of the IO, e.g. within the ventromedial reticular formation or may descend along the IO to the spinal cord (Buisseret-Delmas *et al.*, 1993) and may be inadvertently activated by the IO stimulation electrode.

Our data are in accordance with the evidence that the nucleoolivary projection takes its origin from a population of small GABAergic neurons located in the cerebellar nuclei (Angaut and Sotelo, 1987; De

Zeeuw *et al.*, 1989b; Fredette and Mugnaini, 1991) whereas the projection to the RN (Bernays *et al.*, 1988; Tarnecki, 1988; Toyama *et al.*, 1968) as well as to the adjacent prerubral area and medial nuclei at the mesodiencephalic junction arises from a population of non-GABAergic and excitatory neurons (Batini *et al.*, 1992; Berretta *et al.*, 1991a; De Zeeuw and Ruigrok, 1994). Hence, cerebellar projections to the RN and IO evidently originate from completely separate populations. Therefore, although both types of projection neurons are largely intermingled (Fig. 4.1C, Fig. 4.5) and, thus, in theory, may be influenced by efferents from a single Purkinje cell zone, elements of both groups are not necessarily activated in the same way. E.g. recent evidence suggests that climbing fiber collaterals do not appear to innervate the GABAergic nucleoolivary neurons (Van der Want *et al.*, 1994), indicating that olivary activity may have different monosynaptic effects on nucleoolivary and nucleo-rubral neurons.

Legends to figures

Fig. 4.1. Color microphotography showing retrograde double labeling experiments with CTb and WGA-BSA-gold. **A**: CTb injection site centered on RNm in case R42. **B**: WGA-BSA-gold injection site in the inferior olive (case R42). **C**: retrogradely labeled cells in the LCN of case R45. Medium and large-sized neurons projecting to the RNp are labeled with brown DAB reaction product and are intermingled with small neurons containing black gold-silver particles, indicating their termination in the 10. **D**: retrogradely labeled neurons in the interposed nucleus. Note that one neuron contains both labels. Bar represents 1 mm in A and B, and 25 μm in C and D. **See p. 275.**

Fig. 4.2. Diagrammatic representations of the injection sites in the RN and 10 of cases R42 and R45.

Fig. 4.3. Diagrammatic representation of the retrograde labeling in the contralateral CN of cases R42 and R45. CTb labeled neurons are indicated by open circles (approximately one circle for every five labeled cells), gold-silver labeled neurons are indicated by dots (approximately one dot for every five labeled cells). All double labeled neurons are indicated by an asterisk.

Fig. 4.4. Size distribution of single and double labeled neurons. One hundred CTb and one hundred gold labeled neurons were chosen and measured randomly and were supplemented with 12 double labeled neurons. Surface area was estimated by the formula $1/4\pi lw$, where l equals the length and w the width of the neuron. Note that the size distributions of the single, gold or CTb, labeled neurons are almost completely separated and that the double labeled neurons fall within the size distribution of the CTb neurons. The overall size distribution is quite similar to data reported by Chan-Palay (1977).

Fig. 4.5. Camera lucida drawing of part of the LCN in case R45. Non-labeled cells are indicated by open contours, shaded contours denote CTb labeled neurons, black contours indicate gold-silver labeled neurons. No double labeled cells were encountered. Bar equals 100 μm.

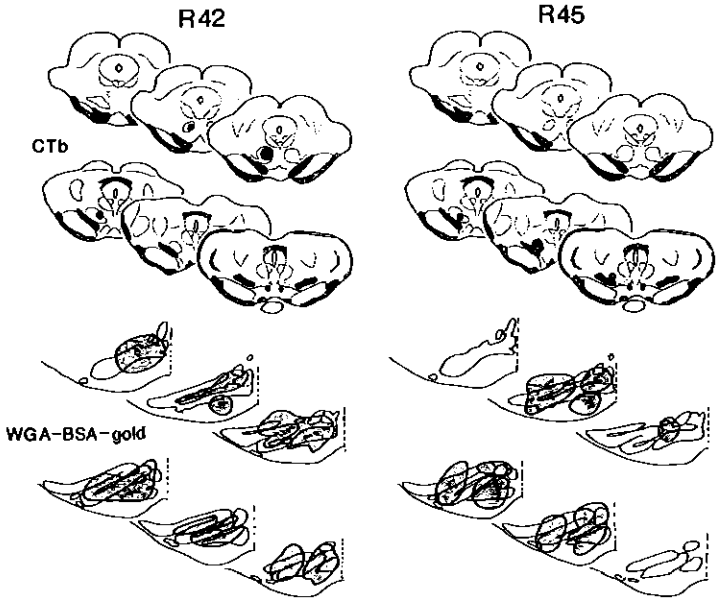

Fig. 4.2

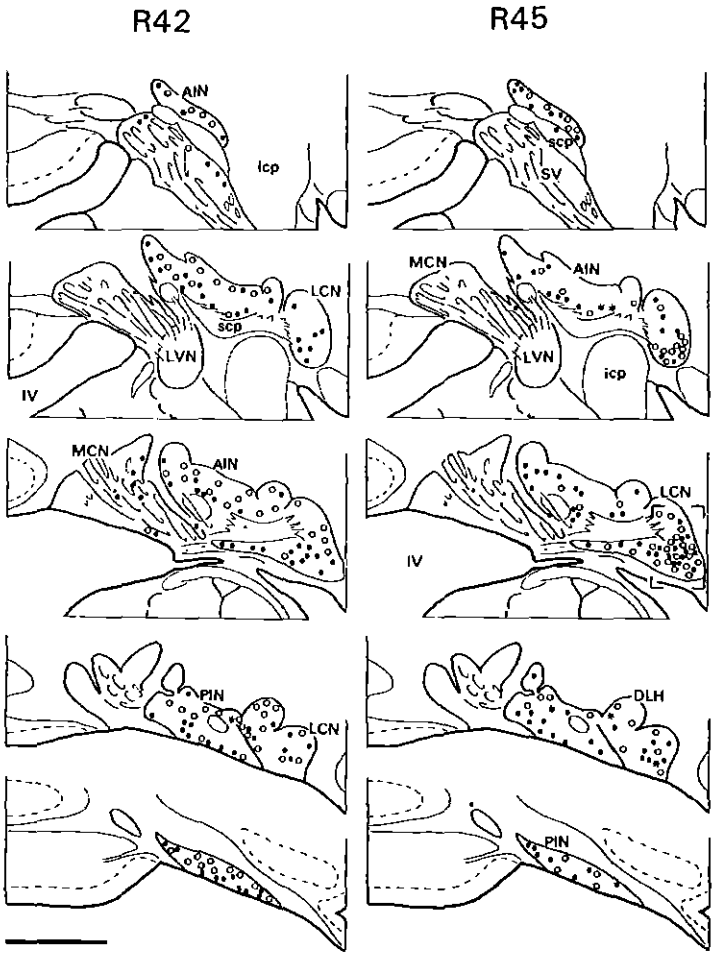

Fig. 4.3

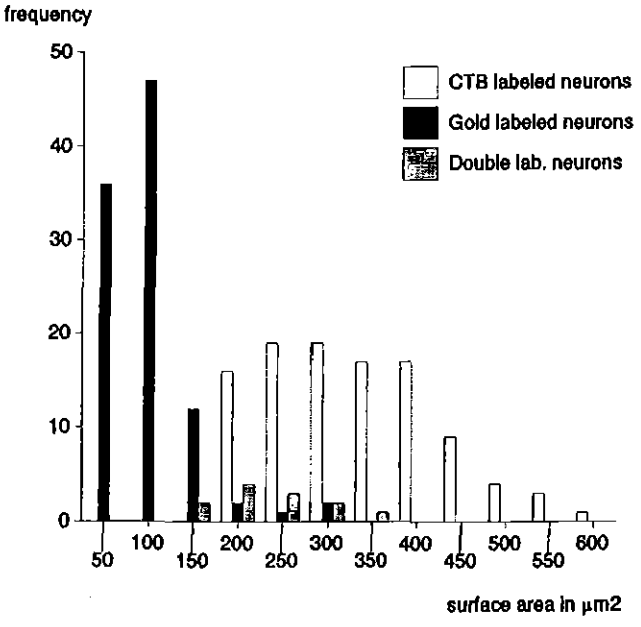
frequency
50
40
30
20
10
0
CTB labeled neurons
Gold labeled neurons
Double lab. neurons
50
100
150
200
250
300
350
400
450
500
550
600
surface area in µm2

Fig. 4.4

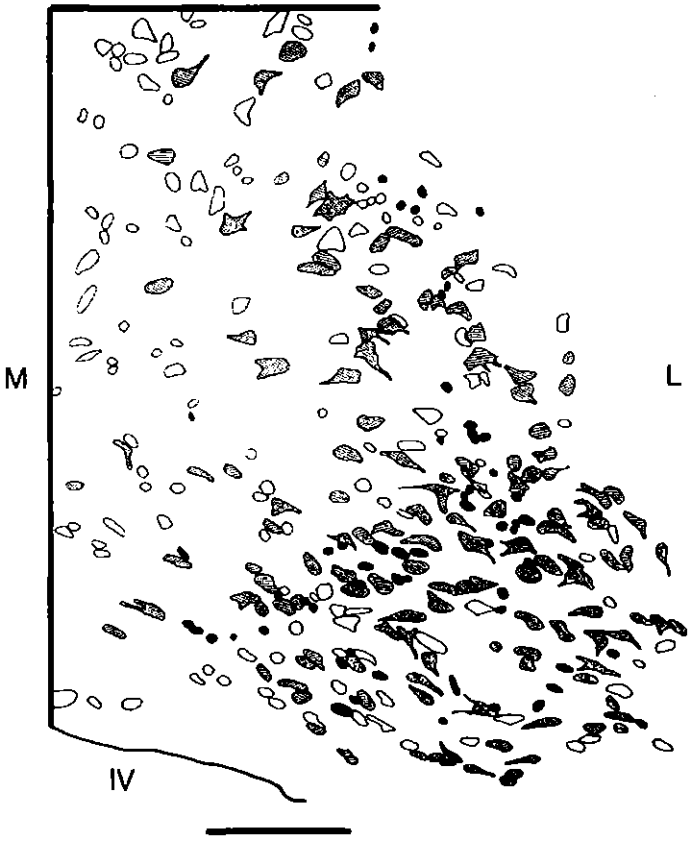

Fig. 4.5

CHAPTER 5:
CEREBELLAR COLLATERALIZATION TO PRERUBRAL, RUBRAL, PONTINE TEGMENTAL RETICULAR AND INFERIOR OLIVARY NUCLEI

A non-fluorescent double retrograde tracing study in the rat

T.M. Teune, J. van der Burg, J. Voogd and T.J.H. Ruigrok

Abstract

The organization of the cerebellum is characterized by a number of parallel longitudinal connection patterns consisting of matching olivo-cortico-nuclear zones, often referred to as modules. The cerebellar nuclei constitute the output stations of these modules. Here, divergent and convergent patterns in the output of the modules to four, functionally distinct brain stem areas, were investigated in the rat.

Two non-fluorescent retrograde tracers, cholera toxin B subunit and a gold-lectin conjugate, were injected into combinations of the following areas: the red nucleus, as an example of cerebellar nuclear projections to premotor areas; the prerubral area, for its relationship with the inferior olive as a preolivary area; the nucleus reticularis tegmenti pontis, as an important source of cerebellar mossy fibers; and the inferior olive, as the sole source of climbing fibers.

The red nucleus received an topographically-arranged projection from the contralateral interposed and lateral cerebellar nuclei. The ventral and dorsal parts of the magnocellular red nucleus received projections from the medial and lateral part of the anterior interposed nuclei, respectively. Projections from the caudal lateral cerebellar nucleus terminated laterally in the parvicellular red nucleus, and more rostral parts of the lateral cerebellar nucleus provided a projection terminating in the ventral and medial part of the parvicellular red nucleus. The medial part of the posterior interposed nucleus supplied afferents to the medial part of the red nucleus. Injections in the prerubral area also resulted in labeling in the interposed and lateral nucleus, but a topographical organization could not be detected. The nucleus reticularis tegmenti pontis was found to receive input from all cerebellar nuclei except for the posterior interposed nucleus. The inferior olivary complex was found to receive discrete projections from most parts of the cerebellar nuclei.

Cerebellar nuclear cells that were retrogradely labeled from inferior olivary injections constitute a distinct population that did not collateralize to any of the other areas, with a possible exception of the NRTP from where a very low percentage of labeled cells was double-labeled.

When tracers were injected in any combination of the red nucleus, the prerubral area or the nucleus reticularis tegmenti pontis, at least 18% and up to 80% of the cells labeled with a particular tracer and located in an area where both types of labeled cells were found, also contained the other tracer. It should be emphasized that double labeled neurons always occur in regions where the neurons labeled from the red nucleus, the prerubral area or the nucleus reticularis tegmenti pontis overlap, or in regions of overlap with any other combination of target nuclei, reported in the literature. These observations suggest that the large- and medium-sized relay cells of the cerebellar nuclei exert their influence on widely dispersed targets varying from the cord to the thalamus through collateralizing axons.

It can be concluded that the cerebellar nuclei contain two populations of relay cells that differ in

the collateralization of their axons. One population corresponding to the GABAergic, nucleoolivary neurons, only targets the inferior olive. The other population of medium- to large-sized non-GABAergic neurons distribute their output to many functionally different areas –such as a premotor area (RN), a preolivary (preRN) and a precerebellar mossy fiber center (NRTP)- through branching axons. Within the nuclei the two populations are completely intermingled. The individual collateralization profiles of the different cerebellar target nuclei are discussed. Cerebellar output to premotor areas such as the red nucleus with simultaneous collateralizing projections to recurrent mossy fiber circuits, as well as with projections incorporating prerubro-olivo-cerebellar circuits and its conjunction with an independent nucleoolivary circuit, are suggested to be a basic characteristic of cerebellar operation.

Introduction

The cerebellum provides its regulatory influence on many aspects of the central nervous system through the cerebellar nuclear output. It has become abundantly clear that cerebellar nuclear efferents terminate, mostly contralaterally, in a great variety of brain stem regions. Cajal (1911) already described that, immediately after their decussation, the fibers of the scp branch in ascending and descending bundles. The descending branch is located in the ventromedial tegmentum and mainly terminates in the nucleus reticularis tegmenti pontis (NRTP), the pontine nuclei, and the pontine and medullary reticular formation and in the inferior olive (IO). The ascending branch terminates in the red nucleus (RN), the prerubral area (including the area surrounding the fasciculus retroflexus), the accessory oculomotor nuclei, the superior colliculus and the thalamus and subthalamus (Chan-Palay, 1977; Faull, 1978; Faull and Carman, 1978). Since the cerebellar nuclei (CN) serve as the output stations of the cerebellar modules as defined by the organization of their cortico-nuclear and olivo-cortical connections (Buisseret-Delmas and Angaut, 1993; Groenewegen and Voogd, 1977; Groenewegen *et al.*, 1979; Oscarsson, 1980; Voogd and Bigaré, 1980), it has become a point of interest to investigate in what way this modular organization becomes implemented within the brain stem circuitry. More detailed knowledge on the distribution of information processed by cerebellar modules has become even more pressing since available evidence suggests that the cerebellar modules may represent functional entities (Bloedel and Roberts, 1971; Godschalk *et al.*, 1994; Sato and Kawasaki, 1990a; van der Steen *et al.*, 1994).

Within the CN, two types of relay cells are intermingled. One type consists of relatively small cells that are GABAergic and predominantly project to the IO (Bentivoglio and Kuypers, 1982; Buisseret-Delmas *et al.*, 1989; Chan-Palay, 1977; De Zeeuw *et al.*, 1989b; Fredette and Mugnaini, 1991) whereas the other group consists of large- and medium-sized cells that are excitatory (Berretta

et al., 1993; Giuffrida *et al.*, 1993; Toyama *et al.*, 1968). Neurons that belong to this group of non-GABAergic relay cells may collateralize to a wide array of target sites as has been shown with fluorescent retrograde double-labeling techniques. In the rat, collateralization has been demonstrated for combinations involving the medullary and pontine reticular formation (or the spinal cord), the thalamus, the superior colliculus, the accessory oculomotor nuclei or the basal pontine nuclei (Bentivoglio and Kuypers, 1982; Gonzalo-Ruiz and Leichnetz, 1987; Lee *et al.*, 1989). The group of medium- and large-sized relay cells does not appear to terminate within the IO (Bentivoglio and Kuypers, 1982; Lee *et al.*, 1989); see also chapter 4. The axons of the small GABAergic neurons of the lateral and interposed cerebellar nuclei, on their way to the contralateral IO, follow a parallel, but slightly different course from the axons of the non-GABAergic relay cells, which ascend in the scp. Nucleoolivary fibers ascend just ventral and lateral to the scp, decussate ventral to the main decussation of the scp and descend ventral to its main descending branch (Legendre and Courville, 1987; Ruigrok and Voogd, 1990). Although electrophysiological data, performed in the cat, suggest otherwise (Andersson and Hesslow, 1987b; Ban and Ohno, 1977; McCrea *et al.*, 1978; Tolbert *et al.*, 1978a), it seems unlikely that in the rat the nucleoolivary pathway gives rise to a crossed ascending branch. Double labeling experiments with combinations of the RN and inferior olive (Teune *et al.*, 1995) or of thalamus or superior colliculus and the caudal ventral medulla (Bentivoglio and Kuypers, 1982) failed to show double-labeled small neurons in the CN.

In the present study, a recently improved non-fluorescent retrograde double labeling method (Ruigrok *et al.*, 1995b; Teune *et al.*, 1995) that makes use of small, confined injections of highly selective and permanently visible, retrogradely transported tracers was used to investigate the degree of collateralization of the individual CN. Since, as outlined above, the output of individual CN may reflect functional characteristics, particularly interest was paid to the potential divergence of this output to four well-known, but functionally different cerebellar target sites. We have selected the RN as an example of a premotor area (Ruigrok and Cella, 1995), the IO as cerebellar climbing fiber source (Desclin, 1974), the nucleus reticularis tegmenti pontis (NRTP), being an important mossy fiber source which also collateralizes to the CN (Mihailoff, 1993; Ruigrok and Cella, 1995), and the prerubral area including the region surrounding the fasciculus retroflexus and from which a major projection to the IO originates (Carlton *et al.*, 1982; Onodera, 1984; Ruigrok and Cella, 1995). The results will be discussed in relation to the coupling of the motor output of the cerebellum with recurrent mossy fiber and climbing fiber paths. Differences in collateralization profiles between different parts of the CN will be discussed in relation to the modular organization of the cerebellum (Buisseret-Delmas and Angaut, 1993; Voogd and Bigaré, 1980).

In order to obtain an overall picture of the distribution of the CN projection neurons to these areas, we will first describe the distribution of CN neurons retrogradely labeled from individual target sites. Double retrograde tracing experiments with combinations of the different target sites will be presented subsequently. Part of these data has been reported as a short communication elsewhere (Teune *et al.*, 1995).

Materials and methods

Surgical procedures and tracer application

All experiments were performed on purposebred male Wistar rats. The experimental procedure was approved by the institute's animal care committee and adhered to NIH guidelines. A total of 36 rats, weighing 250-300 grams, were anesthetized by an intraperitoneal injection with a cocktail of ketamine (80 mg/kg) and xylazine (5 mg/kg) and were subsequently mounted in a stereotactic device according to Paxinos and Watson (1986). Additional dosages of anesthetics were given when needed.

Access to the cerebellum and lower brain stem was gained by partially removing the squamosal part of the occipital bone after partition of the covering skin and muscles through a midline incision over the skull and neck area. The IO was reached by penetrating the medulla oblongata at obex level dorsally, at an angle of 45^0 with the horizontal plane. The RN and preRN were approached through a small hole drilled in the parietal bone directly over these areas, according to coordinates obtained from the atlas of Paxinos and Watson (1986), between 3.0 and 5.0 mm rostral to the interaural line, laterality: 0.8-1.0 mm, with the pipette perpendicular with respect to the horizontal plane. The NRTP was approached stereotactically through the caudal cerebellum (entering between lobule IXb and IXc) at an angle of 34^0 with the horizontal plane. In this way, the electrode would pass ventrally to the CN, avoiding possible spread of tracer to the CN and / or IO.

All injections were made with double barrel glass micropipettes (overall tip diameter: 12-18 μm). One barrel contained the tracer, whereas the other was filled with an electrolyte solution (4 M NaCl) and was connected to standard electrophysiological equipment. In this way, and prior to the actual application of tracers, electrophysiological recordings could be made in order to verify the location of the glass electrode tip. The RN and IO both demonstrate a spontaneous and characteristic firing pattern (Gellman *et al.*, 1983; Ruigrok and Voogd, 1990), which is readily distinguished from electrical discharges recorded from the surrounding nervous tissue. The location of the NRTP was inferred by identifying the medial lemniscus, which demonstrated increased firing rates in response to tapping or touching the animal's contralateral body, and positioning the electrode tip slightly dorsal to this region.

As retrograde tracers, cholera toxin B subunit (CTb: 1% w/v in 0.1M phosphate buffer, pH 7.2; List Biol. Lab. Inc. Campbell, CA; see Luppi *et*

al., 1990) was used in combination with a gold-lectin conjugate, wheatgerm agglutinin coupled to bovine serum albumin and 10 nm gold sol particles (Ruigrok *et al.*, 1995b). CTb was delivered iontophoretically by means of a 4 μA positive current for 10 - 15 min., with a 7 sec on/off cycle. The gold-lectin could be delivered in nanoliter quantities using a homemade pressure device (Gibson *et al.*, 1987; Ruigrok *et al.*, 1995b).

To exclude any influence caused by inadvertent tracer uptake or by tracer transport characteristics in the distribution, the quality and quantity of retrograde labeling, both tracers were applied in individual cases to either of the four selected target areas. In order to reduce potential inadvertent labeling of fibers of passage (Chen, 1995; Ruigrok *et al.*, 1995b), CTb was preferentially injected into the more distal of the injection sites, whereas gold-lectin, which has not been reported to be taken up by passing fibers (Llewellyn-Smith *et al.*, 1992; Menétrey, 1985; Ruigrok *et al.*, 1995b) was predominantly selected for injections more proximal to the CN. However, occasional reversal of tracer application did not appear to influence the resulting labeling.

After injection, all wounds were sutured and the animals were allowed to recover and survived for 4 or 5 days, during which they were checked daily for signs of stress and/or discomfort.

Fixation and immunohistochemistry

Before perfusion, the animals were deeply re-anaesthetized with an overdose of sodium pentobarbital (120 mg/kg i.p.), and transcardially perfusion-fixed, first clearing the cardiovascular system with a rinsing solution (300 ml of a 0.8% NaCl, 0.8% sucrose, 0.4% d-glucose solution in 0.05 M PB, pH 7.2, at room temperature), followed by fixative (1000 ml of a freshly prepared solution containing 4% paraformaldehyde, 4% sucrose, 0.1% glutaraldehyde in 0.05 M PB, pH 7.2, at room temperature).

Brains were extracted, blocked and postfixed for 4 hours at room temperature in postfix-solution (4% paraformaldehyde, 4% sucrose in 0.05 M PB, pH 7.2) under constant agitation. The blocked brains were stored overnight in 10% sucrose in 0.05 M PB for cryoprotection at 4 °C. Next, the brains were gelatin-embedded (10% gelatin, 10 % sucrose in distilled water), hardened in 10% formaldehyde with 30% sucrose for 3 hours and stored until sectioning in 30% sucrose in 0.05 M PB at 4 °C.

With a freezing microtome, 40 μm transverse sections were serially cut and collected in 0.1 M PB, pH 7.2. Free floating sections were processed for CTb immunohistochemistry as follows. First, sections were thoroughly rinsed in TBS+ (0.05 M Tris, 0.5 M NaCl, 0.5% Triton X-100, pH 8.6), and were subsequently incubated for 48 hours in the dark at 4 °C under constant agitation with anti-CTb (1:15,000 in TBS+, List Lab.). Hereafter, sections were thoroughly rinsed with TBS+, and incubated with biotinylated donkey-anti-goat antibodies (1: 2000 in TBS+, List Lab.) at room temperature, under constant agitation for 2 hours. Then, rinsed sections were incubated with the avidine biotine complex (ABC Elite Kit,

1:100 in TBS+, Vector Lab., Burlingame, CA) for 2 hours at room temperature under constant agitation. Following subsequent rinses in 0.05M Tris-HCl, pH 7.3, sections were reacted with diaminobenzidine (37.5 mg DAB per 150 ml Tris-HCl with 25 µl 30% H_2O_2) for 30 minutes. This reaction was stopped by rinsing the sections in 0.1 M PB (pH 7.2). Finally, the gold-lectin labeling was intensified by a silver-enhancement procedure (Aurion, Wageningen, the Netherlands). Sections were stored in 0.1 M PB in the dark at 4 °C until mounting, after which they were air-dried, counterstained with thionin and coverslipped with Permount.

Analysis of sections

Sections were analyzed with a light microscope. In standardized drawings the injection sites of both single and double-labeling experiments were outlined. The resulting CN labeling was plotted with the aid of a computerized plotting device (making use of a Lucivid™ miniature monitor and Neurolucida™ software: MicroBrightField, Inc., Colchester, VT) and was subsequently compilated in a standardized diagram of the flattened, stretched-out CN as based on transverse sections (Fig. 5.1). The lateral vestibular nucleus (LVN) was not included in the analysis.

In order to obtain an estimate of the degree of collateralization, the percentage of double-labeled cells was calculated based on the estimated amount of labeled cells in an overlapping area. To do this, the surface of the areas indicating labeling of either type in the flattened CN diagrams was determined as well as the surface of the overlapping area. From this the number of labeled cells of either type could be estimated based on an assumed equal distribution over the whole surface area. From this the percentage of labeled cells showing both labels could be calculated (Table 5.1, Fig. 5.14).

Nomenclature and definition of areas

Identification and nomenclature of the subdivisions of the IO and of the CN was based on Ruigrok and Voogd (1990) and Korneliussen (1968). The interstitial cell groups (ICG) located between the medial cerebellar (MCN) and the posterior interposed nuclei (PIN) were delineated in accordance with Buisseret-Delmas (1993). Outlines of the NRTP were based on reports by Torigoe *et al.* (1986a; 1986b) and Mihailoff (1981b). The delineation of the RN and adjacent prerubral area were based on descriptions by Reid (1975b), Ruigrok and Cella (1995) and on diagrams in the rat brain atlas of Paxinos and Watson (1986). The approximate border between the magnocellular and parvicellular parts of the RN is situated at level 3, the rostral tip of the parvicellular RN is located between levels 5 and 6 (Figs. 5.4, 5.5, 5.6).

Results

Aspects of injection sites and resulting labeling

CTb injection sites appeared as globular shaped concentrations of a brownish, fine granular substance,

with centrally the darkest coloring and the highest concentration of granules gradually fading towards the edges but with well outlined borders. Gold-lectin injections consisted of an irregularly shaped, but usually well-outlined aggregate of small black particles which appeared to possess an enhanced affinity for white matter compared to neuropil (e.g. see Fig. 5.7 A,B,E,F).

CTb labeled neurons were readily identified in thionin-counter stained sections by their content of brown granules in the somata and proximal dendrites, which frequently gave the soma a solidly brown appearance. Silver-intensified gold-lectin containing neurons were readily identified and discriminated from unlabeled or CTb labeled neurons by their content of small, intensely black particles in the cytoplasm. Gold-particles were evenly distributed through the somata and proximal-most parts of dendrites. Gold-lectin labeled neurons could, in addition, be easily identified at low power magnification with dark-field illumination, in which they appeared as white particles. Double-labeled neurons were identified by the simultaneous occurrence of coarse brown granules and fine black particles in the same neuronal contour (Fig. 5.7C,D,G,H). No indications were found that the resultant retrograde labeling was biased by the choice of tracer (Koekkoek and Ruigrok, 1995; Ruigrok *et al.*, 1995b).

Cerebellar nucleobulbar projections: single tracer studies

From every single case of the 36 experiments, the outline of individual injection sites and the resulting pattern of contralateral CN labeling was analysed. Here, we will report on the results of 44 injections from 26 rats. In the first part of the results, the individual injections will be used to demonstrate the emerging projection pattern between the CN and the selected brain stem areas. In the second part, the results of various tracer combinations made in 18 of these rats will be presented to study the collateralization of nucleobulbar projections.

A: Injections centered on the inferior olivary complex

Ten injections with either gold-lectin or CTb (indicated with * in Figs. 5.2A - 5.6A) into the IO were analyzed. The injection sites of 8 cases and the resultant retrograde labeling in the CN in 5 of these cases are shown in Figs. 5.1 and 5.2. The injection sites and results of additional cases are shown in Figs. 5.8 - 5.10. Fig. 5.1 shows how injections and resulting retrograde labeling in the CN are presented. Injection sites are indicated in a standardized diagram of transverse sections through the IO. The resultant retrogradely labeling was plotted in actual diagrams of the CN, which was subsequently transferred to a standardized diagram of the flattened, separated and partly unfolded CN. Fig. 5.1C,D indicates how data from the actual plots as shown in Fig 5.1B are transferred to this CN scheme. Case T46 together with 4 cases displayed in Fig. 5.2 indicate that it was not possible to make tracer injections limited to a particular olivary subnucleus. In all cases, small-sized retrogradely labeled cells were

observed scattered in various combinations of the contralateral CN. Although the organization of the nucleoolivary projection is difficult to discern from these injections, it appears to be consistent with a description of the organization of the nucleoolivary projection as based on an anterograde tracing study (Ruigrok, 1997; Ruigrok and Voogd, 1990). E.g. cases T39 and T68, which hardly involved the principal olive (PO) in the injection site show labeling at the accessory olives with only a moderate amount of retrogradely labeled cells in the lateral cerebellar nucleus (LCN). Retrograde labeling with injections of the rostral half of the MAO was mostly found in the medial part of the PIN. Its rostral-most tip, which receives its cerebellar nuclear afferents from the caudolateral part of the PIN (Ruigrok, 1997) was never included in the injection site. Involvement of the rostromedial part of the DAO in the injection site (T68 and T53) caused retrograde labeling in the lateral part of the anterior interposed nucleus (AIN), whereas definite involvement of caudal (T39, T46) or lateral parts (T55) of the DAO resulted in labeling within more medial parts of it. Involvement of the ventrolateral outgrowth (VLO) in the injection site always corresponded to a densely labeled patch of neurons in the ventromedial, parvicellular part of the LCN (T46, T53, T55, levels 6, 7 of the CN). Finally, labeling within the dorsolateral hump (DLH) was only noted when the dorsomedial group of the PO (DM) was involved in the injection site (T53).

B: Injections centered on the nucleus reticularis tegmenti pontis

Ten injections that were centered on the NRTP were analyzed. All cases resulted in massive retrograde labeling, mostly of large or medium-sized neurons, in the contralateral CN. An injection centered on the trapezoid body, just caudal to the NRTP, resulted in no labeling within the CN (Fig. 5.3A: case T66). The injection sites of 8 cases are shown in Fig. 5.3A, the remaining injection sites are indicated in Figs. 5.11A and 5.12A. The results of five cases are illustrated in Fig. 5.3B. Note that the corresponding injection sites, all covering the medial part of the NRTP, did not incorporate the contralateral NRTP or major parts of the basal pontine nuclei (Fig. 5.3A). The pattern of retrograde labeling is remarkably consistent in all five cases. Most retrogradely labeled cells are found in the LCN. Injections centered on the caudal part of the NRTP (T61) tend to label the dorsolateral part of the LCN, whereas more rostrally placed injections predominantly label ventromedial parts of the LCN (T44, T69, T58). Within the AIN most retrogradely labeled neurons were observed in its lateral aspects and usually including the DLH (T61,T68). Within the DLH labeling is more concentrated in its caudal part (see also Figs. 5.10, 5.11, 5.12). In the MCN, many labeled neurons were invariably found in its caudal pole. In some cases, labeling is present in the juxtaventricular, rostrolateral part of the MCN (jvMCN). The DLP is devoid of labeled neurons. Within the PIN only a few labeled neurons were detected usually at its ventrorostral aspect close

to the roof of the 4th ventricle (levels 4 and 5 of Fig 5.1B). In some cases, this labeling was continuous with labeled neurons in the rostral parts of the ICG (T68, see also Fig. 5.11: cases T56 and T60, and Fig 5.12: cases T63 and T65), where labeling generally was absent or scanty.

C: Injections centered on the red nucleus

Thirteen injections centered on the RN were analyzed to study the pattern of nucleo-rubral connections. Five injections were centered on the caudal, magnocellular, part of the RN (RNm: Fig. 5.4), whereas the other cases were centered, on its rostral, parvicellular, part (RNp: Fig. 5.5, see also Figs. 5.8, 5.11, 5.13). However, note that, since the border between both RN regions was put between levels 3 and 4 (Daniel *et al.*, 1987; Reid *et al.*, 1975b), many cases were not completely restricted to either part of the RN. In cases where the injection clearly covered parts of the RNm most labeled neurons were observed in the AIN and medial part of the PIN (Fig. 5.4, see also Fig. 5.13 for results of cases R746, R747). The rostromedial part of the AIN was heavily labeled when the injection was centered on the ventrolateral aspect of the RNm (T141, R746, R747), whereas caudolateral AIN was involved when the injection was centered on the dorsomedial part of the RNm (T42). In case T51L, with an injection that was centered on the medial border of the RNm, retrogradely labeling was particularly manifest in the medial part of the PIN, including the caudal aspects of the ICG.

Injections covering the medial, central, and lateral aspects of the RNp are shown in Fig. 5.5 (cases T45, T60, and T143, respectively). In addition, one injection (case T48) is shown that was centered on the pararubral area, located just lateral to the magnocellular RN and merging with the lateral part of the RNp (Ruigrok and Cella, 1995), as well as two injections the results of which are displayed in Figs. 5.8B and 5.11B. Apart from a rather variable labeling within the AIN and PIN in cases T45 and T60, which may be attributed to incorporation of parts of the RNm, most retrograde labeling was found in the LCN (Fig. 5.5B). Caudal aspects of the LCN project to lateral (T143) and dorsal RNp (T42), whereas more rostral areas of the LCN are involved in the medially placed injection (T45). In case T48, retrograde labeling is exclusively found in the ventromedial part of the caudal LCN. Labeling in the DLH is usually weak, especially in its rostral pole, as is the labeling form the ICG. The MCN, including the DLP, were spared, with the exception of the jvMCN, where labeled cells were occasionally found (e.g. Fig. 5.5: case T45, see also Fig. 5.11: for results on cases T56, T64, Fig. 5.8: case T39, Fig. 5.13: cases T118, R746).

D: Injections centered on the prerubral area

Ten injections will be reported on that were placed in the area directly rostral the RN. Most of them involved the prerubral area between the medial part of the medial lemniscus and the fasciculus retroflexus. Eight injections are shown in Fig. 5.6A, the others are displayed in Figs. 5.9A and 5.12A. No

distinctive topography could be discerned between the location of the preRN injections and labeling in the CN. Cases with an injection bordering on the medial lemniscus tended to label neurons in the rostrodorsal part of the LCN (case T118), whereas the caudal aspects of the LCN were more specifically involved when the injection involved the areas surrounding the fasciculus retroflexus (T69, R746). When the injection was situated even more rostrally and involved the ventral part of the parafascicular thalamic nucleus and/or the subparafascicular nucleus, retrogradely labeled neurons were specifically found in the ventromedial LCN and adjacent lateral part of the PIN, with sparse labeling in the AIN (case T186). Larger areas of the PIN, in particular its medial part and including the ICG, as well as the jvMCN were usually involved when the injection bordered on the fasciculus retroflexus (R746, T69). Labeling in the medial AIN included its medial part with injections in the region between the fasciculus retroflexus and the medial lemniscus (T118, R747, T53, T55, T63). In some experiments labeling in the MCN extended up to its caudal pole (Fig. 5.9: T54, Fig. 5.12: T63, T65). In addition, scattered retrograde labeling was often observed throughout the AIN and DLH (see also Figs. 5.9, 5.12, 5.13).

Collateralization of nucleobulbar projections: double-labeling studies

From the diagrams illustrating the distribution of CN labeling resulting from selective injections in any of the four areas, as depicted in Figs. 5.1 to 5.6, it follows that there are few, if any, CN areas that appear to have a brain stem projection that is restricted to a particular nucleus. Rather, it appears to be a rule that projections from a particular CN subnucleus are distributed to several of the investigated areas. This would imply that individual neurons located within such an area could collateralize to all these regions, or, when collateralization is absent, that every type of projection stems from a distinct, but intermingled, population of cells within such a CN subnucleus. These issues will be addressed in the next section where the results will be presented of 18 cases that cover all six potential combinations of injection sites into the four selected brain stem areas (Table 5.1).

A: Combinations involving the inferior olive

A1: IO and RN

Fig. 5.8A shows the injection sites and resultant retrograde labeling in the contralateral CN of case T45. The olivary injection with gold-lectin covered large areas of the PO, central MAO and DAO and resulted in concomitant labeling within large areas of the LCN, PIN, and AIN and of a few cells in the rostromedial MCN. The RN injection with CTb and resultant CN labeling was already described above (Fig. 5.5). These patterns of distribution of labeled neurons are in accordance with those described above. Large areas of overlap are noted, especially when the labeled areas are indicated in the flattened and stretched-out diagrams of the CN (Fig. 5.8B). However, out of a total of 990

labeled neurons only two double-labeled cells were found (Table 5.1). Obviously, not all retrogradely labeled cells are located in regions were both types of cells are encountered (i.e. in an "overlapping" area). Therefore, in order to obtain a better estimate of the amount of potential collateralization, the percentage of double-labeled cells was calculated based on the relative amount of labeled cells in an overlapping area (see Materials and Methods). Thus, for case T45, the two double-labeled neurons were located in an overlapping area where an estimated number of 413 gold-lectin-labeled neurons and 253 CTb-labeled neurons were found in the analyzed sections. This would indicate that in the overlapping areas (i.e. central PIN, lateral AIN and rostral LCN) approximately 0.5% of the gold-lectin-labeled neurons were double-labeled and 0.4% of the neurons that were labeled from the RN injection (Table 5.1, Fig. 5.14).

In two additional cases (T39: gold-lectin injection in IO is shown in Fig. 5.2A, CTb injection in Fig. 5.5A, and T42: CTb injection site in RN is depicted in Fig. 5.4A, gold-lectin injection in IO in Fig. 5.2A), overlapping areas were also found in PIN, AIN and in a relatively small area of the LCN (Fig. 5.8B). Similar to case T45 virtually no double-labeled cells were encountered (0 out of a total of 1121 and 1 out of 870 labeled neurons in T42 and T39, respectively, see also Table 5.1 and Fig. 5.14).

A2: IO and preRN

Case T53 was chosen as a typical example of an IO-preRN injection combination (Fig. 5.9). Here, gold-lectin was injected in the prerubral region but also involved the medial part of the RNp. CTb had been injected in the central and medial aspects of the inferior olivary complex. Although within the overlapping regions of the CN, i.e. the medial part of the PIN, central part of the AIN and most of the LCN, 288 CTb-labeled and 153 gold-lectin-labeled neurons were counted in the analyzed sections, no double-labeled cells were observed (Table 5.1). A similar picture emerged in two additional cases (Fig. 5.9B, T54 and T55: for injections see Fig. 5.2A and 5.6A). Again, despite extensive CN areas where both cell types were intermingled not a single (T54) and only one (T55) double-labeled neuron was found (Table 5.1, Fig. 5.14).

A3: IO and NRTP

Three examples of cases with injections in the IO and NRTP are shown in Fig. 5,10. Case T61 received a gold-lectin injection in the medial half of the NRTP and two iontophoretic CTb injections were centered on the central MAO and DAO, respectively, but also involved parts of the PO. CN regions in which both types of retrogradely labeled neurons were located, were the lateral part of the AIN and the ventrolateral part of the LCN. These overlapping regions contained an estimated number of 147 gold-lectin and 215 CTb labeled neurons. Three, small-sized, double-labeled neurons were found in the caudal DLH (2) and lateral AIN (1) amounting to 2.0% of the gold-lectin-labeled and to 1.4% of the CTb-labeled cells, respectively. In case T58 (CTb injections in IO centered on lateral bend in PO and involving

adjacent DAO and an additional injection centered on central MAO, and gold-lectin centered on the rostroventral aspect of the medial NRTP and involving the dorsomedial part of the basal pontine nuclei to a small extent, see Figs. 5.2A and 5.3A, respectively) the overlapping area was mainly restricted to the LCN where 5 out of 68 gold-lectin and 74 CTb-labeled neurons were double-labeled. In the overlapping area in case T68 (for injection sites see Figs. 5.2A and 5.3A) two labeled neurons were observed, both located in the rostroventral aspect of the PIN, directly bordering the roof of the 4th ventricle (Figs. 5.10B, 5.14 and Table 5.1).

B: Remaining combinations involving the NRTP

B1: NRTP and RN

Fig. 5.11 displays the results of case T56 with a CTb injection that was centered on the RNp but also incorporated part of the RNm, and a gold-lectin injection in the NRTP and only just encroaching upon the dorsal part of the basal pontine nuclei. The emerging pattern of retrogradely labeled neurons in the contralateral CN was in accordance with earlier descriptions. CN regions where both types of retrogradely labeled cells were found encompassed most of the LCN and AIN, a small strip of cells in the rostroventral PIN and to some degree the jvMCN. Double-labeled neurons were present in all areas of the CN where the two populations overlapped. Of the, estimated, 309 CTb-labeled cells that were located in these areas, 225 (73%) were also labeled with gold-lectin. The estimated number of cells projecting to the NRTP (gold-lectin labeled) in these overlapping areas was 415, implying that at least more than half of these cells (54%), collateralize to the RN. Two additional cases, T60 and T64, had CTb injections that centered on the RNp and involved part of the RNm, combined with gold-lectin injections into the medial NRTP (injections shown in Figs. 5.3A and 5.5A, for injections of T64 also see Fig. 5.7A,B). As in T56, many double-labeled neurons were encountered in the LCN, lateral half of the AIN, and in the rostral part of the ICG and rostroventral part of the PIN (Fig. 5.7C,D, Fig. 5.14, Table 5.1).

B2: NRTP and preRN

T63 serves as a typical example of a case with a combination of injections in the NRTP (with gold-lectin) and in the prerubral area (Fig. 5.12). Gold-lectin labeling in the CN was in general agreement with earlier descriptions of other injections. CTb-labeled cells were found mostly throughout the LCN and PIN, and scattered cells were encountered in the AIN/DLH and the caudal MCN. Thus, most of the LCN, the lateral AIN/DLH, caudal MCN and the rostroventral PIN/rostral ICG constitute regions where both celltypes were intermingled. Indeed, in all these areas double-labeled cells were encountered, contributing to about 27% of the number of gold-lectin labeled cells (projecting to the NRTP) and to more than half of the CTb labeled cells (53%, projecting to the prerubral area, Table 5.1, Fig. 5.14). Basically similar results were obtained in two additional cases, displayed in Fig. 5.12B (T65 and T69: for NRTP injection sites see Fig. 5.3A, for CTb

injections see Fig. 5.6A. Note that in all cases the ratio of double-labeled cells appears to be highest in the LCN.

C: Remaining combinations involving the RN: RN and preRN

In this combination gold-lectin injections were made that were centered on the RN and CTb injections that were centered on the prerubral area. Care was taken to select only those cases with clearly separated injection sites. Three cases will be presented here (Fig. 5.13). The preRN injection of case T118 was already described above (Fig. 5.6, see also Fig. 5.7E) and resulted in many CTb-labeled neurons in the rostrodorsal LCN, medial AIN, and, more sparsely, in the rostral PIN. Neurons labeled from a rather large gold-lectin injection into the RN (Fig. 5.7F) were observed throughout most of the cerebellar nuclear complex except rostral MCN and ventromedial LCN. In all overlapping areas, i.e. dorsal LCN, medial AIN and rostral PIN, double-labeled neurons were encountered, amounting to about 20% of the gold-labeled cells but to almost 70% of the CTb labeled neurons (Fig. 5.7G,H, Fig. 5.14, Table 5.1). In two additional cases, the preRN injections were centered just between the medial lemniscus and the retroflex bundle in case R746, and slightly more dorsomedially in case R747 (injection sites shown in Fig. 5.6A). The gold-lectin injections were almost identical and were centered on the caudal aspect of the RNm (Fig. 5.4A). In both cases overlapping areas and many double-labeled neurons were observed in the medial halves of the AIN and PIN/ICG and, more sparsely, in the LCN (Fig. 5.13B, 5.14, Table 5.1).

Discussion

Objective of this study

This study was prompted by evidence that cerebellar modules exert a differential control over different motor systems (Bloedel, 1992; Godschalk *et al.*, 1994; Oscarsson, 1980; Sato and Kawasaki, 1990a; van der Steen *et al.*, 1994; Voogd and Bigaré, 1980). Therefore, the distribution of the output of these modules through their cerebellar or vestibular target nuclei is of special interest.

The four investigated brain stem areas were selected on the basis of their efferent projections. Since it is well known that perhaps the most obvious function of the cerebellum is concerned with motor control, cerebellar projections to premotor areas such as the "motor" thalamus, the medial reticular formation, the superior colliculus and the RN, have already been described in literature (for review see (Voogd, 1995) and chapter 2). We have chosen to investigate the RN as premotor nucleus because it is a relatively small, reasonable well delineated area. Moreover, most of its projection neurons may be considered as premotor neurons since they enter the rubrospinal tract (for review see Ruigrok and Cella, 1995). Many of the projections of the cerebellar nuclei are involved in recurrent cerebellar circuits. Cerebellar projections to the NRTP (for review see Ruigrok and

Cella, 1995) but also to the basal pontine nucleus (Mihailoff *et al.*, 1989), give rise to cerebellar mossy fiber activity and collateral activation of the CN, whereas the source of climbing fibers, the IO, also receives a direct and prominent cerebellar nuclear projection. The IO is also heavily afferented by areas located at the mesodiencephalic junction such as the nucleus of Darkschewitsch, the prerubral area, the accessory oculomotor nucleus and the interstitial nucleus of the medial longitudinal fascicle (Carlton *et al.*, 1982; Ruigrok and Cella, 1995; Rutherford *et al.*, 1984), areas which are known to receive cerebellar input (Berretta *et al.*, 1991a; De Zeeuw and Ruigrok, 1994; Faull and Carman, 1978) and are collectively known as the area prerubralis parafascicularis (Carlton *et al.*, 1982). Indeed, stimulation of the brachium conjunctivum in cat can result in disynaptic activation of olivary cells (Ruigrok and Voogd, 1995a). Hence, as an excitatory preolivary area, the prerubral area was included in our study on the degree of convergence and divergence of cerebellar nuclear projections.

Using a new non-fluorescent double retrograde tracer technique, we found extensive collateralization of the axons of relay cells of the CN nuclei between the nucleus reticularis tegmenti pontis (NRTP), innervated by the crossed descending branch of the scp, and the red nucleus (RN) and prerubral area (preRN), both provided by its crossed ascending branch. Moreover, a large proportion of the CN neurons projecting to RN also has terminations in the prerubral area. Neurons that provide an input to the inferior olive, however, do not collateralize to these areas.

Methodological considerations

Most studies investigating axonal branching of CN neurons make use of combinations of retrogradely transported fluorescent tracers (Bentivoglio and Kuypers, 1982; Bentivoglio and Molinari, 1981; Gonzalo-Ruiz and Leichnetz, 1987; Huisman *et al.*, 1983; Lee *et al.*, 1989). Although the development of these and related techniques have greatly furthered our understanding on the collateralization of fiber projections, some major disadvantages are recognized. Fluorescent tracers such as Fast Blue, Diamino Yellow and Nuclear Yellow are difficult to dissolve, frequently result in large injection sites and may result in considerable tissue necrosis and potential tracer uptake by damaged fibers of passage (Keizer *et al.*, 1983). Moreover, the pattern of labeling tends to fade upon illumination and in time. Also, with fluorescent microscopy, the identification of cytoarchitectural boundaries may be difficult. Using immunocytochemically detected tracing with CTb in combination with silver-enhanced detection of transported gold-lectin, most of these disadvantages can be overcome. Relatively small injection sites can be obtained with either tracer without any apparent tissue necrosis. Moreover, standard verification of the injection site by recording either directly through the tracer solution or using a double barrel pipette greatly increases the success rate of well-placed injections (Luppi *et al.*, 1990;

Ruigrok *et al.*, 1995b). Various gold-lectin conjugates such as WGA-HRP-gold, WGA-apoHRP-gold (Menétrey, 1985), CTb-gold (Llewellyn-Smith *et al.*, 1992) and WGA-BSA-gold (Ruigrok *et al.*, 1995b) have been shown to have excellent retrograde uptake capabilities without obvious risk of inadvertent labeling by damaged or passing fibers. This risk may be present when using CTb as a tracer (Chen, 1995; Ruigrok *et al.*, 1995b), but is minimal when only low iontophoretic currents and short survival times are employed (Luppi *et al.*, 1995; Luppi *et al.*, 1990; Ruigrok *et al.*, 1995b). Nevertheless, for this reason we routinely changed gold-lectin and CTb injections in any combination of injection sites, with exception of the NRTP which, since the nucleoolivary pathway runs directly through and just dorsal to the NRTP (Legendre and Courville, 1987; Ruigrok and Voogd, 1990) and therefore would be exceptionally prone to inadvertently label nucleoolivary neurons, always received the gold-lectin injection. Risk of inadvertent tracer uptake by passing nucleoolivary fibers indeed appeared to be minimal since no labeled CN neurons were encountered when the gold-lectin injection was centered just caudal to the NRTP in the trapezoid body. Although not specifically investigated we have noted no obvious differences in retrograde uptake characteristics between CTb and gold-lectin as based on the relation of injection site and size and number of retrogradely labeled cells (see also Koekkoek and Ruigrok, 1995; Teune *et al.*, 1995).

Organization of cerebellar nuclear projections to IO, NRTP, RN and prerubral area

A: Inferior olive

Nucleoolivary neurons in general can be distinguished from other cerebellar nuclear relay neurons by their size and immunoreactive characteristics. They are small-sized, spindle shaped neurons (Buisseret-Delmas *et al.*, 1989; Chan-Palay, 1977; Fredette and Mugnaini, 1991), and contain GABA as their main neurotransmitter (De Zeeuw *et al.*, 1989b; Fredette and Mugnaini, 1991). In our series of experiments, neurons labeled from IO injections displayed a compatible morphology. Since virtually all injections were made in the center of the IO complex (in order to maximize the amount of retrograde labeled cells without risk of tracer spillage to extraolivary regions), not much information is available on the results of injections into the caudal- and rostral-most aspects of the olivary complex. Nevertheless, the pattern of retrograde labeling following these injections was completely compatible with a detailed report by Ruigrok and Voogd (Ruigrok and Voogd, 1990), which was based on anterograde tracing studies. In brief, injection sites involving the PO resulted in labeling in the LCN. Labeled neurons in the PIN were found after an injection involving the rostral MAO; the AIN contained labeled cells when the injection incorporated the DAO (excluding its dorsal fold). Injections involving the dorsomedial group resulted in labeling in the DLH. The organization of the nucleoolivary projections appears to be neatly reciprocated by a matching

olivonuclear projection by the climbing fiber collaterals (Ruigrok, 1997).

B: Nucleus reticularis tegmenti pontis

Projections from the CN to the contralateral NRTP have been described in many species such as rat (Angaut *et al.*, 1985a; Torigoe *et al.*, 1986b; Watt and Mihailoff, 1983a; Watt and Mihailoff, 1983b), see also chapter 2; opossum (Yuen *et al.*, 1974); cat (Brodal *et al.*, 1972a; Voogd, 1964) and monkey (Asanuma *et al.*, 1983a). Using anterograde tracing techniques, the projections from the MCN onto the NRTP have been described as relatively sparse and to terminate mainly in a dorsomedial column throughout the NRTP (Cicirata *et al.*, 1982; Mihailoff *et al.*, 1988; Watt and Mihailoff, 1983a). In our retrograde study we have noted that the NRTP injections, which usually involved the medial part of the NRTP resulted in many retrogradely labeled neurons usually limited to the caudal pole of the MCN, but sometimes including the base of the DLP and the jvMCN. This is in partial accordance with a degeneration study in opossum which suggest that terminal degeneration is only found in the NRTP when the caudomedial part of the MCN was involved in the lesion (Yuen *et al.*, 1974). Since a prominent projection to the medial pontine reticular formation has been described to (partly) originate from the MCN (Gonzalo-Ruiz and Leichnetz, 1987), the possibility of false positive labeling by inadvertent spread or leakage of the tracer to this overlying area may have been present. However, since one of our injections, using a similar approach, only just missed the NRTP (T 66: Fig. 5.3A) and subsequently did not result in any labeling within the CN, the risk of false positive labeling was judged to be minimal.

In all cases, most of the retrogradely labeled neurons were observed in the LCN. In agreement with anterograde tracing studies by Angaut (Angaut *et al.*, 1985a) reported in chapter 2 of this thesis, we noted that injections that were centered on the caudal part of the NRTP tended to result in labeling of neurons in the rostrodorsal part of the LCN, whereas labeling in caudomedial LCN resulted from more rostrally placed injections. Within the interposed nuclei most labeling was observed within the DLH and lateral part of the AIN. The absence of the NRTP projections of the medial AIN is not in accordance with the observations made in the anterograde tracing studies reported in chapter 2. Here, medial injections of the AIN resulted in distinct or sparse labeling in the lateral NRTP and the adjacent pontine nuclei. The exclusion of PIN in the cerebellar nuclear projections to the NRTP was already noted by Torigoe (Torigoe *et al.*, 1986b), in the cat by Brodal (Brodal *et al.*, 1972a) and in the monkey by Asanuma (Asanuma *et al.*, 1983a). However, in our material, there was some, but consistent retrograde labeling of neurons that were located directly dorsal to the roof of the 4th ventricle, a transition area that could be designated as part of the PIN (Voogd, 1995) and which was continuous with labeling in the rostral part of the interstitial cell groups that are located between the medial part of the AIN and the MCN.

C: Red nucleus

For the description of the RN in the rat, we have followed the description of Reid (Reid *et al.*, 1975b). In our figures, the border between the magnocellular and parvicellular parts is located approximately at level 3, which corresponds to level 6 of Reid et al. (Reid *et al.*, 1975b). The organization of cerebellar nuclear projections to the RN in the rat has been investigated using anterograde and retrograde tracing techniques (Angaut *et al.*, 1987; Caughell and Flumerfelt, 1977; Daniel *et al.*, 1987). Basically, the results presented here are in agreement with those studies. The medial part of the AIN projects to the ventrolateral RNm, the lateral AIN projects to the dorsomedial RNm and the medial part of the PIN contains labeled neurons when the medial border of the RN was included in the injection site. Although our injections that were centered on the RNp never resulted in exclusive labeling of the LCN, we concur with other authors that most cerebellar terminals to this part of the RN originate from the LCN (Angaut *et al.*, 1987; Caughell and Flumerfelt, 1977; Flumerfelt, 1978). The topography in the projection of the rostral LCN to medial and ventrolateral RNp and caudal LCN to lateral and dorsal RNp is in partial agreement with the observations of Angaut (1987) that were based on anterograde tracing studies. An essentially similar pattern has been reported for other animals such as the monkey (Flumerfelt *et al.*, 1973) and cat (Condé, 1988; Courville, 1966). The MCN is usually devoid of labeling with exception of some neurons in the jvMCN. In some cases (e.g. T 118: Fig. 5.13) additional labeling within the MCN may have been caused by inadvertent spread of the tracer to overlying accessory oculomotor areas (Gonzalo-Ruiz and Leichnetz, 1987).

An injection directly lateral to the RNm resulted in retrograde labeling within a small area in the caudal part of the ventromedial LCN. This projection has recently also been shown by anterograde techniques (Ruigrok and Cella, 1995), see also chapter 2, and resulted in a definite and rather circumscript terminal field which merged rostrally with the boundaries of the RNp. This region was indicated as the pararubral area by Ruigrok and Cella (Ruigrok and Cella, 1995). It is not known to what extent this pararubral region should be considered as a premotor or a preolivary region (Newman, 1985a).

D: Prerubral area

The medial part of the mesodiencephalic junction has received much attention as an area from which a prominent projection to the IO originates (Carlton *et al.*, 1982; De Zeeuw *et al.*, 1989b; Onodera, 1984; Ruigrok and Cella, 1995; Rutherford *et al.*, 1984; Spence and Saint-Cyr, 1988) (Ruigrok and Voogd, 1995a). More specifically, this area includes the prerubral field (medial to the medial lemniscus and dorsal and lateral to the fasciculus retroflexus), the medial accessory oculomotor nucleus, the rostral part of the nucleus of Darkschewitsch, the subparafascicular nucleus and the rostral interstitial nucleus of the medial longitudinal fascicle (for review see Ruigrok and Cella, 1995). Here, this area is collectively referred to as

prerubral area (preRN). Claims that in the rat an olivary projection originates from the RNp (Swenson and Castro, 1983a; 1983b) have been denied on several occasions (Carlton *et al.*, 1982; Rutherford *et al.*, 1984). For this reason, the preRN rather than the RNp of the rat has been considered as a homologue of the primate parvicellular RN (Kennedy *et al.*, 1986; Ruigrok and Cella, 1995).

Cerebellar projections to the mesodiencephalic junction have been mainly investigated in cat and appear to originate predominantly from the LCN and PIN (Cohen *et al.*, 1958; Voogd, 1964), but projections to the nucleus of Darkschewitsch have also been shown to arise from AIN and MCN (Kawamura *et al.*, 1982; Onodera and Hicks, 1995; Sugimoto *et al.*, 1982). Indeed, in the cat, it has been demonstrated that neurons in the mesodiencephalic junction mediate a disynaptic excitatory pathway between the CN and the IO (De Zeeuw and Ruigrok, 1994; Ruigrok and Voogd, 1995a). In accordance with the situation in cat, injection with retrograde tracers in the prerubral region of the rat mostly result in retrograde labeling in the LCN and PIN, as well as in the AIN including the DLH. Labeled neurons were usually found scattered throughout the entire LCN, including its ventromedial, parvicellular part. In the PIN labeling extended into the ICG and into the lateral and caudal pole of the nucleus. In some cases labeled cells were present in the jvMCN and in the caudal pole of this nucleus.

Collateralization of cerebellar nuclear output

Our experiments are in agreement with and extend the generally held concept that the CN harbor at least two different populations of projection neurons. One group, the nucleoolivary neurons, consists of small-sized neurons which are distributed throughout the CN and reportedly all contain GABA as neurotransmitter (Angaut and Sotelo, 1987; Bentivoglio and Kuypers, 1982; Buisseret-Delmas *et al.*, 1989; De Zeeuw *et al.*, 1989b; Fredette and Mugnaini, 1991; Legendre and Courville, 1987). The question remains, however, to what extent the nucleoolivary neurons may collateralize to other cerebellar projection areas such as the bulbar reticular formation (Buisseret-Delmas *et al.*, 1989), the thalamus or the basal pontine nuclei and/or NRTP (Aas and Brodal, 1990; Border *et al.*, 1986; Verveer *et al.*, 1997).

The second group of projection neurons consists of medium- to large-sized cells, which may show a rather extensive collateralization to these latter areas, while observing regional differences in their projection pattern. These neurons, most likely, are all excitatory (De Zeeuw and Ruigrok, 1994; Giuffrida *et al.*, 1993; Toyama *et al.*, 1968). Here, we will discuss our observations in relation with these two populations of cerebellar projection neurons.

A: Nucleoolivary neurons

The collateralization of nucleoolivary neurons to other brain stem regions has been investigated by many groups employing both

anatomical and electrophysiological techniques. The fluorescent double-labeling studies by Bentivoglio (1982) in the rat, investigating cerebellar nuclear collateralization to the cervical cord, the caudal medulla, the mesencephalon (superior colliculus and RN) and the thalamus, were suggestive of a non-collateralizing projection from small-sized neurons to the IO. However, definite conclusions were hampered by the large injection sites that covered sizable parts of the caudal medulla oblongata. In the cat, and in line with an unique nucleoolivary projection, Legendre (1987) and Bharos (1981) were unable to find collateralizing nucleoolivary neurons to the thalamus. Lee (1989), on the other hand, found evidence of a small, collateral projection of nucleoolivary neurons to the contralateral basilar pontine nuclei in the rat. This would be in line with observations in both the rat and the cat of a cerebellar derived GABAergic projection to the basilar pontine nuclei (and NRTP: Aas and Brodal, 1990; Border *et al.*, 1986). Electrophysiologically obtained data in the rat (Berretta *et al.*, 1991a) appear to collaborate this notion but are not in line with a similar study in the cat where only excitatory monosynaptic responses could be elicited in NRTP neurons after stimulation of the LCN (Kitai *et al.*, 1976). Our data indicate that only a relatively low portion of the nucleoolivary fibers may collateralize to the NRTP. At best only 5 out of 68 labeled neurons in an overlapping region (case T 58) was double-labeled in a combination involving the NRTP and IO. It should be realized, however, that, although specifically for this reason gold-lectin was used as the injected tracer, the interpretation of a potential collateralization of nucleoolivary fibers to the NRTP may be hampered by the risk of false positive double-labeling which may result from inadvertent uptake by damaged axons of the crossed descending limb of the scp that runs directly dorsal to and through the NRPT and which contains most of the nucleoolivary fibers (Legendre and Courville, 1987; Ruigrok and Voogd, 1990). In the cat, a recently published ultrastructural study failed to establish a GABAergic projection originating from the CN to the NRTP (Verveer *et al.*, 1997). Nevertheless, especially since Lee (1989) -see also Aas and Brodal, 1990- made use of a ventral approach to the BPN, thus minimizing the risk of false positive labeling, it would seem possible that a very small number of nucleoolivary neurons truly may have collaterals to the basal pontine nuclei and/or NRTP.

In the cat, several publications have suggested that at least part of the nucleoolivary neurons possess ascending collaterals to the thalamus (Andersson and Hesslow, 1987b; Ban and Ohno, 1977; McCrea *et al.*, 1978; Tolbert *et al.*, 1978a). This conclusion was mainly based on electro-physiological studies of recordings in the interpositus nuclei and employing antidromic stimulation and collision experiments from thalamus and IO. However, it should be noted that at least part of the PIN neurons, especially located in its medial part, project to the contralateral cervical cord and course just dorsal to the IO (Bharos *et al.*, 1981; Horn *et al.*, 1995). Since at least a part of these

cervical cord projecting PIN neurons possess ascending collaterals to the thalamus (Bharos *et al.*, 1981), only a slight current spread from the IO-placed stimulation electrode may explain the above mentioned electrophysiological observations.

In conclusion, despite the possibility that a very small proportion of the nucleoolivary neurons may collateralize to the NRTP, it is evident that this population of, GABAergic, cerebellar nuclear neurons is unique in its projection to the IO.

B: Other nucleobulbar relay neurons

Several anatomical studies, including our own, have shown that many of the medium- and large-sized, excitatory relay cells project to two or more different brain stem areas (Bentivoglio and Kuypers, 1982; Bentivoglio and Molinari, 1986; Gonzalo-Ruiz and Leichnetz, 1987; Lee *et al.*, 1989). Bentivoglio (1982) demonstrated with the fluorescent double-labeling technique that many cerebellar efferents traveling in the crossed ascending limb of the scp to the superior colliculus and/or thalamus bifurcate and send their collaterals via the descending limb to the medulla oblongata and/or cervical spinal cord. Most double-labeled neurons were found in the MCN, in the medial part of the interposed nuclei, especially in the area now designated as the interstitial cell groups (ICG; Buisseret-Delmas *et al.*, 1998), and in the dorsomedial part of the LCN and DLH. These data are largely in accordance with similar experiments performed in the cat (Bharos *et al.*, 1981). In a later study, Bentivoglio (1986) demonstrated a projection of neurons in the DLH and adjoining AIN and LCN to the ipsilateral bulbar reticular formation. The cells located just outside the DLH in AIN and LCN also collateralize to the contralateral thalamus. Collateralization of many neurons located in the LCN and of a few in the AIN to the basilar pontine nuclei and thalamus were demonstrated by Lee (1989). The same authors also describe a collateral projection to the basilar pontine nuclei and the superior colliculus arising from several LCN neurons. Gonzalo-Ruiz (Gonzalo-Ruiz and Leichnetz, 1987) observed double-labeled neurons predominantly in the MCN but also in the LCN after double fluorescent tracer injections in combinations of several areas involved in eye movement control such as the superior colliculus, the paraoculomotor region and the medial pontine reticular formation.

In our study, we found double-labeled cells projecting to the NRTP and to the RN or the prerubral area in all areas of the CN which also project to the former nucleus. No areas were found that contained large quantities of retrograde labeled neurons of either type, yet without any double-labeled neurons. Double-labeled neurons were notably absent from the medial AIN and PIN, with the exception of its rostroventral, juxtaventricular area. In addition, our study shows that many CN neurons that project to the RN also provide terminals to the preRN. The occurrence of double-labeled neurons varied between experiments but, in some instances, could amount to more than 70% of the total number of labeled cells in an area where both types of labeling were found (e.g. case T56, T747, Table 5.1). Our

observation that double labeled neurons are present in all regions where single labeled neurons from combinations of the red nucleus, the prerubral area or the NRTP overlap is not unique. Similar observations have been made by all previous authors using retrograde double labeling from other combinations of cerebellar target nuclei in many different regions, including the cord, visual effector regions, the pontine nuclei, the reticular formation and the thalamus (Bentivoglio and Kuypers, 1982; Bharos *et al.*, 1981; Gonzalo-Ruiz and Leichnetz, 1987; Lee *et al.*, 1989). It can be concluded that a large proportion, if not all, medium- to large-sized non-GABAergic project to at least more than one area. For this reason, it seems quite probable that some neurons, especially in the LCN, may project to more than two of these areas. In addition, Shinoda (1988), using intra-axonal injection of HRP, was unable to find cerebellar nuclear axons with terminals within the RN that did not continue to the thalamus.

Output profiles of cerebellar modules

The present data should be discussed in relation to the modular organization of the CN, which is based on the strict organizational pattern of longitudinal strips of Purkinje cells, which terminate upon a specific part of the CN. This organization is mimicked by climbing fibers that originate from particular subdivisions of the IO to the same longitudinal strips of Purkinje cells and that, simultaneously, provide a collateral projection to the CN target nucleus of these strips (Buisseret-Delmas and Angaut, 1993; Voogd, 1995; Voogd and Bigaré, 1980). In this way, the output of the cerebellar cortex is organized as a series of discrete, parallel olivo-cortico-nuclear modules. The modular organization of the cerebellum of the rat was reviewed by Buisseret-Delmas and Angaut (1993). It differs on some essential points from the situation in the cat, where the MCN, lateral vestibular nucleus (Deiters' nucleus: LVN), PIN, AIN, and dorsal and ventral LCN are considered as the target nuclei of the cerebellar modules (Voogd and Bigaré, 1980). Several subdivisions of the CN of the rat, which serve as target nuclei of independent modules, were not recognized in the cat by Voogd (1980). These subnuclei include the dorsolateral protuberance (DLP) of the MCN and target nucleus of the lateral extension of the A zone (Buisseret-Delmas, 1988a); the interstitial cell groups (ICG) located between the MCN and AIN and target nucleus of the vermal X and hemispheral Cx zones (Buisseret-Delmas *et al.*, 1993; Campbell and Armstrong, 1985); and the dorsolateral hump (DLH) which is the target nucleus of the D0 zone (Buisseret-Delmas and Angaut, 1989b). Moreover, the spatial arrangement of the projections of several cortical zones to the nuclei appears to be different for cat and rat. The C1, C2 and C3 zones of the cortical pars intermedia of the cat project to the AIN, PIN and AIN, but in the rat, C1, C2 and C3 project to medial AIN and PIN, central AIN and lateral PIN, and lateral AIN, respectively (Buisseret-Delmas, 1988b). Also, the projection of the D1 and D2 zones of the hemisphere of cat cerebellum to the ventromedial,

parvicellular LCN and the rostrodorsal LCN, respectively, appears to be reversed in the rat (Buisseret-Delmas and Angaut, 1989a).

A-module. In Table 5.2 we summarize our single and double-labeling studies with respect to the modular organization of the rat cerebellum. Basically, the MCN in the rat can be divided into a rostral, a caudal and the rostrolateral, juxtaventricular subdivisions. The DLP, in addition, may be considered as a separate subnucleus. These differences in the brain stem projections originating from these four MCN target areas may be related to the presence of subzones restricted to certain cerebellar lobules (Voogd *et al.*, 1996b). However, in the rat, little is known about the corticonuclear projections to these different MCN areas. Projections from the rostral part of the MCN have been documented to terminate in the medial bulbar reticular formation and spinal cord (Bentivoglio and Kuypers, 1982). The caudal part of the MCN receives Purkinje cell axons from the lobules VIb,c - IX, including the vermal visual area (Godschalk *et al.*, 1997; Päällysaho *et al.*, 1990; Umetani and Tabuchi, 1988), see also chapter 2. Neurons in this MCN subdivision have been shown to project to the thalamus, the superior colliculus, the basilar pontine nuclei, the medullary reticular formation and the cord and to several preoculomotor nuclei (Bentivoglio and Kuypers, 1982; Gonzalo-Ruiz and Leichnetz, 1987; Lee *et al.*, 1989). In our study, it was identified as the main MCN subnucleus with projections to the NRTP and, to a lesser extent, to the prerubral area. Many of these projections arise as branches of the same neurons. Projections of the MCN to the lateral horn of the RN and to the pararubral area were noticed in the anterograde tracing studies reported in chapter 2. In cases T118 and R747 from this chapter, retrograde labeling after injections of lateral (para-)rubral areas was noticed in the caudal MCN and the base of the DLP. No double labeling in these regions was observed.

The DLP receives a projection from Purkinje cells in the hemisphere of the lobules VI and VII (lateral extension of the A zone: Buisseret-Delmas, 1988a). It gives rise to a major, crossed, projection to the medial bulbar reticular formation, which partly branches to the thalamus (Bentivoglio and Kuypers, 1982), but not to the areas investigated in this study.

X-module. The ICG is the target nucleus of the X zone, which is located between the A and B zones in the anterior vermis, with possible extensions in the posterior lobe (Buisseret-Delmas *et al.*, 1993; Ruigrok, 1997; Voogd and Ruigrok, 1997; Yatim *et al.*, 1995b). Although it possesses diverging projections and collateralizes to the RN, the preRN and, to a lesser degree, to the NRTP, its most typical feature is found in its projections to the medial medullary reticular formation and, especially, to the spinal cord with collateralizations to the thalamus (Bentivoglio and Kuypers, 1982).

B-module. The LVN, not specifically included in our analysis, is the target nucleus of the B zone of the anterior vermis (Buisseret-Delmas, 1988a; Voogd *et al.*, 1991). It gives rise to the lateral vestibulospinal tract,

and does not participate in any of the ascending projections, although it does have a projection, to the dorsal fold of the DAO from which it also receives a collateral climbing fiber innervation (Ruigrok and Voogd, 1990; Voogd and Ruigrok, 1997).

C-modules. Within the interposed nuclei, there are important differences in projection between medial and lateral areas, which would derive their significance from the mediolateral pattern in the terminations of the C1, C2 and C3 zones of the pars intermedia, as described by Buisseret-Delmas (1988b). Medial AIN and PIN, which receive Purkinje cell axons from the C1 zone, lack a projection to the NRTP, but both project and collateralize to the RN and preRN. The lack of a projection to the NRTP of the medial AIN, which was a consistent feature of our experiments with retrograde (double) labeling, is at variance with some of the cases with anterograde tracing from the AIN, as reported in chapter 2 (T89, T83), which showed terminal labeling in the lateral NRTP and the adjacent pontine nuclei. Projections from the medial-most part of the PIN may posses similar features as the neurons in the ICG with respect to their projections to the cervical cord and thalamus (Bentivoglio and Kuypers, 1982). Cells in the intermediate and lateral part of the AIN are the targets of the C2 and C3 zones, respectively, whereas the lateral PIN only receives Purkinje cell axons from the C2 zone. In our material, the lateral AIN is characterized by its abundant projections to the dorsal part of the magnocellular RN with collateralizations to the NRTP and, somewhat more sparsely, to the preRN. In addition, collateralizing projections have been described to the contralateral thalamus, superior colliculus and medial bulbar reticular formation, and to the ipsilateral lateral medulla oblongata (Bentivoglio and Kuypers, 1982; Bentivoglio and Molinari, 1986). The lateral PIN, on the other hand, does not project to the NRTP, but projects to the preRN and, to a lesser extent, to the parvicellular part of the RN. Collateralizing cells from this region have furthermore been described to the superior colliculus and thalamus (Bentivoglio and Kuypers, 1982).

D-modules. The DLH is the target nucleus of the D0 zone of Buisseret-Delmas and Angaut (1989b), located in the lateral hemisphere of the lobules III-VIII, between the C2 and D1 zones. Like the lateral AIN, the DLH is characterized by branched projections to the ipsilateral lateral medulla oblongata and the thalamus (Bentivoglio and Molinari, 1986). However, neurons in this area may also collateralize to RN and NRTP, and more sparsely, to the preRN. In addition, the DLH may issue projections to oculomotor related areas (Gonzalo-Ruiz and Leichnetz, 1987).

In the rat, the ventromedial (and caudal) LCN and dorsolateral (and rostral) LCN are proposed to be the recipients of Purkinje cell axons of the D1 and D2 zones, respectively, of the cerebellar hemisphere (Buisseret-Delmas and Angaut, 1989b; Buisseret-Delmas and Angaut, 1993). However, no systematic differences were noted between the caudal and rostral LCN and their projections to NRTP, RN and

preRN. Both subdivisions issue collateralizing projections to the NRTP, the RN (mainly to its parvicellular part) and to the preRN. (Double) labeling was confined to the rostrodorsal LCN with injections laterally in the prerubral field (T118, R746) and to the ventral and caudal LCN with injections located more medially, touching the fasciculus retroflexus or extending rostrally into the subparafascicular nucleus. Collateralization from the LCN was also noted to the superior colliculus, the thalamus, the medial reticular formation, the basal pontine nuclei and from caudal LCN to several oculomotor related nuclei (Bentivoglio and Kuypers, 1982; Gonzalo-Ruiz and Leichnetz, 1987; Lee *et al.*, 1989). Indeed, it would appear that extensive collateralization to large variety of brain stem structures is a specific feature of the output nucleus of the D-zone.

Functional considerations

The cerebellum is suggested to be involved in a great variety of functions which effect the coordination, adaptation, timing and learning of motor programs as well as of cognitive and visceral functions (Haines *et al.*, 1990; Ito, 1994; Schmahmann, 1996). Nevertheless, cerebellar function is thought to involve a characteristic operation that is performed across various, structurally homogeneous components (Bloedel, 1992). The functional heterogeneity of the cerebellum reflects the multiplicity of functions subserved by the central targets receiving the outputs of different cerebellar regions. Bloedel suggests that the functional unit of the cerebellum is the sagittal zone, i.e. the cerebellar module. Evidence for this view may be found by the control on compensatory eye movements by floccular zones (Sato and Kawasaki, 1990b; van der Steen *et al.*, 1994), on saccadic eye movements by the visual vermis (Godschalk *et al.*, 1994) and on the reach to grasp movements by the C1 and C3 zones (Gibson *et al.*, 1996). As such, functional heterogeneity among sagittal zones should be reflected in the systems innervated by the target nucleus. Our study provides information on the level and organization of cerebellar control on motor behaviour, through the RN, the preRN, the NRTP and the IO. The observation that from a particular cerebellar nuclear region projections to several brain stem regions may originate, indicates that a particular cerebellar module may influence these various brain stem areas simultaneously. Thus, non-olivary projecting neurons in the LCN and AIN may simultaneously regulate activity in NRTP, RN and preRN, whereas individual neurons in the PIN do not appear to be involved in the control of the NRTP, but project to the RN and preRN area. The MCN does not appear to be heavily involved in the control of the RN and preRN area. Scattered throughout all CN, and therefore constituents of the output of all cerebellar modules, small, GABAergic, neurons are found with specific projections to the IO. Although the influence on the IO originates from a distinct neuronal population, these neurons are completely intermingled with the medium- and large-sized relay cells of the CN (e.g. see Teune *et al.*, 1995) and, thus, are likely to be

influenced simultaneously by a particular Purkinje cell zone. Indeed, recent evidence has been presented that a single Purkinje cell axon can influence both types of projection neurons (De Zeeuw and Berrebi, 1995a; De Zeeuw and Berrebi, 1995b; Tempia *et al.*, 1991; Teune *et al.*, 1998).

The projections to the NRTP should be viewed with respect to its role as major supplier of cerebellar mossy fibers with a distinct collateral input to the CN. According to the electrophysiological studies of Tsukahara (1983) a two-neuron excitatory loop exists between the nucleus interpositus of the cat cerebellum and the NRTP, based on the observation that stimulation of one area produced monosynaptic excitation in the other. The activity of such a self-activating reverberating circuit appears to be curbed by the cerebellar cortex since removal of the cerebellar cortical input to the interposed nuclei resulted in long-lasting depolarizations and bursting of neurons in the interposed nuclei, NRTP, but also in the RN (Tsukahara *et al.*, 1983). Tsukahara's observations on cerebello-precerebellar reverberating circuits have received renewed interest from Houk's cerebellar model where positive feedback within premotor loops, regulated by inhibition from the cerebellar cortex, may explain the distributed nature of the motor commands in behaving animals (Houk *et al.*, 1993; Houk and Wise, 1995). Our findings on the occurrence of neurons with projections to the RN or preRN and to the NRTP in certain CN, both extend and qualify the existence of these two-neuron excitatory loops. When our retrograde labeling experiments are compared to the results of an anterograde tracing study of the projections from the NRTP and basal pontine nuclei (Mihailoff, 1993), it appears that closed loops may be present between the NRTP and the lateral portion of the AIN, the LCN and the caudal MCN (excluding DLP). Both connections are lacking for the medial AIN, whereas the PIN receives input from the NRTP but does not reciprocate it. In addition, reciprocal projections may exist between the interposed nuclei and the RN (Huisman *et al.*, 1983). The collateral projections of these loops to the RN and the prerubral area probably all proceed to the thalamus (Shinoda *et al.*, 1988). It is not known whether the ascending collaterals from these loops also terminate in other target areas of the CN, such as the superior colliculus, oculomotor-related areas and the reticular formation. The obvious absence of major afferent and efferent connections between the medial AIN and medial PIN with the NRTP, may be compensated by a three neuron-loop, between the RN, lateral reticular nucleus and the medial parts of the interposed nuclei (Ruigrok and Cella, 1995; Tsukahara *et al.*, 1983). The lateral reticular nucleus may also be involved in reciprocal connections to the MCN (for review see Ruigrok *et al.*, 1995a).

The prerubral area may be particularly involved in establishing a 3-neuron excitatory loop between the CN and the IO. Excitatory connections between the interposed nuclei, the nucleus of Darkschewitsch (one of the nuclei in the prerubral area), and the

inferior olivary nuclei have been established in the cat with both morphological and electrophysiological techniques (De Zeeuw and Ruigrok, 1994; Ruigrok *et al.*, 1990; Ruigrok and Voogd, 1995a). The olivary nuclei, in particular the principal and medial accessory olives are involved in this circuitry (Carlton *et al.*, 1982; Onodera, 1984; Saint-Cyr, 1987; Spence and Saint-Cyr, 1988). On their turn they provide an excitatory collateral projection to the PIN and LCN (Kitai *et al.*, 1977; Ruigrok, 1997). The function of these excitatory, CN-prerubral-IO-CN circuits is not well understood. Interactions of the corticospinal system and cerebellar output at the level of the parvicellular RN/preRN (Saint-Cyr, 1987) may also be essential for motor learning. According to Kennedy (1990) the mesodiencephalic projection to the IO may act as a switching device designed for automatization of learned movements. Once movements are learned by combined actions of the corticospinal system and the cerebellum, the (pre-)rubro-olivary pathway, by way of its projections to the cerebellum, automatizes this learned movement by involving the magnocellular RN and its output to the spinal cord. Collateralizating output from the interposed and lateral CN to both prerubral and rubral areas, as reported in this study, might corroborate such a notion.

At the level of the IO the excitatory cerebello-midbrain-olivary-cerebellar circuit interacts with the GABAergic nucleoolivary pathway (Ruigrok and Voogd, 1995a). Since this projection to the IO does not appear to posses major diverging projections (if any at all) to extra-olivary regions, the information carried by this pathway may be completely independent from the information to other brain stem areas. However, recently, it was shown that single Purkinje cells may simultaneously influence nucleoolivary as well as other CN relay neurons (De Zeeuw and Berrebi, 1995b; Teune *et al.*, 1998). Activity patterns in both CN cell types may thus be well correlated and explain why, during movement, activity of the IO appears to be reduced (Horn *et al.*, 1996). In addition, the nucleoolivary pathway may be involved in regulation of the electrotonic coupling between olivary cells, thus regulating the synchronicity in olivary firing characteristics. This may be an important feature of selection and timing of motor functions executed by the cerebellum (Llinás *et al.*, 1974; Welsh *et al.*, 1995)

Legends to figures

Fig. 5.1. Results of an injection with gold-lectin into the left inferior olivary complex of case T 46. **A**: displays a standardized equidistant (160 μm) series of diagrams of the IO in transverse sections. Caudal-most level is at the lower left hand corner (1), rostral-most level is at the upper right hand (16). The injection is indicated as the stippled area. **B**: Neurolucida™ plotted, equidistant (160 μm) series of transverse diagrams of the cerebellar nuclear complex contralateral to the injection site (caudal: level 1, rostral: level 11). Every dot represents one retrogradely labeled cell. **C**: Conversion of the transverse plots into a standardized diagram of the cerebellar nuclei. The first panel shows the transverse plot of level 6, the second panel shows the delineation of nuclei and subnuclei at this particular level. The third panel indicates how the different parts of the nuclei are transformed into a number of flat lines. Note that the dLCN and vLCN are represented as an unfolded strip of cells. The dorsal-most part of the dLCN is disconnected from the DLH (at *). A similar transformation of the other levels results in the standardized view of the separated, flattened and partly unfolded CN in which the location of labeling can be indicated as shown in **D**. A subjectively high density of labeled cells is indicated with dark shading, areas with a more diffuse pattern of labeled neurons is indicated with stippling. The numbers correspond to the approximate transverse levels depicted in B.

Fig. 5.2. Injection sites and results of cases with injections centered on the inferior olivary complex. **A**: Injection sites of seven cases indicated in standardized transverse diagrams of the IO. * indicates that the olivary injection was made with CTb. **B**: Location of retrograde labeling of four cases depicted in the standard diagram of the CN and constructed as indicated in Fig. 5.1. Results of cases T 42, T 54* and T 58* are shown in Figs. 5.8, 5.9, 5.10, respectively.

Fig. 5.3. Injection sites and results of cases with injections centered on the NRTP. **A**: Injection sites of eight cases indicated in a series of standardized, equidistant (320 μm) diagrams of the NRTP. In an additional case (T 66) the injection was located just caudal to the NRTP. Bottom level of the panels is caudal, top level is rostral. **B**: Localization of resultant retrograde labeling of five of these cases in standardized diagrams of the contralateral CN. T 66 did not result in retrograde labeling within the CN. Results of T 64, T 60 and T 65 are shown in Figs. 5.11, 5.12. Diagrams were constructed as indicated in Fig. 5.1.

Fig. 5.4. Injection sites and results of cases with injections centered on the caudal, magnocellular, RN. **A**: Injection sites five cases indicated in a series of standardized, equidistant (320 μm) diagrams of the mesencephalon. * indicates that the RN injection was made with CTb. Top level of the panels is rostral (level 5). **B**: Localization of resultant retrograde labeling of three cases in standardized diagrams of the contralateral CN. the results of R 746 and R 747 are shown in Fig. 5.13. Diagrams were constructed as indicated in Fig. 5.1.

diagrams of the contralateral CN. the results of R 746 and R 747 are shown in Fig. 5.13. Diagrams were constructed as indicated in Fig. 5.1.

Fig. 5.5. Injection sites and results of cases with injections centered on the rostral, parvicellular, RN. **A**: Injection sites of five cases indicated in a series of standardized diagrams of the mesodiencephalon. In addition, a case is shown (T 48) in which the injection was centered in the pararubral area. * indicates that the RN injection was made with CTb. Top level of the panels is rostral (level 6). **B**: Localization of resultant retrograde labeling of three cases with injections into the RNp and of case T 48 in standardized diagrams of the contralateral CN. The results of T 39* and T 64* are shown in Figs. 5.8 and 5.11, respectively. Diagrams were constructed as indicated in Fig. 5.1.

Fig. 5.6. Injection sites and results of cases with injections centered on the prerubral area. **A**: Injection sites of eight cases indicated in a series of standardized diagrams of the mesodiencephalon. * indicates that the RN injection was made with CTb. Top level of the panels is rostral (level 9). **B**: localization of resultant retrograde labeling of four cases in standardized diagrams of the contralateral CN. the results of cases T 54 and T 55*, T 65*, R 747* are depicted in Figs. 5.9, 5.12, 5.13, respectively. Diagrams were constructed as indicated in Fig. 5.1.

Fig. 5.7. Color photomicrographs of cases T 64 (A,B,C,D) and T 118 (E,F,G,H). **A**: CTb injection site centered on the RN in case T 64. **B**: Gold-lectin injection centered on the ipsilateral NRTP in the same animal. **C**: resultant labeling in the contralateral LCN; neurons labeled with gold-lectin only are indicated by open arrow heads, neurons labeled with CTb are indicated by black arrow heads, arrows depict neurons that contain both labels. **D**: Higher magnification of single and double-labeled cells in the AIN. **E**: CTb injection centered in the prerubral area in case T 118. **F**: Gold-lectin injection centered on the RN of the same animal. **G**: Single and double-labeled neurons in the contralateral AIN. **H**: Single and double-labeled neurons in the contralateral LCN. Several double-labeled neurons are indicated by arrows. Scale bars equal 500 μm in A,B,E,F and 25 μm in C,D,G,H. **See p. 272.**

Fig. 5.8. **A**: Injection sites and resultant retrograde labeling in the contralateral CN of case T 45. The CTb injection was centered on the ventromedial RN (upper left hand panel) and the gold-lectin injection covered large areas of the IO (lower left hand panel). Right hand panel depicts retrogradely labeled cells in Neurolucida™-prepared plots of 5 equidistant (360 μm) levels of the CN. Every symbol indicates one labeled neuron. **B**: Single and double-labeling of T 45 indicated in the standardized diagram and supplemented with the same combination of injections of two other cases (T42 and T39: injection sites shown in Figs. 5.2A, 5.4A and 5.5A). In these cases virtually no double-labeled neurons were encountered.

Fig. 5.9. **A**: Injection sites and resultant retrograde labeling in the CN of case T 53. The gold-lectin injection was centered on the prerubral area and medial part of the RNp, whereas the CTb injection covered the medial half of the IO (upper and lower left hand panels, respectively). Right hand panel depicts distribution of retrogradely labeled cells in 5 transverse levels of the contralateral CN. Every symbol indicates one labeled neuron. **B**: Distribution of retrogradely labeled neurons of case T 53 and of two additional cases (T 54 and T 55: injection sites shown in Figs. 5.2A, 5.6A) with injections in the IO and preRN in standardized diagrams of the CN. In these cases virtually no double-labeled neurons were encountered.

Fig. 5.10. **A**: Injection sites and resultant retrograde labeling in the CN of case T 61. Injections of gold-lectin in the NRTP and of CTb in the IO are depicted in upper and lower left hand panels. The distribution of retrograde labeling in the CN is shown in the right hand side panel. The distribution of labeled cells in the standardized CN diagrams is shown in **B** together with two other cases (T 58 and T 68: injection sites shown in Figs. 5.2A, 5.3A) with the same combination of injections. Only very few double-labeled neurons were found.

Fig. 5.11. **A**: Injection sites and resultant retrograde labeling in the CN of case T 56. The injection of CTb was centered on the RNp and gold-lectin covered the medial aspect of the NRTP and dorsomedial part of the basal pontine nuclei. Resultant retrograde labeling in the contralateral CN is shown in 5 equidistant transverse sections. **B**: Distribution of single and double-labeled neurons of case T 56 and of two additional cases (T 60 and T 64: injection sites shown in Figs. 5.3A and 5.5A) with a similar injection combination in the standardized CN diagrams. Many double-labeled neurons are found in overlapping regions, especially in the lateral AIN and LCN.

Fig. 5.12. **A**: Injection sites and resultant retrograde labeling in the CN of case T 63. The CTb injection was centered dorsally in the prerubral area whereas gold-lectin covered ventromedial NRTP and extended somewhat into the basal pontine nuclei. Resultant retrograde labeling in the contralateral CN is shown in 5 equidistant transverse sections. **B**: Distribution of single and double-labeled neurons of case T 63 and of two other cases (T 65 and T 69: injection sites shown in Figs. 5.3A and 5.6A) in the standardized CN diagrams. Many double-labeled neurons are found in overlapping CN regions.

Fig. 5.13. **A**: Injection sites and resultant retrograde labeling in the CN of case T 118. The CTb injection was centered laterally in the prerubral area, whereas the gold-lectin was centered on the RN. Resultant retrograde labeling in the contralateral CN is shown in 5 equidistant transverse sections. **B**: Distribution of single and double-labeled neurons of case T 63 and of two other cases (R 756 and R 747: injection sites shown in Figs. 5.4A and 5.6A) in the standardized CN diagrams. Many double-labeled neurons are found in overlapping CN regions.

Fig. 5.14. Diagram of the percentage of double-labeled neurons found in overlapping areas for all 18 analysed cases displayed in Figs. 5.8-5.13 and sorted by combination of injections (see Table 5.1). Grey bars refer to the percentage of cells that project to the first mentioned area of the injection combination but containing both labels. Black bars refer to the percentage of double-labeled cells that project to the other injection site.

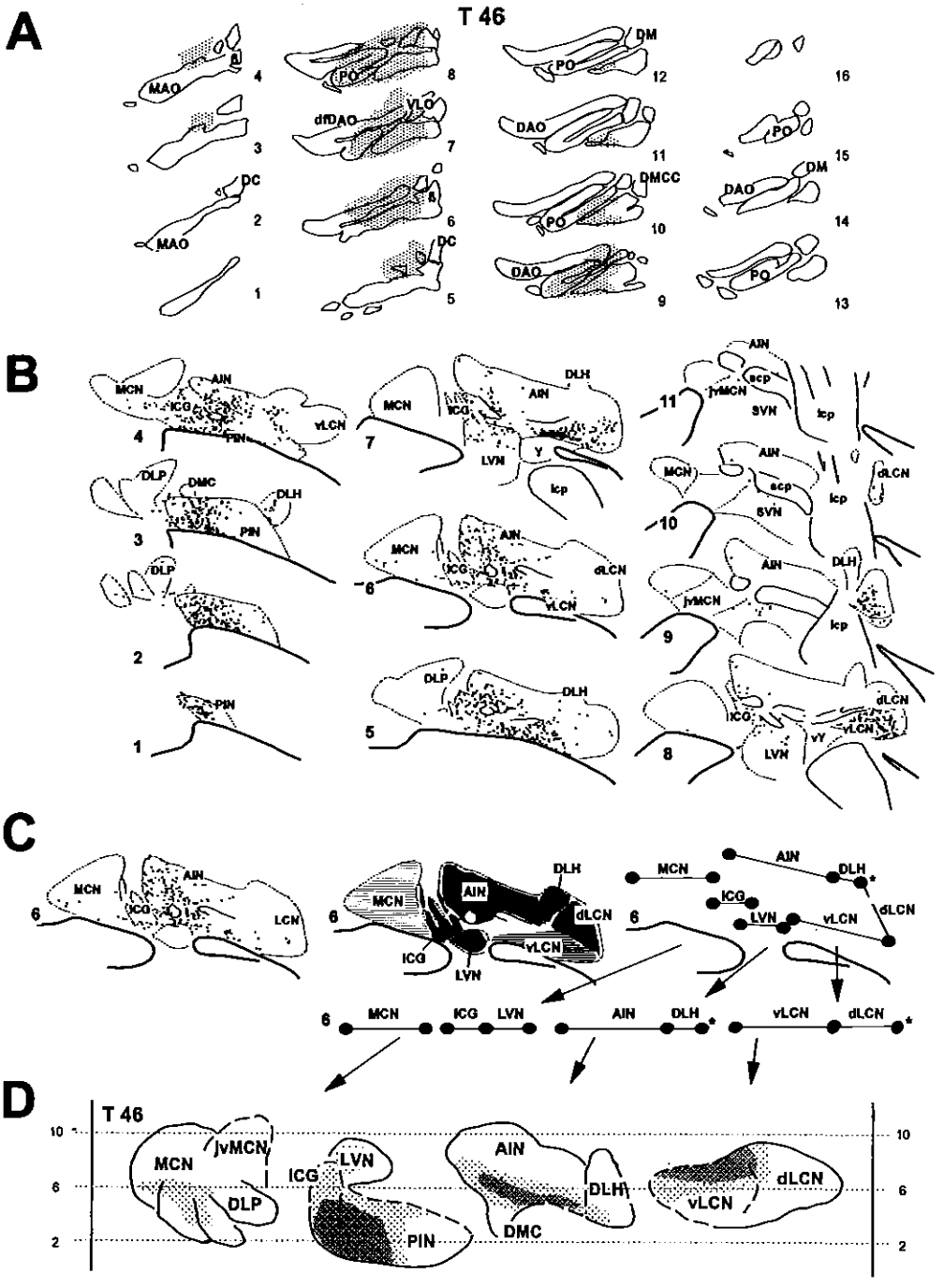
A
T 46
MAO
PO
DM
DAO
VLO
dfDAO
DC
DMCC
B
MCN
AIN
ICG
vLCN
PIN
DLP
DMC
DLH
LVN
Y
lcp
dLCN
jvMCN
scp
SVN
vY
C
LCN
LVN
D
jvMCN
DLP
PIN

Fig. 5.1

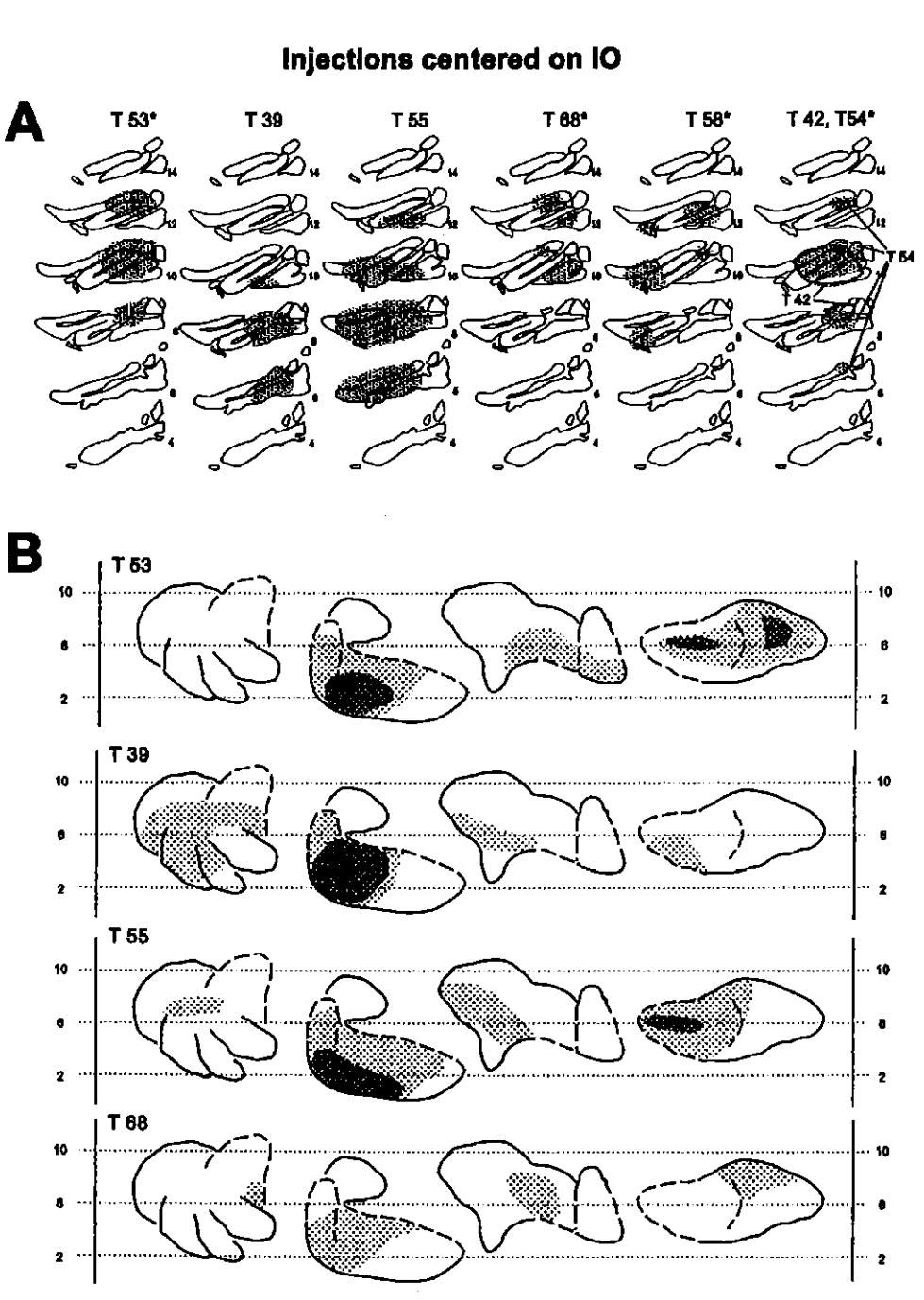
Injections centered on IO
A
T 53*
T 39
T 55
T 68*
T 58*
T 42, T54*
T 54
T 42
B
T 53
T 39
T 55
T 68
10
8
2

Fig. 5.2

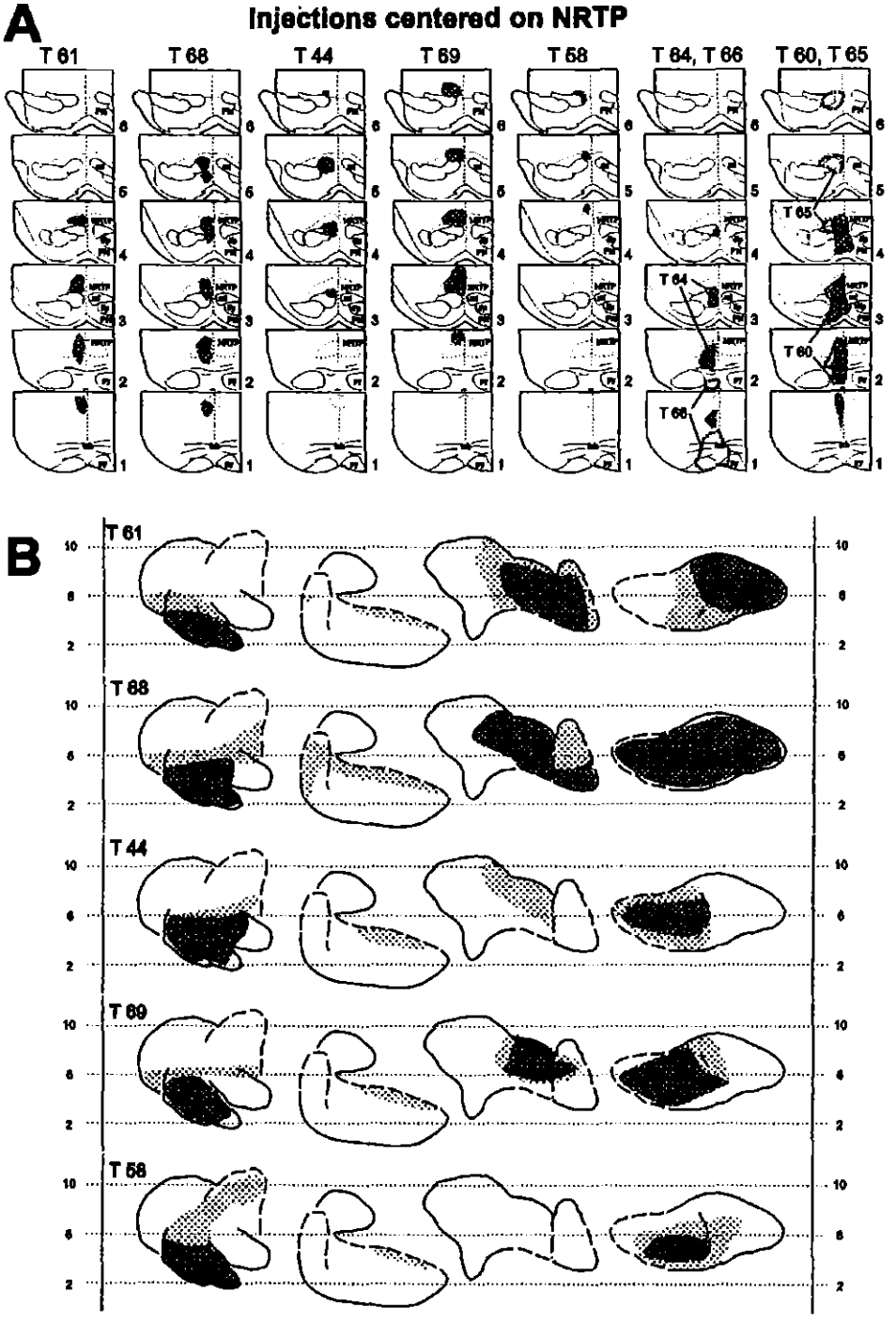
A
Injections centered on NRTP
T 61
T 68
T 44
T 69
T 58
T 64, T 66
T 60, T 65
T 65
T 64
T 60
T 66
B
T 61
T 68
T 44
T 69
T 58

Fig. 5.3

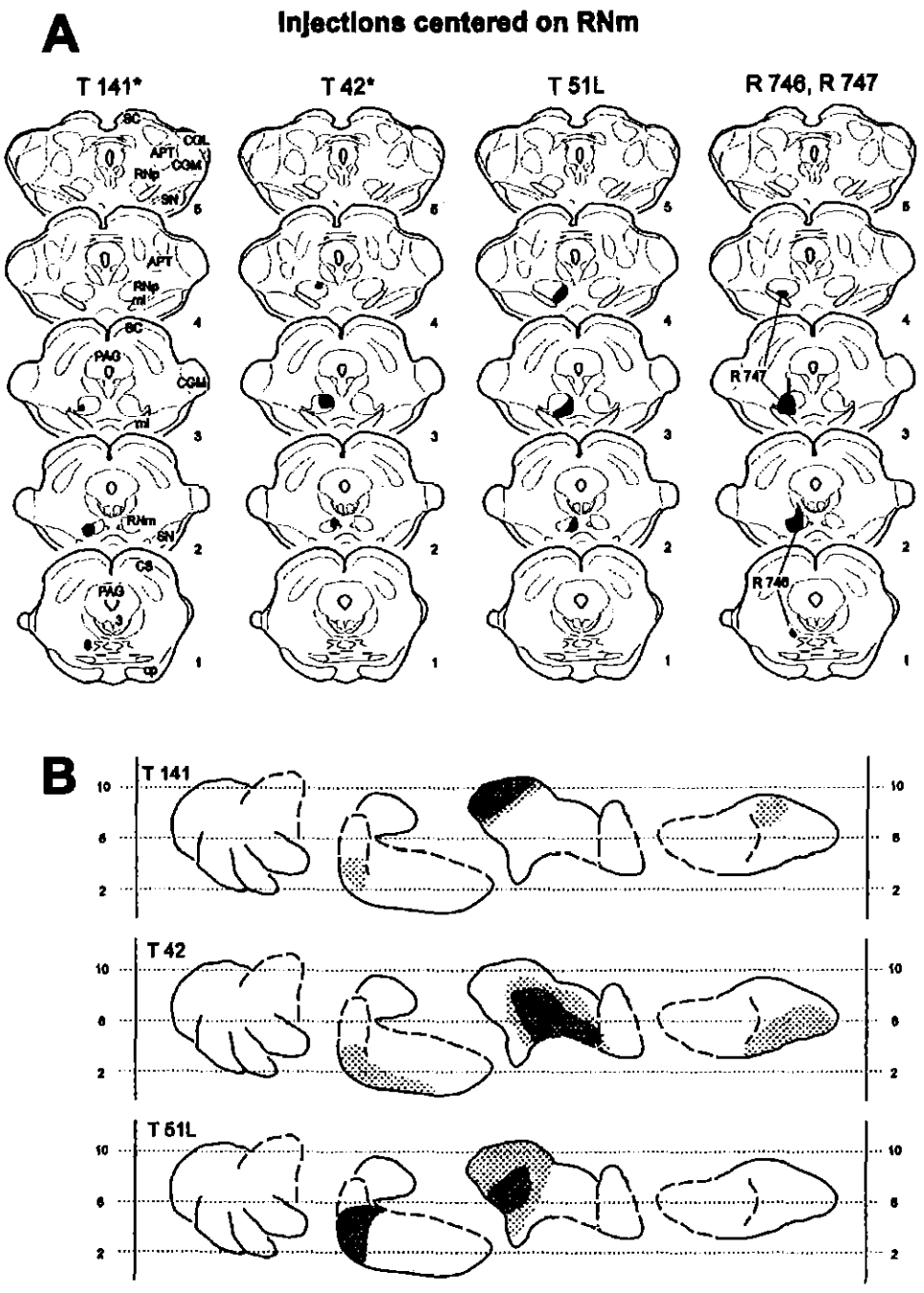
A
Injections centered on RNm
T 141*
T 42*
T 51L
R 746, R 747
SC
APT
CGL
CGM
RNp
SN
PAG
RNm
CS
cp
R 747
R 746
B
T 141
T 42
T 51L
10
6
2

Fig. 5.4

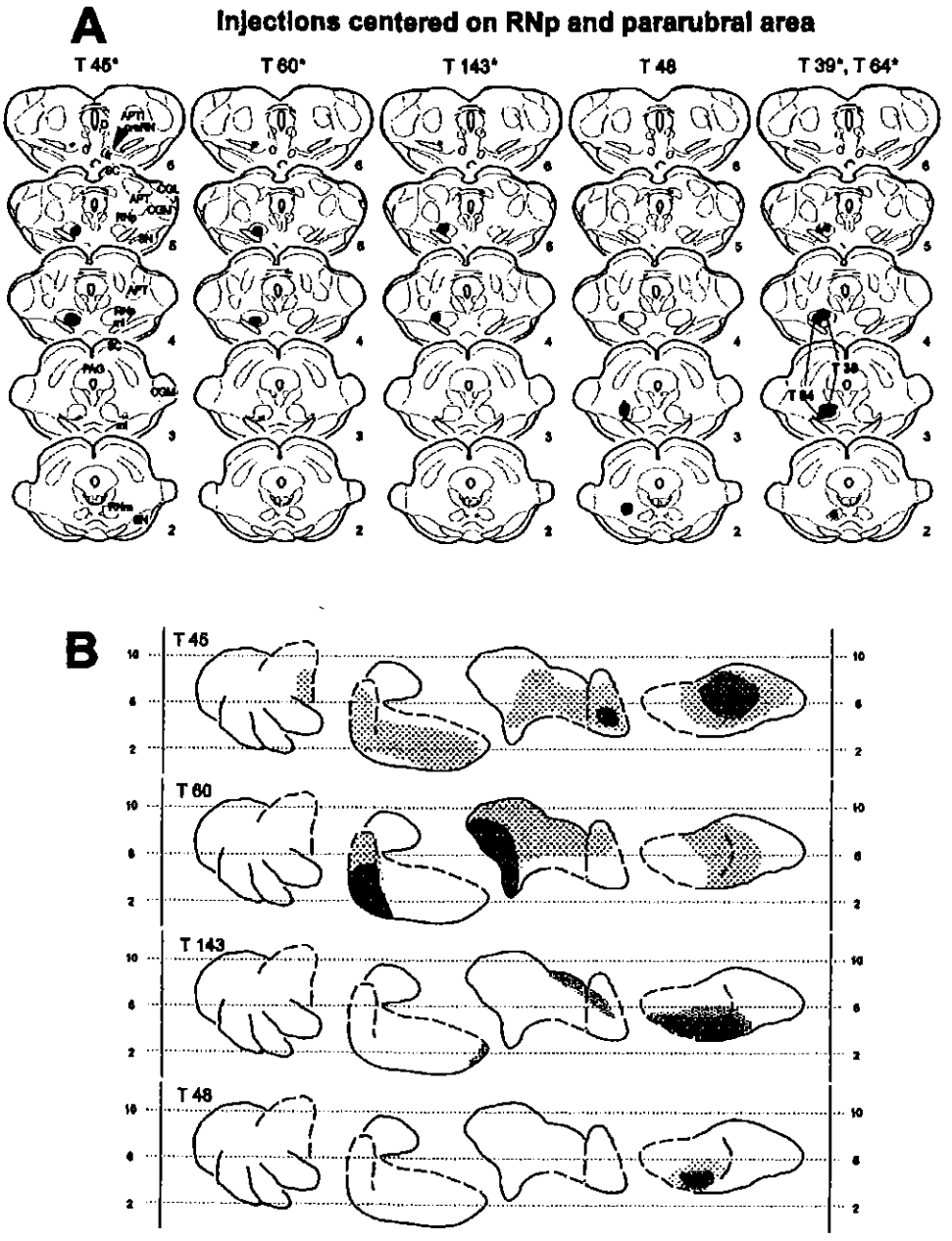
A
Injections centered on RNp and pararubral area
T 45*
T 60*
T 143*
T 48
T 39*, T 64*
B
T 45
T 60
T 143
T 48

Fig. 5.5

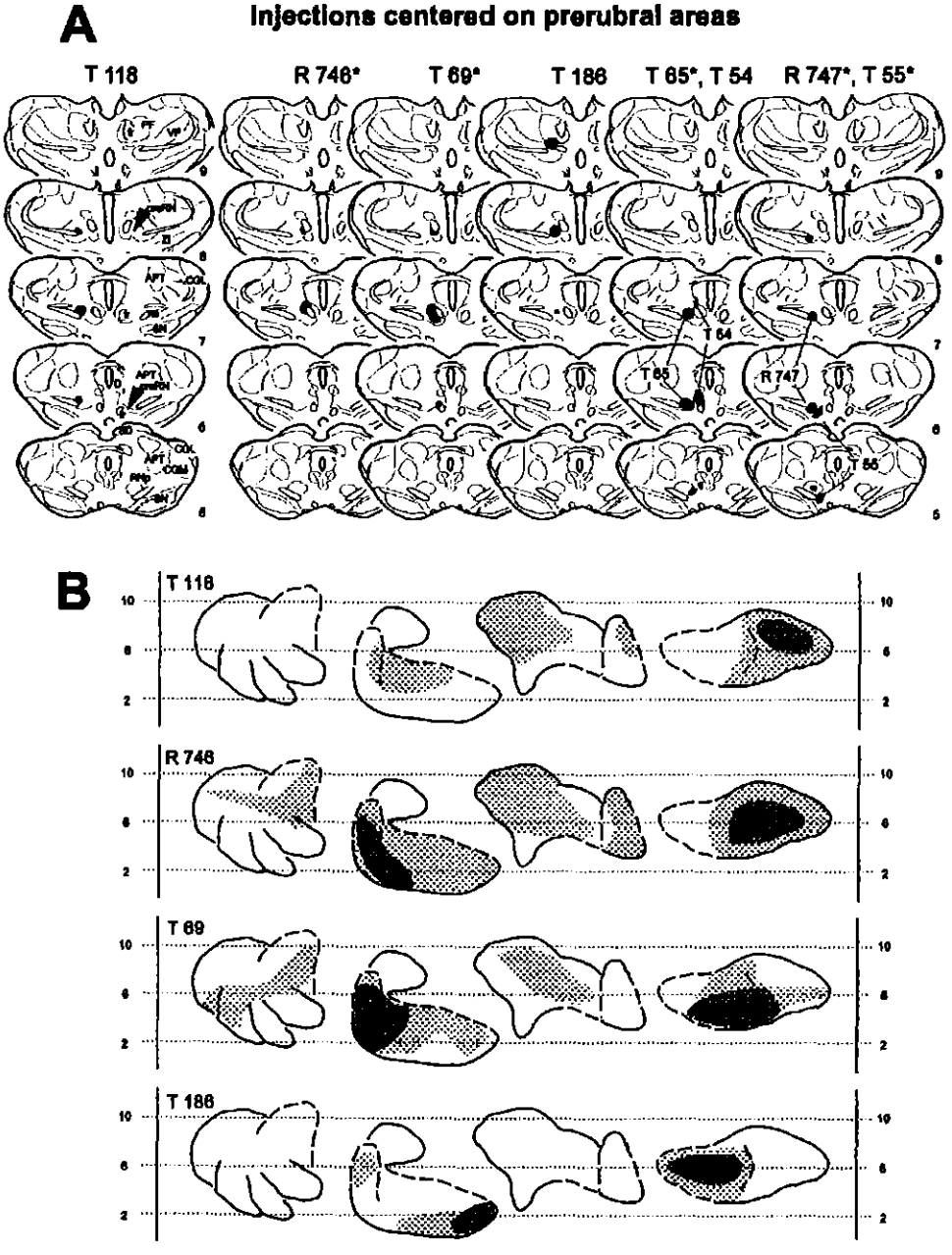
A
Injections centered on prerubral areas
T 118
R 746*
T 69*
T 186
T 65*, T 54
R 747*, T 55*
T 64
T 65
R 747
T 55
B
T 118
R 748
T 69
T 186

Fig. 5.6

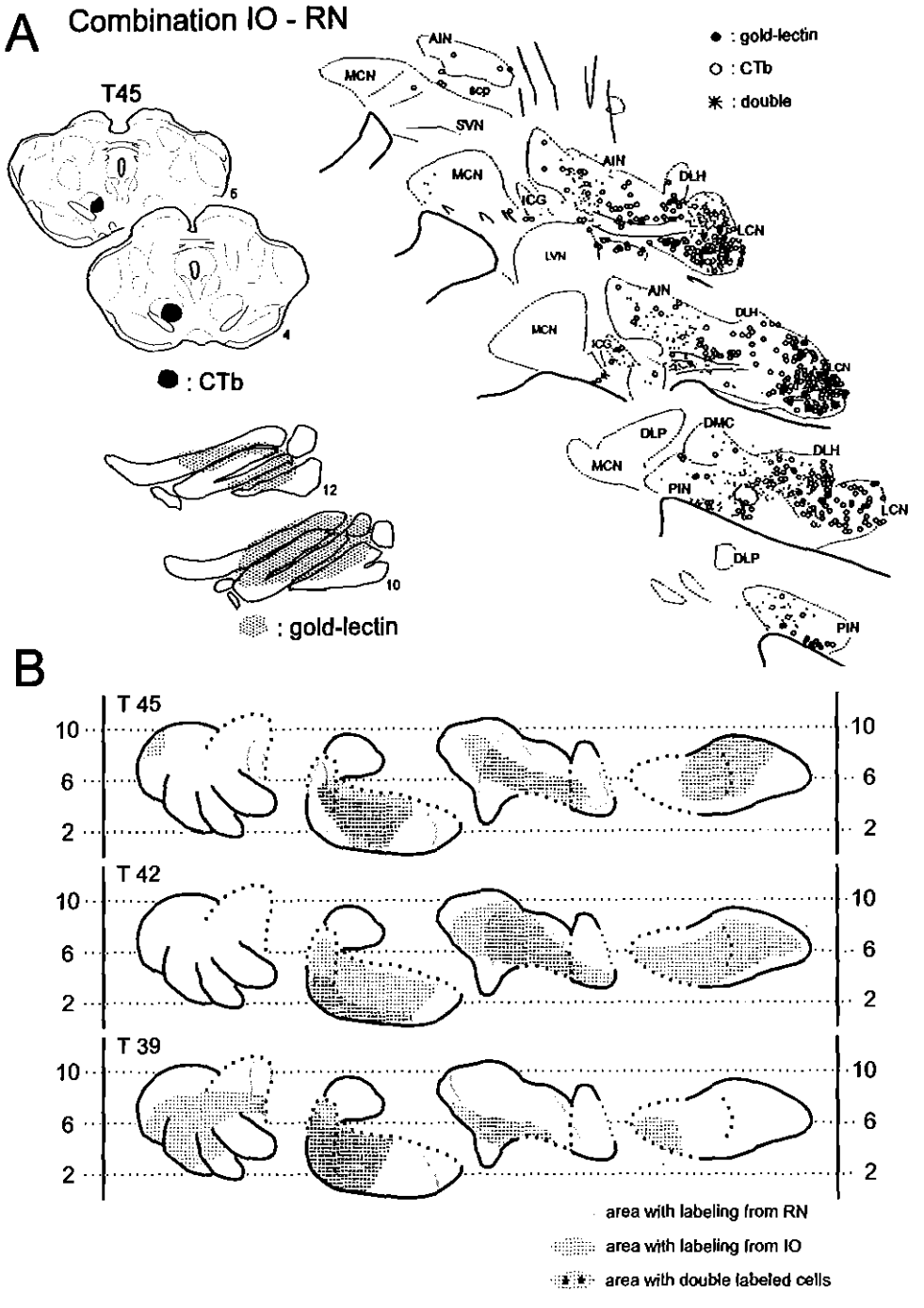
A
Combination IO - RN
T45
6
4
: CTb
12
10
: gold-lectin
AIN
MCN
scp
SVN
ICG
DLH
LCN
LVN
DMC
DLP
PIN
: gold-lectin
: CTb
: double
B
T 45
T 42
T 39
10
6
2
area with labeling from RN
area with labeling from IO
area with double labeled cells

Fig. 5.8

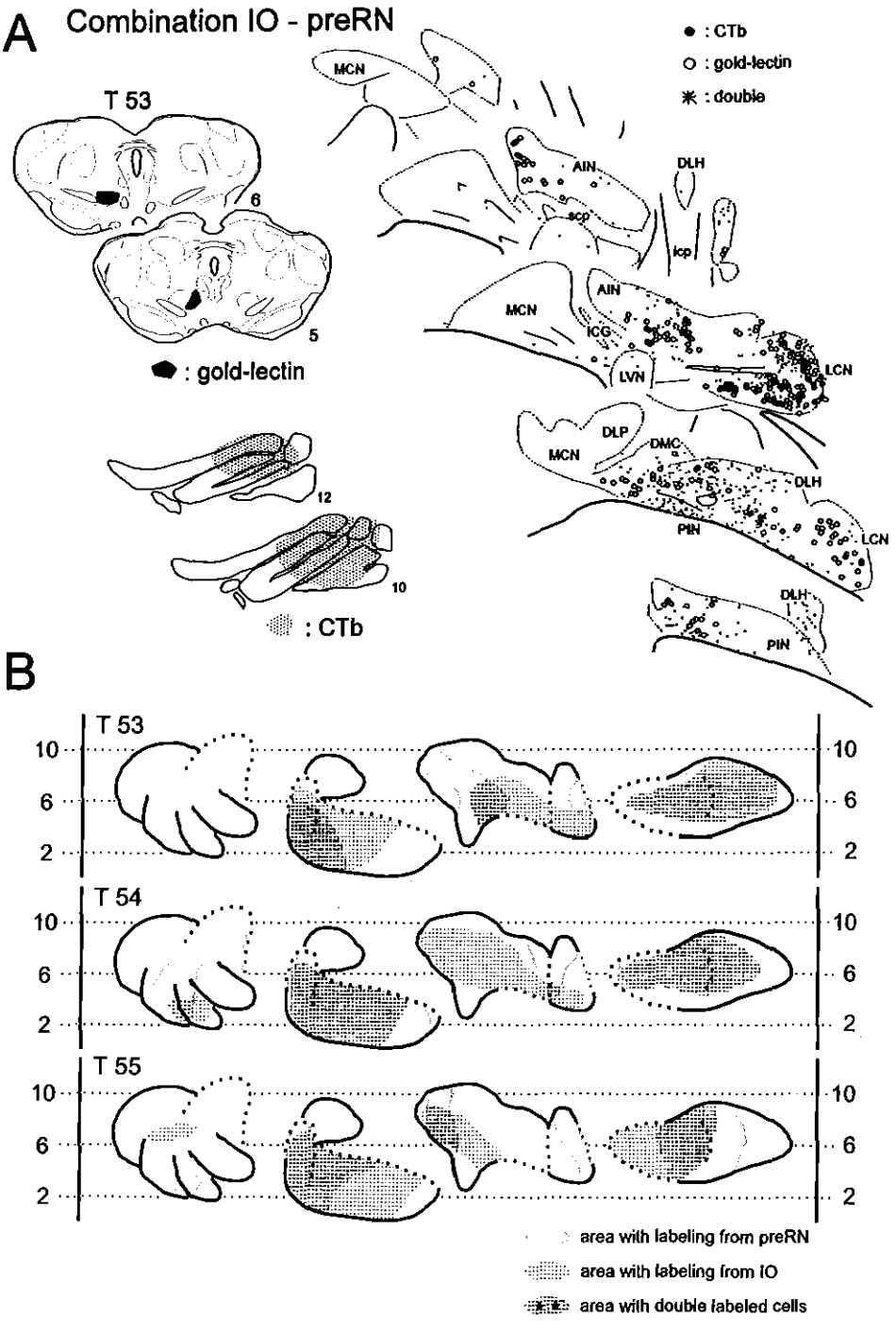
A
Combination IO - preRN
● : CTb
○ : gold-lectin
✳ : double
T 53
6
5
● : gold-lectin
12
10
: CTb
MCN
AIN
DLH
scp
icp
AIN
MCN
ICG
LVN
LCN
DLP
MCN
DMC
DLH
PIN
LCN
DLH
PIN
B
T 53
10
6
2
T 54
10
6
2
T 55
10
6
2
area with labeling from preRN
area with labeling from IO
area with double labeled cells

Fig. 5.9

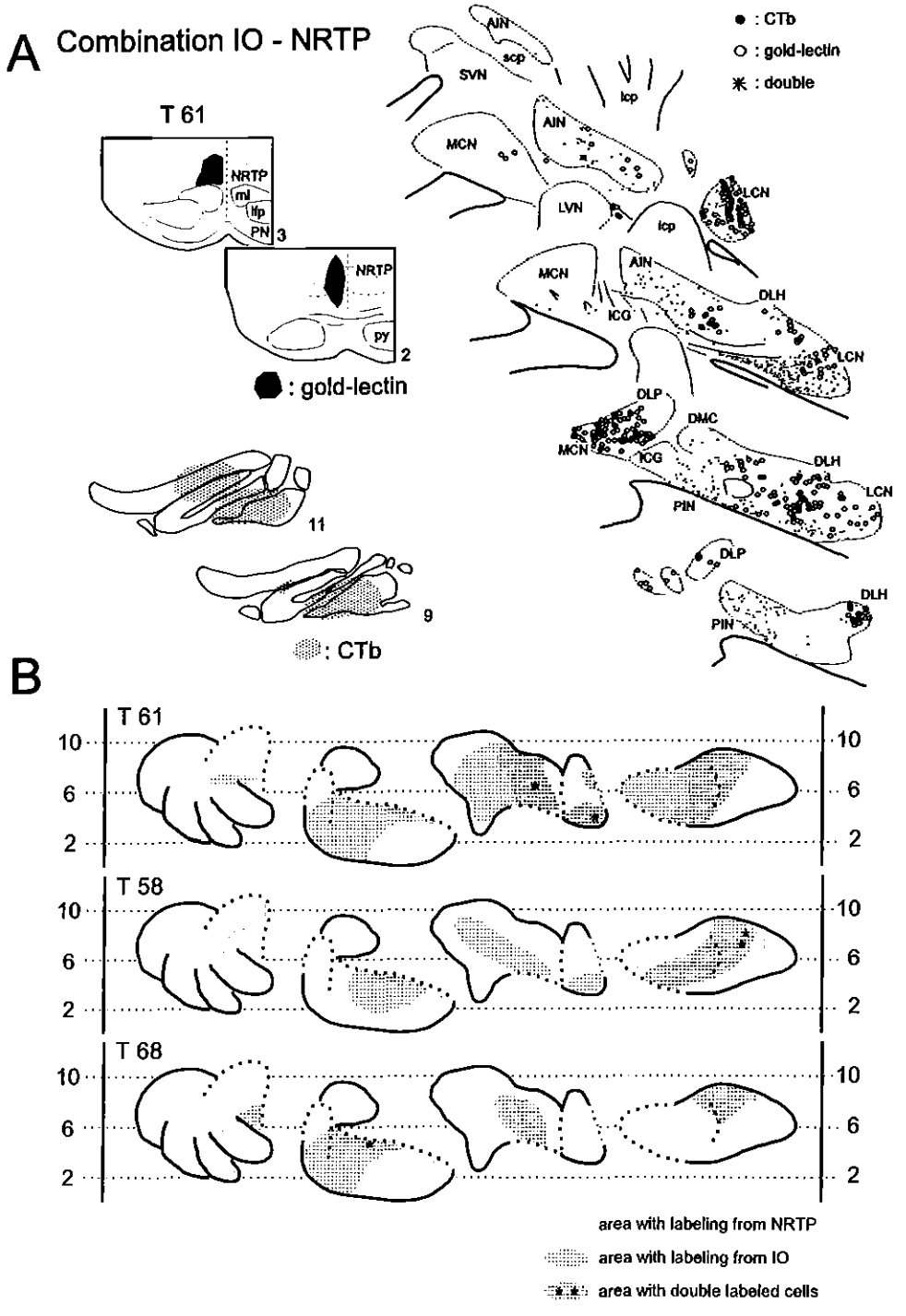
A
Combination IO - NRTP
T 61
NRTP
ml
lfp
PN
3
NRTP
py
2
: gold-lectin
11
9
: CTb
: CTb
: gold-lectin
: double
AIN
scp
SVN
icp
AIN
MCN
LVN
LCN
icp
MCN
AIN
DLH
ICG
LCN
DLP
DMC
MCN
ICG
DLH
LCN
PIN
DLP
DLH
PIN
B
T 61
T 58
T 68
10
6
2
area with labeling from NRTP
area with labeling from IO
area with double labeled cells

Fig, 5.10

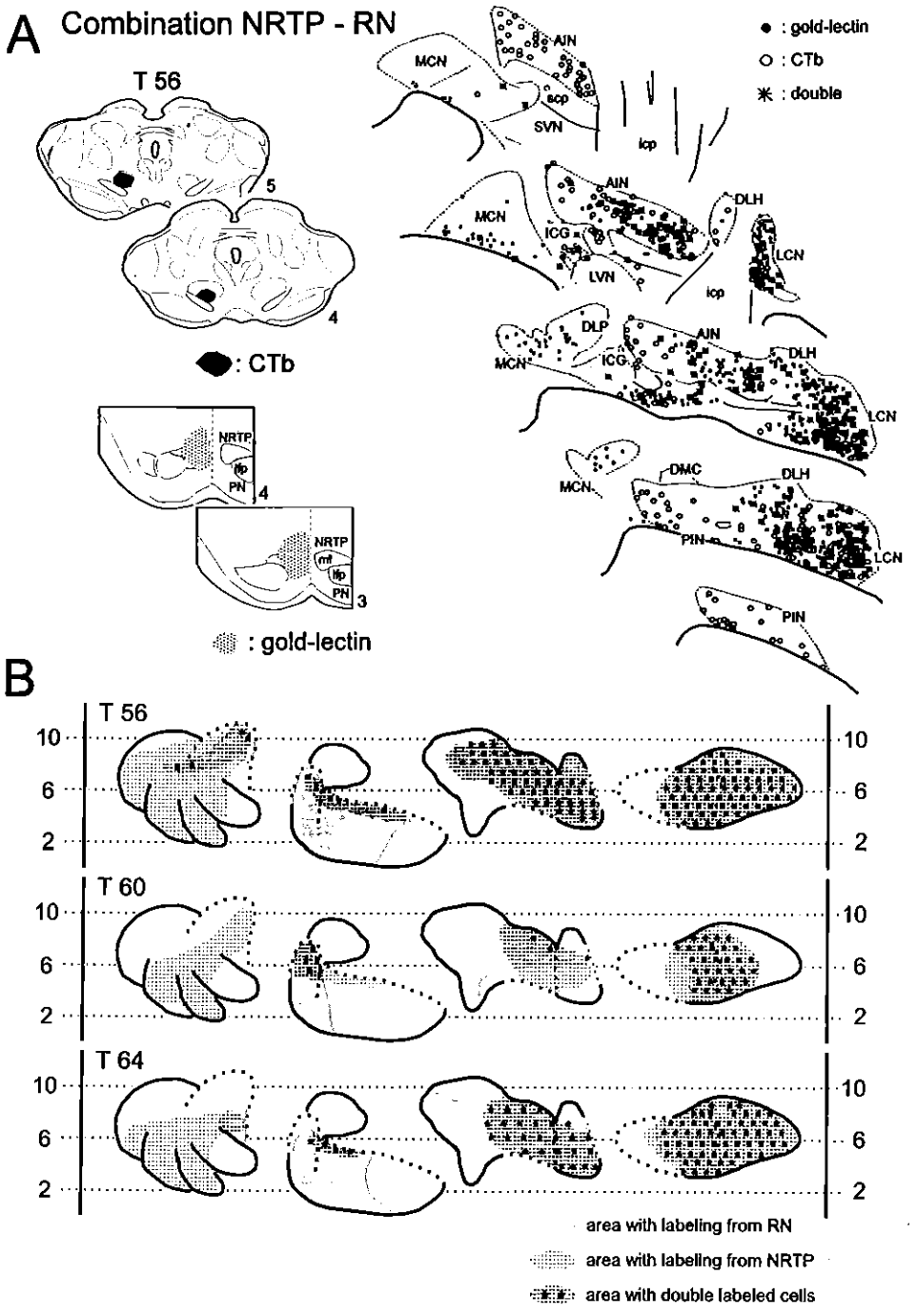
A
Combination NRTP - RN
T 56
: CTb
: gold-lectin
● : gold-lectin
○ : CTb
✳ : double
MCN
AIN
scp
SVN
icp
DLH
ICG
LVN
LCN
DLP
DMC
PIN
NRTP
lfp
PN
mf
B
T 56
T 60
T 64
10
6
2
area with labeling from RN
area with labeling from NRTP
area with double labeled cells

Fig. 5.11

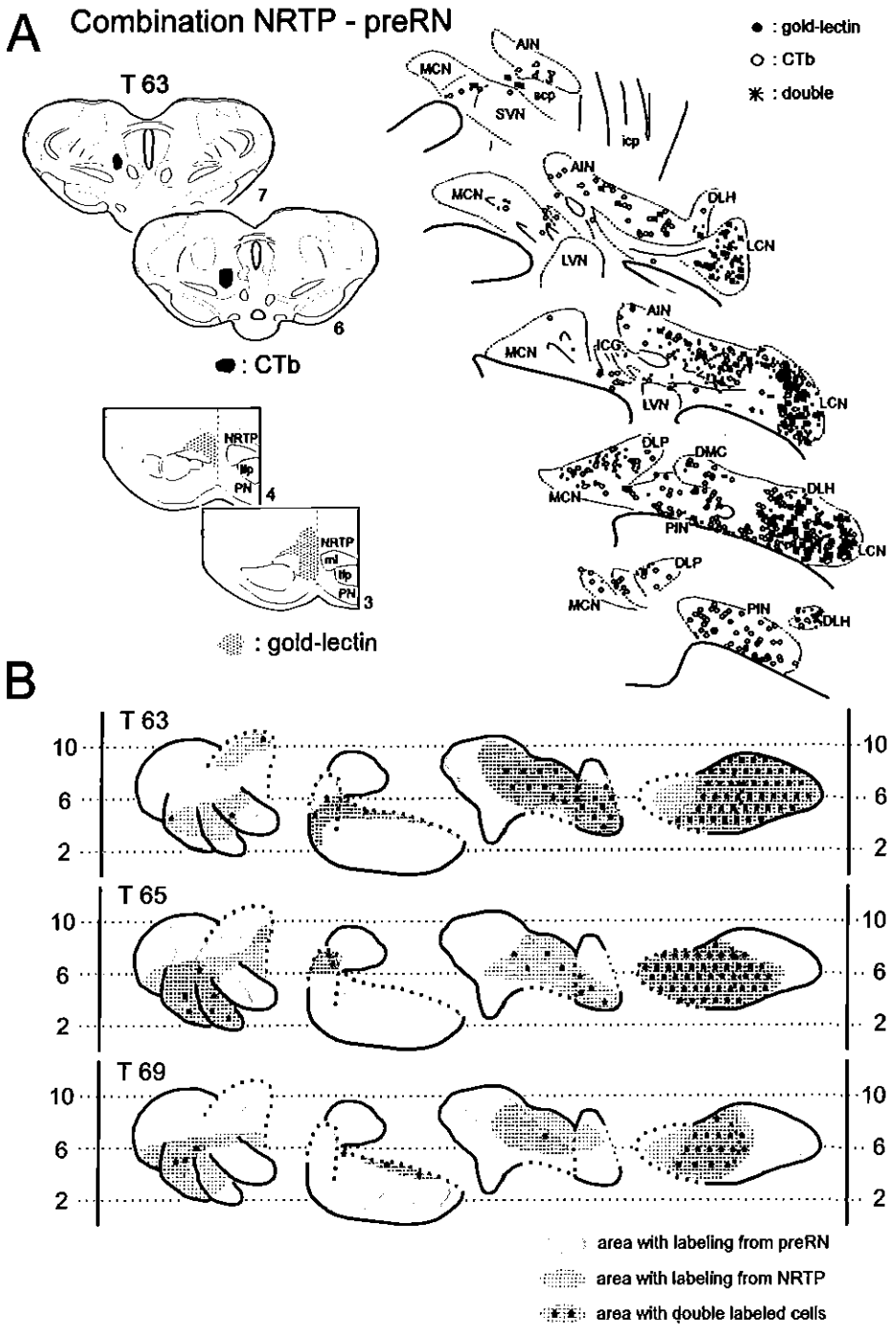
A
Combination NRTP - preRN
T 63
7
6
: CTb
NRTP
llp
PN
4
NRTP
ml
llp
PN
3
: gold-lectin
: gold-lectin
: CTb
: double
AIN
MCN
SVN
scp
icp
AIN
MCN
DLH
LCN
LVN
AIN
MCN
ICG
LVN
LCN
DLP
DMC
DLH
MCN
PIN
LCN
DLP
MCN
PIN
DLH
B
T 63
10
6
2
T 65
10
6
2
T 69
10
6
2
area with labeling from preRN
area with labeling from NRTP
area with double labeled cells

Fig. 5.12

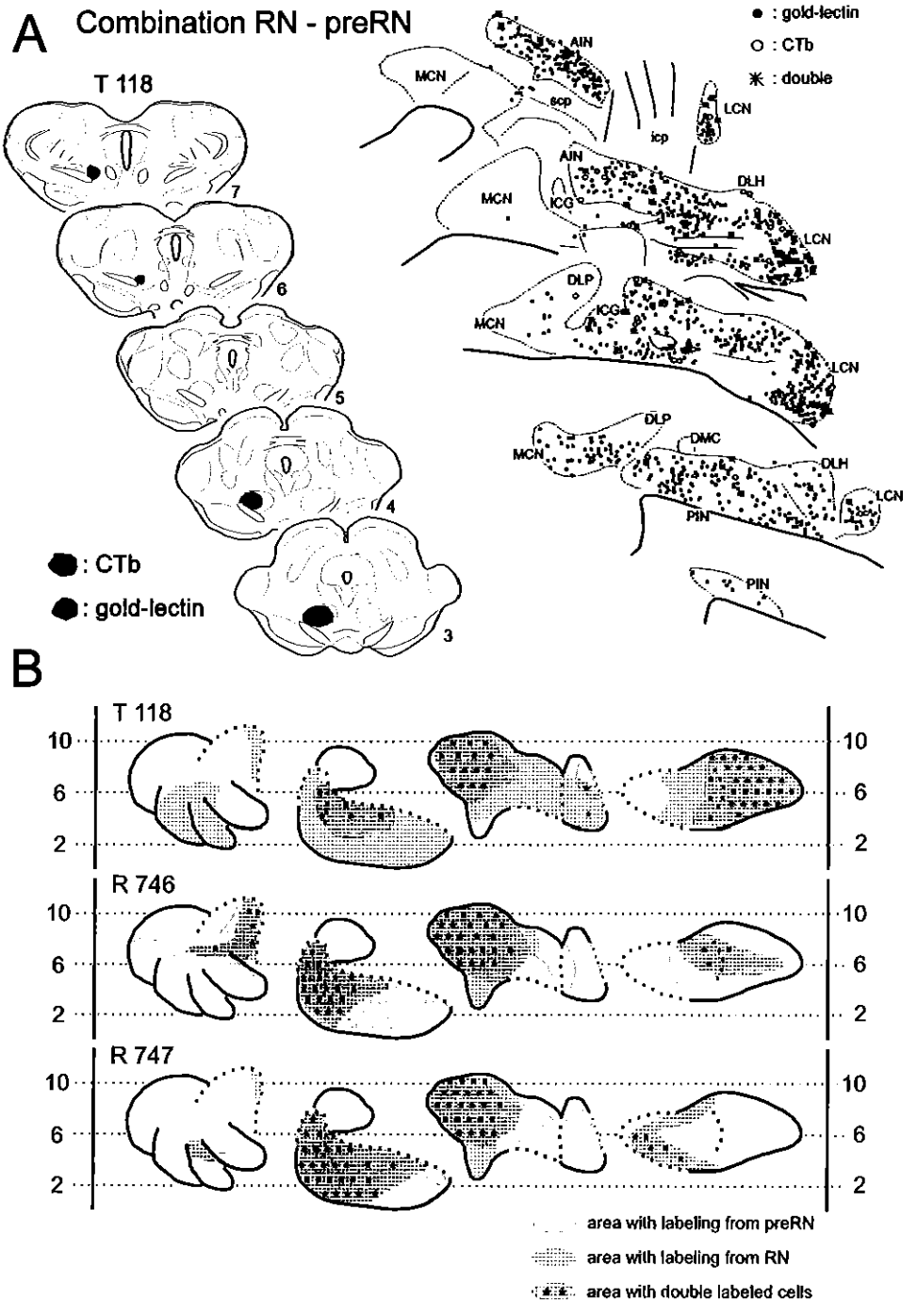
A
Combination RN - preRN
T 118
: gold-lectin
: CTb
: double
AIN
MCN
scp
icp
LCN
DLH
ICG
DLP
DMC
PIN
7
6
5
4
3
: CTb
: gold-lectin
B
T 118
R 746
R 747
10
6
2
area with labeling from preRN
area with labeling from RN
area with double labeled cells

Fig. 5.13

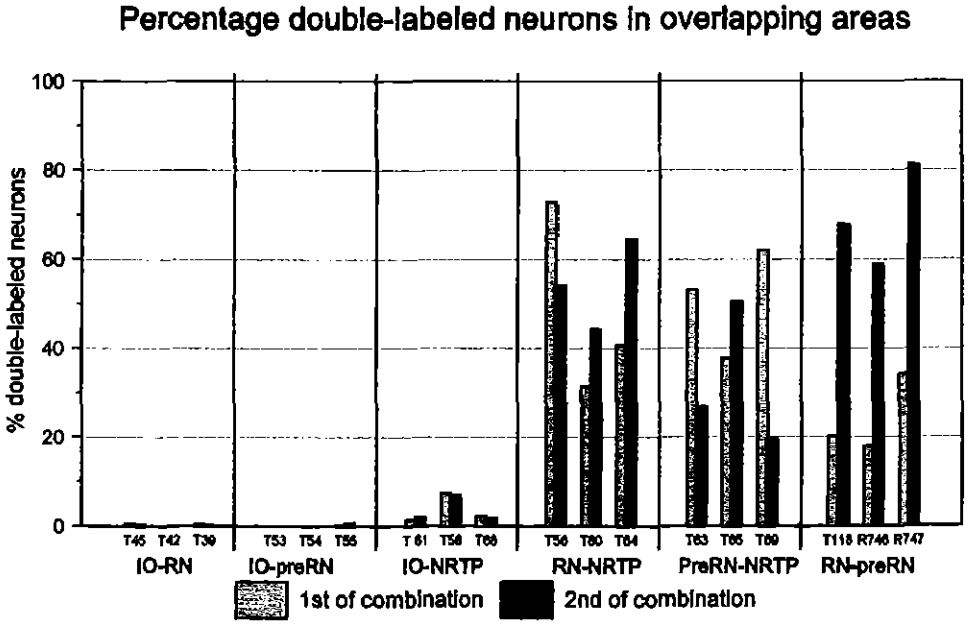
Percentage double-labeled neurons in overlapping areas
% double-labeled neurons
100
80
60
40
20
0
T45 T42 T39
IO-RN
T53 T54 T55
IO-preRN
T 61 T58 T68
IO-NRTP
T56 T80 T84
RN-NRTP
T63 T85 T89
PreRN-NRTP
T118 R746 R747
RN-preRN
1st of combination
2nd of combination

Fig. 5.14

Table 5.1. Total numbers of single and double-labeled neurons in 5 equidistant sections of the CN. Overlap#1 and Overlap#2 refer to the estimated number of labeled neurons as determined from the labeled surface area in the flattened and stretched-out diagram of the CN. % Double 1 and % Double 2 are the estimate percentages of labeled neurons that are located within the overlapping area and projecting to injection site 1 and 2, respectively.

Combination	Case	Total #1	Total #2	Overlap#1	Overlap#2	#Double	%Double1	%Double2
	T 45	527	463	413	253	2	0.5	0.4
1: IO - 2: RN	T 42	698	423	250	357	0	0	0
	T 39	491	379	253	113	1	0.4	0.3
	T 53	474	240	288	153	0	0	0
1: IO - 2: preRN	T 54	503	282	322	148	0	0	0
	T 55	827	237	0	139	1	0.2	0.7
	T 61	511	293	215	147	3	1.4	2
1: IO - 2: NRTP	T 58	193	252	68	74	5	7.3	6.8
	T 68	167	513	92	107	2	2.2	1.9
	T 56	615	460	415	309	225	54.2	72.8
1: NRTP - 2: RN	T 60	375	493	176	247	78	44.4	32.5
	T 64	399	779	278	443	180	64.7	40.7
	T 63	521	425	474	240	127	26.8	53
1: NRTP - 2: preRN	T 65	315	62	278	371	140	50.4	37.8
	T 69	322	149	208	65	40	19.3	61.9
	T 118	967	106	353	105	71	20.1	67.8
1: RN - 2: preRN	R 746	543	287	480	146	86	17.9	59
	R 747	582	452	515	217	176	34.2	81.2

Table 5.2. Projection and collateralization patterns from the CN to the four investigated brain stem areas and related to the modular organization of the rat cerebellum (Buisseret-Delmas and Angaut, 1993). Filled black and small open circles indicates that a major or minor projection, respectively, was noted between the listed CN areas and the investigated brain stem areas. Circles linked by a pulled or hatched lines indicate that many or some double-labeled neurons, respectively, were encountered in the part of the CN of the same row. Fine dashed line linking the NRTP and IO in C2,C3 zones and D1,2 zones rows indicate the very few neurons in lateral AIN and LCN, respectively, that were double labeled after NRTP and IO injections.

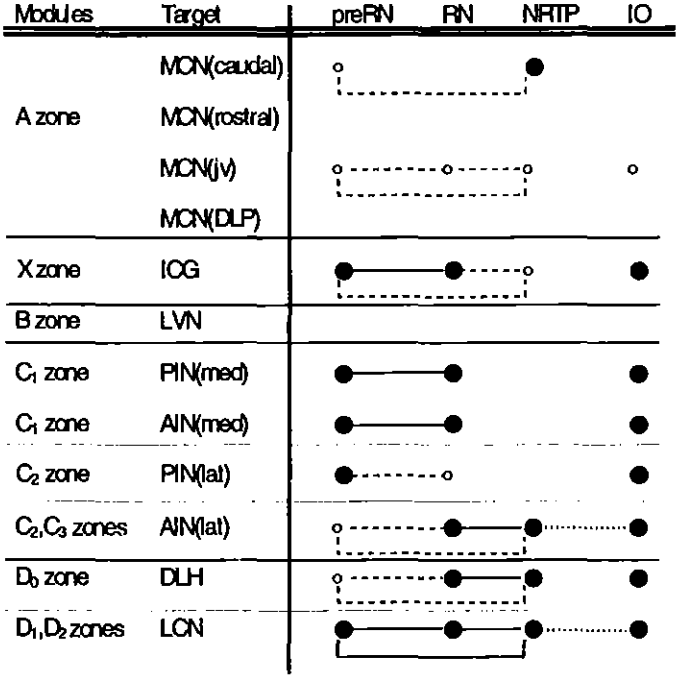

CHAPTER 6:
PRESERVATION OF THE CEREBELLAR MODULAR ORGANIZATION IN NUCLEO-BULBAR PROJECTIONS

A non-fluorescent anterograde double labeling study in the rat

T.M. Teune, J. Voogd, J. van der Moer, J. van der Burg and T.J.H. Ruigrok

Abstract

The modular organization of the cerebellum is based on the topography of projections from parasagittally arranged strips of the Purkinje cells to selected parts of the cerebellar nuclei and which is matched by the topography of climbing fiber projection from the inferior olive to the cerebellar cortex and, as collaterals of the climbing fibers, to the cerebellar nuclei. As such, the cerebellar nuclei represent the core as well as the output stations of the cerebellar modules. Here, we have investigated in the rat to what extent the output of different parts of the cerebellar nuclei, i.e. modules, remain separated in the brain stem circuitry.

The cerebellar nuclear projection onto the brain stem (nucleobulbar projection) was investigated with the application of two, non-fluorescent, anterogradely transported tracers (biotinylated dextran amine and the plant lectin *Phaseolus vulgaris* leucoagglutinin). The simultaneous distribution of both types of terminal labeling was examined in four typical, but functionally different, major targets of the cerebellar nuclei: the inferior olive (source of climbing fibers), the nucleus reticularis tegmenti pontis (a mossy fiber source), the red nucleus (premotor nucleus) and the prerubral area (a source of olivary afferents).

The distribution of terminal fields in selected areas largely confirmed earlier reports based on retrograde tracer studies. All injections resulted in small terminal patches of labeling within selected portions of the inferior olive. Likewise, injections centered on the anterior and posterior interposed and lateral cerebellar nuclei resulted in distinct fields of labeling in the red nucleus. Patchlike terminal fields were also noted in the nucleus reticularis tegmenti pontis upon injections in the anterior interposed, lateral and medial cerebellar nuclei. Terminal fields were somewhat less distinct in the prerubral area. In all cases, even when the tracers had been applied within the same nucleus, the terminal fields essentially remained separated. We conclude that, like the nucleoolivary projection, the projections from the individual cerebellar nuclei (or parts thereof) to the red nucleus, the nucleus reticularis tegmenti pontis and the prerubral area remain segregated. The role of the cerebellum and the recurrent reticulocerebellar mossy fiber circuit in cerebellar integration are discussed.

Introduction

The cerebellar nuclei (CN) are the target nuclei of Purkinje cell zones in the cerebellar cortex. This type of modular organization of the cerebellar output was studied and specified for the rat by Buisseret-Delmas and colleagues (Buisseret-Delmas and Angaut, 1993). The CN neuronal population is composed of two both morphologically and physiologically distinct types of neurons, which are randomly distributed over the nuclei (Batini *et al.*, 1992; Chan-Palay, 1977; Fredette and Mugnaini, 1991). One group is formed by the small GABAergic neurons which project to the inferior olive (IO), apparently

without collateralizing to other brain stem areas (chapters 2, 4 and 5). Within the GABAergic, nucleoolivary projection of the rat, a strict topographical pattern, without apparent overlap of the terminations of the individual CN within the IO subnuclei, has been described (Ruigrok and Voogd, 1990). This projection was found to be essentially reciprocal (Ruigrok, 1997).

The other CN neuronal population consists of medium- to large-sized non-GABAergic projection neurons (Batini *et al.*, 1992; Chen and Hillman, 1993). Among the target sites of these projection neurons we can distinguish: 1) premotor nuclei (red nucleus -RN-, vestibular nuclei, reticular formation, and different visual premotor centers such as the superior colliculus, the pretectum, and the rostral interstitial nucleus of the medial longitudinal fascicle); 2) precerebellar nuclei giving rise to mossy fibers (nucleus reticularis tegmenti pontis -NRTP-, pontine nuclei -Pn-, nucleus reticularis lateralis); 3) pre-olivary nuclei projecting to the IO (cellgroups located in the area prerubralis parafascicularis at the mesodiencephalic junction, the parasolitary nucleus) and 4) nuclei located in the subthalamus (zona incerta) and subnuclei of the thalamus, which are connected with motor and association areas in the cerebral cortex (see chapter 2 for particulars).

From retrograde double labeling experiments, it became evident that the projection of these medium- and large-sized neurons is divergent, i.e. their axons branch and project simultaneously to functionally different target sites (Bentivoglio and Kuypers, 1982; Bharos *et al.*, 1981; Gonzalo-Ruiz and Leichnetz, 1987; Lee *et al.*, 1989; Teune *et al.*, 1999). E.g. the large- and medium-sized projection neurons of the lateral cerebellar nucleus (LCN) and interposed nuclei have been shown to collateralize to the thalamus and the Pn, the medullary reticular formation, the spinal cord or the SC (Bentivoglio and Kuypers, 1982; Bentivoglio and Molinari, 1986; Bharos *et al.*, 1981; Lee *et al.*, 1989), to the SC and the Pn (Lee *et al.*, 1989), to various visual premotor areas in the brain stem (Gonzalo-Ruiz and Leichnetz, 1987) and to the NRTP and the RN or the prerubral area, the RN and the preRN (see chapter 5). The tracing of single axons from the CN confirmed and extended these observations (Aumann and Horne, 1996; Shinoda *et al.*, 1988).

However, converging projecting patterns emanating from these medium- and large-sized projection neurons have also been noted, i.e. a single nucleus or area in the brain stem usually receives input from neurons located in different CN or in different parts of the same cerebellar nucleus. Neurons located within the LCN, AIN, and of some in the MCN, were found to project to the NRTP (McCrea *et al.*, 1978; Teune *et al.*, 1999; Torigoe *et al.*, 1986b; Watt and Mihailoff, 1983a). The magnocellular red nucleus (RNm) receives input from both the AIN and PIN (Angaut *et al.*, 1986; Daniel *et al.*, 1988). The ventrolateral thalamus is known to receive input from the AIN, PIN and LCN (Aumann *et al.*, 1994; Haroian *et al.*, 1981; Nakano *et al.*, 1980). Convergence in the projections of different CN has been noticed for most of the premotor, precerebellar, pre-

olivary and thalamic target sites. In this paper we will use an anterograde double-labeling technique to investigate to what extent this apparent convergence results in actual overlap of the terminal fields which are derived from different CN or from different parts of the same cerebellar nucleus in three target sites (RN, preRN and NRTP) which also were the subject of our previous studies (see chapters 4 and 5). Projections to the IO will serve as a control on the discreteness and the non-overlap of the injection sites.

Materials and methods

Surgical techniques

The experiment protocol had been approved by the institute's animal care committee, and adhered to NIH guidelines.

Male adult purpose-bred Wistar rats (n=53) were anesthetized with a cocktail of ketamine 10% (10 mg / kg i.p.) and thiazine-hydrochloride 2% (3 mg / kg i.p.). When necessary, additional doses of ketamine were given intraperitoneally to maintain anesthesia. Animals were mounted in a Kopf stereotactic device according to Paxinos and Watson's (1986) atlas of the rat brain. Access to the cerebellum was obtained through a midline nuchal incision and lateral spread of skin and muscles, followed by partial removal of the occipital bone and dura. Guided by stereotactic coordinates, and under continuous monitoring of the spontaneous electrical activity of the nervous tissue (see (Ruigrok *et al.*, 1995b) for details), a single barrel pulled glass pipette (tip diameter 10 - 12 μm) was advanced onto the CN, perpendicular to the earbars in the horizontal plane. The pipette contained either biotinylated dextran amine (BDA, List Laboratories, 10% in 0.05 M phosphate buffered saline, PBS, pH 7.2) or the plant lectin *Phaseolus vulgaris* leucoagglutinin (PhaL, Sigma, 2.5% in 0.05 M Tris buffered saline, TBS, pH 8.6). Upon reaching a suitable position, both tracers were iontophoretically deposited (at +4 μA, for 10 minutes, with a 7 sec. on/off cycle). After the consequent application of the two tracers, the dura was appositioned, the muscles were sutured, the skin was closed with stainless steel surgical staples, and the animals were allowed to recover from surgery. During the survival period, they were checked bidiurnally for any signs of discomfort or stress.

After a survival time of 5-8 days, the animals were deeply reanesthetized with an intraperitoneal application of sodium pentobarbital (120 mg / kg). The brains were perfusion-fixated through transcardial application of 250 ml of a rinsing solution (0.8% NaCl, 0.8% sucrose and 0.4% d-glucose in 0.05 M phosphate buffered saline -PBS-, pH 7.2), followed by 1000 ml of a freshly prepared fixative containing 0.5% paraformaldehyde, 2.5% glutaraldehyde and 4% sucrose in 0.05 M PBS, pH 7.2. Hereafter, the brains were removed from the calvarinae, blocked and kept in the fixative for postfixation, for 2 hours under constant agitation at room temperature. For cryoprotection, the brains were submerged in 10% sucrose in 0.05 M PBS, pH 7.2 in the

cold, over night. Next, the brains were embedded in gelatin (10% gelatin, 10% sucrose in distilled water), stored for 2 hours in 10% formaline and 30% sucrose at room temperature under constant agitation. The embedded blocks were subsequently stored in 30% sucrose in 0.05 M PBS, pH 7.2, at 4 °C until sectioning.

Immunohistochemical processing

Transverse sections, 40 μm thick, were cut on a freezing microtome and serially collected in 0.05 M PBS, pH 7.2. Adjacent sections were processed free floating to visualize either BDA or PhaL or both.

BDA immunohistochemistry involved incubation of the sections with the avidine-biotine-complex (ABC, 1:100 in 0.05 M Tris buffered saline, pH 8.4, with 0.5% Triton X-100, TBST; Vector, ABC Elite Kit) for 2 hours under constant agitation at room temperature. Following thorough rinses with 0.05 M PB, pH 7.2, sections were submerged in a diaminobenzidine solution containing cobalt chloride, to obtain a permanent, black stained, product (75 mg DAB, with 3 ml 1% $CoCl_2$ in 150 ml 0.05 M PB, pH 7.2, with 50 μl 30% H_2O_2; 15 min., room temperature). The reaction stopped by rinsing the sections several times in 0.05 M PB, pH 7.2. BDA-single stained sections were stored in 0.05 M PB, pH 7.2 in the cold until mounting. Other sections were further processed to visualize the resulting PhaL labeling as well, together with those sections assigned to demonstrate PhaL only.

To demonstrate PhaL labeling, sections were incubated with a goat-anti-Phaseolus-antibody (1:4000, in 0.05 M TBST, pH 8.4; Vector) for 48 to 72 hours, in the cold, under constant agitation. After several rinses with 0.05 M TBST, pH 8.4, sections were incubated with a rabbit-anti-goat secondary antibody (RAG, 1:200 in 0.05 M TBST, pH 8.4; Sigma) for 2 hours at room temperature under constant agitation. Again after several rinses with 0.05 M TBST, pH 8.4, sections were incubated for 1.5 hours at room temperature with periodic-acid-peroxidase (PAP, 1:400 in 0.05 M TBST, pH 8.4; Sigma), under constant agitation. After a final series of rinses with 0.05 M PB, pH 7.2, sections were DAB-reacted to render a brown stained reaction product (37.5 mg DAB in 150 ml 0.05 M PB, pH 7.2, with 25 μl 30% H_2O_2) for 30 to 45 minutes. The reaction was stopped with several rinses with 0.05 M PB, pH 7.2. Then the sections were mounted, air dried, counter stained with thionin, dehydrated and cleared with serial runs through ethanol and xylene, and, finally, cover slipped with Permount.

Analysis of sections

Sections were analyzed with an Olympus light microscope, equipped with a Lucivid™ miniature monitor and Neurolucida™ software. A selection of successfully combined injection sites was made by discarding those experiments in which tracer deposits had either been deposited in other structures than the CN, or in which injection sites showed overlap, either within the CN subnuclei or in the IO labeling pattern. In all, 23 (out of 53) combinations met these criteria, and were selected for further analysis. The

combinations of the injection sites of the selected series are given in Table 6.1.

The resulting labeling pattern in three of the four selected target sites (the RN, the preRN and the NRTP) was plotted using a 20x objective in a 1 mm^2 square that was superimposed on the sections before plotting and that covered the vicinity and center parts of the selected target nuclei. Within these squares, the resulting terminal labeling pattern, i.e. tracer-filled varicosities (Wouterlood and Groenewegen, 1985), was plotted from double labeled sections (after prior consultation of single labeled sections). In this way, five serial levels through NRTP were analysed as well as ten serial levels through the RN and advancing into the prerubral region and thalamus. Injection sites and patterns of terminal labeling in the IO were manually entered in standardized maps of the CN and IO (Ruigrok, 1997; Ruigrok and Cella, 1995; Ruigrok and Voogd, 1990). Ten cases were selected for detailed description.

Anatomy and nomenclature

In the rat, four subnuclei of the cerebellar nuclear complex are recognized according to the description and terminology of Korneliussen (1968; Voogd, 1995). From medial to lateral, the medial cerebellar nucleus (MCN), the posterior and anterior interposed nuclei (PIN and AIN, respectively) and the lateral cerebellar nucleus (LCN) can be distinguished. The MCN features a medial portion, a dorsolateral protuberance (DLP) and a caudomedial part, all with characteristic cytoarchitecture. Buisseret-Delmas *et al.* (1993) defined the outlines of the interstitial cell group (ICG), a separate entity wedged between the MCN and the PIN and AIN. Characteristic of the AIN is the dorsomedial crest which protrudes caudomedially over the PIN. Between the lateral parts of the interposed nuclei and the LCN, the dorsolateral hump (DLH) is located. The LCN is divided into a small-celled ventromedial part lining the fourth ventricle, and a large-celled dorsolateral part.

The terminology of Azizi and Woodward (1987) was adopted to identify the different constituents of the IO complex. The main subdivisions, in brief, are the medial accessory olive (MAO), the dorsal accessory olive (DAO) and the principal olive (PO). In the rat, the MAO is the largest of the subnuclei and constitutes the caudal pole of the IO. At caudal levels, the dorsal fold of the DAO (dfDAO) lies immediately dorsal to the MAO, but, more rostrally, the PO is situated between the MAO and the main body of the DAO. At their rostral layers, the DAO and the PO fuse and form the rostral pole of the IO. Other subnuclei of the IO are the nucleus β, the dorsal cap of Kooy (DC), the ventrolateral outgrowth (VLO) and the dorsomedial group (DM); for a detailed description, see (Ruigrok and Cella, 1995).

The cytoarchitecture of the NRTP of the rat has been described elsewhere (Mihailoff, 1983; Torigoe *et al.*, 1986a; 1986b) and will be adhered to in this study (see also Ruigrok and Cella, 1995).

In the rat, the RN is divided into a caudal, magnocellular part and a

rostral, parvicellular part (Reid *et al.*, 1975b; Ruigrok and Cella, 1995). The area extending from the rostral borders of the RNp, surrounding the fasciculus retroflexus (fr), extending from the zona incerta (ZI) laterally to the nucleus of Darkschewitsch in the periaquaeductal gray (PAG) medially was defined as the area prerubralis parafascicularis by Carlton *et al.* (1982). This area encompasses the rostral interstitial nucleus (RI), the prerubral field (preR), the ventral tegmental relay zone (VTRZ), the nucleus of Darkschewitsch (Dk) and its rostral component, the rostral nucleus of Darkschewitsch (rDk), and the subthalamic nucleus (SPF: Paxinos and Watson, 1986). Ventral to the rostral part of the preR, the nucleus of the fields of Forel (FF) are situated. In addition, labeling was examined within the ventral tegmental relay zone (VTRZ), interstitial nucleus of Cajal (INC), medial accessory oculomotor nucleus (MA3), periaquaeductal gray (PAG), deep mesencephalic nucleus (DpMe) and pararubral area (paraR).

Results

Characteristics of injections and resulting labeling

The appearance of the cobalt-DAB intensified BDA injection sites was usually round-shaped, and consisted of a cluster of heavily labeled fibers with a core of densely labeled cell bodies. Surrounding the injection site, Golgi-like labeled cell bodies were occasionally observed. The density of the labeling gradually decreased towards the borders of the injection site. With bright-field illumination, fibers and terminals containing BDA were identified as containing a homogenous, black stained substance. With dark-field illumination, BDA-labeled structures stood out as heavily filled, yellow to orange colored strands of fibers and varicosities.

The contours of the PhaL injection sites were also circular. The DAB-reacted PhaL occasionally appeared to be packed in very fine particles. Bright-field illumination revealed brown stained fibers and varicosities, whilst with dark-field illumination the PhaL containing structures appeared to be silver to white in color. Because of the apparent difference in quality of either tracer, the distinction between BDA or PhaL labeled structures was easily made, as is demonstrated in Fig. 6.1.

Below, ten cases will be described and are illustrated in detail (Figs. 6.2-6.11). BDA injections and resultant terminal labeling are shown in blue and PhaL labeling is depicted in red.

Combinations of injection sites and resulting anterograde labeling

MCN and LCN (case T194)

The PhaL injection was centered in the ventrolateral part of the MCN, in its rostral juxtaventricular part. BDA had been deposited in the caudal LCN, at levels caudal to the MCN injection (Fig. 6.2A). Within the IO, the BDA injection resulted in terminal labeling in the PO, where labeled varicosities could be found rostrally in its ventral lamellae. The caudolateral MAO contained PhaL stained beads. In addition, some PhaL labeled terminals were found ventrally in the rostral part of nucleus β.

At the level of the NRTP, numerous PhaL labeled terminal arborizations were observed in the gigantocellular reticular nucleus, pars oralis, of the pons (PnO). Within the NRTP two small tufts of PhaL containing structures could be identified, mediodorsally and dorsolaterally in the nucleus, flanking a large cluster of BDA labeled terminals. The BDA labeled terminals were found mediodorsally at the center and caudal levels of the nucleus. A little more rostrally (Fig. 6.2B, level 3), BDA labeled terminals fanned out in a sheet-like arrangement from the dorsomedial outline of the nucleus to the ventrolateral border. Small patches of PhaL labeling were also found scattered throughout the Pn.

Within the mesodiencephalon, BDA labeling was present in the dorsal half of the rostral RNp. Ventral to the RNp, the VTRZ also contained BDA labeled terminals. The prerubral field displayed numerous BDA containing varicosities. Structures confined to the area prerubralis parafascicularis, such as the RI, the SPF, the FF, the DK and the rDK all contained some BDA labeling. More impressive terminal labeling was found, however, in the DpMe and paraRN (Fig. 6.2C, levels 3-6). Mesodiencephalic PhaL labeling was not abundantly present. An occasional PhaL labeled terminal could be seen in the lateral horn of the RNm. The preR demonstrated only a few PhaL labeled structures. The medial part of the FF contained some PhaL labeling, as did the caudal RI and the SPF. The MA3 and the INC, however, showed numerous PhaL labeled terminals (Fig. 6.2C, levels 3-4). In the rDK, some PhaL labeled terminals could be seen, ventral to some BDA labeling (Fig. 6.2C, level 9).

MCN and AIN (case T199)

In this case, BDA had been deposited in the ventral, juxtaventricular part of the MCN, at approximately the same position, only slightly more caudal, as in case T194. The PhaL injection covered ventral aspects of the lateral AIN, directly dorsal to the fibers emerging from the LCN subnuclei that give rise to the scp (Fig. 6.3A).

The lateral part of the caudal MAO contained BDA labeled terminals. The medial part of the DAO, at its rostralmost levels, and the DM contained PhaL labeled structures (conform the labeling in T84 and T151). The involvement of the DM illustrates the involvement of the DLH in the AIN injection site (Fig. 6.3A).

The NRTP contained predominantly PhaL labeled terminals. PhaL labeled varicosities could be found in all levels of the NRTP, but the largest concentration was present in the caudal half of the nucleus. Rostral levels showed a passing of fibers, loaded with numerous terminals, from the NRTP to the Pn. The medial Pn contained a few PhaL labeled beads. A few BDA terminals could be identified in the mediodorsal part in the middle third levels of the NRTP. A more prominent BDA projection was noted in the PnO. Here, only very few PhaL labeled terminals were observed (Fig. 6.3B).

The RNm contained a large cluster of PhaL labeled terminals, advancing into the RNp. They occupied most of the dorsomedial area of this part of the nucleus. A small patch of BDA labeled

varicosities was identified in the lateral horn of the RNm and in the DpMe. A separated and more prominent involvement of the DpMe was noted for the AIN injection (PhaL), which continued into the APT. Scant labeling was noted in MA3. Virtually no terminals labeled with either tracer were found in the prerubral area (levels 8-10, Fig. 6.3C).

AIN and LCN (T96, T92)

In case T96, BDA had been injected in the intermediate part of the rostral AIN. PhaL had been deposited ventrally in the rostral LCN (Fig. 6.4A). The resulting IO labeling pattern displayed PhaL labeled terminals in the ventral lamellae of the caudal PO, next to its caudal pole. Some labeled terminals were present in the VLO. BDA containing beads were located slightly lateral to the central part of the rostral DAO (Fig. 6.4A).

Labeled varicosities are located in the ventromedial part of the nucleus at caudal levels and more prominently along its ventrolateral and medial periphery and its rostral pole at more rostral levels. The caudal levels of the NRTP contained BDA labeled varicosities from the AIN in its ventral and central parts. The medial Pn also contained some PhaL labeled terminal patches (Fig. 6.4B).

The RNm contained BDA labeled varicosities from the AIN which were restricted to the dorsolateral part of the nucleus. Ventrally in the RNm, some PhaL labeled varicosities from the LCN were seen (Fig. 6.4, level 3), which developed into a large patch of PhaL labeled varicosities in the ventral and ventromedial part of the RNp, which extended somewhat in the VRTZ.. The MA3, the PAG, the INC, and the Dk, with exception of the rostral part of this nucleus, also contained PhaL labeled varicosities. Scattered PhaL labeling, in addition was found in the SPF and FF. None of these areas received a projection from the AIN. In the DpMe only sparse labeling was found (Fig. 6.4C).

Case T92 resembled T96 in many respects. Here, the AIN injection (BDA) was centered on somewhat more caudolateral parts of the AIN compared to the AIN injection in T96. This injection was combined with a LCN injection (PhaL), at approximately the same rostrocaudal level as in case T96, but located more dorsally (Fig. 6.5A).

The IO labeling in T92 from the LCN now consisted of PhaL labeled terminals in the bend and dorsal lamellae of the PO, and BDA containing varicosities from the AIN were located in more medial parts of the rostral DAO as compared with the previous case. In the DM, a few BDA labeled varicosities were found as well, indicative of (minimal) involvement of the DLH in the injection site (Fig. 6.5A, level 12).

The NRTP pattern of labeling showed a rostrocaudal shift compared to the labeling in T96. BDA labeled structures from the AIN injection site were found caudally and centrally in the NRTP, extending more caudally when compared with the labeling in T96. Labeling from the LCN injection in T92 was found along the ventral outlines of this nucleus, in a more caudal, lateral and ventral position than where the terminals were found in case T96 with a more ventral injection of the LCN. Similarly, in the Pn,

terminal labeling resulting from the LCN injection site was observed, in T92 at somewhat more rostral levels than in T96.

In case T92 BDA labeling from the AIN in the RNm was located in a dense cluster in a more dorsomedial position than in case T94. It extended somewhat into the RNp. PhaL labeling from the LCN was seen in the ventrolateral part of the caudal RNp, and centrally in the rostral levels of this part of the nucleus, laterally and dorsally to the labeling in the previous case with a more ventral injection of the LCN. The preRN contained predominantly PhaL labeled terminals from the LCN, in the VTRZ, the dorsal part of the ZI, and in the preR. The ventral part of the ZI contained some BDA labeled varicosities. The FF contained both PhaL and a few BDA labeled terminals. In contrast to case T96, no PhaL labeling was found in the MA3, the Dk, the INC, or SPF.

AIN and DLH (T84)

In this case, the BDA injection was centered on and remained confined to the rostrolateral aspect of the AIN. The PhaL injection was placed laterally in the DLH. Corresponding labeling in the IO consisted of BDA labeled terminals that were restricted to the rostrolateral DAO and of PhaL containing varicosities that remained confined to the DM, where they could be found bilaterally (not shown) but with a contralateral preponderance (Fig. 6.6A).

In the NRTP, PhaL labeled terminals from the DLH were found centrally at the caudal half of the nucleus. BDA labeled varicosities from the AIN were found ventral to of the PhaL labeling in the central part of the NRTP. At rostral levels, a few BDA-filled terminals were seen dorsal to the PhaL labeled structures. In the medial Pn, a few PhaL- and BDA-labeled patches could be identified. Dorsal to the NRTP, within the PnO, a few labeled beads could be identified, labeled with either tracer (Fig. 6.6B).

The RN contained a cluster of BDA labeling from the AIN dorsolaterally in its magnocellular subdivision but which extended into its parvicellular subdivision. Scattered PhaL labeled terminals from the DLH were found along the medial and dorsomedial border of the RNm, and extending into the VTRZ. Labeling in the DpMe was mostly derived from the DLH. The preRN contained only a few labeled varicosities, predominantly labeled with PhaL from the DLH. These PhaL labeled terminals could be identified in the preRN, the RI, the rDk, and in the FF. A few BDA labeled terminals from the AIN were observed in the lateral aspects of the SPF, and scattered throughout the preR and FF (Fig. 6.6C).

LCN and DLH (T94)

The injection sites in this case involved the DLH, extending a little into the adjacent dorsolateral AIN (BDA), and a rather large PhaL injection centered on the caudal LCN (Fig. 6.1D, Fig. 6.7A). In the IO complex, BDA terminal labeling was present in the DM, ascending into the dorsomedial aspect of the DAO, which is consistent with the incorporation of part of the AIN in the injection site. PhaL containing terminals were only found in the ventral lamellae of the

rostral PO, indicating that this tracer had remained confined to the LCN (Fig. 6.1E, Fig. 6.7A).

This case displayed a remarkably large amount of PhaL labeled terminals from the caudal LCN in the reticular areas, such as the PnO. Within the NRTP, also predominantly PhaL labeled terminals were found especially along the dorsal margin of the nucleus. BDA labeled terminals from the DLH could be identified ventrally of the PhaL labeling, in the central levels of the nucleus (Fig. 6.1F, Fig. 6.7B, levels 3-5). The Pn showed patches of BDA labeled beads, medially and laterally, separated from a few laterally located PhaL containing terminals.

In the mesodiencephalon, labeled terminals were present in abundance. Again, the predominant tracer was PhaL. In the RNm, a cluster of BDA labeled varicosities of the DLH was present in the mediodorsal part of this nucleus and as scattered terminals within the DpMe. BDA labeling extended into the APT. Also, some BDA labeling was present in the RI and laterally in the preR. Abundant PhaL labeling from the caudal LCN was found in the DpMe, and in the paraRN, extending into the lateral part of the RNp. Within the PAG, abundant labeling was noted, especially in the MA3, which, more rostrally, became continuous with labeling in the VTRZ. The DK and the INC were virtually devoid of labeling. Pronounced terminal labeling was found in the preR, rDk, ZI and FF. Patches of labeling were also noted in the hypothalamic areas surrounding the mammillothalamic tract (mt, level 9,10 of Fig. 6.7C). Note, that despite large amounts of labeling in these areas, actually very little, if any, overlap of terminal fields in NRTP, RN and preRN was observed (Fig. 6.7C).

PIN and PIN (T108)

In case T108 (Fig. 6.8) both tracers were centered on the PIN. The PhaL injection was situated in caudoventrally in the central part of the nucleus, and the fading zone of tracer substance overlapped just a little with the fading zone of tracer substance from the BDA injection site, which was located slightly more rostrolaterally in the nucleus (Fig. 6.1G, Fig. 6.8A).

The absence of labeling in the PO indicates that both injections spared the LCN. Terminal labeling in the IO was only observed in the rostral part of the MAO. BDA labeled terminals were found at levels more rostral than the PhaL labeled ones. They also occupied a more dorsal and medial position in the rostral MAO. Only a single section revealed both (separated) fields of terminal labeling (Fig. 6.1H, Fig. 6.8A).

Within the NRTP, an occasional fiber of passage could be identified, but, consistent with other experiments in which the PIN had been one of the injected CN subnuclei (T79, T07, T109), no terminal labeling was found within the nucleus. Neither the Pn, nor the PnO contained terminal labeling from these injection sites (Fig. 6.8B).

In the RNm, a few PhaL containing varicosities from the medial injection site could be found along its ventral border. Only occasionally, BDA labeled terminals from the lateral injection site were observed in the RNm and RNp. Scattered terminals, labeled with BDA or PhaL, were located in the DpMe, the PAG, MA3,

and the INC. Virtually no labeling was found in the Dk. The rDk, in contrast, displayed in its caudolateral part a small area occupied with PhaL labeled terminals from the medial injection site, clearly separated from an area located more ventromedially in this nucleus that was BDA labeled from the lateral injection site (Fig. 6.11). The VTRZ contained only a few labeled terminals, predominantly filled with PhaL. Distinct, essentially non-overlapping terminal fields were observed in the SPF and ZI. Scattered labeling was found in the preR and FF.

LCN and LCN (T98)

In this experiment, both tracers had been deposited in the LCN. The PhaL injection site was located in the small-celled ventral part of the LCN, in the roof of the fourth ventricle. The BDA injection had been deposited adjacent to but somewhat dorsal of the PhaL injection at slightly more rostral levels, and also occupied the ventral half of the LCN (Fig. 6.9).

BDA labeled terminals from the dorsal injection site were restricted to the dorsal leaf of the PO. PhaL labeling from the ventral injection site extended from the ventral leaf of the PO into the VLO. Both patches of terminal labeling remained completely separated.

In the NRTP, BDA labeled terminals from the dorsal injection site were located in the central part and ventrally in this nucleus, at middle and rostral levels. PhaL containing varicosities from the ventral injection site were positioned dorsal and ventral to the BDA labeling. The Pn contained a few BDA labeled patches.

The RN demonstrated a few labeled terminals from the ventral PhaL deposit, located in the ventrolateral part of the nucleus at the transition between the magnocellular and parvicellular level. The majority of labeled terminals in the RN were BDA labeled and came from the dorsal injection site, and could be found ventromedially. Rostrally in the RNp BDA and PhaL terminals overlap. The medial part of the VTRZ contained BDA labeled terminals, whereas the lateral part of the VTRZ contained PhaL labeled terminals. The preRN, the SPF and the parafascicular nucleus were mostly BDA labeled from the dorsal site. The FF showed both a few PhaL and some BDA labeled beads. The MA3, the Dk, and the rDk as well as the oculomotor nuclei were strongly PhaL labeled from the ventral injection site.

AIN and AIN (T150, T151)

In two experiments, both tracers had been deposited in the AIN (Figs. 6.10,6.11). In T151, BDA and PhaL had been applied at approximately the same antero-posterior level. PhaL was centered in the caudomedial aspects of the AIN, whereas the BDA injection was placed in the lateralmost aspect of the AIN, bordering on the DLH (Fig. 6.10A).

In the IO, the fields with terminal labeling remained virtually confined to the DAO. BDA-filled terminals from the lateral AIN were found in the rostrolateral tip of the DAO. Some varicosities were observed in the DM group, indicating the incorporation of (a very small part of) the DLH in the injection site. PhaL labeled terminals from the more medial AIN were found

in the caudolateral aspects of the DAO.

The NRTP contained labeling from both injection sites mainly in its central parts. The laterally placed injection site (BDA) resulted in a more prominent projection compared to more the medially placed injection (PhaL). PhaL terminal labeling from the medial AIN was more scattered and surrounded the centrally and ventrally positioned BDA labeled field. The Pn contained patches of BDA labeled terminals, laterally of a patch with PhaL-filled beads. The overlying PnO contained some scattered labeled terminals (BDA as well as PhaL: Fig. 6.10B).

The RN contained labeled terminals in its caudal pole. PhaL-filled terminals from the medial AIN were located in the caudal pole and in the ventral part of the RNm. BDA labeling was observed more dorsally in the RNm (Fig. 6.10C, level 4,5). Both terminal fields extended into the RNp. The DpMe contained scattered BDA labeled terminals, which appeared clustered in a ribbon-like aggregation and extending into the caudal aspects of the APT. The DpMe contained only a few PhaL labeled terminals. The rostral APT, however, showed PhaL labeled terminals, contrasting with the more caudally located cluster of BDA labeled varicosities. Both injection sites resulted in scattered labeling within the preR. The MA3 displayed a few BDA labeled beads whereas a more dense projection was noted to the FF.

In contrast with T151, the BDA injection in case T150 was centered medial to the PhaL injection. Compared with T151, the injection sites were also positioned closer to each other; the medial-most placed tracer (BDA) was located more centrally in the AIN, whereas the position of the laterally placed injections were very similar (Fig. 6.1A, Fig. 6.11A).

The rostral tip of the DAO contained PhaL labeled terminals from the lateral injection site, corresponding with the pattern of labeling from the lateral AIN injection in T151. In T150, however, the labeling from the lateral AIN remained limited to the DAO, indicating that the adjacent DLH was not involved. BDA-filled terminals from the injection in the central part of the AIN were found at more rostral and central levels in the DAO, compared to the labeling resulting from the medial AIN injection in T151 (cf. Figs. 6.10A and 6.11A; also see Fig. 6.1B).

The pattern of labeling in the NRTP in T150 was quite similar, although reversed with respect to the identity of the tracers, to the distribution of terminals in T151 (Fig. 6.11B).

In the mes- and diencephalon, PhaL labeling was quite similar to the pattern displayed by the BDA-filled beads in T151. BDA-filled terminals in T150 were found adjacent to the patch with PhaL-filled varicosities (Fig. 6.1C). The field with terminal labeling from the centrally placed injection site in T150 was located more dorsal than the labeling arising from the more medially placed injection site in T151. In T150, the ventral aspect of the RNm remained devoid of labeling (Fig. 6.11C, level 3,4). The distribution of labeling in the preR was essentially similar in both cases. In level 4 through 8 (Fig. 6.10 and 6.11), the reversed pattern of terminal labeling in the DpMe and APT can be appreciated: in

T150, PhaL labeling was found in the caudal DpMe and APT, whereas at rostral levels BDA-filled terminals were seen. In agreement with the labeling in T151, MA3 contained some labeling resulting from the laterally positioned injection site.

Discussion

In this paper we used a double anterograde tracing technique to study overlap in the converging projections of the CN to the NRTP, the RN and the prerubral area. Nucleoolivary projections (Ruigrok and Voogd, 1990) were used to check the discreteness of the injection sites. We found that terminal fields in these nuclei, resulting from injections confined to a single nucleus, remained separated. This non-overlapping distribution of terminals supports the notion of a parallel alignment of projections from the CN to the brain stem and suggests that the modular organization of the cerebellum is not only maintained in its connections to the IO (Ruigrok and Voogd, 1990) but also in its projections to diverse brain stem areas.

Methodological considerations

Convergence of projections from different CN in nuclei of the brain stem has been established with retrograde labeling (chapter 5). However, to establish the actual overlap or segregation of the terminations from individual nuclei anterograde tracing methods should be employed. Despite the wealth of information that may be extracted from studies using a single anterograde tracer, it remains difficult to decide to what extent injections made in different individuals may show overlapping terminal fields, due to differences in cutting angle, staining procedure, fixation, size etc. Obviously, double or multiple anterograde tracing studies may partially overcome this problem since the terminal fields can be directly related to one another. Therefore, anterograde double labeling studies have been employed using various combinations of tracers (Aumann *et al.*, 1994; 1996; Dolleman-Van der Weel and Wouterlood, 1994). Here, we have chosen for light microscopical visualisation of BDA (DAB-Cobalt incubated) and PhaL (DAB incubated) in line with Dolleman-Van der Weel (1994). In this way, it proved possible to simultaneously visualize and plot both tracers in counterstained sections. This proved to be invaluable in assessing the cytoarchitectonic boundaries in conjunction with the labeling. In cases of doubt adjacent sections, processed for either BDA or PhaL only, were compared. Due to the Cobalt intensification of the DAB reaction procedure employed for BDA visualisation, labeled fibers and terminals not only could be distinguished by the black colour of their reaction product but also tended to be somewhat coarser compared to the, brown, PhaL -labeled fibers, which further helped in distinguishing type of labeling. Moreover, both types of label could be further differentiated using dark field illumination.

The transport characteristics of both tracers appeared to be rather similar, i.e. in when comparing the results of two cases in which the location of the injected tracers was

almost identical but with reversed tracers, the results were more or less comparable (cf. T150 and T151).

Finally, another important factor in our choice of anterograde tracers that can be visualized with normal light microscopy is their resistance to fading, thus enabling reliable analysis of the cases even after years of storage.

CN - IO projections

The projections from the CN to the IO have been studied in great detail (see (Ruigrok and Cella, 1995; Voogd, 1995) for review). Our observations are in full agreement with these and other reports (Ruigrok and Voogd, 1990). Some new, additional observations concern the organization of the AIN projections onto the DAO in which a caudolateral to rostromedial topography was recognized to match a rostromedial to caudolateral olivary topography: i.e. the caudolateral AIN supplied the rostromedial DAO with input. Within this topography more rostrally located AIN areas tend to project to more lateral DAO regions (e.g. compare BDA injections and olivary projections in cases T92 and T84). The DLH projected to the DM (T94, T84). When the nucleoolivary projection is compared to the somatotopical organization of the DAO and the DM, it appears that the hindlimb is located in the rostromedial AIN, and the forelimb in more lateral and caudal parts of this nucleus, with the face in the DM. Projections from the LCN are confined to the PO: caudal (T194 PhaL, T94 PhaL) and ventral (T96, T98) injections project predominantly to the ventral leaf of the PO, whereas rostral and dorsal injections (T92, T98 BDA) project caudally, predominantly in the dorsal leaf of the PO. The VLO was densely innervated when the ventromedial, parvicellular part of the LCN (levels 6,7) was involved in the injection site (e.g. cases T98-PhaL).

The clear-cut, point to point relation between the nuclear masses of the cerebellum and the IO becomes even more obvious in this material with dual tracers. Even when both injections were made in the same nucleus such as the AIN (T150, T151), PIN (T108) or LCN (T98) distinct, non-overlapping, labeling was observed in the olivary complex. In fact, assessment of the location of labeled terminals within the IO proves to be a very valuable instrument in judging the boundaries of the actual effective injection site.

CN - NRTP and Pn projections

The CN projections onto the NRTP have been studied in different species (rat: Angaut *et al.*, 1985a; Teune *et al.*, 1999; Torigoe *et al.*, 1986a; Torigoe *et al.*, 1986b; Watt and Mihailoff, 1983a; Watt and Mihailoff, 1983b; opossum: Yuen *et al.*, 1974; cat: Brodal *et al.*, 1972b; Voogd, 1964, and monkey: Asanuma *et al.*, 1983a) with both retrograde and anterograde tracing techniques. Clearly, the largest contribution in this projection is supplied by the LCN followed by AIN and MCN. The PIN reportedly does not project to the NRTP. However, not much information is available on the level of convergence. In the monkey, Asanuma and collaborators (Asanuma *et al.*, 1983a) noted overlap of MCN projections with the lateral and

interposed nuclei in the lateral and medial-most aspect of the NRTP. However, Angaut *et al.* (1985a), in an autoradiographic study in the rat proposed another scheme with caudal parts of the LCN projecting to more rostral regions and vice versa. Also, the projections from the interposed nucleus were reported to be found more ventrally within the NRTP. In previous chapters 2 and 5 we found convergence of caudal MCN, AIN, DLH and LCN onto the NRTP and confirmed Angaut's (1985) reversed rostrocaudal topography in the projection of the LCN to the NRTP. Rostral and dorsal injections of the LCN, with labeling in the dorsal leaf of the PO (T98, T92) mainly project to laterocentral parts of the NRTP and ventral into its rostral pole. Ventral injections of the LCN, with nucleo-olivary labeling in the caudal ventral leaf of the PO (T98, T96) label the periphery of the NRTP and the rostral pole. Injections of the caudal LCN, with a nucleoolivary projection to the rostral part of the ventral lead (T194, T94), strongly project to the dorsolateral periphery and dorsally in or to the rostral pole of the NRTP. A rostrocaudal topography in the LCN, with diverging nucleoolivary projections could not be confirmed. In case T98, with injections in adjacent parts of the LCN, with diverging nucleoolivary projections to the dorsal and ventral leaf of the PO, the terminal fields of the NRTP did not overlap. We could confirm the somewhat more ventral localization of terminal fields when the AIN was injected. When all cases with injections in the AIN and the DLH are ordered according to their nucleo-olivary projection from rostrolateral DAO to caudomedial DAO and DM (i.e. according to the somatotopical gradient lower limb - upper limb - face, i.e. T151, T150, T96, T92, T199, T150, T151, T94, T84), the rostromedial AIN, the caudolateral AIN and the DLH were found to project to successively more dorsal areas in the caudal two thirds of the central NRTP. From a comparison of the single injections these projections appeared to overlap somewhat, but in three cases with two paired injections in the AIN and/or the DLH (T84, T150, T151) no such overlap of the terminal fields was observed.

Although the caudomedial part of the MCN has been shown to be specifically incorporated in the projection of this nucleus to the NRTP (Teune *et al.*, 1999), no injections specifically involved this area. Nevertheless, case T194 demonstrated a projection to the mediodorsal parts of the NRTP which was supplemented with a sparse projection to the lateral NRTP (T194). This pattern is basically in line with the report on cerebellar projections to the NRTP in the monkey (Asanuma *et al.*, 1983a) and in the rat (Cicirata *et al.*, 1982; Watt and Mihailoff, 1983a). The PIN, agreeing with previous reports, was the only CN subnucleus that did not project to the NRTP (Angaut, 1970; Asanuma *et al.*, 1983a; Brodal *et al.*, 1972b; McCrea *et al.*, 1978; Teune *et al.*, 1999; Torigoe *et al.*, 1986a; Voogd, 1995; Yuen *et al.*, 1974).

Most injections in the MCN, AIN, DLH and LCN resulted in small but distinct patches of terminal labeling within the Pn. However, as in the NRTP, no overlapping patches were observed.

The general picture of the cerebello-reticular projection to the NRTP which emerges from our studies is that of a central, somatotopically arranged area, containing the projection from the AIN and the DLH, with strong projections from the LCN and a minor contribution from the MCN located in the periphery and the rostral pole of the nucleus. Afferents from the zona incerta, the pretectum (Mihailoff *et al.*, 1985), and the superior colliculus terminate in the periphery of the NRTP, with the crossed tectopontine pathway from deep and intermediate layers of the SC terminating dorsomedially (rat: Burne *et al.*, 1981; rabbit: Wells *et al.*, 1989) and, therefore, would overlap with the cerebellar nuclear projections from the LCN and the caudal MCN. The corticopontine projection to the NRTP has not been studied systematically. In the cat, these afferents distribute to the ventral parts of this nucleus; the hindlimb somatosensory cortex projects laterally, the forelimb and face in successively more ventromedial parts of the nucleus (Brodal and Brodal, 1971; Chiba, 1980). Afferents from the frontal eye fields have been located in the medial and dorsal periphery of the NRTP in the monkey (Stanton, 1980). The visual corticopontine projection does not appear to terminate in the NRTP (Brodal, 1972; Wells *et al.*, 1989).

The projection of the NRTP to the cerebellum is characterized by the collateralization of its mossy fibers to the cerebellar nuclei. A projection to the vestibular nuclei and the nucleus prepositus hypoglossy, advocated by Balaban (1983) and Cazin *et al.* (1984), was denied by Gerrits (Gerrits and Voogd, 1986; Gerrits *et al.*, 1984b). In the rat, the mossy fiber projection of the NRTP has only been analyzed with retrograde tracing methods. In the cat, these mossy fibers were traced to all lobules of the cerebellum, with exception of lobule X, with an emphasis on lobules VI, VII, and IX of the caudal vermis, the lateral anterior lobe, and the simplex, ansiform and paramedian lobules, the proximal dorsal paraflocculus, the ventral paraflocculus and the rostral flocculus (Gerrits *et al.*, 1984a; Gerrits and Voogd, 1982; 1986; Kawamura and Hashikawa, 1981a; 1981b). In the monkey, projections to the dorsal paraflocculus and lobule IX later were excluded by Glickstein (1994).

The projection of the NRTP to the flocculus was found to originate from the dorsomedial NRTP (Gerrits *et al.*, 1984a; Glickstein *et al.*, 1994), i.e. from the area receiving the tecto-pontine pathway and projections from the caudal MCN and the LCN. In the rat the projections to the caudal vermis, including the vermal visual area, also arise from cells in the dorsal, medial and ventral periphery of the nucleus (Azizi *et al.*, 1981; Batini *et al.*, 1987), partially overlapping the floccular-projecting cells. The hemisphere is innervated from more central parts of the nucleus (Mihailoff *et al.*, 1981a). Similar observations were made in the cat (Hoddevik, 1978) and in the monkey (Brodal, 1980a; 1980b; 1982; Thielert and Thier, 1993). A topical projection of ventral parts of the nucleus to its dorsal folia was observed by Grottel *et al.* (1988) in the rabbit. This topical projection would be in accordance with the somatotopical pattern in the AIN / DLH

projection to the central NRTP described in this study, and the known somatotopical localization in the paramedian lobule (Snider and Stowell, 1944) hindlimb located ventrally and the forelimb and the face dorsally both in the NRTP and the paramedian lobule.

The collaterals of the mossy fibers of the NRTP to the cerebellar nuclei were traced by Mihailoff (1993) in the rat. They were found to terminate in the LCN, DLH, lateral AIN, PIN and caudal and ventral MCN, confirming the observations by Gerrits and Voogd (1987) in the cat. Some of the collateral nuclear projections from the NRTP may reciprocate the connections from the cerebellar nuclei, but the prevailing property of the cerebellar-reticular connections is that they function as an open loop. The cerebellar nuclear and cortical projections from the NRTP are bilateral and include all nuclei, zones and lobules of the cerebellum, whereas the nucleo-reticular limb of the loop is closed and lacks the reciprocal connections of the PIN, the rostral MCN and the medial AIN with the NRTP.

CN - RN projections

The RN receives a somatotopically organized projection from the CN as has been shown in rat (Angaut *et al.*, 1987; Angaut and Sotelo, 1987; Caughell and Flumerfelt, 1977; Daniel *et al.*, 1988; Daniel *et al.*, 1987) and other species (Condé and Condé, 1980; Courville, 1966; Flumerfelt *et al.*, 1973). Our results confirm and extend these observations. Here, we show that the organization of projections from the AIN and the DLH to the RNm appears to be very precise and resembles the level of specificity seen in the cerebellar nuclear projection to the IO. E.g. when comparing the RN projections in cases T150, T151 and T84, it is obvious that paired injections of these nuclei, placed in close proximity, result in terminal fields in the RN that are adjacent, but not overlapping. Basically, our studies confirm the observations of (Angaut, 1970; Daniel *et al.*, 1987; Robinson *et al.*, 1987; Teune *et al.*, 1999) and our observations from chapters 2 and 5. When the AIN and DLH injections, reported in this chapter, are ordered according to their projection to the DAO, ranging from rostrolateral DAO (which contains the localization of the hindpaw) to caudomedial DAO and DM (forepaw and face) the terminal fields from rostromedial AIN (T151) shift from a caudal and ventrolateral position to the dorsomedial and more rostral RN, where the terminal fields from the DLH are found (T94). The projection from the most lateral DLH injection (T94-BDA) is found along the dorsomedial border of the RN. The ventromedial RNm remains unlabeled and may contain the projection from the medial PIN. Unfortunately, we have no specific combination of injections in the AIN and medial PIN, and therefore are not able to confirm or deny the suggestion made by Daniel *et al.* (1987) that these areas will show overlap in their projections to the RNm. In variance with the report by Daniel *et al.* (1987), we have shown that the projections from the AIN are not restricted to the caudal, magnocellular, part of the RN, but advance well into its parvicellular part.

The LCN is reported to be connected exclusively with the RNp (Angaut *et al.*, 1987; Caughell and Flumerfelt, 1977) and T94-PhaL. Although the projections of the LCN do not appear to overlap with terminal fields originating from the AIN or DLH (T92, T96, and T94, respectively), there may be some overlap when both injections are made in the LCN (case T98). This would illustrate the somewhat less specific character of LCN projections to the RNp compared to its projections to the IO or when comparing AIN projections to the RN. However, it should be noted that in case T98 both injections were close to each other located both in the ventral half of the LCN. We concur with the description by Angaut et al. (Angaut *et al.*, 1987) that the rostral LCN projects ventromedially in the RNp, whereas caudally placed injections terminate in dorsolateral regions (cf. terminal fields in cases T96-PhaL and T98-BDA with T194-BDA and T94-PhaL). However, a superimposed ventral to lateral somatotopy could not be confirmed with the present material (e.g. case T 98-PhaL). Rather, the terminal field of caudally placed injections appears to extend caudally along the lateral margin of the RNm into the pararubral region (Ruigrok and Cella, 1995). This topographic arrangement would be in line with recent findings based on retrograde tracing (Teune *et al.*, 1999).

Our injections centered on the MCN did not reveal a major projection to the RN. However, some terminal patches were observed in or near the lateral horn of the RN (Reid *et al.*, 1975b; Ruigrok and Cella, 1995).

CN - preRN projections

In our definition, the prerubral area includes regions rostral and directly medial to the RN. Here, numerous retrogradely labeled cells can be observed after injections in the IO (Carlton *et al.*, 1982; Ruigrok and Cella, 1995; Rutherford *et al.*, 1984; Teune *et al.*, 1999). It encompasses the medial accessory oculomotor nucleus (MA3), the ventral tegmental relay zone (VTRZ), the prerubral field (preR), the Dk, the subparafascicular nucleus (SPF), the rostral interstitial nucleus of Cajal (RI). The definitions of these nuclei differ for different authors (Carlton *et al.*, 1982; Kennedy, 1990; Ruigrok and Cella, 1995; Swenson and Castro, 1983a; 1983b). Here, we basically follow the outlines indicated by the atlas of Paxinos and Watson (1986), but include the rDk located just dorsally and medially to the fasciculus retroflexus (Ruigrok and Cella, 1995). This distinction was prompted by the observation that in the rat no olivary afferents appear to originate from either the Dk or from the RNp (Carlton *et al.*, 1982; Ruigrok and Cella, 1995; Rutherford *et al.*, 1984), whereas Darkschewitsch' nucleus definitely projects to the IO in the cat (Onodera, 1984). It has been suggested that, in the rat the prerubral area, rather than the RNp is the homologue of the primate RNp (Kennedy *et al.*, 1986; Ruigrok and Cella, 1995).

Based on the experiments reported in chapter 5 of this thesis, using retrogradely transported tracers injected into the prerubral area most projections appear to originate from the LCN and PIN. However, retrogradely labeled cells were also

observed in the medial AIN and in the lateral and central, but also occasionally caudal, MCN. A clear topographic relation could not be found. Nevertheless, the notion, obtained in cat (Onodera, 1984; Voogd, 1964) that in this region the PIN predominantly projects to the rDk, RI and SPF, whereas the LCN rather connects with the MA3, VTRZ, and preR, could be verified. Within the projections from the PIN a topography may be recognized: within the rDk and RI, the medial PIN terminates caudally and dorsolaterally whereas lateral PIN terminations are found rostrally and ventromedially (T108). Projections to MA3 and VTRZ specifically arise from injections in the ventral part (T96-PhaL; T98-PhaL) or caudal part (T94-PhaL) of the LCN. Labeling in the oculomotor nuclei is only observed when the ventral-most part of the LCN is incorporated in the injection site (T98). The injection may have extended into Gacek's infracerebellar nucleus (Gacek, 1977; 1979) which is the rat□s equivalent of the dorsal nucleus y (Highstein and Reisine, 1979; Tan *et al.*, 1995) which has been shown to connect to the oculomotor nuclei in cat and rabbit (for review see Rubertone *et al.*, 1995a; Voogd *et al.*, 1996a). Cerebellar efferents to MA3 also originate from the MCN (T194-PhaL) as was described earlier (Gonzalo-Ruiz and Leichnetz, 1987; 1990) and PIN (T108). However, in the available combinations of injections no cases were found displaying conspicuous overlap of terminal arborizations within these oculomotor-related areas.

Consistent with our retrograde study, most cases resulted in terminal labeling within the preR, located directly rostral to the RNp and wedged between the medial lemniscus and fasciculus retroflexus. The scp courses through this region on its route to the thalamus. Most fibers appear to show some sparse and scattered terminal-like varicosities along their path. Here, overlap of terminal fields may be apparent (e.g. between MCN and LCN: T194; AIN and LCN: T92).

The question which CN target the preolivary neurons in this area and, whether these connections are reciprocally organized, i.e. whether the neurons of the cerebellar target nucleus of a particular module selectively terminate on the preolivary neurons projecting to the olivary subnucleus which innervates the same module, is still difficult to answer. Discrete projections from Darkschewitsch' nucleus and the subparafascicular nucleus to the rostral MAO and the dorsomedial cell column (DMCC), Bechterew's medial accessory oculomotor nucleus to the dorsal lead of the PO and the parvicellular RN to the ventral leaf were described by Onodera (1984) in the cat. The results of the tracing study of Swenson and Castro (1983a; 1983b) in the rat were basically similar, though less precise, with the periaquaeductal gray and Darkschewitsch' and subparafascicular nuclei projecting to the rostral MAO, DMCC and PO, the medial part of the deep mesencephalic nucleus (which may include part of the pararubral area) to the dorsal leaf of the PO and the lateral part of the deep mesencephalic nucleus (which may include the pretectum) to the DAO.

The discrete, non-overlapping projections of different parts of the PIN to the rostral nucleus of Darkschewitsch (T108) confirm a similar projection in the cat (Ruigrok and Voogd, 1988; Voogd, 1964) and would support the existence of a strict modular organization of the cerebello-mesencephalic-olivary loop. However, our material is not sufficient to recognize a similar, modular organization for the projections of the LCN, the DLH, and the caudal MCN to the prerubral area. The rostral MCN, the DLP and the AIN seem to lack projections to preolivary neurons in this area. The AIN, however, is involved in a cerebello-mesencephalic-olivary loop, which includes the pretectum as a preolivary relay nucleus.

Projections to other midbrain areas

Besides the generally rather specific projection to the investigated areas, it was observed that injections in some cases resulted in labeling within surrounding areas such as the oral part of the pontine reticular formation (PnO: T94-PhaL, T194-PhaL, T199-BDA), DpMe (DpMe: most cases), pretectum (APT: e.g. T151 and T150) and ZI (most cases). It should be appreciated that in all cases the actual overlap within most of these areas actually is very small. E.g. see labeling in DpMe in case T94, in APT in cases T151 and T150, in ZI in case T108. Only within the PnO a potential convergence of projections from the caudal LCN and central MCN may occur (cf. cases T194-PhaL and T94-PhaL).

Functional implications

Available evidence suggests that the cerebellum may be involved in a large variety of functions, not only in the coordination, adaptation, timing and learning of motor programs (Ito, 1984), but also in cognitive (Fiez, 1996; Leiner *et al.*, 1986; Schmahmann, 1996) and visceral functions (Haines *et al.*, 1990). The output of the cerebellum is organized as a number of parallel, and structurally identical, modules which are considered as the functional units of the cerebellum (Bloedel, 1992; Voogd, 1964). Evidence that distinct sagittal zones, incorporated in the modules, are involved in different aspects of movement control has been presented in studies on the control of compensatory eye movements (Sato and Kawasaki, 1990b; van der Steen *et al.*, 1994), on saccadic eye movements (Godschalk *et al.*, 1994) and on the reach to grasp movements (Gibson *et al.*, 1996). Since the individual CN (or parts thereof) function as output stations of the modules, the question arises as to how this differential control is implemented in the brain stem.

Two different systems should be recognized in the output of each cerebellar nucleus. One, the GABAergic nucleoolivary system, precisely reciprocates the olivo-nuclear projection. The likelihood of a similar reciprocity in the superimposed, cerebello-mesencephalic-olivary loop was discussed in the previous section. The other system consists of large and medium sized non-GABAergic neurons with widely diverging,

branching axons, terminating in premotor, precerebellar, and preolivary centers in the brain stem and the cord and in the thalamus. The collateralization profile of the neurons of each cerebellar nucleus appears to be quite specific, but collaterals of different cerebellar nuclei converge on many of their target nuclei in the brain stem and the thalamus.

In the present report, the convergence of different CN in three functionally diverse brain stem areas were investigated with a double anterograde tracing technique. These areas include a premotor area (the RN), an area that supplies mossy fibers to the cerebellar cortex and a collateral projection to the CN (NRTP) and finally a preolivary area (the prerubral area). The projections to the IO were included in our study, to check the localization and the discreteness of the injection sites.

Although these three areas clearly subserve different functions, it will be obvious that the existence of a cerebellar output to these areas does not critically depend on a particular module. Rather, input from many modules to several or all three areas would appear to be the rule (also see (Teune *et al.*, 1999) and chapter 5). This would imply that proper functioning of most modules apparently requires a direct as well as an indirect (via preR) feedback signal to the climbing fiber source, supplemented by a feedback connection to a mossy fiber source in order to be able to adequately influence premotor areas. In some instances, the modular input to one of the four brain stem areas appears to be minimal or non-existent (e.g. PIN input to the NRTP, AIN input to the preR, MCN input to the RN). However, it would appear very likely that other brain stem areas receiving cerebellar input may represent similar functions (i.e. AIN input to pretectal areas from which olivary afferents may originate (Kitao *et al.*, 1989; Walberg *et al.*, 1981); MCN input to the vestibular nuclei and/or reticular formation which may serve as premotor areas (Holstege and Kuypers, 1987).

Despite the fact that the output of several recognized cerebellar modules may converge on the investigated brain stem areas, the present study provides evidence that within these areas the output from different parts of the same cerebellar nucleus or from different CN is not processed conjunctively but in parallel. Indeed, even when both injections were centered on the same cerebellar nucleus no conspicuous overlap of terminal fields was usually noted in the investigated brain stem nuclei. Separated terminal fields resulting from both injected tracers are most clearly recognized in the RNm, followed by the NRTP and preRN, and the RNp. The apparent lack of overlap in the projections from different parts of the same nucleus or from different CN suggests that integration at the level of the brain stem nuclei, of signals processed by different parts of the cerebellum is not a characteristic of their functioning. Similar observations have been made in the thalamus, The different CN project, through branching neurons, to different thalamic nuclei (Aumann *et al.*, 1994). Within these nuclei their terminal fields remain separated (Aumann and Horne, 1996). Even in regions where

the projections of different cerebellar nuclei appear to overlap (i.e. PIN and LCN in the medial VL nucleus of the thalamus, Aumann and Horne, 1996) their terminations interdigitate, but do not overlap on the same thalamic neurons.

Overlap with convergence of different CN on single neurons may occur in certain areas of the brain stem, such as the reticular formation, the deep mesencephalic nucleus, the pretectal area, the prerubral field and, for the LCN, in the parvicellular red nucleus, but most of these regions have not yet been sufficiently analysed with the appropriate morphological and electrophysiological techniques.

The presence of parallel processing in many centers in the brain stem and the thalamus, which serve as target nuclei of the cerebellum, raises the question where the integration, which should be a major property of cerebellar function, occurs. Two comments can be made on this question. One is obvious, integration should occur within the cerebellar cortex, mainly through parallel fibers, and in the CN, where many Purkinje cell axons converge upon a small number of the nuclear cells. The nature of the integration by parallel fibers remains unknown. The convergence of Purkinje cells onto the cells of the CN will be analyzed in chapter 7 of this thesis. The second remark concerns the organization of the reciprocal mossy fiber pathways from the NRTP and other reticular nuclei. In contrast to the cerebello-olivary circuits, which seem to operate on a strictly reciprocal basis, the reticular nuclei, may set up reverberating circuits, which would involve increasingly wider regions of the cortex and the nuclei of the cerebellum. In what way the various types of potentially reverberating cerebello-bulbar circuits interact in order to result in an adjustable and meaningful signal to a particular type of effector remains to be investigated. The integrative properties, characteristic of cerebellar functioning, therefore, are likely to reside within the cerebellum, rather than being the result of extensive convergence of the cerebellar output in the brain stem.

Table 6.1

Summary of cases with combinations of PhaL (rows) and BDA (columns) injections centered on parts of the cerebellar nuclei. Bold print refers to cases that are illustrated and described in the text. AIN: anterior interposed nucleus; DLH: dorsolateral hump; ICG: interstitial cell group; MCN: medial cerebellar nucleus; LCN: lateral cerebellar nucleus; PIN: posterior interposed nucleus.

	LCN	AIN	PIN	DLH	MCN
LCN	**T98**	T83			**T194**
AIN	T77, T89,**T92**,T93, **T96**	T150, T151		**T84**, T121	
PIN	T79, T90, T109, T109	T176	**T108**		
DLH	**T94**				
ICG		T82			
MCN		T195, T198, **T199**			

Legends to figures (see pages 276-287)

Fig. 6.1. Color microphotographs showing examples of injection sites and resulted anterograde labeling taken from cases T150 (A,B,C), T94 (D,E,F) and T108 (G,H,I). Black arrows depict BDA labeling, white arrows point to PhaL labeling. **A**: BDA and PhaL injection sites in the AIN of case T150. **B**: anterograde BDA (B1) and PhaL (B2) labeling in the DAO. **C**: Distinct BDA and PhaL labeled patches in the RNm. Compare with Fig. 6.11. **D**: BDA and PhaL injection sites in the DLH and LCN, respectively, of case T94. **E**1,2: Resulting BDA and PhaL labeling in the medial part of the DAO and DM, and in the ventral part of the PO, respectively. **F**: High magnification micrograph of a part of the NRTP showing tufts of BDA labeling surrounded by PhaL terminal arborizations. **G**1,2: Micrographs depicting two levels of the PIN and indicating centers of the PhaL and BDA injection sites of case T108. **H**: a PhaL and BDA patch of terminal labeling in the MAO. **I**: Differential distribution of BDA and PhaL labeled terminals in the rDk. Scale bars: 1000 μm in A,D; 500 μm in E,G; 100 μm in B,C,F,H,I.

Fig. 6.2. Plots injection sites in MCN and LCN and anterograde labeling in the IO, pontine and mesodiencephalic area of case T194. BDA injections sites and labeled varicosities are indicated in blue, PhaL labeling is indicated in red. **A**: Right hand panels depict the injection sites indicated in standardized diagrams of the cerebellar nuclei in the right hand side of the brain (Ruigrok and Voogd, 1990). Left hand panels depict anterograde labeling indicated in standardized diagrams of the contralateral inferior olivary complex. Numbers in both series of diagrams refer to respective caudorostral levels and are taken at 160 μm intervals. **B**: Computer generated plots of labeling in and around the contralateral NRTP. Every dot represents essentially one labeled varicosity. Five consecutive caudorostral levels (1 to 5) are shown. **C**: Computer generated plots of the contralateral red nucleus and prerubral area shown in 10 consecutive caudorostral levels. Every dot represents essentially one labeled varicosity. The aquaeduct or third ventricle is indicated in the upper right hand corner of the square. The square measures 1 mm^2. Abbreviations in this and following Figures: 3: oculomotor nucleus, AIN: anterior interposed nucleus, APT: anterior pretectal nucleus, ß: nucleus β, bp: brachium pontis, DAO: dorsal accessory olive, DC: dorsal cap of Kooy, dfDAO: dorsal fold of DAO, Dk: nucleus of Darkschewitsch, DLH: dorsolateral hump, DLP: dorsolateral protuberance, DM: dorsomedial group of the PO, DMCC: dorsomedial cell column, DpMe: deep mesencephalic nucleus, dtgx: dorsal tegmental decussation, FF: nucleus of the fields of Forel, fr: fasciculus retroflexus, ICG: interstitial cell groups, INC: interstitial nucleus of Cajal, LCN: lateral cerebellar nucleus, lfp: longitudinal fascicle of the pons, ll: lateral lemniscus, LVN: lateral vestibular nucleus: MA3: medial accessory oculomotor nucleus, MAO: medial accessory olive, MCN: medial cerebellar nucleus, ml: medial lemniscus, mlf: medial longitudinal fascicle, MTN: medial terminal nucleus, NRTP: nucleus reticularis tegmenti pontis, PAG:

periaquaeductal gray, paraRN: pararubral area, PF: parafascicular nucleus, PIN: posterior interposed nucleus, Pn: basilar pontine nuclei, PO: principal olive, preR: prerubral field, py: pyramidal tract, rDk: rostral part of the nucleus of Darkschewitsch, rostral interstitial nucleus, RNm: magnocellular part of the red nucleus, RNp: parvicellular part of the red nucleus, scp: superior cerebellar peduncle, SN: substantia nigra, SNc: pars compacta of SN, SO: superior olive, SPF: subparafascicular nucleus, SVN: superior vestibular nucleus, tz: trapezoid body, VLO: ventrolateral outgrowth, VP: ventroposterior thalamus, VTRZ: visual tegmental relay zone, ZI: zona incerta.

Fig. 6.3. Plots of the injection sites in the AIN and MCN and anterograde labeling in the IO, pontine and mesodiencephalic regions of case T199. See text and Fig. 6.2 for further explanation.

Fig. 6.4. Plots of the injection sites in the LCN and AIN and anterograde labeling in the IO, pontine and mesodiencephalic regions of case T96. See text and Fig. 6.2 for further explanation.

Fig. 6.5. Plots of the injection sites in the LCN and AIN and anterograde labeling in the IO, pontine and mesodiencephalic regions of case T92. See text and Fig. 6.2 for further explanation.

Fig. 6.6. Plots of the injection sites in the AIN and DLH and anterograde labeling in the IO, pontine and mesodiencephalic regions of case T84. See text and Fig. 6.2 for further explanation.

Fig. 6.7. Plots of the injection sites in the LCN and DLH, and anterograde labeling in the IO, pontine and mesodiencephalic regions of case T94. See text and Fig. 6.2 for further explanation.

Fig. 6.8. Plots of the injection sites in the PIN and anterograde labeling in the IO, pontine and mesodiencephalic regions of case T108. See text and Fig. 6.2 for further explanation.

Fig. 6.9. Plots of the injection sites in the LCN and anterograde labeling in the IO, pontine and mesodiencephalic regions of case T98. See text and Fig. 6.2 for further explanation.

Fig. 6.10. Plots of the injection sites in the AIN and anterograde labeling in the IO, pontine and mesodiencephalic regions of case T151. See text and Fig. 6.2 for further explanation.

Fig. 6.11. Plots of the injection sites in the AIN and anterograde labeling in the IO, pontine and mesodiencephalic regions of case T150. See text and Fig. 6.2 for further explanation.

CHAPTER 7:
SINGLE PURKINJE CELL CAN INNERVATE MULTIPLE CLASSES OF PROJECTION NEURONS IN THE CEREBELLAR NUCLEI OF THE RAT:
A light microscopic and ultrastructural triple tracer study

T.M. Teune, J. van der Burg, C.I. De Zeeuw, J. Voogd, and T.J.H. Ruigrok

The Journal of Comparative Neurology 392: 164-178 (1998)

Abstract

Two different populations of projection neurons are intermingled in the cerebellar nuclei. One group consists of small, γ-aminobutyric acid-containing (GABAergic) neurons that project to the inferior olive, and the other group consists of larger, non-GABAergic neurons that provide an input to one or more, usually premotor, centers in the brain stem, such as the red nucleus, the thalamus, and the superior colliculus. All cerebellar nuclear neurons are innervated by GABAergic Purkinje cells. In this study, we investigated whether individual Purkinje cells of the C1 zone of the paramedian lobe of the rat innervate both groups of projection neurons in the anterior interposed nucleus. Two different, retrogradely transported tracers, either cholera toxin B subunit (CTb) or wheat germ agglutinin coupled to horseradish peroxidase (WGA-HRP) and a gold lectin tracer were injected into the red nucleus and the inferior olive, respectively, whereas Purkinje cell axons were anterogradely labeled with biotinylated dextran amine (BDA) injected into the paramedian lobule.

Cerebellar nuclear sections studied with the light microscope demonstrated a close relation of varicosities from BDA-labeled Purkinje cell axons with both gold lectin- and CTb-labeled neurons. Branches of individual axons could be traced to both retrogradely labeled cell populations. At the ultrastructural level, synapses of labeled Purkinje cell terminals with profiles of WGA-HRP-labeled projection neurons predominated over contacts with gold lectin-containing neurons. Nine out of 367 investigated BDA-labeled terminals were observed to be presynaptic to a WGA-HRP-labeled profile as well as to a gold lectin-labeled profile. This indicates that nuclear cells that project to the inferior olive as well as those that project to premotor centers are under the influence of the same Purkinje cells. Such an arrangement would suggest an in-phase cortical modulation of the activation patterns of the inhibitory cells that project to the inferior olive and excitatory cells that project to premotor nuclei, which could explain why olivary neurons, especially those of the rostral part of the DAO, appear to be unresponsive to stimuli generated during active movement.

Introduction

The main targets of the cerebellar Purkinje cells (PCs) are the cerebellar nuclei (CN) and the vestibular nuclear (VN) complex. PCs located within longitudinal cortical zones project to a particular CN and/or to the VN, which, in turn, receive olivocerebellar fibers that originate from a specific part of the inferior olivary (IO) complex and that provide the corresponding PC zone with a climbing fiber input. This type of organization is known as the modular organization of the cerebellum (Voogd and Bigaré, 1980). The neuronal population of the CN consists of projection neurons and interneurons (Batini *et al.*, 1992; Chan-Palay, 1977; Chen and Hillman, 1993; Teune *et al.*, 1995). The projection neurons can be divided into a

population of small, γ-aminobutyric acid-containing (GABAergic) neurons, which project to the IO (Angaut and Sotelo, 1987; De Zeeuw *et al.*, 1989b; Fredette and Mugnaini, 1991; Nelson and Mugnaini, 1984; Ruigrok and Voogd, 1990), and a group of medium to large-sized neurons, which use glutamate and/or aspartate as a neurotransmitter (Bernays *et al.*, 1988; Chen and Hillman, 1993; Monaghan *et al.*, 1986). The latter neurons project to one or more other centers in the brain stem, such as the red nucleus (RN), the superior colliculus, the mesodiencephalic junction, the basilar pontine and reticular pontine nuclei, the reticular formation of the medulla oblongata, the VN, and the spinal cord as well as projecting to several thalamic areas (Bentivoglio and Kuypers, 1982; Berretta *et al.*, 1993; Chan-Palay, 1977; De Zeeuw and Ruigrok, 1994; Faull, 1978; Faull and Carman, 1978; Ito, 1984; Legendre and Courville, 1987; Teune *et al.*, 1995). A number of small to medium-sized CN neurons colocalize glycine and GABA and are thought to represent interneurons (Chen and Hillman, 1993; De Zeeuw and Berrebi, 1995b). Both types of projection neurons and the interneurons appear to be completely intermingled (Chan-Palay, 1977; Chen and Hillman, 1993; Teune *et al.*, 1995).

For a better understanding of the cerebellar modules as functional units (see, e.g. (Ekerot *et al.*, 1995; Sato *et al.*, 1991; van der Steen *et al.*, 1994), it is important to know whether the synaptic inputs of both types of projection neurons are similar or dissimilar. Dissimilarity with respect to the climbing fiber collateral input to the projection neurons was suggested in a recent preliminary report by Borsello (1994), in which it was suggested that climbing fiber collaterals did not contact the nucleoolivary cells (however, see also De Zeeuw *et al.*, 1997). With respect to the PC input to the neurons of the CN, De Zeeuw (De Zeeuw and Berrebi, 1995a; De Zeeuw and Berrebi, 1995b) provided evidence that both GABAergic and non-GABAergic neurons within the interposed and lateral CN receive input from the same varicosities of a PC axon. The latter investigators, however, used immunocytochemical methods, and they could not identify the localization of the PCs with a double projection and did not distinguish between projection neurons and possible GABA- and glycine-colocalizing interneurons in the CN. Therefore, the present study was designed to investigate whether individual axons from PCs of a particular zone of the cerebellar cortex of the rat (the C1 zone) make synaptic contact both with neurons in the anterior interposed nucleus (AIN) that project to the IO and with neurons in the same cerebellar nucleus that project to the RN.

To identify the two types of projection neurons in the CN, we applied two different, retrogradely transported tracers to their target areas: either wheat germ agglutinin coupled to horseradish peroxidase (WGA-HRP) or cholera toxin B subunit (CTb) to the RN and a gold lectin conjugate (Ruigrok *et al.*, 1995b; Teune *et al.*, 1995) to the IO. The axons and terminal arborizations of a small number of PCs were labeled by a localized injection of an

anterogradely transported tracer, biotinylated dextran amine (BDA), into the presumed C1 zone of the paramedian lobule (PM). The position of the C1 zone was determined by recording surface potentials over the cortex of the PM (cat: Trott and Apps, 1993; rat: Atkins and Apps, 1996). The distribution of BDA-labeled terminals with respect to the location of the nucleoolivary and RN-projecting neurons was studied both at the light microscopic (LM) and electron microscopic (EM) levels.

Materials and methods

Surgical procedures

All experiments were performed on purpose-bred male Wistar rats. The experimental procedure was approved by the institute's animal care committee and adhered to the National Institutes of Health guidelines. Eighteen rats were anesthetized with intraperitoneal application of a mixture of ketamine (10 mg/kg) and thiazine-hydrochloride (3 mg/kg), and they were placed in a stereotactic frame. Additional doses of ketamine were applied intraperitoneally to maintain anesthesia when necessary.

Although previous LM studies indicated that gold lectin, WGA-HRP, and CTb tracers have comparable retrograde tracing and detection capabilities (Koekkoek and Ruigrok, 1995; Ruigrok *et al.*, 1995b; Teune *et al.*, 1995), we noted that the density of gold lectin label was higher in small cells compared with the density of label in larger cells. For this reason, we chose to inject the gold lectin label in the IO in the expectation that, especially at the ultrastructural level, the identification of gold lectin-labeled (small) neurons would be facilitated. CTb (LM experiments) or WGA-HRP (EM experiments) was injected into the RN area, and BDA was injected into the contralateral cerebellar cortex.

All tracer injections were made with glass micropipettes (10-15 μm tip diameter). For injections of BDA (10% in Tris-buffered saline; List Biological Laboratories, Campbell, CA) into the cerebellar cortex and of gold lectin into the IO, the atlantooccipital membrane was opened, and the occipital bone was largely removed. For the injections of WGA-HRP (n = 14; 7% in saline; Sigma, St. Louis, MO) or CTb (n = 4; 1% in 0.1 M phosphate buffer (PB), pH 7.2; List Biological Laboratories) into the RN, small holes were drilled in the parietal bone close to the sagittal suture (Teune *et al.*, 1995).

Recordings of spontaneous activity were used to verify the location of the IO, the RN, and the molecular layer of the cerebellar cortex. For the RN, the stereotactic atlas of the rat of Paxinos and Watson (1986) was used as an additional reference. Upon reaching the intended injection site, WGA-HRP and gold lectin were pressure injected, whereas CTb and BDA were iontophoretically applied (+4 μA; 7 seconds on/off cycle for 10 minutes). In several cases (n = 5), the location of the C1 zone in the PM was established prior to the BDA injection by percutaneous stimulation of the ipsi- and contralateral forepaw while recording surface potentials over the PM with a tungsten electrode

(impedance 200-500 kΩ; Atkins and Apps, 1996; Trott and Apps, 1993).

Animals were allowed to recover and survived for 3 days, during which they were checked daily for signs of stress and/or discomfort. Subsequently, they were anesthetized with an overdose of sodium-pentobarbital (120 mg/kg i.p) and transcardially perfused with 100 ml 0.9% NaCl followed by 1 liter of fixative containing 2% glutaraldehyde and 0.5% paraformaldehyde in 0.1 M PB, pH 7.2. After perfusion, the brains were removed, blocked, and kept in fixative for 1 hour. For CTb injections, animals were perfused with 4% paraformaldehyde, 0.5% glutaraldehyde, and 4% sucrose solution for fixation, and the intact brains were transferred to 30% sucrose in 0.05 M PB solution and were embedded in gelatin (Teune *et al.*, 1995) until sectioning on a freezing microtome. For EM experiments, only the mesodiencephalon, the caudal medulla oblongata, and the blocked and gelatin-embedded caudal part of the cerebellum containing the PM were stored in 30% sucrose in 0.05 M PB at 4 °C, and the remainder of the cerebellum, which contained the CN, was stored in 0.1 M PB at 4 °C.

Immunocytochemical and EM procedures

For LM experiments, sections were processed for CTb, as described previously (Teune *et al.*, 1995). Briefly, sections were incubated with an anti-CTb antibody (1:20,000 in (pH 8.6) Tris buffer, 0.05 M, with 0.5% Triton X-100 and 0.5 M NaCl; List Biological Laboratories) for 72 hours at 4 °C under frequent agitation. Next, after several rinses, a 2 hour incubation at room temperature in biotinylated donkey anti-goat antibodies (1:2,000 in the same Tris buffer with 0.5% Triton X-100; List Biological Laboratories), and further rinses, sections were incubated with the avidin-biotin complex (ABC) product (1:100 in 0.05 M PB (pH 7.2); ABC Elite kit; Vector Laboratories, Burlingame, CA) for 3 hours under frequent agitation at room temperature. Thereafter, following a thorough rinse in 0.05 M PB, sections were reacted with diaminobenzidine (DAB; 37.5 mg with 25 µl 30% H_2O_2 in 150 ml PB) for 45 minutes. Finally, the gold lectin label was enhanced by silver intensification (Aurion, Wageningen, the Netherlands; (Ruigrok *et al.*, 1995b; Teune *et al.*, 1995), and sections were mounted, air dried, counterstained, and coverslipped.

The tissue blocks containing the WGA-HRP, gold lectin, and BDA injection sites were cut transversely on a freezing microtome at 40 µm and were collected in 0.05 M PB. Cerebellar sections containing the BDA injection site were incubated in ABC (1:100 in 0.05 M PB) for 2 hours at room temperature, in the dark, and under frequent agitation. Together with the brain stem sections containing the WGA-HRP injection site, they were rinsed and incubated in DAB for 15-30 minutes. After thorough rinses in 0.05 M PB, sections were mounted, air-dried, counterstained, and coverslipped. Medullary sections were mounted without prior processing.

For ultrastructural studies, the cerebella were sectioned transversely

on a Vibratome at 40-80 μm. For LM purposes, the blocked brains were cut transversely on a freezing microtome at 40 μm or 80 μm. The sections were collected in 0.05 M PB, and were processed according to a modified tetramethyl benzidine (TMB) procedure to stabilize the WGA-HRP labeling (Lemann *et al.*, 1985). Briefly, the free-floating sections were rinsed in 0.05 M sodium-acetate buffer, pH 4.8, for 15 minutes and were then preincubated in 0.5% TMB with 0.8% sodium- pentacyano-nitrosulferrate in 0.05 M sodium-acetate buffer (pH 4.8). After 10 minutes, 30 μl 30% H_2O_2 was added. After 45 minutes, the sections were rinsed thoroughly in sodium-acetate buffer and were subsequently reacted with 75 mg DAB, 3 ml 1% $CoCl_2$, and 50 μl 30% H_2O_2 in 150 ml PB (DAB-cobalt) for 15 minutes. After a thorough rinse in sodium-acetate buffer and a Tris-HCl rinse (0.05 M Tris buffer, pH 7.6), WGA-HRP histochemistry was immediately followed by the procedures to visualize BDA. The sections were incubated in ABC (1:50) in Tris-HCl at 4 °C in the dark under frequent agitation. After 48-72 hours of incubation, sections were rinsed in Tris-HCl and were incubated with DAB for 45 minutes. Thereafter, the sections were rinsed and stored in 0.05 M PB (pH 7.2).

All thoroughly rinsed, wet sections were subsequently examined under the light microscope. Selected sections containing parts of the AIN with abundant WGA-HRP gold lectin, and BDA labeling were transferred to 0.1 M cacodylate buffer (pH 4.8) and fixed in 2% osmium tetroxide with 8% d-glucose. To enhance the gold lectin label, the osmicated sections were rinsed in distilled water, silver enhanced (Aurion) for 20 minutes, rinsed in distilled water, stained in 2% aqueous uranyl acetate, rinsed again in distilled water, then dehydrated in a graded series of ethanol and propylene oxide, and finally flat embedded in Araldite.

Subsequently, 0.50-0.75 mm pyramids from the selected sections of the AIN were prepared. Serial ultrathin (65 nm) sections from the superficial layer (≤ 5 μm) were mounted on Formvar-coated nickel grids, counterstained with uranyl acetate and lead citrate, and examined in a Philips CM 100 electron microscope (Philips Industries, Eindhoven, The Netherlands).

Collection and analysis of data

The ultrastructural data are based on four cases from which a total of five pyramids were prepared. From each pyramid at least 50-200 sections were cut serially and mounted onto grids. The BDA-labeled profiles were analyzed for each pyramid in three single sections, which were spaced ten grids apart (the grids usually contained four to seven serially collected sections). These sections were scanned for BDA-labeled profiles. All positively identified profiles were subsequently examined, and the identified vesicle-containing boutons that made synaptic contact with one or more other profiles were scored. The postsynaptic structure(s) was identified as labeled or unlabeled and was classified as some, proximal, or distal dendrite. Dendritic structures with diameters greater than 5 μm and

with ribosomes and saccules of endoplasmatic reticulum were classified as proximal dendrites, if they were smaller in size and contained a relatively low amount of ribosomes, they were classified as distal dendrites. Adjacent serial sections through the same PC terminal were routinely examined to verify the identity of the postsynaptic structures.

Results

Alignment of injection sites

To assess the termination of PCs on either type of projection neurons in the AIN, it was essential to center all injection sites on locations known to project or to receive afferents from this nucleus. Retrograde labeling from the RN and the DAO, therefore, was combined with anterograde labeling from the C1 zone of the PM (Buisseret-Delmas and Angaut, 1993; Ruigrok and Voogd, 1990; Teune *et al.*, 1995; Voogd and Bigaré, 1980). The use of electrophysiological recording techniques proved invaluable for optimal alignment of the injection sites. Recordings of the characteristic firing pattern of the RN and the IO neurons was instrumental in verifying the correct location of these nuclei. In most cases, these recordings enabled us to center the CTb and WGA-HRP injections on the magnocellular part of the RN and to incorporate at least part of the DAO into the gold lectin injection site. The presumed C1 zone in the rat was identified by recording evoked potentials on the surface of the PM after percutaneous stimulation of the ipsilateral and contralateral forepaw. In all investigated rats (n = 5), we noted a rather conspicuous positive peak after ipsilateral stimulation at a laterality of 2.4-2.7 mm, with a latency of approximately 15 msec (Fig. 7.1). In accordance with results obtained in the cat and in the rat (Atkins and Apps, 1996; Oscarsson, 1980; Trott and Apps, 1993), this evoked potential was interpreted as a climbing fiber response in the C1 zone mediated by the dorsal funiculus spinoolivocerebellar pathway. Because this recording procedure was time consuming (especially in combination with recordings from other injection sites) and because the location of peak response varied only slightly between rats, most BDA injections into the PM were made at a laterality of 2.5 without recording.

LM studies

In ten rats, the injections produced overlap of all three labels in the AIN. From these ten rats, four cases contained an injection of CTb that was centered on and remained confined to the RN (Fig. 7.2A). In the other six cases, WGA-HRP had been injected into and around this nucleus. In the latter cases, the DAB-incubated sections of the brain stem usually demonstrated some spread of the WGA-HRP from the caudal thalamus to the decussation of the scp and into the reticular formation surrounding the RN. In the CN, WGA-HRP-labeled neurons were identified by the characteristic black, needle-like reaction product of cobalt-stabilized TMB in the cell body and in the proximal, second-, or third-order

dendrites. Labeled cells were usually encountered in both interposed nuclei and within the LCN. In the CTb-injected cases, retrogradely labeled neurons were identified easily by their coarse, brownish, granular contents, which filled most of the cell body, the proximal dendrites, and, sometimes, the higher order dendrites. The location of CTb-labeled neurons varied somewhat from case to case but usually included the medial half of the posterior interposed nucleus (PIN) and areas throughout the AIN and the LCN (Fig. 7.3A).

The extent of the gold lectin injections varied considerably but always incorporated at least part of the DAO. Usually, parts of the principal olive and MAO, in various combinations, were incorporated into the injection site (Fig 7.2B). In the selected cases, the tracer did not spread beyond the boundaries of the IO. Gold lectin-containing neurons could be identified readily by the numerous black, apparently regularly shaped, small particles in the cytoplasm of the somata and the proximal dendrites (see also Ruigrok *et al.*, 1995b; Teune *et al.*, 1995). The localization of gold lectin-labeled neurons varied from case to case but was positively correlated to the olivary areas that were incorporated in the injection site (Fig. 7.3A; Ruigrok and Voogd, 1990). In accordance with a previous investigation (Teune *et al.*, 1995), CN neurons labeled both from the RN and the IO were not observed.

The BDA injection site remained restricted to the superficial layers of the cerebellar cortex of the PM (Fig. 7.2C) and appeared as a homogenous, densely stained deposit. At the borders of the injection site somata, dendritic trees and axons of individual PCs were stained. From the injection site, axons could be followed in the subcortical white matter en route to the CN. Within the CN, the labeled PC axons started to diverge and also lost their smooth appearance, whereas the axonal diameter gradually decreased. In any one section, ten to 15 varicosities (diameter 2.0-3.8 μm) per single PC axon segment were usually found at equal distances (4.5-8.0 μm). The heavily branched terminal parts of PC axons contained two to five small, spherical varicosities. The course and appearance of these terminal arborizations are in agreement with earlier observations by Chan-Palay (1977).

All cortical injections with BDA invariably resulted in terminal labeling within the caudal AIN, usually within its lateral parts. Frequently, however, some terminal arborizations were also encountered in more rostral regions of the PIN, within the dorsolateral protuberance (DLP) of the medial cerebellar nucleus (MCN), or within the dorsolateral hump (DLH).

In Figures 7.2 and 7.3, data from case T138 are shown as an example. Here, the CTb injection was centered on the transition of the magnocellular and parvicellular RN and resulted in retrogradely labeled neurons in the medial PIN, in the AIN (predominantly caudomedially), and dorso-laterally throughout the lateral cerebellar nucleus. The gold lectin injection was centered on the medial part of the DAD and included the medial part of ventral leaf of the principal olive with the dorsomedial subnucleus and the rostral part of the medial accessory

olive and encroached upon the medial part of the dorsal leaf of the principal olive. Most gold lectin-labeled neurons were encountered in the DLH, the rostral PIN, the lateral part of the caudal AIN, and the ventromedial part of the lateral cerebellar nucleus. The BDA injection in this case was made at a laterality of 2.2 and resulted in terminal labeling in the caudolateral AIN at its border with the PIN and within the DLP. Figure 7.3A,B shows that overlap of all three labels was apparent in the caudolateral AIN. Here, single-labeled, varicose axons were found in close apposition with both CTb- and gold lectin-labeled neurons (Figs. 7.2D,E, 7.3B).

The close proximity of these varicosities to neuronal structures is highly suggestive of a synaptic contact between individual PC axons and both types of projection neurons. These synaptic contacts were verified in the following ultrastructural studies.

EM studies

General observations. From the six cases with injections of WGA-HRP into the RN and overlap of all three tracers within the boundaries of the AIN, four cases were selected for EM analysis. The injection sites and resulting CN labeling pattern of these cases were essentially similar to the LM observations described above.

At the ultrastructural level, the characteristic WGA-HRP labeling consisted of large, irregular crystals within large profiles containing ovoid-shaped nuclei with regular contours. Frequently, dendritic and axonal profiles were also filled with the tracer substance. In any ultrathin section, WGA-HRP-labeled somata were usually contacted and surrounded by large numbers (ranging from 5 to 27) of terminals.

Most of the synapses were symmetric, but asymmetric synapses and attachment plaques were also observed. Symmetric synapses coincided on occasion with coated vesicles in the presynaptic cytoplasm, but the latter structures were usually seen in association with attachment plaques or in terminals without obvious synapses.

In contrast with LM observations, the ultrastructural appearance of the silver-enhanced gold lectin was characterized by the presence of irregularly shaped, evenly black particles with sharp and pointed edges (Figs. 7.4, 7.5). In any one ultrathin section, up to 17 gold particles were found in the labeled somata and in the proximal dendrites. Occasionally, gold particles were encountered in more distal dendrites (Fig. 7.5B). Neurons containing gold lectin usually were smaller in size and had fewer terminals on their somata. Neuronal somata containing gold lectin label were contacted on average by up to nine terminals in any one ultrathin section.

BDA-labeled profiles were characterized by a homogenous electron-dense substance (Figs. 7.3-7.6). Within the BDA-labeled terminals mitochondria and vesicles could be identified. Positive identification of the vesicle type was usually not possible due to the distribution of the DAB reaction product and/or inadequate histology. Figure 7.4 demonstrates that the three tracers were readily distinguished from

either background staining and from one another.

Synapses between labeled structures. In accordance with earlier reports, the synaptic contacts of the BDA-labeled terminals with labeled and unlabeled postsynaptic profiles could all be classified as symmetric. From a total of 367 analyzed BDA-labeled terminal profiles, 105 were found to make a synapse with an identified, labeled postsynaptic structure (Table 7.1). Of these 105 BDA-labeled terminals, 81 (77.1%) terminated on WGA-HRP-labeled somata, proximal and distal dendrites (Fig. 7.5C). Synapses with gold lectin-labeled cell bodies and/or proximal dendrites, on the other hand, were found on 24 occasions (22.9%); (Fig. 7.5B,D). BDA-labeled PC terminals synapsing with either gold lectin-containing profiles or with WGA-HRP-labeled structures possessed a similar size distribution (1.6 ± 0.3 mm (mean ± S.E.M.), n = 21 vs. 2.1 ± 0.8 mm, n = 54, respectively; this difference is not significant according to the Mann-Whitney test; P = 0.05).

On 21 occasions (5.7%), labeled PC terminals were observed to make a synaptic contact with more than one postsynaptic profile within the same ultrathin section (Table 7.1). In four cases (19.1%), the postsynaptic profiles were identified as both a WGA-HRP-labeled structure and a gold lectin-containing structure (Fig. 7.6); in two cases (9.5%), the BDA-labeled terminal contacted a gold lectin-labeled structure and an unlabeled profile. Other combinations involved WGA-HRP-labeled and unlabeled profiles (33.3%), two WGA-HRP-labeled profiles (14.8%), and two unlabeled postsynaptic profiles (23.8%).

From the batch of 81 BDA-labeled terminals that made a synapse with a WGA-HRP-labeled postsynaptic structure five were observed to make an additional contact with a gold lectin-labeled profile in an adjacent section. Hence, at least nine out of the 367 (2.5%) identified PC terminals were observed to make synaptic contact with both a gold lectin-labeled and a WGA-HRP-labeled neuronal structure.

Labeled profiles postsynaptic to BDA-labeled terminals as mentioned above and as shown in Table 7.1 were most frequently identified as somata or proximal dendrites. This is in contrast to the distribution of the 241 profiles of labeled PC terminals (65.7%) contacting unlabeled profiles. These unlabeled postsynaptic structures predominantly represented distal dendrites (67.2%), some were identified as proximal dendrites (25.3%), and a few represented somata (7,5%).

Discussion

Within the CN, at least two populations of projection neurons can be recognized. One population is formed by small GABAergic neurons that selectively project to the IO (De Zeeuw *et al.*, 1989b; Fredette and Mugnaini, 1991; Graybiel *et al.*, 1973; Ruigrok and Voogd, 1990; Teune *et al.*, 1995). The other group consists of medium- to large-sized excitatory neurons that collateralize to various other brain stem areas and to the

thalamus (Bentivoglio and Kuypers, 1982; Bernays *et al.*, 1988; Berretta *et al.*, 1993; Chen and Hillman, 1993; Faull, 1978). Furthermore, a small group of glycinergic/GABAergic neurons has been identified that may represent interneurons (Chen and Hillman, 1993; De Zeeuw and Berrebi, 1995a) and/or nucleocortical neurons (Batini *et al.*, 1992). The main objective of this study was to investigate whether or not single PCs that belong to a particular zone, as defined by their projection to a particular part of the CN (Voogd, 1995; Voogd and Bigaré, 1980), terminate on both types of projection neurons.

Methodological considerations

Because the input and output relations of the CN are known to be critically dependent upon the part of the CN involved (see, e.g. Angaut and Cicirata, 1988; Buisseret-Delmas and Angaut, 1993; Daniel *et al.*, 1988; Ruigrok and Voogd, 1990), it was essential that all injection sites were properly aligned in order to obtain an optimal amount of both types of retrograde and of anterograde labeling in the same CN locus. A number of practical reasons were decisive in our focussing on the AIN. First, the efferent connections of this part of the CN are well known and include a consistent and excitatory projection to the magnocellular part of the RN (Daniel *et al.*, 1988) and to the DAO as the recipient of the nucleoolivary projection neurons of the AIN (Ruigrok and Voogd, 1990). The AIN receives its cortical input from the paravermal C1 and C3 zones (Voogd, 1995), which are present in the PM (Buisseret-Delmas and Angaut, 1993; Umetani, 1989). Moreover, and essential for making optimally aligned injections, all of these areas are relatively easy to reach and to identify with electrophysiological methods. The RN is readily localized by recording the large and vigorous action potentials (Ruigrok *et al.*, 1995b; Ruigrok and Voogd, 1990) upon entering the nucleus. Similarly, recording, through the injection pipette, the slow and irregular spontaneous firing of olivary units responding to the tapping of contralateral body parts (Gellman *et al.*, 1983) assists in determining the location of the DAO. The C1 zone of the rat PM was identified by recording the powerful and robust climbing fiber evoked potentials after percutaneous stimulation of the ipsilateral forepaw (Atkins and Apps, 1996; Trott and Apps, 1993).

In ten experiments, these conditions were fulfilled, and the three tracers could be identified in the AIN either with LM alone (n = 4) or with LM and EM (n = 6). Neurons were never double labeled from the RN and the IO, as demonstrated previously (Legendre and Courville, 1987; Teune *et al.*, 1995). The BDA-labeled fibers, which were densely filled with DAB reaction product, were easy to identify and could be distinguished from structures containing the granular reaction product of the CTb and/or WGA-HRP tracers. Although BDA has been reported to be transported in a strict anterograde direction (Veenman *et al.*, 1992; Wouterlood and Jorritsma-Byham, 1993), care has to be taken to exclude the possibility of inadvertent labeling of mossy fiber

collaterals due to initially retrograde transport of tracer out of the injection site. Indeed, especially over short distances and by particular systems, retrograde transport of BDA may occur (Yatim *et al.*, 1995b). Even upon coinjection of excitotoxic substances, such as n-methyl-D-aspartate, exceptionally good retrograde labeling may occur in some systems (Jiang *et al.*, 1993). In our material, however, we have several reasons to believe that our analysis was not hampered by labeled mossy fiber collaterals. First, BDA-labeled neurons with solid label in their somata and dendrites were encountered only occasionally in the CN. These neurons apparently represent retrogradely labeled nucleocortical neurons (Angaut *et al.*, 1997; Batini *et al.*, 1992). However, careful examination failed to show evidence of local recurrent collaterals arising from these neurons. Nevertheless, in the selection of the pyramids, special care was taken to exclude these BDA-labeled neurons. Second, although we usually encountered a few, lightly BDA-labeled fibers in the distal regions of the middle and inferior cerebellar peduncles in our LM-processed material, no BDA-labeled neurons were observed in classic sources of mossy fibers, such as the basal pontine nuclei, the nucleus reticularis tegmenti pontis, the VN, the reticular formation, or the lateral reticular nucleus (Rubertone *et al.*, 1995b; Ruigrok and Cella, 1995; Voogd, 1995). Finally, the mossy fiber system is generally believed to be excitatory (McCrea *et al.*, 1978; Murphy and Sabah, 1971b). Hence, the terminals of mossy fiber collaterals, as opposed to PC terminals, would be expected to make asymmetric synapses (Peters *et al.*, 1991), which have indeed been reported in several instances (see, e.g. Mihailoff, 1994; van der Want *et al.*, 1987). However, from the ultrastructural analysis, it was obvious that none of the BDA-labeled terminals in the CN could be classified as making an asymmetric synapse. Therefore, we are confident that all investigated BDA-labeled fibers represent anterogradely labeled PC axons.

At the LM level, the distinction between gold lectin and cobalt-stabilized TMB reaction product of the WGA-HRP is less straight forward compared with the combination of CTb and gold lectin labeling (Ruigrok *et al.*, 1995b), especially in osmicated and plastic-embedded sections. However, ultrastructural examination leaves no doubt about the nature of the tracer present in any particular structure. A restriction in the use of BDA for EM purposes may be the low yield of labeled fibers in the deeper parts of the Vibratome sections and plastic-embedded pyramids, which is most likely related to the poor penetration of the ABC product in the absence of Triton X-100 or any other detergent. For this reason, we routinely examined the superficial layers (3-5 μm) only.

LM studies

Retrograde CN labeling corresponded to earlier reported patterns observed in the same and other species. Tracer injections into the magnocellular RN mainly labeled neurons in the AIN and the medial

PIN, whereas injections into the parvicellular RN and the prerubral area labeled neurons in the lateral cerebellar nucleus as well as in the AIN and the PIN (Angaut and Sotelo, 1987; Asanuma *et al.*, 1983a; Bentivoglio and Kuypers, 1982; Bharos *et al.*, 1981; Daniel *et al.*, 1987; Teune *et al.*, 1995). Few labeled neurons were found in the MCN. Small nucleoolivary neurons were found scattered throughout various parts of the CN subnuclei. Their distribution depended critically on the areas of the IO complex that were included in the injection site. The location of labeled cells was in accordance with the pattern described in the anterograde tracing study of the nucleoolivary projection in the rat by Ruigrok (Ruigrok and Voogd, 1990). In most areas of the CN, both types of retrogradely labeled neurons appeared to be randomly intermingled (Legendre and Courville, 1987; Teune *et al.*, 1995).

BDA-labeled PC axons ran from the cortical injection site in small bundles toward the CN, which they entered mainly from their dorsal aspect. In agreement with others (Courville *et al.*, 1973; Umetani, 1989), the BDA injections in the forepaw area of the PM resulted in PC terminal labeling mainly in the caudolateral AIN, but terminal arborizations in the more rostral areas of the PIN were also observed. In some cases, terminal labeling within the DLP of the MCN was present. This is in accordance with the description of a medial zone in the PM of the rat (the lateral extension of the A zone of Buisseret-Delmas (1993) to the DLP, (Atkins and Apps, 1996; Buisseret-Delmas, 1988b; Umetani, 1989). According to Umetani (1989), a C1 zone projection to the AIN is absent in the PM of the rat. Buisseret-Delmas (1988b) and Atkins (1996), however, have identified a C1 zone in the PM that is bordered laterally by the C2 zone, which projects to the PIN. Indeed, our case T138 (Figs. 7.2, 7.3) most likely reflects a BDA injection centered on the C1 zone, with some involvement of the neighboring lateral extension of the A zone and of the C2 zone, because PC terminal labeling was observed in the DLP and in the transition area of the AIN and the PIN. Other cases with injections based on electrophysiological data made at a laterality of 2.4-2.6 usually showed labeling only in the caudolateral AIN and, occasionally, in the PIN and the dorsolateral hump. From our data, it is not possible to speculate on the existence of a C3 zone in the PM (Buisseret-Delmas and Angaut, 1993).

Two observations are relevant in relation to the objective of this paper. The first is that, within a particular focus of BDA terminal labeling in the AIN, the BDA-labeled varicosities are apposed to nucleoolivary as well as nucleorubral neurons. This would imply that, in such a terminal focus, no apparent preference of PC terminals for either type of neuron is present. Furthermore, we noted in many instances that varicosities of a particular labeled PC axon, when followed through the AIN, contacted neurons that were labeled with the two different tracers, suggesting that individual PCs may contact both nucleoolivary and other projection neurons.

EM studies

In accordance with the LM data, it was established that small BDA injections confined to a single cortical zone resulted in labeled PC axons that synapsed with nucleorubral as well as with nucleoolivary neurons. Occasionally, individual terminals were observed to make synaptic contact with both types of neurons. These findings agree well with previous ultrastructural studies suggesting that individual PC axons contact both large and small neurons of the CN (Chan-Palay, 1977) or both GABAergic and non-GABAergic cells of the CN and the VN (De Zeeuw and Berrebi, 1995b).

In the latter study, De Zeeuw and Berrebi estimated that 79% of the L7+ PC terminals made synaptic contact with non-GABAergic postsynaptic profiles and that 21% made synaptic contact with GABAergic postsynaptic profiles. This distribution is remarkably similar to the percentages of BDA-labeled terminals synapsing with WGA-HRP-labeled (77%) and with gold lectin-labeled (23%) postsynaptic profiles, respectively, found in the present study. It should be realized that, in our material, nonlabeled postsynaptic structures constitute a third and separate group; whereas, in the analysis by De Zeeuw (1995a), only two types of postsynaptic profiles were identified (i.e., GABAergic and non-GABAergic). Thus, in both studies, the identity of the unlabeled profiles cannot be established unequivocally due to potential failure and weak or only partial labeling. Another reason that the data of L7+ contacts with GABAergic and non-GABAergic dendrites cannot be compared directly with BDA-labeled contacts upon gold lectin- vs. WGA-HRP-labeled dendrites pertains to differences in penetration and labeling characteristics of axonal tracers compared with the use of immunocytochemical markers. Nevertheless, it would appear that the classes of GABAergic and non-GABAergic profiles are very similar to our gold lectin- and WGA-HRP-labeled profiles, respectively. Especially with regard to the percentages of synaptic contacts with somata only, for which the possibility of false-negative labeling would seem less likely, the data of De Zeeuw and Berrebi are very similar to those of the present study. Approximately twice as many L7+ PC terminals were found on non-GABAergic somata (8%) compared with GABAergic somata (4%), which corresponds well with the 6.6% (23 in 346) of the BDA-labeled terminals that were found on WGA-HRP-labeled cell bodies and the 3.5% (12 in 346) that contacted gold lectin-labeled somata.

The observation that only about two times more PC terminals were encountered on either non-GABAergic or WGA-HRP-labeled profiles compared with GABAergic or gold lectin-labeled profiles is somewhat puzzling. The size distribution, based on the diameters of the somata of the GABAergic nucleoolivary neurons, peaks at 10 μm, and that of the other excitatory neurons peaks at about 20 μm (Batini *et al.*, 1992; Chan-Palay, 1977; De Zeeuw and Berrebi, 1995b; Teune *et al.*, 1995). Furthermore, Batini (1992) showed that only about 31% of the neurons in the CN contain

GABA and belong to the small-sized category. When the distribution of PC terminals on both types of projection neurons is equal, and when the number of cells and the differences in surface areas of their somata are taken into account, approximately nine times as many contacts should be found on the excitatory neurons compared with nucleoolivary cells[1]. Actually, the assumption that PC terminals demonstrate a homogenous distribution upon both types of projection neurons may not be true, because De Zeeuw (De Zeeuw and Berrebi, 1995b) noted that the GABAergic neurons were contacted only infrequently by GABAergic (PC-derived) terminals. This obvious discrepancy in the proportion of observed and estimated numbers of PC terminals on the somata of both populations of projection neurons may be explained by assuming that 1) the actual number of nucleoolivary neurons was underestimated by Batini (1992), see, e.g. (Chan-Palay, 1977; Teune *et al.*, 1995), and 2) the data may be biased by a potential inhomogeneous distribution of both types of projection neurons in the AIN. Nevertheless, based on our data, we conclude that not only the nucleorubral but also the nucleoolivary cells receive a prominent PC input from a focussed cerebellar cortical area.

[1]Based on a total of 100 CN neurons and a globular surface estimate of $\pi \times d^2$ *yields a total cell body surface area of* $3.14 \times 10^2 \times 31 = 9{,}734\ \mu m^2$ *for the batch of nucleoolivary cells and of* $3.14 \times 20^2 \times 69 = 86{,}664\ \mu m^2$ *for the nucleorubral neurons.*

Single PCs innervating two classes of projection neurons

With respect to the question of whether the cortical inputs to the nucleoolivary and nucleorubral neurons are similar or dissimilar, the distribution of terminals from a single PC axon upon both cell types requires consideration. The following options may be contemplated: option A, all individual PCs terminate either on nucleoolivary or on nucleorubral neurons; option B, all individual PCs terminate on both cell types; and option C, some PCs may terminate on both cell types, whereas others are specific for a particular cell class.

De Zeeuw (1995a) that 3% and up to 9% of the L7+terminals contacted both GABAergic and non-GABAergic postsynaptic profiles in nonserial and serial analyses, respectively. Accordingly, the present study demonstrated that about 1% (4 in 367) of the BDA-labeled terminals contacted both a gold lectin- and a WGA-HRP-labeled postsynaptic structure. This percentage could be more than doubled (nine terminals) when serial sections were incorporated in the analysis. These observations would exclude option A (see above). Considering the fact that at least 2% of the individual PC terminals may contact both an identified nucleoolivary and a nucleorubral profile and that a typical PC terminal arborization contains at least dozens of varicosities (Chan-Palay, 1977; De Zeeuw and Ruigrok, 1994), which may all represent terminals, it is obvious that individual PCs have a fair chance of influencing both types of projection cells and

would appear to favor option B. The same conclusion was drawn by De Zeeuw (De Zeeuw and Berrebi, 1995a), based on the assumption that most GABAergic cells indeed represent nucleoolivary cells and that all non-GABAergic profiles represent the other, excitatory class of projection neurons. However, to date, a definite distinction between options B and C is not possible with the available evidence and will have to await further research.

Functional considerations

Recent studies indicate that PCs that belong to an anatomically defined olivocorticonuclear/vestibular module constitute a functional unit (Ekerot *et al.*, 1995; Sato *et al.*, 1991; van der Steen *et al.*, 1994), e.g., stimulation of zonal white matter of the rabbit flocculus or posterior vermis results in clearly circumscribed, slow or saccadic eye movements, respectively (Godschalk *et al.*, 1994; van der Steen *et al.*, 1994). The present study indicates that PCs that belong to the C1 zone contact effector cells that project to the RN as well as to neurons that project to the IO. Indeed, individual PC axons may contact both cell types, even with single boutons. This would imply that both cell types are affected by the same PC activity patterns. Although they were not specifically investigated in this study, it seems likely that parts of the CN that project to other premotor areas (such as the superior colliculus; (Westby *et al.*, 1993), to preolivary areas (such as the prerubral area and nucleus of Darkschewitsch; (De Zeeuw and Ruigrok, 1994; Ruigrok and Voogd, 1995a), or to other precerebellar nuclei (such as the basal pontine and reticular pontine nuclei; for review, see (Ruigrok and Cella, 1995) and their locally intermingled nucleoolivary neurons also receive a similar common PC input. At a first glance, this seems to imply that the phase modulation of both populations of projection neurons could be similar. Unfortunately, to our knowledge, no attempts have been made to record and distinguish the activity patterns of identified nucleoolivary and nucleorubral neurons. Most likely, this is due to the difficulty in isolating the activity of the small nucleoolivary units between the more robust firing of the larger nucleorubral cells. It has been shown by a number of groups that the activity in several regions of the CN, including the AIN, is enhanced during the execution of movement (see e.g. Armstrong and Edgley, 1984; Armstrong and Edgley, 1988; Gibson *et al.*, 1996; Milak *et al.*, 1995; van Kan *et al.*, 1993). This activity most likely reflects the activity of the larger neurons, which, by way of their projections to the RN, superior colliculus, and thalamus, may affect motor programs (Bloedel and Bracha, 1995; Gibson *et al.*, 1996). In this context, it is interesting that, during movement, the excitability of olivary cells in the rostral part of the DAO appears to be diminished (Horn *et al.*, 1996; Lidierth and Apps, 1990). The possibility that the GABAergic (De Zeeuw *et al.*, 1989b; Fredette and Mugnaini, 1991) nucleoolivary projection and the excitatory nuclear projection neurons may be modulated in the same way by the same PCs could explain how a release of cortical

inhibition results both in activity of premotor centers (i.e., the RN) and, simultaneously, in inhibition of IO areas, as suggested by Horn (1996).

Of course, to date, these considerations remain speculative, because it is not known whether the different populations of cerebellar nuclear neurons actually respond similarly to an identical PC input. Moreover, the anatomical and physiological interactions with other, excitatory, afferent inputs, such as mossy and climbing fiber collaterals (see, e.g. Borsello *et al.*, 1994; Kitai *et al.*, 1977; McCrea *et al.*, 1978), or with other inhibitory sources, such as the population of glycinergic/GABAergic interneurons (Chen and Hillman, 1993; De Zeeuw and Berrebi, 1995a), are largely unknown. More detailed knowledge of these properties will prove to be invaluable for a proper understanding of the information flow to and from the cerebellum, as was also concluded from a recent electrophysiological study in the cat in which stimulation of the brachium conjunctivum had different effects on the excitability of olivary neurons, depending on the integrity of the nucleoolivary pathway (Ruigrok and Voogd, 1995a) .

Table 7.1 Biotinylated Dextran Amine-labeled presynaptic profiles[1]

	One postsynaptic profile (n=346)			Two postsynaptic profiles (n=21)						
	Gold	HRP	NL	Gold/gold	HRP/HRP	NL/NL	Gold/NL	HRP/NL	Gold/HRP	Total
Soma	12	23	18	0	2	0	0	0	1	56
Proximal dendrite	8	34	61	0	1	3	0	2	1	110
Distal dendrite	4	24	162	0	0	2	2	5	2	201
Total	24	81	241	0	3	5	2	7	4	367

[1]Distribution of postsynaptic profiles of randomly collected biotinylated dextran amine (BDA)-labeled Purkinje cell (PC) terminals. In four cases, 367 BDA-labeled PC terminals synapsing with postsynaptic structures were collected in single section analysis. Twenty-one PC terminals were found to contact two postsynaptic structures, which, in four cases (19.1%) could be identified as two differently labeled structures. In the case of synapses with two postsynaptic profiles, the contacts were categorized as somatic or dendritic, according to the first indexed label in the rows. Gold: gold-lectin; HRP: wheat germ agglutinin conjugated horse radish peroxidase (WGA-HRP); NL: not labeled.

Legends to figures

Fig 7.1. **A** Diagram of a posterior view of the cerebellum of the rat. The dots in the right paramedian lobule indicate the locations of the electrode tips from which field potentials were recorded while electrically stimulating the ipsilateral forepaw. **B**: Surface evoked potentials recorded from the selected locations on the paramedian lobule. Along the y-axis, the distance from the midline toward the lateral aspect of the hemisphere is indicated, and an averaged recording (ten sweeps) is shown. Note that, at 2.5, at 2.7, and at 2.9 mm from the midline, the field potential demonstrates a definite peak within 20 msec after the stimulus. **C**: Diagram of the peak values of the evoked potentials as measured in four rats. Each case is represented by a different dotted or solid line. All rats demonstrated a similar pattern, with an increase of the field potential at approximately 2.5-2.6 mm lateral from the midline

Fig. 7.2. **A-E**: Color photomicrographs of case T138 showing the cholera toxin B subunit (CTb) injection site into the red nucleus (**A**), the gold lectin deposit in the ipsilateral inferior olive (**B**), and the biotinylated dextran amine (BDA) injection into the contralateral paramedian lobule (PM; **C**). **D** and **E** show the resulting labeling in the cerebellar nuclei ipsilateral to the BDA injection site. In **D**, note the close approximation of the BDA-labeled varicosities with a CTb-labeled, nucleorubral cell (**D**, arrow) and, at a slightly deeper level (E), with a gold lectin-labeled, nucleoolivary cell (E, arrow). Scale bars = 500 μm in A-C, 25 μm in D, E. See p. 288.

Fig. 7.3. A Lucivid-assisted (MicroBrightField, Inc., Colchester, VT) reconstruction of equidistant, transverse sections through the cerebellar nuclei (CN) in case T138 showing the distribution of CTb-labeled neurons (open circles), gold lectin-labeled cells (solid squares) and biotinylated dextran amine (BDA)-labeled Purkinje cell (PC) terminals (crosses) resulting from the injection sites demonstrated in Figure 7.2. In **A**, the lower left drawing is the caudalmost level, and the upper right drawing is the rostralmost level. The midline is toward the left AIN. anterior interposed nucleus; DLH, dorsolateral hump; DLP, dorsolateral protuberance; LCN, lateral cerebellar nucleus; LVN, lateral vestibular nucleus; MCN, medial cerebellar nucleus; PIN, posterior interposed nucleus. **B**: Camera lucida drawing of a selected part of the transition area between the AIN and the PIN, as indicated in A. The small stippled cells represent the nucleoolivary cells, the hatched profiles correspond with the nucleorubral neurons, and the solid profiles represent the BDA-labeled PC axons with terminal tufts and beads. Arrows indicate the close apposition of BDA-filled PC varicosities with neurons with either tracer and illustrate the possibility of one PC axon to terminate on more than one type of neuron. Scale bar = 25 μm.

Fig. 7.4. Electron photomicrograph of a section through the AIN. The three different labels can be distinguished: the dense, irregularly shaped gold lectin

particles in the cytoplasm of a small neuronal profile (delineated by asterisks); the irregular densities of the wheat germ agglutinin coupled to horseradish peroxidase (WGA-HRP) reaction product (thick arrows) in three cells (delineated by hatched lines); and the solid, wall-to-wall biotinylated dextran amine (BDA) deposits (thin arrows) in axonal profiles. Scale bar = 1 μm.

Fig. 7.5. Electron photomicrographs of sections through the anterior interposed nucleus (AIN). **A**: A biotinylated dextran amine (BDA)- labeled axon terminal is shown in close proximity with a dendritic structure labeled with wheat germ agglutinin coupled to horseradish peroxidase (WGA-HRP) (thick arrow) and synapsing with unlabeled. structures (thin arrows). **B**: An axon terminal labeled with BDA is shown to synapse (thin arrow) with a postsynaptic profile containing gold lectin (arrowhead) and is in close apposition with a profile containing WGA-HRP label (thick arrow). **C**: A BDA-containing axon terminal (thin arrow) is shown to synapse with a neuron labeled with WGA-HRP (thick arrow), **D**: A synaptic contact of a BDA-labeled terminal (arrow) with a gold lectin-containing (arrowhead) structure. Scale bars = 1 μm.

Fig. 7.6. **A**: Overview of a biotinylated dextran amine (BDA)-labeled bouton synapsing with both a dendrite containing wheat germ agglutinin coupled to horseradish peroxidase (WGA-HRP) label (arrows) and a neuronal some containing gold lectin particles (arrowheads). **B-D**: Higher magnifications of the same labeled structures in adjacent serial sections. Note both symmetrical synapses (arrows) in C and D.
Scale bars = 1,000 nm in A, 500 nm in B, 300 nm in D, E.

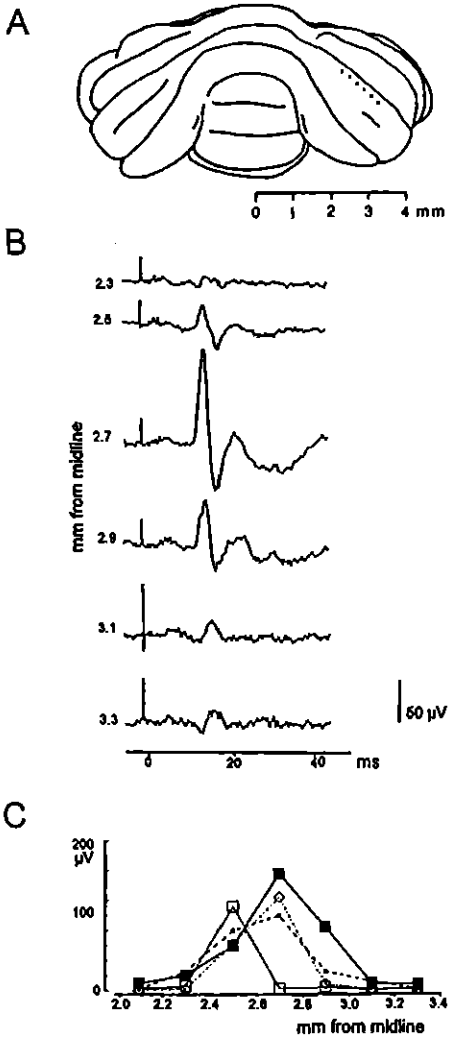
A
0 1 2 3 4 mm
B
2.3
2.5
2.7
2.9
3.1
3.3
mm from midline
60 µV
0 20 40 ms
C
200 µV
100
0
2.0 2.2 2.4 2.6 2.8 3.0 3.2 3.4
mm from midline

Fig. 7.1

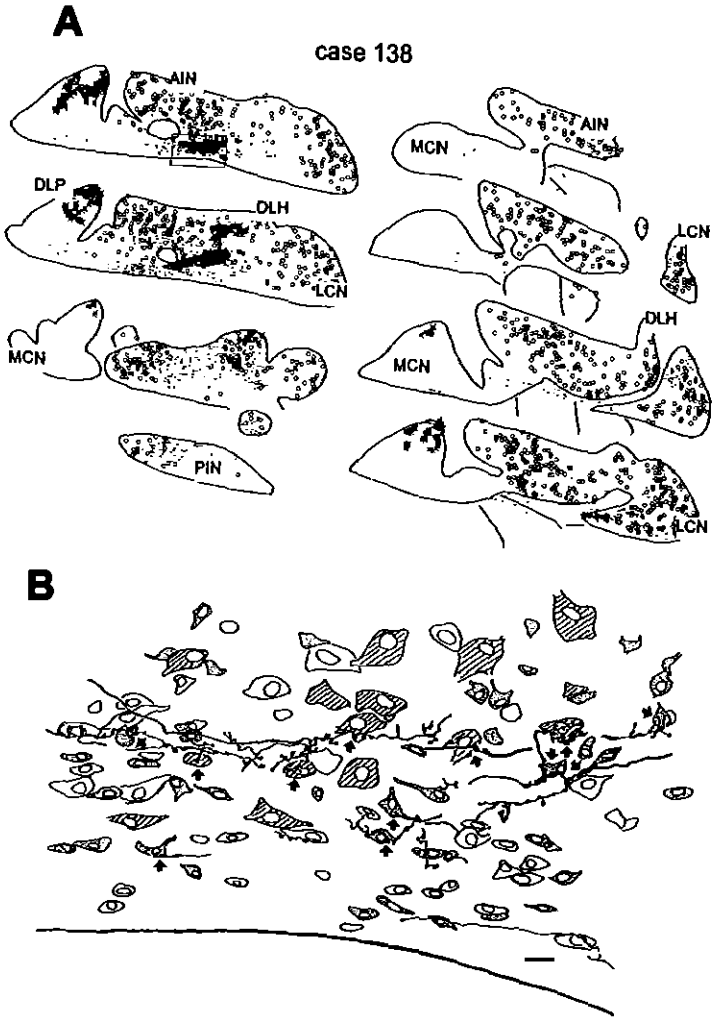

Fig. 7.3

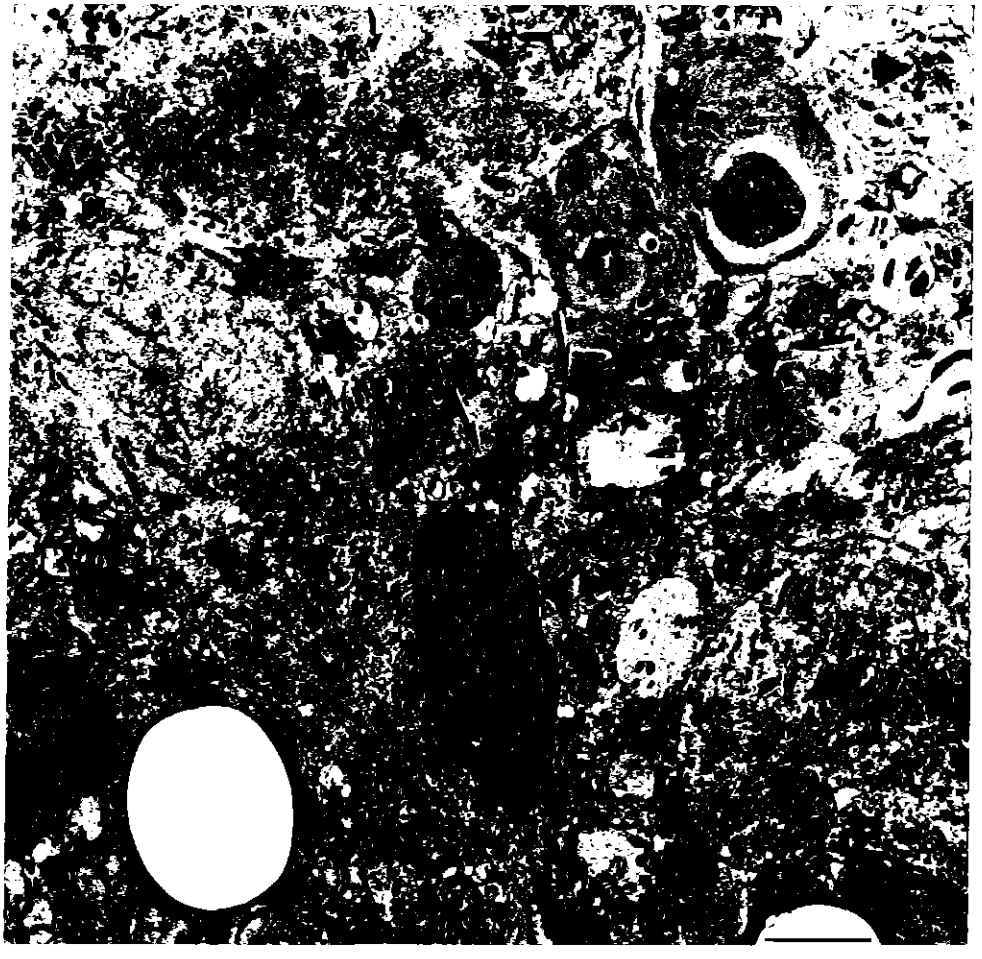

Fig. 7.4

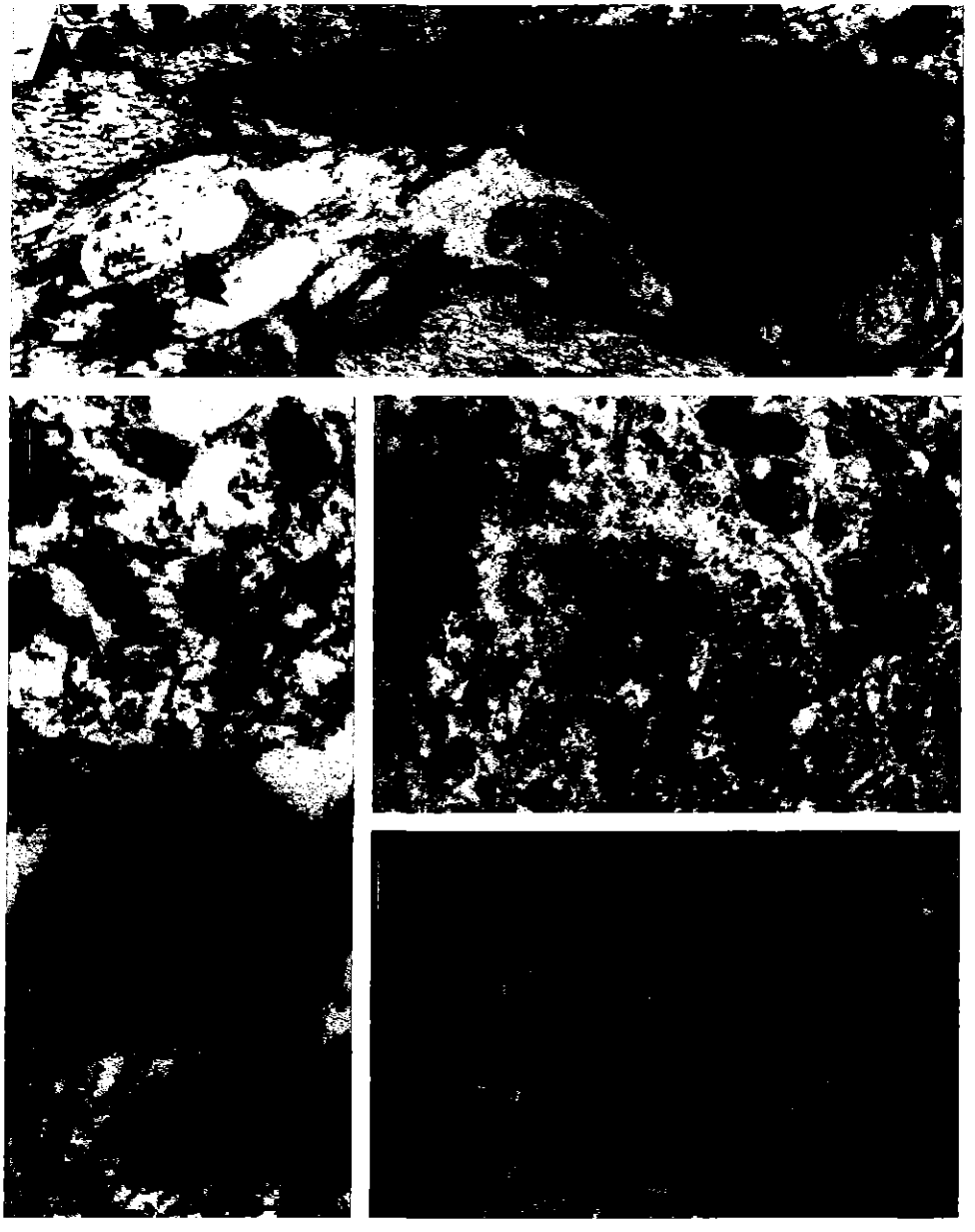

Fig. 7.5

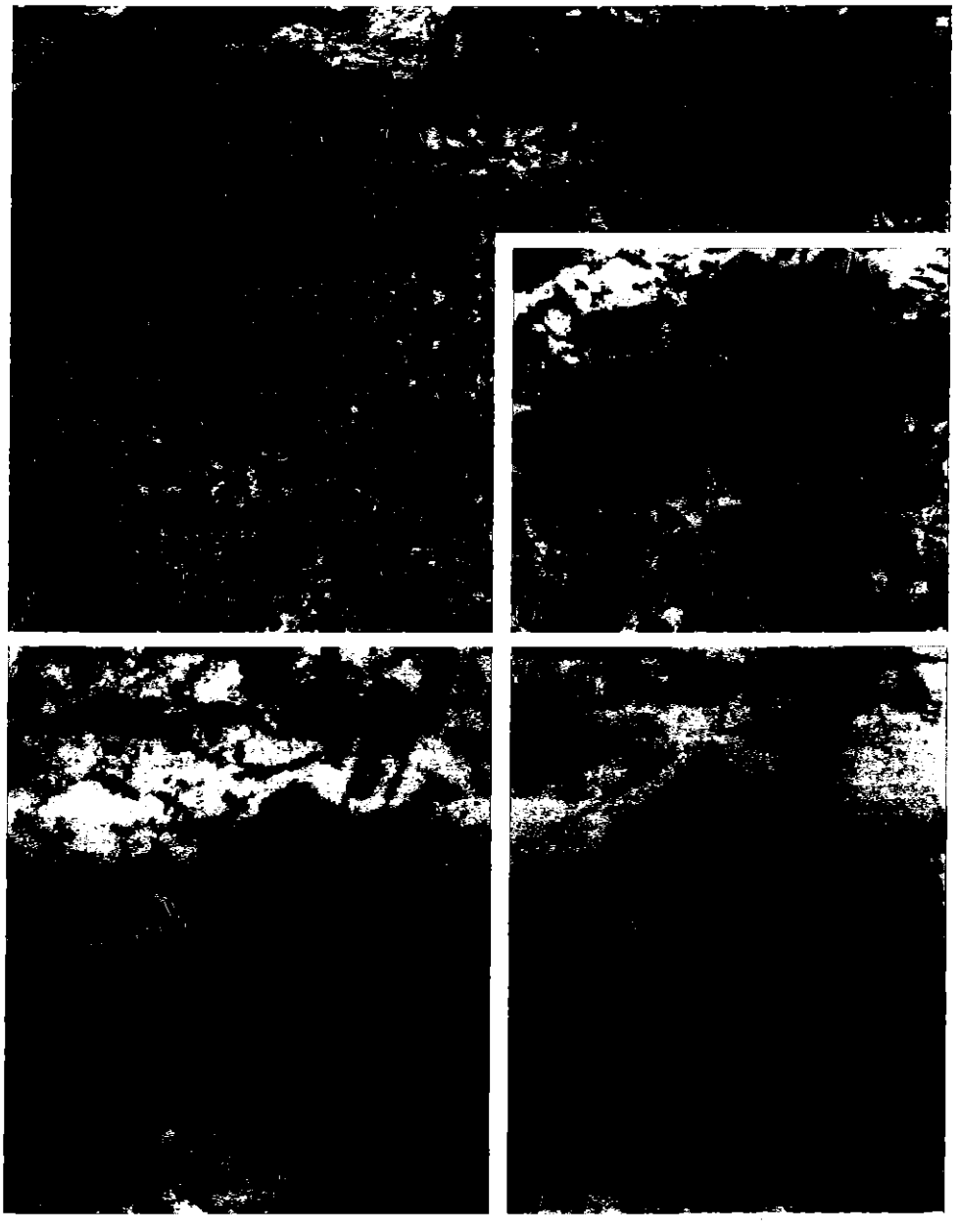

Fig. 7.6

CHAPTER 8:
SUMMARY AND GENERAL DISCUSSION

Summary and general discussion

Cerebellar modules

The cerebellum receives its input from the spinal cord and from the brain stem via the mossy fiber system and from the inferior olive through the climbing fibers. This double input is used to coordinate movements. However, as has become evident more recently, over and above coordinating motor behaviour, the cerebellum has been shown to be involved in the initiation, adaptation and potentially even in the learning not only of movements but also of visceral processes, affective behaviour and cognitive tasks.

This diversity of cerebellar function is in striking contrast with the relative uniform structure of the cerebellar cortex. Apparently the information supplied by climbing and mossy fibers to different parts of the cerebellar cortex is subjected to the same operation, in spite of the different functions to which it is applied. At the meta-level of the topographical organization of the input and the output of the cerebellar cortex the cerebellum is less uniform. Mossy fibers of different origin are organized in complicated patterns of patches and stripes, which may alternate or overlap in different regions of the cortex. Purkinje cells with an output to a particular cerebellar or vestibular target nucleus are arranged in discrete zones, and the distribution of their climbing fiber afferents follows a similar pattern. Collateral projections from the climbing fibers, as well as projections from the cerebellar nuclei to the inferior olive appear to match the basic olivocorticonuclear organization. In this modular organization the cerebellar (and vestibular) nuclei constitute the output of the modules.

Topic of this thesis

Although it is well known that cerebellar efferents can influence a great variety of brain stem areas it is less clear to what extent the organization of the cerebellar modules may be reflected in their projection patterns to the brain stem. The basic subject of this thesis, therefore, was to investigate how the modular organization of the olivocorticonuclear connections relates to the organization of projections from the cerebellar nuclei to the brain stem of the rat.

Cerebellar modules and the brain stem

In Chapter 2, using anterograde tracer techniques, it is shown that the cerebellar efferents which originate from only a part of a cerebellar nucleus, thus composing the output of only part of a module, are directed to a wide variety of brain stem areas which are located from the spinal cord to the rostral-most parts of the thalamus. Based on the number of plotted varicosities, which constitute presumed terminals, i.e. sites of information transfer, it was concluded that the different cerebellar target nuclei differ greatly in their overall distribution over the rostrocaudal extent of the brain stem. The medial cerebellar nucleus mainly distributes to

the lower brain stem, with a shift to more rostral levels for its dorsolateral protuberance and the caudal part of the nucleus. The distribution of the terminals that originate from interstitial cell groups is wide and ranges from the spinal cord (not considered in this thesis) to the thalamus. The posterior interposed nucleus mainly projects to the mes- and diencephalon, and only targets the inferior olive in the lower brain stem. The distribution of the anterior interposed nucleus is similar to that of the former nucleus, with a slightly higher projection to the caudal brain stem. The dorsolateral hump distributes strongly to the ipsilateral lower brain stem and more moderately to the mes- and diencephalon. The entire brain stem receives projections from the lateral cerebellar nucleus. These distributions show that the relative impact of the cerebellar projections to the red nucleus and ventrolateral thalamus may be overrated in the literature, whereas other projections to e.g. the reticular formation, the zona incerta and the parafascicular thalamic nucleus deserve more attention. Differences as well as similarities were noted in the projection patterns that originate from various parts of the same cerebellar nucleus as well as between parts of different cerebellar nuclei.

These observations suggest that the organization of the output of modules follows an intricate pattern of diverging and converging projections. Although specific clear-cut differences were noted between the output patterns of different modules, in some cases the output of certain cerebellar nuclei may be quite specific (i.e. the projection of all cerebellar nuclei to particular subnuclei of the inferior olive, of the rostral MCN to the vestibular nuclei, the AIN to the magnocellular red nucleus and the DLH to the ipsilateral parvicellular reticular formation), the same brain stem areas are innervated by multiple nuclei, e.g. the reticular formation, the nucleus reticularis tegmenti pontis, the red nucleus, the superior colliculus, the pretectum, the area prerubralis parafascicularis and several of the thalamic nuclei. It was concluded that the output of the modules can be characterized by the *combination* of target nuclei innervated by each cerebellar nucleus (by its "profile"), i.e. the rostral MCN combines an innervation of the vestibular nuclei with the reticular formation, the projection of the DLH only terminates in the reticular formation, AIN and PIN both innervate the magnocellular red nucleus, but the AIN combines this connection with a projection to the nucleus reticularis tegmenti pontis, whereas such a reticular projection is absent in the case of the PIN. Convergent and divergent patterns in the projections of the cerebellar nuclei were further investigated using modern multiple tracer techniques for studying neural connections.

Selection of characteristic brain stem nuclei

Because, using these tracer techniques, it is not feasible to investigate the complete brain stem, four areas were selected which are representative for the different functional centers that receive the cerebellar output. These areas include

1) the inferior olive, which, as the source of the climbing fibers and the recipient of cerebellar nuclear afferents has been implicated in the cerebellar modular organization, 2) the nucleus reticularis tegmenti pontis which is known to supply a major mossy fiber projection to the cerebellar cortex, with a collateral projection to the cerebellar nuclei, 3) the red nucleus which has amply been established to function as a premotor center, and, finally, 4) the prerubral area which is known as a major source of afferents to the inferior olive and, as such, has been implicated in an indirect cerebello-olivary loop. Both a double retrograde tracing study and a double anterograde tracing study were conducted to study the organization of the cerebellar nuclear connections to these four areas.

A new double retrograde tracing technique

In order to be able to conduct the first part, a method employing a new combination of retrogradely transported tracers was developed which is described in Chapter 3. Most important advantage of this technique over previously used methods that made use of fluorescent tracers is found in the fact that with the new technique a robust and permanent labeling is acquired in counterstained sections which makes analysis much more straightforward.

Organization of cerebellar projections to four brain stem nuclei. 1. retrograde double tracing

The retrograde double labeling experiments (Chapters 4 and 5), confirmed that the inferior olive received its input from a separate group of neurons, that could be found scattered throughout all four main divisions of the cerebellar nuclei. These nucleoolivary neurons did not collateralize to any of the other three investigated cerebellar nuclear targets. The red nucleus, nucleus reticularis tegmenti pontis and prerubral area received input from specific combinations from medium- to large-sized neurons that were distributed over diverse and multiple parts of the cerebellar nuclei. Moreover, many of these neurons collateralize extensively to combinations of these three, functionally different, target areas. This would imply that certain effects always are combined in the output of a particular group of nuclear cells, i.e. neurons that project to both the red nucleus and the nucleus reticularis tegmenti pontis may, upon activation, participate in both the triggering of a motor behaviour and the recurrent activation of the cerebellum by means of mossy fibers and their nuclear collaterals. Likewise, collateral innervation of the red nucleus and the prerubral area, may result in (near-) simultaneous activation of motor systems and the inferior olive. Although not specifically investigated in the present study, the occurrence of double labeled cells in virtually all regions of the cerebellar nuclei containing single labeled neurons after injection of a single target nucleus in the brain stem or the cord, in our

double labeling study, or in all previously published double labeling studies of the cerebellar nuclei, suggests that the output of the non-GABAergic relay cells of the cerebellar nuclei consists of branching axons which collateralize to most, if not all, of their targets in the brain stem, the cord and the thalamus. This conclusion is supported by the single-axon studies of the cerebellar nuclei published thus far. As a consequence the output of the cerebellar nuclei would consist of two systems: the one the highly focussed, GABAergic, nucleoolivary system, the other a non-GABAergic, branching system, innervating a combination of targets specific for each cerebellar nucleus.

Organization of cerebellar projections to four brain stem nuclei. 2. anterograde double tracing

Apart from the collateralization of cerebellobulbar projections, another one prominent feature of the connections of the cerebellar nuclei is that neurons located in different parts of the same nucleus, or different cerebellar nuclei, converge upon several of the investigated areas. Thus, parts of both the interposed nuclei and the lateral cerebellar nucleus were found to project to the red nucleus; projections to the nucleus reticularis tegmenti pontis originated from the medial cerebellar nucleus, anterior interposed and lateral cerebellar nucleus etc. Using retrograde tracers, it is not possible to study whether or not the terminal fields from these different parts of the cerebellar nuclei actually overlap. This question was specifically studied in a subsequently executed set of experiments employing a double anterograde tracing in order to visualize the projections from the individual cerebellar nuclei or from different parts of the same nucleus onto the four selected targets (Chapter 6). It was noted that the terminal fields originating from different parts of the cerebellar nuclei, or even from different parts of the same nucleus did rarely overlap within the four selected brain stem areas. In the central part of the nucleus reticularis tegmenti pontis, and, more prominently in the magnocellular red nucleus, a somatotopical projection was identified from the anterior interposed nucleus, which also includes the dorsolateral hump. The terminations of these nuclei extend into the parvicellular red nucleus, where they remain segregated from the projections of the lateral cerebellar nucleus. Some overlap of the terminal fields of the lateral cerebellar nucleus in the parvicellular red nucleus appears to be present. Potential regions for convergence of different cerebellar nuclei onto the same relay cells also include the deep mesencephalic nucleus and the pretectum. Within the medial prerubral parafascicular area, which contains the preolivary neurons, the terminal fields from different parts of the posterior interposed nucleus and the lateral and medial cerebellar nuclei appear to remain separated.

Parallel processing of information from the cerebellar nuclei in the brain stem and the thalamus, therefore, appears to be the rule. This raises the question of where the integration of the actions of single muscles for simple movements into a smooth and timely behaviour, which is an essential

feature of cerebellar functioning, actually occurs. This role of the cerebellar cortex and of the recurrent circuits established by the reticular nuclei of the brain stem in this type of integration is briefly discussed.

Purkinje cell input to two populations of cerebellar nuclear neurons

It was concluded from the retrograde double labeling studies reported in chapters 4 and 5 that the output of the cerebellar nuclei consists of two systems: the one the highly focussed, GABAergic, nucleoolivary system, the other a non-GABAergic, branching system, innervating a combination of targets specific for each cerebellar nucleus. In this chapter the question is studied whether these two types of relay cells of the cerebellar nuclei receive the same information from the Purkinje cells of the cerebellar cortex. In a light microscopical and ultrastructural study employing three different tracers, it was shown that a single Purkinje cell may contact neurons that project to the red nucleus as well as to adjacent cells that evidently project to the inferior olive. Although, this does not necessarily means that the nucleo-olivary cells respond in a similar way as the other projection neurons to the incoming information from the cerebellar cortex, it is attractive to speculate that the activities of both cell populations are modulated in phase with each other. Since the nucleo-olivary projection is GABAergic and therefore most likely inhibitory, this would explain why the execution of movements (e.g. by cerebellar activation of premotor nuclei such as the red nucleus) is often accompanied by inhibition of olivary responses. Also, the, as yet not understood, but potentially interesting interactions with simultaneously activated excitatory cerebello-midbrain-olivary circuits and excitatory and potentially reverberating cerebello-precerebellar circuits may appear to be essential constituents for proper cerebellar functioning.

Conclusion

In conclusion, a single cerebellar module can influence many different centers involved in motor control by the cord, the brain stem and the cerebral cortex, and in recurrent activation of the cerebellum by recurrent mossy and climbing fiber paths, simultaneously by branching axons. Different modules use the same target nuclei in the brain stem, the cord and the thalamus, but this information does not appear to be integrated at that level. These findings are in support of the recent notion that the cerebellar zones may represent functional entities, and need to be considered in further studies on the functioning of the rat cerebellum. Cerebellar integration probably occurs within and between the modules and requires processing of the incoming information by the cortex, convergence of Purkinje cells onto the two types of neurons in the cerebellar nuclei and feedback of information from the brain stem through recurrent mossy and climbing fiber paths.

Literature cited

Aas J-E, Brodal P. (1990) GABA and glycine as putative transmitters in subcortical pathways to the pontine nuclei. A combined immunochemical and retrograde tracing study in the cat with some observations in the rat. Neurosci. 34: 149-162.

Achenbach KE, Goodman DC. (1968) Cerebellar projections to pons, medullar and spinal cord in the albino rat. Brain Behav. Evol. 1: 43-57.

Akaike T. (1992) The tectorecipient zone in the inferior olivary nucleus in the rat. J. Comp. Neurol. 320: 398-414.

Allen GI, Tsukahara N. (1974) Cerebrocerebellar communication system. Physiol. Rev. 54: 957-1006.

Allen GV, Hopkins DA. (1990) Topography and synaptology of mamillary body projections to the mesencephalon and pons in the rat. J. Comp. Neurol. 301: 214-231.

Altman J, Bayer SA. (1987a) Development of the precerebellar nuclei in the rat: II. The intramural olivary migratory stream and the neurogenetic organization of the inferior olive. J. Comp. Neurol. 257: 490-512.

Altman J, Bayer SA. (1987b) Development of the precerebellar nuclei in the rat: IV. The anterior precerebellar extramural migratory stream and the nucleus reticularis tegmenti pontis and the basal pontine gray. J. Comp. Neurol. 257: 529-552.

Anderson RF. (1943) Cerebellar distribution of the dorsal and ventral spino-cerebellar tracts in the white rat. J.Comp.Neurol. 79: 415-423.

Andersson G, Garwicz M, Hesslow G. (1988) Evidence for a GABA-mediated cerebellar inhibition of the inferior olive in the cat. Exp. Brain Res. 72: 450-456.

Andersson G, Hesslow G. (1987a) Activity of Purkinje cells and interpositus neurones during and after periods of high frequency climbing fibre activation in the cat. Exp. Brain Res. 67: 533-542.

Andersson G, Hesslow G. (1987b) Inferior olive excitability after high frequence climbing fibre activation in the cat. Exp. Brain Res. 67: 523-532.

André D, Vuillon-Cacciuttolo G, Bosler O. (1987) GABA nerve endings in the rat red nucleus combined detection with serotonin terminals using dual immunocytochemistry. Neurosci. 23: 1095-1102.

André P, D'Ascanio P, Gennari A, Pirodda A, Pompeiano O. (1991) Microinjections of α1- and α2-noradrenergic substances in the cerebellar vermis of decerebrate cats affect the gain of the vestibulospinal reflexes. Arch. Ital. Biol. 129: 113-160.

Angaut P. (1969) The fastigio-tectal projections. An anatomical experimental study. Brain Res. 13: 186-189.

Angaut P. (1970) The ascending projections of the nucleus interpositus posterior of the cat cerebellum: an experimental anatomical study using silver impregnation methods. Brain Res. 24: 377-394.

Angaut P, Batini C, Billard JM, Daniel H. (1986) The cerebellorubral projection in the rat: retrograde anatomical study. Neurosci. Lett. 68: 63-68.

Angaut P, Bowsher D. (1970) Ascending projections of the medial cerebellar (fastigial) nucleus: an experimental study in the cat. Brain Res. 24: 49-68.

Angaut P, Cicirata F. (1982) Cerebello-olivary projections in the rat. An autoradiographic study. Brain Behav. Evol. 21: 24-33.

Angaut P, Cicirata F. (1988) The dentatorubral projection in the rat: an autoradiographic study. Behav. Brain Res. 28: 71-73.

Angaut P, Cicirata F, Pantò M-R. (1985a) An autoradiographic study of the cerebellopontine projections from the interposed and lateral cerebellar nuclei in the rat. J. Hirnforsch. 26: 463-470.

Angaut P, Cicirata F, Serapide F. (1985b) Topographic organization of the cerebellothalamic projections in the rat. An autoradiographic study. Neurosci. 15: 389-401.

Angaut P, Cicirata F, Serapide MF. (1987) The dentatorubral projection. An autoradiographic study in rats. Brain Behav. Evol. 30: 272-281.

Angaut P, Compoint C, Buisseret-Delmas C, Batini C. (1997) Synaptic connections of Purkinje cell axons with nucleo-cortical neurones in the cerebellar medial nucleus of the rat. Neurosci. Res. 26: 345-348.
Angaut P, Sotelo C. (1987) The dentato-olivary projection in the rat as a presumptive GABAergic link in the olivo-cerebello-olivary loop. An ultrastructural study. Neurosci. Lett. 83: 227-231.
Angaut P, Sotelo C. (1989) Synaptology of the cerebello-olivary pathway. Double labelling with anterograde axonal tracing and GABA immunocytochemistry in the rat. Brain Res. 479: 361-365.
Apps R, Trott JR, Dietrichs E. (1991) A study of branching in the projection from the inferior olive to the x and lateral c1 zones of the cat cerebellum using a combined electrophysiological and retrograde fluorescent double labeling technique. Exp.Brain Res. 87: 141-152.
Armstrong DM, Edgley SA. (1984) Discharges of nucleus interpositus neurones during locomotion in the cat. J. Physiol. 351: 411-432.
Armstrong DM, Edgley SA. (1988) Discharges of interpositus and Purkinje cells of the cat cerebellum during locomotion under different conditions. Journal of Physiology 400: 425-445.
Armstrong DM, Harvey RJ, Schild RF. (1971) Distribution in the anterior lobe of the cerebellum of branches from climbing fibers to the paramedian lobule. Brain Res. 25: 203-206.
Armstrong DM, Harvey RJ, Schild RF. (1973) Branching of the inferior olivary axons to terminate in different folia, lobules or lobes of the cerebellum. Brain Res. 54: 365-371.
Arshavsky YI, Gelfand IM, Orlovsky GN, Pavlova GA. (1978) Messages conveyed by spinocerebellar pathways during scratching in the cat. I. Activity of neurons of the lateral reticular nucleus. Brain Res. 151: 479-491.
Asanuma C, Thach WT, Jones EG. (1983a) Brainstem and spinal projections of the deep cerebellar nuclei in the monkey, with observations on the brainstem projections of the dorsal column nuclei. Brain Res. Rev. 5: 299-322.
Asanuma H, Thach CW, Jones EG. (1983b) Distribution of cerebellar terminations and their relation to other afferent terminations in the ventral lateral thalamic region of the monkey. Brain Res. Rev. 5: 237-265.
Atkins MJ, Apps R. (1996) Somatotopical organisation within the inferior olive projection to the posterior lobe of the rat cerebellum. Soc.Neurosci.Abstr. 22: 1630.
Audinat E, Gähwiler BH, Knöpfel T. (1992) Excitatory synaptic potentials in neurons of the deep nuclei in olivo-cerebellar slice cultures. Neurosci. 49: 903-911.
Aumann TD, Horne MK. (1996) Ramification and termination of single axons in the cerebellothalamic pathway of the rat. J Comp Neurol. 376: 420-430.
Aumann TD, Rawson JA, Finkelstein DI, Horne MK. (1994) Projections from the lateral and interposed cerebellar nuclei to the thalamus of the rat: a light and electron microscopic study using single and double anterograde labelling. J.Comp.Neurol. 349: 165-181.
Aumann TD, Rawson JA, Pichitpornchai C, Horne MK. (1996) Projections from the cerebellar interposed and dorsal column nuclei to the thalamus in the rat: a double anterograde labelling study. J Comp Neurol. 368: 608-619.
Azizi SA. (1989) Principles of organization within the olivary system in the rat. Exp.Brain Res. 46-51.
Azizi SA, Mihailoff GA, Burne RA, Woodward DJ. (1981) The pontocerebellar system in the rat: An HRP study. I. Posterior vermis. J. Comp. Neurol. 197: 543-558.
Azizi SA, Woodward DJ. (1987) Inferior olivary nuclear complex of the rat: morphology and comments on the principles of organization within the olivocerebellar system. J. Comp. Neurol. 263: 467-484.
Babinski JFF. (1902) Sur le rôle du cervolet dans les actes volitionnels nécessitant une succession rapide de mouvements (diadococinésie). Revue Neurologique 10: 1013-1015.
Balaban CD. (1983) A projection from nucleus reticularis tegmenti pontis of Bechterew to the medial vestibular nucleus in rabbits. Exp. Brain Res. 51: 304-309.
Ban M, Ohno T. (1977) Projection of cerebellar nuclear neurones to the inferior olive by descending collaterals of ascending fibers. Brain Res. 133: 156-161.
Barmack NH, Baughman RW, Eckenstein FP. (1992a) Cholinergic innervation of the cerebellum of rat, rabbit, cat, and monkey as revealed by choline acetyltransferase activity and immunohistochemistry. J. Comp. Neurol. 317: 233-249.
Barmack NH, Baughman RW, Eckenstein FP, Shojaku H. (1992b) Secondary vestibular cholinergic projection to the cerebellum of rabbit and rat as revealed by choline acetyltransferase immunohistochemistry, retrograde and orthograde tracers. J. Comp. Neurol. 317: 250-270.

Barmack NH, Fagerson M, Fredette BJ, Mugnaini E, Shojaku H. (1993) Activity of neurons in the beta nucleus of the inferior olive of the rabbit evoked by natural vestibular stimulation. Exp.Brain Res. 94: 203-215.

Barmack NH, Fredette BJ, Mugnaini E. (1998) Parasolitary nucleus: a source of GABAergic vestibular information to the inferior olive of rat and rabbit. J Comp Neurol. 392: 352-72.

Basbaum AI, Menétrey D. (1987) Wheat germ agglutinin-apoHRP gold: a new retrograde tracer for light- and electronmicroscopic single- and double-label studies. J. Comp. Neurol. 261: 306-318.

Batini C, Compoint C, Buisseret-Delmas C, Daniel H, Guegan M. (1992) Cerebellar nuclei and the nucleocortical projections in the rat: retrograde tracing coupled to GABA and glutamate immunohistochemistry. J. Comp. Neurol. 315: 74-84.

Batini C, Daniel H, Ramirez RD. (1987) Release of cerebellar inhibitory activity by partial destruction of the inferior olive with kainic acid in rat. Brain Res. 403: 186-191.

Batton RR, Jayaraman D, Ruggiero D, Carpenter MB. (1977) Fastigial afferent projections in the monkey: an autoradiographic study. J. Comp. Neurol. 174: 281-306.

Bechterew W. (1885) Zur Anatomie der Schenkel des Kleinhirns, insbesondere der Brückenarme. Neurol.Zbl. 4: 121-125.

Beitz AJ. (1976) The topographical organization of the olivo-dentate and dentato-olivary pathways in the cat. Brain Res. 115: 311-317.

Beitz AJ, Chan-Palay V. (1979) A Golgi analysis of neuronal organization in the medial cerebellar nucleus of the rat. Neurosci. 4: 47-63.

Bentivoglio M, Kuypers HGJM. (1982) Divergent axon collaterals from rat cerebellar nuclei to diencephalon, mesencephalon, medulla oblongata and cervical cord. Exp. Brain Res. 46: 339-356.

Bentivoglio M, Kuypers HGJM, Catsman-Berrevoets CE. (1980a) Retrograde neuronal labeling by means of bisbenzimide and nuclear yellow (Hoechst S769121). Measures to prevent diffusion of the tracers out of retrogradely labeled neurons. Neurosci. Lett. 18: 19-24.

Bentivoglio M, Kuypers HGJM, Catsman-Berrevoets CE, Loewe H, Dann O. (1980b) Two new fluorescent tracers retrograde neuronal tracers which are transported over long distances. Neurosci. Lett. 18: 25-30.

Bentivoglio M, Molinari M. (1981) Axonal branches of the same cerebellar neurons terminate bilaterally in the thalamus. Neurosci.Lett. 23: 291-296.

Bentivoglio M, Molinari M. (1984) The interrelations between cell groups in the caudal diencephalon of the rat projecting to the striatum and to the medulla oblongata. Exp. Brain Res. 54: 57-65.

Bentivoglio M, Molinari M. 1986) Crossed divergent axon collaterals from cerebellar nuclei to thalamus and lateral medulla oblongata in the rat. Brain Res. 362: 180-184.

Berkley KJ, Hand PJ. (1978) Projections to the inferior olive of the cat. II. Comparisons of input from the gracil, cuneate and the spinal trigeminal nuclei. J. Comp. Neurol. 180: 253-264.

Berkley KJ, Worden IG. (1978) Projections to the inferior olive of the cat. I. Comparisons of input from the dorsal column nuclei, the lateral cervical nucleus, the spino-olivary pathways, the cerebral cortex and the cerebellum. J. Comp. Neurol. 180: 237-252.

Bernays RL, Heeb L, Cuenod M, Streit P. (1988) Afferents to the rat red nucleus studied by means of D-[^{3}H]choline and non-selective tracers. Neurosci. 26: 601-619.

Berrebi AS, Mugnaini E. (1988) Effects of the murine mutation 'nervous, on neurons in cerebellum and dorsal cochlear nucleus. J. Neurocytol. 17: 465-484.

Berretta S, Bosco G, Giaquinta G, Smecca G, Perciavalle V. (1993) Cerebellar influences on accessory oculomotor nuclei of the rat: A neuroanatomical, immunohistochemical, and electrophysiological study. J. Comp. Neurol. 338: 50-66.

Berretta S, Bosco G, Smecca G, Perciavalle V. (1991a) The cerebellopontine system: an electrophysiological study in the rat. Brain Res. 568: 178-184.

Berretta S, Perciavalle V, Poppele RE. (1991b) Origin of cuneate projections to the anterior and posterior lobes of the rat cerebellum. Brain Res. 556: 297-302.

Bharos TB, Kuypers HGJM, Lemon RN, Muir RB. (1981) Divergent collaterals from deep cerebellar neurons to thalamus and tectum, and to the medulla oblongata and spinal cord: retrograde fluorescent and electrophysiological studies. Exp. Brain Res. 42: 399-410.

Billard JM, Batini C, Buisseret-Delmas C, Daniel H. (1989) The inferior olive innervation from the cerebellar and lateral vestibular nuclei: evidence for a longitudinal zonal segregation of the

cortico-nucleo-olivary connection in the rat. In: Strata P, editor. The olivocerebellar system in motor control. Vol 17. Berlin: Springer-Verlag; 117-120.
Bishop GA. (1992) Calcitonin gene-related peptide in afferents to the cat's cerebellar cortex: distribution and origin. J.Comp.Neurol. 322: 201-212.
Bishop GA, Ho RH. (1984) Substance P and serotonin in the rat inferior olive. Brain Res. Bull. 12: 105-113.
Bishop GA, Ho RH. The distribution and origin of serotonin immunoreactivity in the rat cerebellum. Brain Res. 1985; 331: 195-207.
Bishop GA, King JS. (1986) Reticulo-olivary circuits: an intracellular HRP study in the rat. Brain Res. 371: 133-145.
Blanks RH, Precht W, Torigoe Y. (1983) Afferent projections to the cerebellar flocculus in the pigmented rat demonstrated by retrograde transport of horseradish peroxidase. Exp. Brain Res. 52: 293-306.
Blanks RHI. (1988) Cerebellum. In: Büttner-Ennever JA, editor. Neuroanatomy of the oculomotor system. Vol 2. Amsterdam, New York, Oxford: Elsevier Science Publishers; 225-272.
Bloedel JR. (1992) Functional heterogeneity with structural homogeneity: How does the cerebellum operate? Behav. Brain Sci. 15: 666-678.
Bloedel JR, Bracha V. (1995) On the cerebellum, cutaneomuscular reflexes, movement control and the elusive engrams of memory. Behav. Brain Res. 68: 1-44.
Bloedel JR, Roberts WJ. (1971) Action of climbing fibers in cerebellar cortex of the cat. J.Neurophys. 34: 17-31.
Boesten AJP, Voogd J. (1975) Projections of the dorsal column nuclei and the spinal cord on the inferior olive in the cat. J. Comp. Neurol. 161: 215-238.
Boivie J. (1988) Projections from the dorsal column nuclei and the spinal cord to the red nucleus in the cat. Behav. Brain Res. 28: 75-79.
Border BG, Kosinski RJ, Azizi SA, Mihailoff GA. (1986) Certain basilar pontine afferent systems are GABA-ergic: combined HRP and immunocytochemical studies in the rat. Brain Res. Bull. 17: 169-179.
Border BG, Mihailoff GA. (1985) GAD-immunoreactive neural elements in the basilar pontine nuclei and nucleus reticularis tegmenti pontis of the rat. I. Light microscopic studies. Exp. Brain. Res. 59: 600-614.
Borsello T, Rossi F, Van der Want J, Strata P. (1994) Collaterals of olivocerebellar pathway synapse only onto non-GABAergic neurons of the deep cerebellar nuclei. Soc. Neurosci. Abstr. 20: 1750.
Bower JM, Woolston DC. (1983) Congruence of spatial organization of tactile projections to granule cell and Purkinje cell layers of cerebellar hemispheres of the albino rat: vertical organization of cerebellar cortex. J.Neurophys. 49: 745-766.
Bradley DJ, Paton JFR, Spyer KM. (1987) Cardiovascular and respiratory responses evoked from the posterior cerebellar cortex and fastigial nucleus in the cat. J. Physiol. (Lond.) 393: 107-121.
Brodal A, Brodal P. (1971) The organization of the nucleus reticularis tegmenti pontis in the cat in the light of experimental anatomical studies of its cerebral cortical afferents. Exp.Brain Res. 13: 90-110.
Brodal A, Destombes J, Lacerda AM, Angaut P. (1972a) A cerebellar projection onto the pontine nuclei. An experimental anatomical study in the cat. Exp.Brain Res. 16: 115-139.
Brodal A, Gogstad AC. (1954) Rubro-cerebellar connections. An experimental study in the cat. Anat. Rec. 118: 455-485.
Brodal A, Kawamura K. (1980) Olivocerebellar projection: a review. Adv. Anat. Embryol. Cell Biol. 64: 1-140.
Brodal A, Lacerda AM, Destombes J, Angaut P. (1972b) The pattern in the projection of the intracerebellar nuclei onto the nucleus reticularis tegmenti pontis in the cat. An experimental anatomical study. Exp.Brain Res. 16: 140-160.
Brodal A, Szikla G. (1972) The termination of the brachium conjunctivum descendens in the nucleus reticularis tegmenti pontis. An experimental anatomical study in the cat. Brain Res. 39: 337-351.
Brodal A, Walberg F, Berkley KJ, Pelt A. (1980) Anatomical demonstration of branching olivocerebellar fibres by means of a double retrograde labelling technique. Neurosci. 5: 2193-2202.
Brodal P. (1972) The cortico-pontine projection from the visual cortex in the cat. I. The total projection and the projection from area 17. Brain Res. 39: 297-317.

Brodal P. (1980a) The cortical projection to the nucleus reticularis tegmenti pontis in the Rhesus monkey. Exp.Brain Res. 38: 19-27.
Brodal P. (1980b) The projection from the nucleus reticularis tegmenti pontis to the cerebellum in the Rhesus monkey. Exp.Brain Res. 38: 29-36.
Brodal P. (1982) Further observations on the cerebellar projections from the pontine nuclei and the nucleus reticularis tegmenti pontis in the Rhesus monkey. J.Comp.Neurol. 204: 44-55.
Brodal P, Dietrichs E, Walberg F. (1986) Do pontocerebellar mossy fibres give off collaterals to the cerebellar nuclei? An experimental study in the cat with implantation of crystalline HRP-WGA. Neurosci. Res. 4: 12-24.
Brodal P, Mihailoff G, Border B, Ottersen P, Storm-Mathisen J. (1988) GABA-containing neurons in the pontine nuclei of rat, cat and monkey. An immunocytochemical study. Neurosci. 25: 27-45.
Brown JT, Chan-Palay V, Palay SL. (1977) A study of afferent input to the inferior olivary complex in the rat by retrograde axonal transport of horseradish peroxidase. J. Comp. Neurol. 176: 1-22.
Brown LT. (1974) Corticorubral projections in the rat. J. Comp. Neurol. 154: 149-168.
Buisseret-Delmas C. (1988a) Sagittal organization of the olivocerebellonuclear pathway in the rat. I. Connections with the nucleus fastigii and the nucleus vestibularis lateralis. Neurosci.Res. 5: 475-493.
Buisseret-Delmas C. (1988b) Sagittal organization of the olivocerebellonuclear pathway in the rat. II. Connections with the nucleus interpositus. Neurosci.Res. 5: 494-512.
Buisseret-Delmas C, Angaut P. (1988) The cerebellar nucleo-cortical projections in the rat. A retrograde labeling study using horseradish peroxidase combined to a lectin. Neurosci.Lett. 84: 255-260.
Buisseret-Delmas C, Angaut P. (1989a) Anatomical mapping of the cerebellar nucleo-cortical projections in the rat: a retrograde labeling study. J.Comp.Neurol. 288: 297-310.
Buisseret-Delmas C, Angaut P. (1989b) Sagittal organization of the olivocerebellonuclear pathway in the rat. III. Connections with the nucleus dentatus. Neurosci. Res. 7: 131-143.
Buisseret-Delmas C, Angaut P. (1993) The cerebellar olivo-cortico-nuclear connections in the rat. Progr. Neurobiol. 40: 63-87.
Buisseret-Delmas C, Angaut P, Compoint C, Diagne M, Buisseret P. (1998) Brainstem efferents from the interface between the nucleus medialis and the nucleus interpositus in the rat. J. Comp. Neurol. 402: 264-275.
Buisseret-Delmas C, Batini C, Compoint C, Daniel H, Menetrey D. (1989) The GABAergic neurones of the cerebellar nuclei: projection to the caudal inferior olive and to the bulbar reticular formation. Exp.Brain Res. 17: 108-110.
Buisseret-Delmas C, Yatim N, Buisseret P, Angaut P. (1993) The X zone and CX subzone of the cerebellum in the rat. Neurosci. Res. 16: 195-207.
Bull MS, Berkley KJ. (1991) Cerebellar projections to the somatic pretectum in the cat. Somatosens. Motor Res. 8: 117-126.
Bull MS, Mitchell SK, Berkley KJ. (1990) Convergent inputs to the inferior olive from the dorsal column nuclei and pretectum in the cat. Brain Res. 525: 1-10.
Burne RA, Azizi SA, Mihailoff GA, Woodward DJ. (1981) The tectopontine projection in the rat with comments on visual pathways to the basilar pons. J. Comp. Neurol. 202: 287-307.
Büttner-Ennever JA, Büttner U. (1988) The reticular formation. In: Büttner-Ennever JA, editor. Neuroanatomy of the oculomotor system. Vol 2. Amsterdam, New York, Oxford: Elsevier Science Publishers; 119-176.
Cadusseau J, Roger M. (1985) Afferent projections to the superior colliculus in the rat, with special attention to the deep layers. J. Hirnforsch. 26: 667-681.
Cajal R y.(1911) Histology du Systeme Nerveux de l'homme et des Vertebres. 2.
Campbell KJ, Takada M. (1989) Bilateral tectal projection of single nigrostriatal cells in the rat. Neurosci. 33: 311-321.
Campbell NC, Armstrong DM. (1985) Origin in the medial accessory olive of climbing fibers to the x and lateral c1 zones of the cat cerebellum: a combined electrophysiological / WGA-HRP investigation. Exp.Brain Res. 58: 520-531.
Carlton SM, Leichnetz GR, Mayer DJ. (1982) Projections from the nucleus parafascicularis prerubralis to medullary raphe nuclei and inferior olive in the rat: a horseradish peroxidase and autoradiography study. Neurosci. Lett. 30: 191-197.

Carpenter MB, Batton III RR. (1982) Connections of the fastigial nucleus in the cat and monkey. Exp.Brain Res. Suppl.6: 250-291.
Carpenter MB, Stevens GH. (1957) Structural and functional relationships between the deep cerebellar nuclei and the brachium conjunctivum in the rhesus monkey. J.Comp.Neurol. 107: 109-163.
Caughell KA, Flumerfelt BA. (1977) The organization of the cerebellorubral projection: an experimental study in the rat. J. Comp. Neurol. 176: 295-306.
Cazin L, Lannou J, Precht W. (1984) An electrophysiological study of pathways mediating optokinetic responses to the vestibular nucleus in the rat. Exp. Brain Res. 54: 337-348.
Cella F, Ruigrok TJH, Voogd J. (1991) Identification of a somatotopical arrangement of spinal projections to the lateral reticular nucleus in the rat. Eur. J. Neurosci. Suppl. 4: 318.
Chambers WW, Sprague JM. (1955a) A functional localization in the cerebellum: I. Organization in longitudinal corticonuclear zones and their contribution to the control of posture, both extrapyramidal and pyramidal. J.Comp.Neurol. 103: 105-130.
Chambers WW, Sprague JM. (1955b) Functional localization in the cerebellum: II. Somatotopic organization in the cortex and nuclei. Arch.Neurol.Psychiat. 74: 653-680.
Chan-Palay V. (1977) Cerebellar dentate nucleus: organization, cytology and transmitters. Berlin: Springer-Verlag.
Chan-Palay V, Palay SL, Brown GT, Van Itallie C. (1977) Sagittal organization of olivocerebellar and reticulocerebellar projections: autoradiographic studies with ^{35}S-methionine. Exp. Brain Res. 30: 561-576.
Chen S. (1995) Evidence that cholera toxin B subunit (CTb) can be avidly taken up and transported by fibers of passage. Brain Res. 674: 107-111.
Chen S, Hillman DE. (1993) Colocalization of neurotransmitters in the deep cerebellar nuclei. J. Neurocytol. 22: 81-91.
Chiba M. (1980) Patterns of organization of comments on the corticopontine projections in the cat with the pontocerebellar projection. J.Hirnforsch. 21: 89-99.
Cholley B, Wassef M, Arsénio-Nunes L, Bréhier A, Sotelo C. (1989) Proximal trajectory of the brachium conjunctivum in rat fetuses and its early association with the parabrachial nucleus. A study combining in vitro HRP anterograde axonal tracing and immunocytochemistry. Devel.Brain Res. 45: 185-202.
Cicirata F, Panto MR, Angaut P. (1982) An autoradiographic study of the cerebellopontine projections in the rat. I. Projections from the medial cerebellar nucleus. Brain Res. 253: 303-308.
Cohen D, Chambers WW, Sprague JM. (1958) Experimental study of the efferent projections from the cerebellar nuclei to the brainstem of the cat. J. Comp. Neurol. 109: 233-259.
Colin F, Manil J, Desclin JC. (1980) The olivocerebellar system. I. Delayed and slow inhibitory effects: An overlooked salient feature of cerebellar climbing fibers. Brain Res. 187: 3-27.
Compoint C, Buisseret-Delmas C, Diagne M, Buisseret P, Angaut P. (1997) Connections between the cerebellar nucleus interpositus and the vestibular nuclei: an anatomical study in the rat. Neurosci. Lett. 238: 91-94.
Condé F. (1988) Cerebellar projections to the red nucleus of the cat. Behav. Brain Res. 28: 65-68.
Condé F, Condé H. (1980) Demonstration of a rubrothalamic projection in the cat, with some comments on the origin of the rubrospinal tract. Neurosci. 5: 789-802.
Corvaja N, Grofova I, Pompeiano O, Walberg F. (1977) The lateral reticular nucleus in the cat. I. An experimental anatomical study of its spinal and supraspinal afferent connections. Neurosci. 2: 537-553.
Courville J. (1966) Rubrobulbar fibres to the facial nucleus (nucleus of the lateral funiculus). An experimental study in the cat with silver impregnation methods. Brain Res. 1: 317-337.
Courville J, Brodal A. (1966) Rubro-cerebellar connections in the cat: an experimental study with silver impregnation methods. J.Comp.Neurol. 140: 241-254.
Courville J, Cooper CW. (1970) The cerebellar nuclei of Macaca mulatta: a morphological study. J.Comp.Neurol. 140: 241-254.
Courville J, Diakiw N, Brodal A. (1973) Cerebellar corticonuclear projection in the cat. The paramedian lobule. An experimental study with silver methods. Brain Res. 50: 25-45.
Crandall WF, Keller EL. (1985) Visual and oculomotor signals in nucleus reticularis tegmenti pontis in alert monkey. J.Neurophys. 54: 1326-1345.

Cruce JF. (1977) An autoradiographic study of the descending connections of the mammillary nuclei of the rat. J. Comp. Neurol. 176: 631-644.
Daniel H, Angaut P, Batini C, Billard JM. (1988) Topographic organization of the interpositorubral connections in the rat. A WGA-HRP study. Behav. Brain Res. 28: 69-70.
Daniel H, Billard JM, Angaut P, Batini C. (1987) The interposito-rubrospinal system. Anatomical tracing of a motor control pathway in the rat. Neurosci. Res. 5: 87-112.
De Zeeuw CI. (1990) Ultrastructure of the cat inferior olive. An anatomical study using three new combination techniques. Anatomy. Rotterdam: Erasmus University Rotterdam; 198.
De Zeeuw CI, Berrebi AS. (1995a) Individual Purkinje cell axons terminate on both inhibitory and excitatory neurons in the cerebellar and vestibular nuclei. Ann.New York Acad.Sci. 781: 607-610.
De Zeeuw CI, Berrebi AS. (1995b) Postsynaptic targets of Purkinje cell terminals in the cerebellar and vestibular nuclei of the rat. Eur.J.Neurosci. 7: 2322-2333.
De Zeeuw CI, Gerrits NM, Voogd J, Leonard CS, Simpson JI. (1994) The rostral dorsal cap and ventrolateral outgrowth of the rabbit inferior olive receive a GABAergic input from dorsal group Y and the ventral dentate nucleus. J.Comp.Neurol. 341: 420-432.
De Zeeuw CI, Holstege JC, Calkoen F, Ruigrok TJH, Voogd J. (1988) A new combination of WGA-HRP anterograde tracing and GABA-immunocytochemistry applied to afferents of the cat inferior olive at the ultrastructural level. Brain Res. 447: 369-375.
De Zeeuw CI, Holstege JC, Ruigrok TJH, Voogd J. (1989a) The cerebellar, mesodiencephalic and GABAergic innervation of the glomeruli in the cat inferior olive. A comparison at the ultrastructural level. In: Strata P, editor. The olivocerebellar system in motor control. Vol 17. Berlin: Springer-Verlag, 111-116.
De Zeeuw CI, Holstege JC, Ruigrok TJH, Voogd J. (1989b) Ultrastructural study of the GABAergic, cerebellar and mesodiencephalic innervation of the cat medial accessory olive: anterograde tracing combined with immunocytochemistry. J. Comp. Neurol. 284: 12-35.
De Zeeuw CI, Holstege JC, Ruigrok TJH, Voogd J. (1990) Mesodiencephalic and cerebellar terminals terminate upon the same dendritic spines within the glomeruli of the cat and rat inferior olive: an ultrastructural study using a combination of ^{3}H-leucine and WGA-HRP anterograde tracing. Neurosci. 34: 644-655.
De Zeeuw CI, Ruigrok TJH. (1994) Olivary projecting neurons in the nucleus of Darkschewitsch in the cat receive excitatory monosynaptic input from the cerebellar nuclei. Brain Res. 653: 345-350.
De Zeeuw CI, van Alphen AM, Hawkins RK, Ruigrok TJH. (1997) Climbing fibre collaterals contact neurons in the cerebellar nuclei that provide a GABAergic feedback to the inferior olive. Neurosci. 80: 981-986.
De Zeeuw CI, Wentzel P, Mugnaini E. (1993) Fine structure of the dorsal cap of the inferior olive and its GABAergic and non-GABAergic input from the nucleus prepositus hypoglossi in rat and rabbit. J. Comp. Neurol. 327: 63-82.
Desclin JC. (1974) Histological evidence supporting the inferior olive as the major source of cerebellar climbing fibers in the rat. Brain Res. 77: 365-388.
Dietrichs E, Walberg F. (1985) The cerebellar nucleo-olivary and olivo-cerebellar nuclear projections in the cat as studied with anterograde and retrograde transport in the same animal after implantation of crystalline WGA-HRP. II. The fastigial nucleus. Anat. Embryol. 173: 253-261.
Dietrichs E, Walberg F. (1986) The cerebellar nucleo-olivary and olivo-cerebellar nuclear projections in the cat as studied with anterograde and retrograde transport in the same animal after implantation of crystalline WGA-HRP. III. The interposed nuclei. Brain Res. 373: 373-383.
Dietrichs E, Walberg F. (1989) Direct bidirectional connections between the inferior olive and the cerebellar nuclei. In: Strata P, editor. The olivocerebellar system in motor control. Vol 17. Berlin: Springer-Verlag; 61-81.
Dietrichs E, Walberg F, Nordby T. (1985) The cerebellar nucleo-olivary and olivo-cerebellar nuclear projections in the cat as studied with anterograde and retrograde transport in the same animal after implantation of crystalline WGA-HRP. I. The dentate nucleus. Neurosci. Res. 3: 52-70.
Dolleman-Van der Weel MJ, Wouterlood FG. (1994) Multiple anterograde tracing, combining Phaseolus vulgaris-leucoagglutinin with rhodamine- and biotin-conjugated dextran amine. J. Neurosci. Meth. 51: 9-21.

Dom R, King JS, Martin GF. (1973) Evidence for two direct cerebello-olivary connections. Brain Res. 57: 498-501.
Dornan WA, Peterson M, Matuszewich L, Malen P. (1991) Ibotenic acid-induced lesions of the medial zona incerta decrease lordosis behavior in the female rat. Behav. Neurosci. 105: 210-214.
Eccles J, Ito M, Szentagothai J. (1967) The cerebellum as a neuronal machine. Springer, Berlin 1967.
Eccles JC. (1973) The cerebellum as a computer: patterns in space and time. J.Physiol. 229: 1-32.
Eccles JC, Llinás R, Sasaki K. (1966) The excitatory synaptic action of climbing fibers on the Purkinje cells of the cerebellum. J. Physiol. (Lond.) 182: 268-296.
Eccles JC, Rosen I, Scheid P, Taborikova H. (1974a) Temporal patterns of responses of interpositus neurons to peripheral afferent stimulation. J.Neurophys. 37: 1424-1437.
Eccles JC, Sabah NH, Taborikova H. (1974b) The pathways responsible for excitation and inhibition of fastigial neurons. Exp. Brain Res. 19: 78-99.
Edwards DA, Isaacs S. (1991) Zona incerta lesions: effects on copulation, partner-preference and other socio-sexual behaviors. Behav. Brain Res. 44: 145-150.
Edwards SB. (1972) The ascending and descending projections of the red nucleus in the cat: an experimental study using an autoradiographic tracing method. Brain Res. 48: 45-63.
Ekerot C-F. (1990) The lateral reticular nucleus in the cat. VI. Excitatory and inhibitory afferent paths. Esp. Brain Res. 79: 109-119.
Ekerot C-F, Garwicz M, Jörntell H. (1997) The control of forelimb movements by intermediate cerebellum. In: De Zeeuw CI, Strata P and Voogd J, editors. The cerebellum: from structure to control. Vol 114. Amsterdam: Elsevier Science; 423-429.
Ekerot C-F, Jorntell H, Garwicz M. (1995) Functional relation between corticonuclear input and movements evoked on microstimulation in cerebellar nucleus interpositus anterior in the cat. Exp.Brain Res. 106: 365-376.
Ekerot C-F, Larson B. (1980) Termination in overlapping sagittal zones in cerebellar anterior lobe of mossy and climbing fiber paths activated from dorsal funiculus. Exp.Brain Res. 38: 163-172.
Ekerot C-F, Larson B. (1982) Branching of olivary axons to innervate pairs of sagittal zones in the cerebellar anterior lobe of the cat. Exp.Brain Res. 48: 185-198.
Elekes I, Patthy A, Lang T, Palkovits M. (1986) Concentrations of GABA and glycine in discrete brain nuclei. Neuropharm. 25: 703-709.
Faber DS, Murphy JT. (1969) Axonal branching in the climbing fiber pathway to the cerebellum. Brain Res. 15: 262-267.
Faull RLM. (1978) The cerebellofugal projections in the brachium conjunctivum of the rat. II. The ipsilateral and contralateral descending pathways. J. Comp. Neurol. 178: 519-536.
Faull RLM, Carman JB. (1978) The cerebellofugal projections in the brachium conjunctivum of the rat. I. The contralateral ascending pathway. J. Comp. Neurol. 178: 495-518.
Fiez JA. (1996) Cerebellar contributions to cognition. Neuron 16: 13-15.
Fiez JA, Petersen SE, Cheney MK, Raichle ME. (1992) Impaired non-motor learning and error detection associated with cerebellar damage. A single case study. Brain 115: 155-178.
Flourens M-J-P. (1823) Recherches physiques sur les propriétés et les fonctions du système nerveux dans les animaus vertébrés. Arch.Génerale de Médicine 2: 321-370.
Flumerfelt BA. (1978) Organization of the mammalian red nucleus and its interconnections with the cerebellum. Experientia 34: 1178-1180.
Flumerfelt BA, Gwyn DG. (1974) The red nucleus of the rat: its organization and interconnections. J. Anat. 118: 374.
Flumerfelt BA, Hrycyshyn AW. (1985) Precerebellar nuclei and red nucleus. In: Paxinos G, editor. The rat nervous system: Academic Press Australia, 221-250.
Flumerfelt BA, Hrycyshyn AW, Kapogianis EM. (1982) Spinal projections to the lateral reticular nucleus in the rat. Anat. Embryol. 165: 345-359.
Flumerfelt BA, Otabe S, Courville J. (1973) Distinct projections to the red nucleus from the dentate and interposed nuclei in the monkey. Brain Res. 50: 408-414.
Fredette BJ, Mugnaini E. (1991) The GABAergic cerebello-olivary projection in the rat. Anat. Embryol. 184: 225-243.
Furber SE, Watson CRR. (1983) Organization of the olivo-cerebellar projection in the rat. Brain Behav. Evol. 22: 132-152.

Gacek RR. (1977) Localization of brain stem neurons projecting to the oculomotor nucleus in the cat. Exp.Neurol. 57: 725-749.
Gacek RR. (1979) Localization of trochlear vestibulo-ocular neurons in the cat. Exp.Neurol. 66: 692-706.
Gellman R, Houk JC, Gibson AR. (1983) Somatosensory properties of the inferior olive of the cat. J. Comp. Neurol. 215: 228-243.
Gerrits NM. (1987) Afferent control of the cerebellum. An hypothesis to explain the differences in the mediolateral distribution of mossy fibre terminals in the cerebellar cortex. In: Glickstein M, Yeo D and Stein J, editors. Cerebellum and neuronal plasticity. New York: Plenum Publisher Corporation, 83-100.
Gerrits NM, Epema AH, Voogd J. (1984a) The mossy fiber projection of the nucleus reticularis tegmenti pontis to the flocculus and adjacent ventral paraflocculus in the cat. Neurosci. 11: 627-644.
Gerrits NM, Voogd J. (1981) Cerebellar efferents of the nucleus reticularis tegmenti pontis in the cat. Acta Morphol.Neerla.-Scand. 19: 57-57.
Gerrits NM, Voogd J. (1982) The climbing fiber projection to the flocculus and adjacent paraflocculus in the cat. Neurosci. 7: 2971-2991.
Gerrits NM, Voogd J. (1986) The nucleus reticularis tegmenti pontis and the adjacent rostral paramedian reticular formation: differential projections to the cerebellum and the caudal brain stem. Exp. Brain Res. 62: 29-45.
Gerrits NM, Voogd J. (1987) The projection of the nucleus reticularis tegmenti pontis and adjacent regions of the pontine nuclei to the central cerebellar nuclei in the cat. J. Comp. Neurol. 258: 52-69.
Gerrits NM, Voogd J, Magras N. (1985) Vestibular afferents of the inferior olive and the vestibulo-olivo-cerebellar climbing fiber pathway to the flocculus in the cat. Brain Res. 332: 325-336.
Gerrits NM, Willemse-Van der Geest L, Kornet M. (1984b) Some observations on the cerebellopontine projections in the cat - with a hypothesis to explain species differences. Neurosci.Lett. 44: 65-70.
Gibson AR, Horn KM, Stein JF, Van Kan PLE. Activity of interpositus neurons during a visually guided reach. Can J Physiol Pharmacol 1996; 74: 499-512.
Gibson AR, Robinson FR, Alam J, Houk JC. Somatotopic alignment between climbing fiber input and nuclear output of the cat intermediate cerebellum. J. Comp. Neurol. 1987; 260: 362-377.
Giuffrida R, Aicardi G, Canedi A, Rapisarda C. (1993) Excitatory amino acids as neurotransmitters of cortical and cerebellar projections to the red nucleus: an immunocytochemical study in the guinea pig. Somatosens.Motor Res. 10: 365-376.
Giuffrida R, Li Volsi G, Perciavalle V. (1988a) Influences of cerebral cortex and cerebellum on the red nucleus of the rat. Behav. Brain Res. 28: 109-111.
Giuffrida R, Palmeri A, Raffaele R, Ricca G, Sapienza S. (1988b) Convergence pattern of cortical and interposital influences on rubrospinal neurons of the cat. Behav. Brain Res. 28: 113-116.
Glickstein M, Gerrits N, Kralj-Hans I, Mercier B, Stein J, Voogd J. (1994) Visual pontocerebellar projections in the macaque. J.Comp.Neurol. 349: 51-72.
Glickstein M, Voogd J. (1995) The cerebellum. In: Bannister LH, Berry MM, Collins P, Dyson M, Dussek JE and Fergusson MWJ, editors. Gray's anatomy. Edinburgh: Churchill Livingstone; 1027-1065.
Godschalk M, De Zeeuw CI, Holman FA, van der Burg J. (1997) Corticonuclear projections from functionally distinct sagittal zones in the cerebellar vermis of the rabbit. Soc. Neurosci. Abstr. 27: 1829.
Godschalk M, Van der Burg J, Van Duin B, De Zeeuw CI. (1994) Topography of saccadic eye movements evoked by microstimulation in rabbit cerebellar vermis. J. Physiol. 480: 147-153.
Gonzalo-Ruiz A, Leichnetz GR. (1987) Collateralization of cerebellar efferent projections to the paraoculomotor region, superior colliculus, and medial pontine reticular formation in the rat: a fluorescent double labeling study. Exp.Brain Res. 68: 365-378.
Gonzalo-Ruiz A, Leichnetz GR. (1990) Connections of the caudal cerebellar interpositus complex in a new world monkey (*Cebus apella*). Brain Res. Bull. 25: 919-927.
Gonzalo-Ruiz A, Leichnetz GR, Hardy SGP. (1990) Projections of the medial cerebellar nucleus to oculomotor-related midbrain areas in the rat: an anterograde and retrograde HRP study. J.Comp.Neurol. 296: 427-436.

Gonzalo-Ruiz A, Leichnetz GR, Smith DJ. (1988) Origin of cerebellar projections to the region of the oculomotor complex, medial pontine reticular formation, and superior colliculus in new world monkeys: a retrograde horseradish peroxidase study. J.Comp.Neurol. 268: 508-526.
Goodman DC, Hallett RE, Welch RB. (1963) Patterns of localization in the cerebellar corticonuclear projections of the albino rat. J.Comp.Neurol. 121: 51-63.
Graham J. (1977) An autoradiographic study of the efferent connections of the superior colliculus in the cat. J.Comp.Neurol. 173: 629-654.
Graybiel AM. (1974) Visuo-cerebellar and cerebello-visual connections involving the ventral lateral geniculate nucleus. Exp.Brain Res. 20: 303-306.
Graybiel AM, Nauta HJW, Lasek RJ, Nauta WJH. (1973) A cerebello-olivary pathway in the cat: an experimental study using autoradiographic tracing techniques. Brain Res. 58: 205-211.
Groenewegen HJ, Voogd J. (1977) The parasagittal zonation within the olivocerebellar projection. I. Climbing fiber distribution in the vermis of cat cerebellum. J. Comp. Neurol. 174: 417-488.
Groenewegen HJ, Voogd J, Freedman SL. (1979) The parasagittal zonation within the olivocerebellar projection. II. Climbing fiber distribution in the intermediate and hemispheric parts of cat cerebellum. J.Comp.Neurol. 183: 551-602.
Grottel K, Zimny R, Kowalski K. (1988) The pontocerebellar efferents from the pontine reticular tegmental nucleus in the rabbit: differential projections to the paramedian sublobules as revealed with tracing of retrograde axonal transport of horseradish peroxidase. J.Hirnforsch. 29: 203-216.
Gwyn DG. (1971) Histochemical evidence for a somatotopic organization of the rubrospinal projection in the rat. Experientia 27: 819-821.
Gwyn DG, Flumerfelt BA. (1974) A comparison of the distribution of cortical and cerebellar afferents in the red nucleus of the rat. Brain Res. 1974: 130-135.
Haines DE, Dietrichs E, Mihailoff GA, McDonald EF. (1997) The cerebellar-hypothalamic axis: basic circuits and clinical observations. Rev. Neurobiol. 41: 83-107.
Haines DE, May PJ, Dietrichs E. (1990) Neuronal connections between the cerebellar nuclei and hypothalamus in *Macaca fascicularis*: cerebello-visceral circuits. J. Comp. Neurol. 299: 106-122.
Hammond WA. (1869) The physiology and pathology of the cerebellum. Quarterly Journal of Physiological Medicine and Medical Jurisprudence 3: 209-244.
Haroian AJ. (1982) Cerebello-olivary projections in the rat: an autoradiographic study. Brain Res. 235: 125-130.
Haroian AJ, Massopust LC, Young PA. (1981) Cerebellothalamic projections in the rat: an autoradiographic and degeneration study. J. Comp. Neurol. 197: 217-236.
Harting JK. (1977) Descending pathways from the superior colliculus: an autoradiographic analysis in the rhesus monkey (Macaca mulatta). J.Comp.Neurol. 173: 583-612.
Hatschek R. (1907) Zur vergleichenden Anatomie des nucleus ruber tegmenti. Arb.Neurol.Inst.WienUniv. 15: 89.
Highstein SM, Reisine H. (1979) Synaptic and functional organization of vestibulo-ocular reflex pathways. Prog.Brain Res. 50: 431-442.
Hinman A, Carpenter MB. (1959) Efferent fiber projections of the red nucleus in the cat. J. Comp. Neurol. 113: 61-81.
Hinrichsen CFL, Watson CD. (1983) Brain stem projections to the facial nucleus of the rat. Brain Behav. Evol. 22: 153-163.
Ho CP, Leong SK. (1977) A cerebellar projection onto the pontine nuclei in the albino rat. Exp.Brain Res. 30: 149-154.
Hoddevik GH. (1978) The projection from the nucleus reticularis tegmenti pontis onto the cerebellum in the cat. Anat.Embryol. 153: 227-242.
Hökfelt T, Fuxe K. (1969) Cerebellar monoamine nerve terminals, a new type of afferent fibers to the cortex cerebelli. Exp. Brain Res. 9: 63-72.
Holmes G, Stewart TG. (1904) Symptomatology of cerebellar tumours: a study of forty cases. Brain 27: 522-591.
Holstege G. (1995) The basic, somatic, and emotional components of the motor system in mammals. In: Paxinos G, editor. The rat central nervous system. New York: Academic Press; 137-154.
Holstege G, Collewijn H. (1982) The efferent connections of the nucleus of the optic tract and the superior colliculus in the rabbit. J.Comp.Neurol. 209: 139-175.

Holstege JC, Kuypers HGJM. (1987) Brainstem projections to spinal motoneurons: an update. Neurosci. 23: 809-821.
Horn KM, Porter CM, Gibson AR. (1995) Spinal connections of cat posterior interpositus. Soc. Neurosci. Abstr. 21: 1190.
Horn KM, Vankan PLE, Gibson AR. (1996) Reduction of rostral dorsal accessory olive responses during reaching. J Neurophysiol 76: 4140-4151.
Hosoya Y, Matsushita M. (1981) Brainstem projections from the lateral hypothalamic area in the rat, as studied with autoradiography. Neurosci. Lett. 24: 111-116.
Houk JC, Keifer J, Barto AG. (1993) Distributed motor commands in the limb premotor network. Trends Neurosci. 16: 27-33.
Houk JC, Wise SP. (1995) Distributed modular architectures linking basal ganglia, cerebellum, and cerebral cortex: their role in planning and controlling action. Cerebral Cortex 5: 95-110.
Hrycyshyn AW, Flumerfelt BA. (1981) A light microscopic investigation of the afferent connections of the lateral reticular nucleus in the cat. J. Comp. Neurol. 197: 477-502.
Hrycyshyn AW, Flumerfelt BA, Anderson WA. (1982) A horseradish peroxidase study of the projections from the lateral reticular nucleus to the cerebellum in the rat. Anat. Embryol. 165: 1-18.
Hrycyshyn AW, Ghazi H, Flumerfelt BA. (1989) Axonal branching of the olivocerebellar projection in the rat: a double labeling study. J.Comp.Neurol. 284: 48-59.
Huerta MF, Frankfurter A, Harting JK. (1983) Studies of the principal sensory and spinal trigeminal nuclei of the rat: projections to the superior colliculus, inferior olive and cerebellum. J. Comp. Neurol. 220: 147-167.
Huisman AM, Kuypers HGJM, Conde F, Keizer K. (1983) Collaterals of rubrospinal neurons to the cerebellum in rat. A retrograde fluorescent double labeling study. Brain Res. 264: 181-196.
Huisman AM, Kuypers HGJM, Verburgh CA. (1981) Quantitative differences in collateralization of the descending spinal pathways from red nucleus and other brain stem cell groups in rat as demonstrated with the multiple fluorescent retrograde tracer technique. Brain Res. 209: 271-286.
Huisman AM, Kuypers HGJM, Verburgh CA. (1982) Differences in collateralization of the descending spinal pathways from red nucleus and other brainstem cell groups in cat and monkey. Progr. Brain Res. 57: 185-218.
Ikeda M, Houtani T, Ueyama T, Sugimoto T. (1991) Choline acetyltransferase immunoreactivity in the cat cerebellum. Neurosci. 45: 671-690.
Ito M. (1984) The cerebellum and neural control. New York: Raven press.
Ito M. (1990) A new physiological concept on cerebellum. Rev. Neurol. (Paris) 146: 564-569.
Ito M. (1991) Structural-functional relationships in cerebellar and vestibular systems. Arch. Ital. Biol. 129: 53-61.
Ito M. (1994) New concepts in cerebellar function. Rev. Neurol. 149: 596-599.
Ito M, Nagao S. (1991) Comparative aspects of horizontal ocular reflexes and their cerebellar adaptive control in vertebrates. Comp. Biochem. Physiol. 98C: 221-228.
Itoh K. (1977) Efferent projections of the pretectum in the cat. Exp. Brain Res. 30: 89-105.
Jaarsma D, Ruigrok TJH, Caffe R, Cozzari C, Levey AI, Mugnaini E, et al. (1997) Cholinergic innervation and receptors in the cerebellum. In: De Zeeuw CI, Strata, P., Voogd, J., editor. The cerebellum: From structure to control. Vol 114. Amsterdam: Elsevier; 67-96.
Jacquin MF, Barcia M, Rhoades RW. (1989) Structure-function relationships in rat brainstem subnucleus interpolaris: IV. Projection neurons. J. Comp. Neurol. 282: 45-62.
Jansen J, Brodal A. (1940) Experimental studies on the intrinsic fibers of the cerebellum. II. The corticonuclear projection. J.Comp.Neurol. 73: 267-321.
Ji Z, Aas J-E, Laake J, Walberg F, Ottersen OP. (1991) An electron microscopic, immunogold analysis of glutamate and glutamine in terminals of rat spinocerebellar fibers. J. Comp. Neurol. 307: 296-310.
Ji Z, Hawkes R. (1994) Topography of Purkinje cell compartiments and mossy fiber terminal fields in lobules II and III of the rat cerebellar cortex: spinocerebellar and cuneocerebellar projections. Neurosci. 61: 935-954.
Jiang X, Johnson RR, Burkhalter A. (1993) Visualization of dendritic morphology of cortical projection neurons by retrograde axonal tracing. J. Neurosci. Meth. 50: 45-60.
Jones BE. (1995) Reticular formation: cytoarchitecture, transmitters, and projections. In: Paxinos G, editor. The rat central nervous system. New York: Academic Press; 155-171.

Kalil K. (1979) Projections of the cerebellar and dorsal column nuclei upon the inferior olive in the Rhesus monkey: an autoradiographic study. J. Comp. Neurol. 188: 43-62.
Kanda K-I, Sato Y, Ikarashi K, Kawasaki T. (1989) Zonal organization of climbing fiber projections to the uvula in the cat. J. Comp. Neurol. 279: 138-148.
Katsumaru HF, Murakami F, Wu JY, Tsukahara N. (1984) GABAergic intrinsic interneurons in the red nucleus of the cat demonstrated with combined immunocytochemistry and anterograde degeneration methods. Neurosci. Res. 1: 35-44.
Katz LC, Burkhalter A, Dreyer WJ. (1984) Fluorescent latex microspheres as a retrograde neuronal marker for *in vivo* and *in vitro* studies of visual cortex. Nature 310: 498-500.
Katz LC, Iarovici DM. (1990) Green fluorescent latex microspheres: a new retrograde tracer. Neurosci. 34: 511-520.
Kawamura K, Hashikawa T. (1981a) Projections from the pontine nuclei proper and reticular tegmental nucleus onto the cerebellar cortex in the cat. J.Comp.Neurol. 201: 395-413.
Kawamura K, Hashikawa T. (1981b) Projections from the pontine nuclei proper and reticular tegmental nucleus onto the cerebellar cortex in the cat. An autoradiographic study. J.Comp.Neurol. 201: 395-413.
Kawamura S, Hattori S, Higo S, Matsuyama T. (1982) The cerebellar projections to the superior colliculus and pretectum in the cat: an autoradiographic and horseradish peroxidase study. Neurosci. 7: 1673-1689.
Keizer K, Kuypers HGJM, Huisman AM, Dann O. (1983) Diamidino Yellow dihydrochloride (DY.2HCl); a new fluorescent retrograde tracer, which migrates only very slowly out of the cell. Exp. Brain Res. 51: 179-191.
Kennedy PR. (1990) Corticospinal, rubrospinal and rubro-olivary projections: a unifying hypothesis. Trends Neurosci. 13: 474-479.
Kennedy PR, Gibson AR, Houk JC. (1986) Functional and anatomic differentiation between parvicellular and magnocellular regions of red nucleus in the monkey. Brain Res. 364: 124-136.
Kennedy PR, Humphrey DR. (1987) The compensatory role of the parvocellular division of the red nucleus in operantly conditioned rats. Neurosci. Res. 5: 39-62.
King JS, Bishop GA. (1990) Distribution and brainstem origin of cholecystokinin-like immunoreactivity in the opossum cerebellum. J.Comp. Neurol. 298: 373-384.
King JS, Bishop GA, Cummings SL, Ho RH. (1989) Localization of neuropeptides within the inferior olivary complex of the opossum. In: Strata P, editor. The olivocerebellar system in motor control. Berlin: Springer-Verlag; 177-186.
King JS, Schwyn RC, Fox CA. (1971) The red nucleus in the monkey (*Macaca mulatta*): a Golgi and an electron microscopic study. J. Comp. Neurol. 142: 75-108.
Kitai ST, Kocsis JD, Kiyohara T. (1976) Electrophysiological properties of nucleus reticularis tegmenti pontis cells: antidromic and synaptic activation. Exp.Brain Res. 24: 295-309.
Kitai ST, McCrea RA, Preston RJ, Bishop GA. (1977) Electrophysiological and horseradish peroxidase studies of precerebellar afferents to the nucleus interpositus anterior. I. Climbing fiber system. Brain Res. 122: 197-214.
Kitao Y, Nakamura Y, Kudo M, Moriizumi T, Tokuno H. (1989) The cerebral and cerebellar connections of pretecto-thalamic and pretecto-olivary neurons in the anterior pretectal nucleus in the cat. Brain Res. 484: 304-313.
Kitzman PH, Bishop GA. (1994) The origin of serotonergic afferents to the cat's cerebellar nuclei. J.Comp.Neurol. 340: 541-550.
Kitzman PH, Bishop GA. (1997) The physiological effects of serotonin on spontaneous and amino acid-induced activation of cerebellar nuclear cells: an in vivo study in the cat. In: De Zeeuw CI, Strata P and Voogd J, editors. The cerebellum: from structure to control. Vol 114. New York: Elsevier Science B.V.; 209-223.
Kneisley LW, Biber MP, LaVail JH. (1978) A study of the origin of brain stem projections to monkey spinal cord using the retrograde transport method. Exp.Neurol. 60: 116-139.
Koekkoek SKE, Ruigrok TJH. (1995) Lack of bilateral projection of individual spinal neurons to the lateral reticular nucleus in the rat: a retrograde, non-fluorescent, double labeling study. Neurosci.Lett. 200: 13-16.
Kooy FH. (1916) The inferior olive in vertebrates. Folia Neurobiol. 10: 205-369.
Korneliussen HK. (1968) On the morphology and subdivision of the cerebellar nuclei of the rat. J. Hirnforsch. 10: 109-122.

Künzle H, (1975) Autoradiographic tracing of the cerebellar projections from the lateral reticular nucleus. Exp. Brain Res. 22: 255-266.
Künzle H, Akert K. (1977) Efferent connections of cortical area 8 (frontal eye field) in Macaca fascicularis. A reinvestigation using the autoradiographic technique. J.Comp.Neurol. 173: 147-164.
Kurimoto Y, Kawaguchi S, Murata M. (1995) Cerebellotectal projection in the rat: anterograde and retrograde WGA-HRP study of individual cerebellar nuclei. Neurosci. Res. 22: 57-71.
Kuypers HGJM, Bentivoglio M, Catsman-Berrevoets CE, Bharos AT. (1980) Double retrograde neuronal labeling through divergent axon collaterals, using two fluorescent tracers with the same excitation wavelength which label different features of the cell. Exp. Brain. Res. 40: 383-392.
Kuypers HGJM, Catsman-Berrevoets CE, Padt RE. (1977) Retrograde axonal transport of fluorescent substances in the rat's forebrain. Neurosci. Lett. 6: 127-135.
Kuypers HGJM, Lawrence DG. (1967) Cortical projections to the red nucleus and the brain stem in the rhesus monkey. Brain Res. 4: 151-188.
Larsell O. (1970) The comparative anatomy and histology of the cerebellum from Monotremes through Apes. Minneapolis: The University of Minnesota Press.
Lee HS, Kosinski RJ, Mihailoff GA. (1989) Collateral branches of cerebellopontine axons reach the thalamus, superior colliculus or inferior olive: a double-fluorescence and combined fluorescence -horseradish peroxidase study in the rat. Neurosci. 28: 725-735.
Lee HS, Mihailoff GA. (1990) Convergence of cortical and cerebellar projections on single basilar pontine neurons: a light and electron microscopic study in the rat. Neurosci. 39: 561-577.
Legendre A, Courville J. (1987) Origin and trajectory of the cerebello-olivary projection: an experimental study with radioactive and fluorescent tracers in the cat. Neurosci. 21: 877-891.
Leichnetz, GR, Gonzalo-Ruiz, A. (1987) Collateralization of frontal eye field (medial precentral / anterior cingulate) neurons projecting to the paraoculomotor region, superior colliculus, and medial pontine reticular formation in the rat: a fluorescent double-labeling study. Exp. Brain Res. 68: 355-364.
Leiner HC, Leiner AL, Dow RS. (1993) Cognitive and language functions of the human cerebellum. Trends Neurosci. 16: 444-447.
Leiner HC, Leiner HC, Dow RS. (1986) Does the cerebellum contribute to mental skills? Behav. Neurosci. 100: 443-454.
Lemann W, Saper CB, Rye DB, Wainer BM. (1985) Stabilization of TMB reaction product for electronmicroscopic retrograde and anterograde fiber tracing. Brain Res.Bull. 14: 277-281.
Lidierth M, Apps R. (1990) Gating in the spino-olivocerebellar pathways to the c1 zone of the cerebellar cortex during locomotion in the cat. J. Physiol. (Lond.) 430: 453-469.
Linauts M, Martin GF. (1978) An autoradiographic study of midbrain-diencephalic projections to the inferior olivary nucleus in the opossum (Didelphis virginiana). J.Comp.Neurol. 178: 325-354.
Llewellyn-Smith IJ, Pilowsky P, Minson JB. (1992) Retrograde tracers for light and electron microscopy. In: Bolam JP, editor. Experimental Neuroanatomy. A practical approach. Oxford: Oxford University Press; 31-59.
Llinás R, Baker R, Sotelo C. (1974) Electrotonic coupling between neurons in the cat inferior olive. J. Neurophys. 37: 560-571.
Lund RD, Webster KE. (1967a) Thalamic afferents from the dorsal column nuclei. An experimental anatomical study in the rat. J. Comp. Neurol. 130: 301-12.
Lund RD, Webster KE. (1967b) Thalamic afferents from the spinal cord and trigeminal nuclei. An experimental anatomical study in the rat. J. Comp. Neurol. 130: 313-28.
Luppi P-H, Aston-Jones G, Akaoka H, Chouvet G, Jouvet M. (1995) Afferent projections to the rat locus coeruleus demonstrated by retrograde and anterograde tracing with cholera-toxin B subunit and Phaseolus Vulgaris Leucoagglutinin. Neurosci. 65: 119-160.
Luppi P-H, Fort P, Jouvet M. (1990) Iontophoretic application of unconjugated cholera toxin B subunit (CTb) combined with immunohistochemistry of neurochemical substances: a method for transmitter identification of retrogradely labeled neurons. Brain Res. 534: 209-224.
Magendie F. (1824) Mémoire sur les fonctions de quelques parties du sytème nerveux. Journal de Physiologie et Expérimentale Pathologie 3: 399-407.
Martin GF, Dom R, King JS, Robards M, Watson CRR. (1975) The inferior olivary nucleus of the opossum (Didelphis marsupialis virginiana) its organization and connections. J.Comp.Neurol. 160: 507-534.

Martin GF, King JS, Dom R. (1974) The projection of the deep cerebellar nuclei of the opossum, *Didelphis marsupialis virginiana*. J. Hirnforsch. 15: 545-573.
Massion J. (1988) Red nucleus: past and future. Behav. Brain Res. 28: 1-8.
Matsumoto RR, Walker JM. (1991) Inhibition of rubral neurons by noxious and non-noxious pressure. Brain Res. 556: 78-84.
May PJ, Porter JD, Gamlin PDR. (1992) Interconnections between the primate cerebellum and midbrain near-response regions. J. Comp. Neurol. 315: 98-116.
McCrea RA, Bishop GA, Kitai ST. (1978) Morphological and electrophysiological characteristics of projection neurons in the nucleus interpositus of the cat cerebellum. J. Comp. Neurol. 181: 397-420.
McDevitt CJ, Ebner TJ, Bloedel JR. (1987a) Changes in the responses of cerebellar nuclear neurons associated with the climbing fiber response of Purkinje cells. Brain Res. 425: 14-24.
McDevitt CJ, Ebner TJ, Bloedel JR. (1987b) Relationships between simultaneously recorded Purkinje cells and nuclear neurons. Brain Res. 425: 1-13.
Mehler WR. (1967) Double descending pathways originating from the superior cerebellar peduncle: An example of neural species differences. Anat. Rec. 157: 374.
Menétrey D. (1985) Retrograde tracing of neural pathways with a protein-gold complex. I. Light microscopic detection after silver intensification. Histochem. 83: 391-395.
Menétrey D, Lee CL. (1985) Retrograde tracing of neural pathways with a protein gold complex. II. Electron microscopic demonstration of projections and collaterals. Histochem. 83: 525-530.
Mihailoff G. (1993) Cerebellar nuclear projections from the basilar pontine nuclei and nucleus reticularis tegmenti pontis as demonstrated with PHA-L tracing in the rat. J. Comp. Neurol. 330: 130-146.
Mihailoff GA. Intrahemispheric and interhemispheric branching in the pontocerebellar system, a fluorescent double label study in the rat. Neurosci. 1983; 10: 141-160.
Mihailoff GA. (1994) Identification of pontocerebellar axon collateral synaptic boutons in the rat cerebellar nuclei. Brain Res. 648: 313-318.
Mihailoff GA, Burne RA, Azizi SA, Norell G, Woodward DJ. (1981a) The pontocerebellar system in the rat: an HRP study. II. Hemispheral components. J. Comp. Neurol. 197: 559-577.
Mihailoff GA, Kosinski RJ, Azizi SA, Border BG. (1989) Survey of noncortical afferent projections to the basilar pontine nuclei: a retrograde tracing study in the rat. J. Comp. Neurol. 282: 617-643.
Mihailoff GA, Kosinski RJ, Border BG, Lee HS. (1988) A review of recent observations concerning the synaptic organization of the basilar pontine nuclei. J. Electr. Microsc. Techn. 10: 229-246.
Mihailoff GA, Lee H, Watt CB, Yates R. Projections to the basilar pontine nuclei from face sensory and motor regions of the cerebral cortex in the rat. J. Comp. Neurol. 1985; 237: 251-263.
Mihailoff GA, McArdle CB, Adams CE. (1981b) The cytoarchitecture, cytology, and synaptic organization of the basilar pontine nuclei in the rat. I. Nissl and Golgi studies. J. Comp. Neurol. 195: 181-201.
Milak MS, Bracha V, Bloedel JR. (1995) Relationship of simultaneously recorded cerebellar nuclear neuron discharge to the acquisition of a complex, operantly conditioned forelimb movement in cats. Exp.Brain Res. 105: 325-330.
Moffett JR, Palkovits M, Namboodiri A, Neale JH. (1994) Comparative distribution of N-acetylaspartylglutamate and GAD67 in the cerebellum and precerebellar nuclei of the rat utilizing enhanced carbodiimide fixation and immunohistochemistry. J.Comp.Neurol. 347: 598-618.
Monaghan PL, Beitz AJ, Larson AA, Altschuler RA, Madl JE, Mullet MA. (1986) Immunocytochemical localization of glutamate-, glutaminase- and aspartate aminotransferase-like immunoreactivity in the rat deep cerebellar nuclei. Brain Res. 363: 364-370.
Mugnaini E, Oertel WH. (1981) Distribution of decarboxylase positive neurons in the rat cerebellar nuclei. Soc.Neurosci.Abstr. 7: 122.
Murakami F, Katsumaru H, Wu JY, Matsuda T, Tsukahara N. (1983) Immunocytochemical demonstration of GABAergic synapses on identified rubrospinal neurons. Brain Res. 267: 357-360.
Murphy JT, Sabah NH. (1971a) Cerebellar Purkinje cell responses to afferent inputs. I. Climbing fiber activation. Brain Res. 25: 449-467.
Murphy JT, Sabah NH. (1971b) Cerebellar Purkinje cell responses to afferent inputs. II. Mossy fiber activation. Brain Res. 25: 469-482.
Murray HM, Gurule ME. (1979) Origin of the rubrospinal tract of the rat. Neurosci.Lett. 14: 19-23.

Nakamura Y, Kitao Y, Okoyama S. (1983) Cortico-Darkschewitsch-olivary projection in the cat: an electron microscope study with the aid of horseradish peroxidase tracing technique. Brain Res. 274: 140-143.
Nakano K, Takimoto T, Kayahara T, Takeuchi Y, Kobayashi Y. (1980) Distribution of cerebellothalamic neurons projecting to the ventral nuclei of the thalamus: an HRP study in the cat. J.Comp.Neurol. 194: 427-439.
Nelson BJ, Mugnaini E. (1984) A GABAergic cerebello-olivary projection in the rat. Soc.Neurosci.Abstr. 10: 539.
Nelson BJ, Mugnaini E. (1988) The rat inferior olive as seen with immunostaining for glutamate decarboxylase. Anat. Embryol. 179: 109-127.
Nelson BJ, Mugnaini E. (1989) Origins of GABAergic inputs to the inferior olive. In: Strata P, editor. The olivocerebellar system in motor control. Vol 17. Berlin Heidelberg: Springer-Verlag; 86-107.
Newman DB. (1985a) Distinguishing rat brainstem reticulospinal nuclei by their neuronal morphology. I. Medullary nuclei. J. Hirnforsch. 26: 187-226.
Newman DB. (1985b) Distinguishing rat brainstem reticulospinal nuclei by their neuronal morphology. II. Pontine and mesencephalic nuclei. J. Hirnforsch. 26: 385-418.
Nicolelis MAL, Chapin JK, Lin RCS. (1992) Somatotopic maps within the zona incerta relay parallel GABAergic somatosensory pathways to the neocortex, superior colliculus, and brainstem. Brain Res. 577: 134-141.
Nieuwenhuys R, Ten Donkelaar HJ, Nicholson C. (1998) The central nervous system of vertebrates. Berlin: Springer Verlag.
Nisimaru N, Okahara K, Nagao S. (1991) Olivocerebellar projection to the cardiovascular zone of rabbit cerebellum. Neurosci. Res. 12: 240-250.
Noda H. (1991) Cerebellar control of saccadic eye movements: its neural mechanisms and pathways. Jap. J. Physiol. 41: 351-368.
Oka H. (1988) Functional organization of the parvocellular red nucleus in the cat. Behav. Brain Res. 28: 233-240.
Oka H, Jinnai K, Yamamoto T. (1979) The Parieto-rubro-olivary Pathway in the Cat. Exp. Brain Res. 37: 115-125.
Olson L, Fuxe K. (1971) On the projections from the locus coeruleus noradrenalin neurons: the cerebellar innervation. Brain Res. 28: 165-171.
Omori O, Umetani T, Sugioka K. (1997) Projections from the subdivisions of the fastigial nucleus to the vestibular complex and the prepositus hypoglossal nucleus in the albino rat: an anterograde tracing study using biocytin. Kobe J.Med.Sci. 43: 37-54.
Onodera S. (1984) Olivary projections from the mesodiencephalic structures in the cat studied by means of axonal transport of horseradish peroxidase and tritiated amino-acids. J. Comp. Neurol. 227: 37-49.
Onodera S, Hicks TP. (1995) Patterns of transmitter labelling and connectivity of the cat's nucleus of Darkschewitsch: a wheat germ agglutinin-horseradish peroxidase and immunocytochemical study at light and electron microscopical levels. J.Comp.Neurol. 361: 553-573.
Oscarsson O. (1969) The sagittal organization of the cerebellar anterior lobe as revealed by the projection patterns of the climbing fiber system. In: Llinas R, editor. Neurobiology of cerebellar evolution and development. Chicago: AMA-ERF 525-537.
Oscarsson O. (1979) Functional units of the cerebellum - sagittal zones and microzones. TINS 2: 143-145.
Oscarsson O. (1980) Functional organization of olivary projections to the cerebellar anterior lobe. In: Courville J, de Montigny C and Lamarre Y, editors. The inferior olivary nucleus, anatomy and physiology. New York: Raven Press; 279-289.
Ostrowska A, Sikora E, Mierzejewska-Krzyzowksa B, Zimny R. (1993) The dentatorubral projection in the rabbit with emphasis on distinction from the interpositorubral connectivity: an HRP retrograde tracer study. J.Hirnforsch. 34: 9-23.
Ottersen OP. (1993) Neurotransmitters in the cerebellum. Rev.Neurol. 149: 629-636.
Päällysaho J, Sugita S, Noda H. (1990) Cerebellar corticonuclear and nucleocortical projections in the vermis of the posterior lobe of the rat as studied with anterograde and retrograde transport of WGA-HRP. Neurosci. Res. 8: 158-178.
Padel Y, Angaut P, Massion J, Sedan R. (1981) Comparative study of the posterior red nucleus in the baboons and gibbons. J.Comp.Neurol. 202: 421-438.

Palkovits M, Mezey E, Hamori T, Szénthàgothài J. (1977) Quantitative histological analysis of the cerebellar nuclei in the cat. I. Numerical data on cells and on synapses. Exp.Brain Res. 28: 189-209.

Paxinos G, Watson C. (1986) The rat brain in stereotaxic coordinates. Sidney: Academic Press.

Peschanski M, Mantyh PW. (1983) Efferent connections of the subfascicular area of the mesodiencephalic junction and its possible involvement in stimulation-produced analgesia. Brain Res. 263: 181-190.

Peters A, Palay SL, Webster HD. (1991) The fine structure of the nervous system. New York, Oxford: Oxford University Press.

Poirier LJ, Bouvier G. (1966) The red nucleus and its efferent nervous pathways in the monkey. J.Comp.Neurol. 128: 223-244.

Pompeiano O, Brodal A. (1957) Experimental demonstration of a somatotopical origin of rubrospinal fibres in the cat. J.Comp.Neurol. 108: 225-252.

Precht W. (1981) Functional organization of optokinetic pathways in mammals. In: Fuchs AF and Becker W, editors. Progress in oculomotor Res.. Amsterdam: Elsevier Science Publishers; 425-433.

Precht W, Strata P. (1980) On the pathway mediating optokinetic responses in vestibular nuclear neurons. Neurosci. 5: 777-787.

Price JL. (1995) Thalamus. In: Paxinos G, editor. The rat nervous system. New York: Academic Press; 629-648.

Qvist H. (1989) Demonstration of axonal branching of fibres from certain precerebellar nuclei to the cerebellar cortex and nuclei: a retrograde fluorescent double-labelling study in the cat. Exp. Brain Res. 75: 15-27.

Qvist H, Dietrichs E, Walberg F. (1984) An ipsilateral projection from the red nucleus to the lateral reticular nucleus in the cat. Anat. Embryol. 170: 327-330.

Ralston DD. (1991) Cortical and cerebellar convergence upon single neurons in the primate red nucleus, an electron microscopic analysis. Soc.Neurosci.Abstr. 17: 469.

Ralston DD. (1994) Red nucleus of Macaca fascicularis: an electron microscopic study of its organization in relation to afferent and efferent connectivity and proposals for the role of the red nucleus in motor mechanisms. Anatomy. Groningen: Rijksuniversiteit Groningen; 114.

Ralston DD, Milroy AM. (1992) Inhibitory synaptic input to identified rubrospinal neurons in *Macaca fascicularis:* an electron microscopic study using a combined immuno-GABA-gold technique and the retrograde transport of WGA-HRP. J. Comp. Neurol. 320: 97-109.

Reid JM, Flumerfelt BA, Gwyn DG. (1975a) An ultrastructural study of the red nucleus in the rat. J. Comp. Neurol. 162: 363-386.

Reid JM, Gwyn DG, Flumerfelt BA. (1975b) A cytoarchitectonic and Golgi study of the red nucleus in the rat. J.Comp. Neurol. 162: 337-362.

Ricardo JA. (1981) Efferent connections of the subthalamic regions of the rat. II. The zona incerta. Brain Res. 214: 43-60.

Robinson FR, Houk JC, Gibson AR. (1987) Limb specific connections of the cat magnocellular red nucleus. J.Comp.Neurol. 257: 553-577.

Roger M, Cadusseau J. (1985) Afferents to the zona incerta in the rat: a combined retrograde and anterograde study. J. Comp. Neurol. 241: 480-492.

Roger M, Cadusseau J. (1987) Anatomical evidence of a reciprocal connection between the posterior thalamic nucleus and the parvocellular division of the red nucleus in the rat. A combined retrograde and anterograde study. Neurosci. 21: 573-583.

Rolando L. (1809) Saggio sopra la vera struttura del cervello dell'uomo e degli animali e sopra le funcioni del sistema nervoso: Sassari: Stamperia Da S.S.R.M.Privilegiata.

Rosina A, Provini L. (1983a) Somatotopy of climbing fiber branching to the cerebellar cortex in cat. Brain Res. 289: 45-63.

Rosina A, Provini L. (1983b) Somatotopy of climbing fiber collaterals of single inferior olive neurons. Brain Res. 289: 45-63.

Rosina A, Provini L. (1987) Spatial distribution of axon collaterals of single inferior olive neurones. J.Comp.Neurol. 256: 317-328.

Roth J. (1983) The colloidal gold marker system for light and electron microscopic cytochemistry. In: Bullock GR and Petrusz P, editors. Techniques in immunocytochemistry. Vol 2. London: Academic Press; 217-284.

Rubertone JA, Haroian AJ, Vincent SL, Mehler WR. (1990) The rat parvocellular reticular formation: I. Afferents from the cerebellar nuclei. Neurosci Lett. 119: 79-82.
Rubertone JA, Mehler WR, Voogd J. (1995a) Vestibular nuclear complex. In: Paxinos G, editor. The rat central nervous system. New York: Academic Press; 773-796.
Rubertone JA, Mehler WR, Voogd J. (1995b) The vestibular nuclear complex. In: Paxinos G, editor. The rat nervous system. Sydney: Academic Press; 773-796.
Ruigrok T, Koekkoek B, Krumm P. (1993) On the existence of cerebellar nucleo-rubro-olivary circuits - an anterograde and retrograde tracer study in the rat. Eur. J. Neurosci. Suppl. 6: 125.
Ruigrok TJH. (1997) Cerebellar nuclei: the olivary connection. In: De Zeeuw CI, Strata P and Voogd J, editors. The cerebellum: from structure to control. Vol Progr. Brain Res. 114: Elsevier Science B.V.; 162-197.
Ruigrok TJH, Cella F. (1995) Precerebellar nuclei and red nucleus. In: Paxinos G, editor. The rat nervous system. Sydney: Academic Press: 277-308.
Ruigrok TJH, Cella F, Voogd J. (1995a) Connections of the lateral reticular nucleus to the lateral vestibular nucleus in the rat. An anterograde tracer study with *Phaseolus vulgaris* leucoagglutinin. Eur. J. Neurosci. 7: 1410-1413.
Ruigrok TJH, de Zeeuw CI, van der Burg J, Voogd J. (1990) Intracellular labeling of neurons in the medial accessory olive of the cat. I. Physiology and light microscopy. J. Comp. Neurol. 300: 462-477.
Ruigrok TJH, Teune TM, van der Burg J, Sabel-Goedknegt H. (1995b) A retrograde double labeling technique for light microscopy. A combination of axonal transport of cholera toxin B-subunit and a gold-lectin conjugate. J. Neurosci. Meth. 61: 127-138.
Ruigrok TJH, Teune TM, van der Burg J, Voogd J. (1994) Electrical stimulation of the inferior olive results in enhanced activity of projection neurons in the cerebellar nuclei of the ketamine anesthetized rat. Soc. Neurosci. Abstr. 20: 1744.
Ruigrok TJH, Voogd J. (1988) Evidence for cerebello-midbrain-olivary circuits in rat using PHA-L anterograde, and gold labeled WGA-BSA retrograde tracing. Europ. J. Neurosci. Suppl. no. 1: 24.
Ruigrok TJH, Voogd J. (1990) Cerebellar nucleo-olivary projections in rat. An anterograde tracing study with *Phaseolus vulgaris*-leucoagglutinin (PHA-L). J. Comp. Neurol. 298: 315-333.
Ruigrok TJH, Voogd J. (1995a) Cerebellar influence on olivary excitability in the cat. Eur. J. Neurosci. 7: 679-693.
Ruigrok TJH, Voogd J. (1995b) Olivary projection to the cerebellar nuclei in the rat. Eur. J. Neurosci. Suppl. 8: 99.
Rutherford JG. (1995) An investigation of a possible direct projection from the medial nucleus of the cerebellum to the paraventricular nucleus of the hypothalamus in the rat: a study using retrograde WGA-HRP and Fluoro-gold tracing techniques. Anat.Embryol. 192: 229-238.
Rutherford JG, Anderson WA, Gwyn DG. (1984) A reevaluation of midbrain and diencephalic projections to the inferior olive in rat with particular reference to the rubro-olivary pathway. J. Comp. Neurol. 229: 285-300.
Saint-Cyr JA. (1987) Anatomical organization of cortico-mesencephalo-olivary pathways in the cat as demonstrated by axonal transport techniques. J. Comp. Neurol. 257: 39-59.
Sakaguchi H, Kubota M, Nakamura M, Tsukahara N. (1984) Effects of amino acids on cat red nucleus neurons in vitro. Exp.Brain Res. 54: 150-156.
Saper CB. (1995) Central autonomic system. In: Paxinos G, editor. The rat central nervous system. New York: Academic Press; 107-135.
Sato Y, Barmack NH. (1985) Zonal organization of olivocerebellar projections to the uvula in rabbits. Brain Res. 359: 281-191.
Sato Y, Kawasaki T. (1990a) Eye movement evoked by stimulation of Purkinje cell zones of the cerebellar flocculus in the cat. Acta Med. Biol. 38: 27-35.
Sato Y, Kawasaki T. (1990b) Operational unit responsible for plane-specific control of eye movement by cerebellar flocculus in cat. J. Neurophys. 64: 551-564.
Sato Y, Kawasaki T, Ikarashi K. (1982) Zonal organization of the floccular Purkinje cells projecting to the group y of the vestibular nuclear complex and the lateral cerebellar nucleus in cats. Brain Res. 234: 430-434.
Sato Y, Kawasaki T, Mizukoshi K. (1991) Eye movement control by Purkinje cell/climbing fiber zones of cerebellar flocculus in cat. Acta Otolaryngol. 481: 237-241.

Sato Y, Miura A, Fushiki H, Kawasaki T. (1993) Barbiturate depresses simple spike activity of cerebellar Purkinje cells after climbing fiber input. J. Neurophys. 69: 1082-1090.
Schmahmann JD. (1991) An emerging concept. The cerebellar contribution to higher function. Arch. Neurol. 48: 1178-1187.
Schmahmann JD. (1996) From movement to thought: anatomic substrates of the cerebellar contribution to cognitive processing. Hum Brain Mapp. 4: 174-198.
Schmahmann JD, Pandya DN. (1995) Prefrontal cortex projections to the basilar pons in rhesus monkey: implications for the cerebellar contribution to higher function. Neurosci. Lett. 199: 175-178.
Schmied A, Amalric M, Dormont JF, Farin D. GABAergic control of rubral single unit activity during a reaction time task. Exp.Brain Res. 1991; 84: 285-296.
Schmued LC, Fallon JH. (1986) Fluoro-Gold: a new fluorescent retrograde axonal tracer with numerous unique properties. Brain Res. 377: 147-154.
Schulman JA, Finger TE, Brecha NC, Karten HJ. (1981) Enkephalin immunoreactivity in Golgi cells and mossy fibers of mammalian, avian, amphibian and teleost cerebellum. Neurosci. 6: 2407-2416.
Sefton AJ, Dreher B. Visual System. In: Paxinos G, editor. The rat nervous system. New York: Academic Press, 1995: 833-898.
Shammah-Lagnado SJ, Costa MS, Ricardo JA. (1992) Afferent connections of the parvocellular reticular formation: a horseradish peroxidase study in the rat. Neurosci. 50: 403-425.
Shammah-Lagnado SJ, Negrao N, Ricardo JA. (1985) Afferent connections of the zona incerta: a horseradish peroxidase study in the rat. Neurosci. 15: 109-134.
Shieh JY, Leong SK, Wong WC. (1983) Origin of the rubrospinal tract in neonatal, developing, and mature rats. J. Comp. Neurol. 214: 79-86.
Shinoda Y, Futami T, Mitoma H, Yokota J. (1988) Morphology of single neurones in the cerebello-rubrospinal system. Behav. Brain Res. 28: 59-64.
Shinonaga Y, Takada M, Mizuno N. (1992) Direct projection from the central amygdaloid nucleus to the globus pallidus and substantia nigra in the cat. Neurosci. 51: 691-703.
Snider RS, Stowell A. (1944) Receiving areas of tactile, auditory and visual systems in the cerebellum. J.Neurophys. 7: 331-357.
Somogyi P, Halasy K, Somogyi J, Storm-Mathisen J, Ottersen OP. (1986) Quantification of immunogold labelling reveals enrichment of glutamate in mossy and parallel fibre terminals in cat cerebellum. Neurosci. 49: 1045-1050.
Sotelo C, Gotow T, Wassef M. (1986) Localization of glutamic-acid-decarboxylase -immunoreactive axon terminals in the inferior olive of the rat, with special emphasis on anatomical relations between GABAergic synapses and dendrodendritic gap junctions. J. Comp. Neurol. 252: 32-50.
Sousa-Pinto A. (1969) Experimental anatomical demonstration of a cortico-olivary projection from area 6 (supplementary motor area?) in the cat. Brain Res. 16: 73-83.
Sousa-Pinto A. (1970) The cortical projection onto the paramedian reticular and perihypoglossal nuclei (nucleus prepositus hypoglossi, nucleus intercalatus and nucleus of Roller) of the medulla oblongata of the cat. An experimental anatomical study. Brain Res. 18: 77-91.
Spence SJ, Saint-Cyr JA. (1988) Comparative topography of projections from the mesodiencephalic junction to the inferior olive, vestibular nuclei, and upper cervical cord in the cat. J. Comp. Neurol. 268: 357-374.
Stanton GB. (1980) Topographical organization of ascending cerebellar projections from the dentate and interposed nuclei in Macaca mulatta: an anterograde degeneration study. J.Comp.Neurol. 190: 699-731.
Steinmetz JE, Sengelaub DR. (1992) Possible conditioned stimulus pathway for classical eyelid conditioning in rabbits. I. Anatomical evidence for direct projections from the pontine nuclei to the cerebellar interpositus nucleus. Behav. Neur. Biol. 57: 103-115.
Strahlendorf JC, Lee M, Strahlendorf HK. (1991) Serotonin modulates muscimol- and baclofen-elicited inhibition of cerebellar Purkinje cells. Eur. J. Pharmacol. 201: 239-242.
Strominger RN, McGiffen JE, Strominger NL. (1987) Morphometric and experimental studies of the red nucleus in the albino rat. Anat. Rec. 219: 420-428.
Sugimoto T, Mizuno N, Uchida K. (1982) Distribution of cerebellar fiber terminals in the midbrain visuomotor areas: an autoradiographic study in the cat. Brain Res. 238: 353-370.

Supko DE, Uretsky NJ, Wallace LJ. (1991) Activation of AMPA/kainic acid glutamate receptors in the zona incerta stimulates locomotor behavior. Brain Res. 564: 159-163.
Swenson RS, Castro AJ. (1983a) The afferent connections of the inferior olivary complex in rats. An anterograde study using autoradiographic and axonal degeneration techniques. Neurosci. 8: 259-275.
Swenson RS, Castro AJ. (1983b) The afferent connections of the inferior olivary complex in rats: a study using the retrograde transport of horseradish peroxidase. Am. J. Anat. 166: 329-341.
Szentágothai J, Rajkovits U. (1959) Über den Ursprung der Kletternfasern des Kleinhirns. Z. Anat. Entwickl.-Gesch. 121: 120-141.
Taber E. (1961) The cytoarchitecture of the brain stem of the cat. I. Brain stem nuclei of the cat. J. Comp. Neurol. 116: 27-69.
Takeda T, Maekawa K. (1984) Collateralized projection of visual climbing fibers to the flocculus and nodulus of the rabbit. Neurosci. Res. 2: 125-132.
Tan J, Gerrits NM, Nanhoe JI, Simpson JI, Voogd J. (1995) Zonal organisation of the climbing fiber projection to the flocculus and nodulus of the rabbit: A combined axonal tracing and acetylcholinesterase histochemical study. J.Comp.Neurol. 356: 23-50.
Tarnecki R. (1988) Functional connections between neurons of interpositus nucleus of the cerebellum and the red nucleus. Behav. Brain Res. 28: 117-125.
Tempia F, Dieringer N, Strata P. (1991) Adaptation and habituation of the vestibulo-ocular reflex in intact and inferior olive-lesioned rats. Exp. Brain Res. 86: 568-578.
ten Donkelaar HJ. (1988) Evolution of the red nucleus and rubrospinal tract. Behav. Brain Res. 28: 9-20.
Terasawa K, Otani K, Yamada J. (1979) Descending pathways of the nucleus of the optic tract in the rat. Brain Res. 173: 405-417.
Teune TM, van der Burg J, De Zeeuw CI, Voogd J, Ruigrok TJH. (1998) Single Purkinje cell can innervate multiple classes of projection neurons in the cerebellar nuclei of the rat: a light microscopic and ultrastructural triple-tracer study in the rat. J. Comp. Neurol. 392: 164-178.
Teune TM, Van der Burg J, Ruigrok TJH. (1995) Cerebellar projections to the red nucleus and inferior olive originate from separate populations of neurons in the rat. A non-fluorescent double labeling study. Brain Res. 673: 313-319.
Teune TM, van der Burg J, Voogd J, Ruigrok TJH. (1999) Cerebellar collateralization to prerubral, rubral, pontine reticulotegmental and inferior olivary nuclei. A non-fluorescent double retrograde tracing study in the rat. J. Comp. Neurol. submitted.
Thach WT. (1996) On the specific role of the cerebellum in motor learning and cognition: clues from PET activation and lesion studies in man. Behav Brain Sci. 19: 411.
Thielert CD, Thier P. (1993) Patterns of projections from the pontine nuclei and the nucleus reticularis tegmenti pontis to the posterior vermis in the rhesus monkey: a study using retrograde tracers. J.Comp.Neurol. 337: 113-126.
Tolbert D, Kultas-Ilinsky K, Ilinsky I. (1980) EM-autoradiography of cerebellar nucleocortical terminals in the cat. Anat.Embryol. 161: 215-223.
Tolbert DL, Alisky JM, Clark BR. (1993) Lower thoracic upper lumbar spinocerebellar projections in rats: a complex topography revealed in computer reconstructions of the unfolded anterior lobe. Neurosci. 55: 755-774.
Tolbert DL, Bantli H, Bloedel JR. (1978a) Multiple branching of cerebellar efferent projections in cats. Exp.Brain Res. 31: 305-316.
Tolbert DL, Bantli H, Bloedel JR. (1978b) Organizational features of the cat and monkey cerebellar nucleocortical projection. J.Comp.Neurol. 182: 39-56.
Tolbert DL, Massopust LC, Murphy MG, Young PA. (1976) The anatomical organization of the cerebello-olivary projection in the cat. J. Comp. Neurol. 170: 525-544.
Tong G, Robertson LT, Brons J. (1993) Climbing fiber representation of the renal afferent nerve in the vermal cortex of the cat cerebellum. Brain Res. 601: 65-75.
Toonen M, van Dijken H, Holstege JC, Ruigrok TJH, Koekkoek SKE, Hawkins RK, et al. (1998) Light microscopic and ultrastructural investigation of the dopaminergic innervation of the ventrolateral outgrowth of the rat inferior olive. Brain Res. 802: 267-273.
Torigoe Y, Blanks RH, Precht W. (1986a) Anatomical studies on the nucleus reticularis tegmenti pontis in the pigmented rat. II. Subcortical afferents demonstrated by the retrograde transport of horseradish peroxidase. J. Comp. Neurol. 243: 88-105.

Torigoe Y, Blanks RHI, Precht W. (1986b) Anatomical studies on the nucleus reticularis tegmenti pontis in the rat. I. Cytoarchitecture, topography, and cerebral cortical afferents. J. Comp. Neurol. 243: 71-87.
Toyama K, Tsukahara N, Udo M. (1968) Nature of cerebellar influences upon the red nucleus neurones. Exp. Brain Res. 4: 292-309.
Travers JB. (1995) Oromotor nuclei. In: Paxinos G, editor. The rat nervous system. New York: Academic Press; 239-255.
Trott JR, Apps R. (1993) Zonal organization within the projection from the inferior olive to the rostral paramedian lobule of the cat cerebellum. Eur.J.Neurosci. 5: 162-173.
Tsukahara N. (1972) The properties of the cerebello-pontine reverberating circuit. Brain Res. 40: 67-71.
Tsukahara N, Bando T, Kitai ST, Kiyohara T. (1971) Cerebello-pontine reverberating circuit. Brain Res. 33: 233-237.
Tsukahara N, Bando T, Murakami F, Oda Y. (1983) Properties of cerebello-precerebellar reverberating circuits. Brain Res. 274: 249-259.
Tucker CL, Kennedy PR. (1990) Re-defining rat red nucleus: cytoarchitectural analysis of red nucleus neurons singly and doubly labelled from spinal cord and inferior olivary nucleus. Neurosci. Abstr. 16: 729.
Tucker CL, Lee SA, Kennedy PR. (1989) Re-defining rat red nucleus: cytoarchitecture and connectivity. Neurosci. Abstr. 15: 405.
Umetani T. (1989) Topographic organization of the corticonuclear fibers from the tuber vermis and paramedian lobule in the albino rat. Brain Behav.Evol. 33: 334-341.
Umetani T, Tabuchi T. (1988) Topographic organization of the corticonuclear and corticovestibular projections from the pyramis and copula pyramidis in the albino rat. Brain Behav.Evol. 32: 160-168.
Van Bockstaele EJ, Aston-Jones G. (1992) Collateralized projections from neurons in the rostral medulla to the nucleus locus coeruleus, the nucleus of the solitary tract and the periaqueductal gray. Neurosci. 49: 653-668.
van der Steen J, Simpson JI, Tan J. (1991) Representation of three-dimensional eye movements in the cerebellar flocculus of the rabbit. In: Schmid R and Zambarbieri D, editors. Oculomotor control and cognitive processes. North Holland: Elsevier Science Publishers B.V.; 63-77.
van der Steen J, Simpson JI, Tan J. (1994) Functional and anatomic organization of three-dimensional eye movements in rabbit cerebellar flocculus. J. Neurophys. 72: 31-46.
Van der Want J, Borsello T, Rossi F, Strata P. (1994) Climbing fibre collateral innervation of the deep cerebellar nuclei in the rat. A combined anterograde tracing and GABA immuno-electronmicroscopic study. Eur. J. Neurosci. Suppl. 7: 12.
van der Want JJL, Gerrits NM, Voogd J. (1987) Autoradiography of mossy fiber terminals in the fastigial nucleus of the cat. J. Comp. Neurol. 258: 70-80.
van der Want JJL, Guegan M, Wiklund L, Buisseret-Delmas C, Ruigrok TJH, Voogd J. (1989) Climbing fibre "collateral" innervation of the central cerebellar nuclei studied with anterograde *Phaseolus vulgaris*-leucoagglutinin (PHA-L) labelling. In: Strata P, editor. The olivocerebellar system in motor control. Vol 17. Berlin: Springer-Verlag; 82-85.
Van Ham JJ, Yeo CH. (1992) Somatosensory trigeminal projections to the inferior olive, cerebellum and other precerebellar nuclei in rabbits. Eur. J. Neurosc. 4: 302-317.
van Kan PLE, Houk JC, Gibson AR. (1993) Output organization of intermediate cerebellum of the monkey. J. Neurophys. 69: 57-73.
Vaudano E, Legg CR. (1992) Cerebellar connections of the ventral lateral geniculate nucleus in the rat. Anat. Embryol. 186: 583-588.
Veenman CL, Reiner A, Honig MG. (1992) Biotinylated dextran amine as an anterograde tracer for single- and double-labeling studies. J.Neurosci. Meth. 41: 239.
Verveer C, Hawkins RK, Ruigrok TJH, De Zeeuw CI. (1997) Ultrastructural study of the GABAergic and cerebellar input t o the nucleus reticularis tegmenti pontis. Brain Res. 766: 289-296.
Von Monakow C. (1909) Der rote Kern, die Haube und die Regio subthalamica bei einige Säugetieren und beim Menschen. 1. Anatomisches und Experimentelles. Arb. Hirnanat. Inst. Zurich 3: 51-267.
Voogd J. (1964) The cerebellum of the cat: Structure and fiber connections. Assen: Van Gorcum.

Voogd J. (1995) The cerebellum. In: Paxinos G, editor. The rat nervous system. Sydney: Academic Press; 309-350.
Voogd J, Bigaré F. (1980) Topographical distribution of olivary and cortico nuclear fibers in the cerebellum: a review. In: Courville J, de Montigny C and Lamarre Y, editors. The inferior olivary nucleus. Anatomy and physiology. New York: Raven Press; 207-234.
Voogd J, Broere G, Rossum J. (1969) The medio-lateral distribution of the spinocerebellar projection in the anterior lobe and the simple lobule in the cat and a comparison with some other afferent systems. Psychiat. Neurol. Neurochir. 72: 137-151.
Voogd J, Epema AH, Rubertone JA. (1991) Cerebello-vestibular connections of the anterior vermis. A retrograde tracer study in different mammals including primates. Arch.Ital.Biol. 129: 3-19.
Voogd J, Gerrits NM, Ruigrok TJH. (1996a) Organization of the vestibulocerebellum. Ann. New York Acad. Sci. 781: 553-579.
Voogd J, H.K.P. F, Schoen JHR. (1990) Cerebellum and precerebellar nuclei. In: Paxinos G, editor. The human nervous system. New York: Academic Press.
Voogd J, Jaarsma D, Marani E. (1996b) The cerebellum: chemoarchitecture and anatomy. In: Swanson LW, Björklund A and Hökfelt T, editors. Handbook of Chemical Neuroanatomy. Vol 12: Elsevier Sience B.V.; 1-369.
Voogd J, Ruigrok TJH. (1997) Transverse and longitudinal patterns in the mammalian cerebellum. In: De Zeeuw CI, Strata P and Voogd J, editors. The cerebellum: From structure to control. Vol Progr.Brain Res.114. Amsterdam: Elsevier; 21-37.
Vuillon-Cacciuttolo G, Bosler O, Nieoullon A. (1984) GABA neurons in the cat red nucleus: a biochemical and immunohistochemical demonstration. Neurosci. Lett. 52: 129-134.
Walberg F. (1956) Descending connections to the inferior olive. An experimental study in the cat. J. Comp. Neurol. 104: 77-174.
Walberg F. (1958) Descending connections to the inferior olive. J.Comp.Neurol. 109: 363-389.
Walberg F, Nordby T, Hoffmann KP, Hollander H. (1981) Olivary afferents from the pretectal nuclei in the cat. Anat.Embryol. 161: 291-304.
Walberg F, Pompeiano O. (1960) Fastigiofugal fibres to the lateral reticular nucleus; an experimental study in the cat. Exp. Neurol. 2: 40-53.
Walberg F, Pompeiano O, Brodal A, Jansen J. (1962) The fastigiovestibular projection in the cat. An experimental study with silver impregnation methods. J.Comp.Neurol. 118: 49-73.
Waldron HA, Gwyn DG. (1969) Descending nerve tracts in the spinal cord of the rat. I. Fibers from the midbrain. J.Comp.Neurol. 137: 143-154.
Waldrop TG, Iwamoto GA. (1991) Cardiovascular responses to chemical stimulation of the inferior olive in the cat. Brain Res. Bull. 26: 667-670.
Watt CB, Mihailoff GA. (1983a) The cerebello-pontine system in the rat. I. Autoradiographic studies. J. Comp. Neurol. 215: 312-330.
Watt CB, Mihailoff GA. (1983b) The cerebellopontine system in the rat. II. Electron microscopic studies. J. Comp. Neurol. 216: 429-437.
Weber JT, Harting JK. (1980) The efferent projections of the pretectal complex: an autoradiographic and horseradish peroxidase analysis. Brain Res. 194: 1-28.
Welker W. (1987) Spatial organization of somatosensory projections to granule cell cerebellar cortex: functional and connectional implications of fractured somatotopy (summary of Wisconsin studies). In: King JS, editor. New concepts in cerebellar neurobiology. New York: Alan R. Liss, Inc.; 239-280.
Wells GR, Hardiman MJ, Yeo CH. (1989) Visual projections to the pontine nuclei in the rabbit: orthograde and retrograde tracing studies with WGA-HRP. J. Comp. Neurol. 279: 629-652.
Welsh JP, Lang EJ, Sugihara I, Llinas R. (1995) Dynamic organization of motor control within the olivocerebellar system. Nature 374: 453-457.
Westby GWM, Collinson C, Dean P. (1993) Excitatory drive from deep cerebellar neurons to the superior colliculus in the rat: an electrophysiological mapping study. Eur.J.Neurosci. 5: 1378-1388.
Wharton SM, Payne JN. (1985) Axonal branching in parasagittal zones of the rat olivocerebellar projection: a retrograde fluorescent double labelling study. Exp.Brain Res. 58: 183-189.
Wigston DJ, Kennedy PR. (1987) Selective reinnervation of transplanted muscles by their original motoneurons in the axolotl. J.Neurosci. 7: 1857-1965.

Wiklund L, Björklund A, Sjölund B. (1977) The indolaminergic innervation of the inferior olive. I. Convergence with direct spinal afferents in the areas projecting to the cerebellar anterior lobe. Brain Res. 131: 1-21.

Wiklund L, Toggenburger G, Cuenod M. (1984) Selective retrograde labelling of the rat olivocerebellar climbing fiber system with D-[^{3}H]aspartate. Neurosci. 13: 441-468.

Woodson W, Angaut P. (1984) The distribution and origin of the ipsilateral descending limb of the brachium conjunctivum. An autoradiographic and horseradish peroxidase study in the rat. Exp.Brain Res. 56: 167-182.

Wouterlood FG, Groenewegen HJ. (1985) Neuroantomical tracing by use of Phaseolus vulgaris - leucoagglutinin (Pha-L): electron microscopy of Pha-L filled neuronal somata, dendrites, axons and axon terminals. Brain Res. 326: 188-181.

Wouterlood FG, Jorritsma-Byham B. (1993) The anterograde neuroanatomical tracer biotinylated dextran-amine: comparison with the tracer *Phaseolus vulgaris*-leucoagglutinin in preparations for electron microscopy. J. Neurosci. Meth. 48: 75-87.

Wylie DR, De Zeeuw CI, DiGiorgi PL, Simpson JI. (1994) Projections of individual Purkinje cells of identified zones in the ventral nodulus to the vestibular and cerebellar nuclei in the rabbit. J.Comp.Neurol. 349: 448-463.

Yamada J, Noda H. (1987) Afferent and efferent connections of the oculomotor cerebellar vermis in the macaque monkey. J. Comp. Neurol. 265: 224-241.

Yarom Y. (1989) Oscillatory behavior of olivary neurons. In: Strata P, editor. The olivocerebellar system in motor control. Vol 17. Berlin: Springer-Verlag; 209-220.

Yarom Y. (1991) Rhythmogenesis in a hybrid system - interconnecting an olivary neuron to an analog network of coupled oscillators. Neurosci. 44: 263-275.

Yatim N, Buisseret-Delmas C, Buisseret P, Compoint C, Angaut P. (1995a) Nucleus medialis-nucleus interpositus interface: its olivary and cerebellocortical projections in the rat. J. Comp. Neurol. 363: 1-14.

Yatim N, Compoint C, Buisseret P, Angaut P, Buisseret-Delmas C. (1995b) On the caudal extension of the X zone in the cerebellar cortex of the rat. Neurosci. Res. 23: 223-227.

Yu DY, Na S, Wilson J, Kennedy PR. (1991) Redefing rat red nucleus: multiple labelling of individual neurons from spinal cord, inferior olivary nucleus and cerebellar nuclei. Neurosci. Abstr. 17: 469.

Yuen H, Dom RM, Martin GF. (1974) Cerebellopontine projections in the American opossum. A study of their origin, distribution and overlap with fibers from the cerebral cortex. J.Comp.Neurol. 154: 257-286.

Abbreviations

3	3rd cranial nerve (oculomotor)
6	6th cranial nerve (abducens)
7	7th cranial nerve (facial)
10	10th cranial nerve (vagus)
12	12th cranial nerve (hypoglossus)
III	3rd ventricle
IV	4th ventricle
A5	area 5 noradrenergic cells
AIN	anterior interposed nucleus
APT	anterior pretectal nucleus
aq	aquaeduct
β	subnucleus β
BDA	biotinylated dextran amine
BPN	basal pontine nuclei
CG	central grey
CN	cerebellar nuclei
cp	cerebral peduncle
CTb	cholera toxin B subunit
cu	cuneate tract
Cu	nucleus cuneatus
DAB	diamino benzidine
DAO	dorsal accessory olive
DC	dorsal cap of Kooy
Dk	nucleus of Darkschewitsch
DLH	dorsolateral hump
DLP	dorsolateral protuberance
DMC	dorsomedial crest
DMCC	dorsomedial cell column
DpG	deep grey layer SC
DpMe	deep mesencephalic nuclei
f	fornix
FF	fields of Forel
fr	fasciculus retroflexus
g7	genu 7th cranial nerve
GABA	γ-amino butyric acid
Gi	gigantocellular reticular nucleus
gr	gracile tract
Gr	nucleus gracilis
ic	internal capsule
IC	inferior colliculus
icp	inferior cerebellar peduncle
InG	intermediate grey layer SC
INC	interstitial nucleus of Cajal
IO	inferior olive
IPSP	inhibitory postsynaptic potential
LCN	lateral cerebellar nucleus
LPGi	lateral paragigantocellular nucleus
LRN	lateral reticular nucleus
LVN	lateral vestibular nucleus
MA3	medial accessory oculomotor nucleus
MAO	medial accessory olive
MCN	medial cerebellar nucleus
Md	medullary reticular field
MDJ	mesodiencephalic junction
MG	medial geniculate nucleus
ml	medial lemniscus
mlf	medial longitudinal fasciculus
MVN	medial vestibular nucleus
Mo5	motor trigeminal nucleus
mp	mammillothalamic peduncle
mt	mammillothalamic tract
NRTP	nucleus reticularis tegmenti pontis
opt	optic tract
PAG	periaquaeductal grey
PB	parabrachial nucleus
PCRt	parvicellular reticular nucleus
PF	parafascicular nucleus
PhaL	*Phaseolus vulgaris* leucoagglutinin
PIN	posterior interposed nucleus
Pn	pontine nuclei
PnC	pontine nuclei, caudal part
PnO	pontine nuclei, oral part
PO	principal olive
Po	posterior thalamic nucleus
Pr5	principal trigeminal nucleus
preR	prerubral field
preRN	prerubral area
PrH	nucleus prepositus hypoglossi
py	pyramidal tract
RI	rostral interstitial nucleus of the medial longitudinal fasciculus
RN	red nucleus
RNm	red nucleus, magnocellular part
RNp	red nucleus, parvicellular part
SC	superior colliculus
scp	superior cerebellar peduncle
SN	substantia nigra
sol	tractus solitarius
Sol	nucleus tractus solitarius
sp5	spinal trigeminal tract
Sp5	nucleus spinal trigeminal tract
SpVN	spinal trigeminal nucleus
STh	subthalamic nucleus
SuG	superficial grey layer SC
SVN	superior trigeminal nucleus
Tz	trapezoid body
VL	ventral lateral thalamic nucleus
VM	ventral medial thalamic nucleus
VN	vestibular nuclei
VTA	ventral tegmental area
VTRZ	visual tegmental relay zone
xopt	decussation optic tract
xpy	decussation pyramidal tract
xscp	decussation superior cerebellar peduncle
ZI	zona incerta

List of publications

Teune, T.M., A.J. Timmers-Reker, J.Bouquet, J.Bijman, H.R. de Jonge, M. Sinaasappel (1996) In vivo measurement of chloride and water secretion in the jejunum of cystic fibrosis patients. Pediatr.Research 40: 522-527

Teune, T.M., J. van der Burg, T.J.H. Ruigrok (1995) Cerebellar projections to the red nucleus and inferior olive originate from separate populations of neurons in the rat. A non-fluorescent double labeling study. Brain Res. 673: 313-319

Ruigrok, T.J.H., T.M.Teune, J. van der Burg, H.Sabel-Goedknegt (1995) A retrograde double labeling technique for light microscopy. A combination of axonal transport of cholera toxin B-subunit and a gold-lectin conjugate. J.Neurosci.Meth. 61: 127-138

Teune, T.M., J. van der Burg, C.I. De Zeeuw, J. Voogd, T.J.H.Ruigrok (1998) Single Purkinje cell can innervate multiple classes of projection neurons in the cerebellar nuclei of the rat: a light microscopic and ultrastructural triple-tracer study in the rat. J.Comp.Neurol. 392: 164-178

Toonen, M., H. van Dijken, J.C. Holstege, T.J.H.Ruigrok, S.K.E. Koekkoek, R.K.Hawkins, T.M.Teune, J. van der Burg, C.I. De Zeeuw (1998) Light microscopic and ultrastructural investigation of the dopaminergic innervation of the ventrolateral outgrowth of the rat inferior olive. Brain Research 802: 267-273

Curriculum vitae

Thea Marieke Teune (18-11-1966, Rijswijk) behaalde in 1985 het VWO examen aan het Thomas More College te Oudenbosch. In datzelfde jaar begon zij aan de studie geneeskunde aan de Erasmus Universiteit Rotterdam, waar zij in 1989 het doctoraal examen behaalde en in 1991 het artsexamen aflegde. In 1988 en 1989 was zij werkzaam als student assistent aan de afdeling Anatomie, o.m. bij Dr. T.J.H. Ruigrok en Dr. N.M. Gerrits. Voor de postdoctorale afstudeeropdracht was zij gedurende 6 maanden werkzaam aan de Johns Hopkins School of Medicine, Baltimore, U.S.A. (Dept. of Neuroanatomy) bij Prof. Dr. M.E. Molliver. Als arts was zij eerst werkzaam als onderzoeker aan de afdeling gastroenterologie van het Sophia Kinderziekenhuis Rotterdam bij Dr. M. Sinaasappel. In juni 1993 startte zij met het hier gepubliceerde onderzoek als OIO aan de afdeling Anatomie van de Erasmus Universiteit, onder leiding van Dr. T.J.H. Ruigrok en Prof. Dr. J. Voogd. Nu volgt zij een opleiding tot klinisch patholoog aan de afdeling Pathologie van het Academisch Ziekenhuis Maastricht onder leiding van Prof. Dr. J.W. Arends.

Dankwoord / Acknowledgements

Dit proefschrift is tot stand gekomen mede dank zij de hulp en steun, in diverse vormen en op verschillende manieren, van vele mensen, naar wie mijn onuitgesproken dank uitgaat. Een aantal van hen wil ik hier in het bijzonder bedanken.
Allereerst Tom Ruigrok, copromotor en dagelijks begeleider. Zonder jouw vertrouwen in het slagen van dit project, je enthousiasme, en je hulp in de laatste fase (vaak op zaterdag) was het niet gelukt (Mary, dank!). Een betere 'baas' kan een OIO zich niet wensen. Hopelijk stopt onze vriendschap niet bij deze laatste pagina.
Jan Voogd, mijn promotor, dank voor het sturen op afstand, en het leggen van verbanden waar Tom en ik ze even niet zagen, en vooral dank dat ik een beroep heb kunnen doen op je fabelachtige geheugen en kennis.
Hans van de Burg, je bent onmisbaar, bij het uitvoeren van de experimenten, bij het voorbereiden van de artikelen en bij eerste hulp bij allerlei lampjes die op dashborden kunnen gaan flikkeren.
Richard Hawkins, dank voor de uitleg en technische ondersteuning bij het EM werk, en voor het openen van nieuwe literaire werelden. May all your dreams come true!
De leden van de examencommissie, Henk Groenewegen, Han van der Want en Han Collewijn, voor het doorworstelen van het 'heavy' manuscript en de adviezen ter verbetering, en Chris de Zeeuw, Alan Gibson, Nico Gerrits en Jan Willem Arends voor het zitting nemen in de promotiecommissie. Alan, thank you so much for your wonderful quote, for sharing your vision on the brain and your suggestions to improve the manuscript. Chris, dank voor de regie bij het EM stuk.
Erika Sabel-Goedknegt, mijn dank voor de technische ondersteuning, maar bovenal voor je vriendschap. Edith Klink, dank voor je luisterend oor van tijd tot tijd en de "secretariële" ondersteuning.
Joost van der Moer, bedankt voor het geduldig plotten van duizenden donkerbruine vs. zwarte varicositeiten tegen een beigebruinblauwe achtergrond, en het mij deelgenoot maken van je ongebreidelde fantasie en bijzondere gevoel voor humor.
EDDIE DALM, zoals beloofd in hoofdletters. Dank voor het afdrukken, scannen, printen, reproduceren, ontwikkelen van vele foto's, figuren en plaatjes, op jouw eigen unieke wijze.
GertJan Kleinrensink, de meest Haagse Harry.
Pierre Wentzel. Woorden schieten te kort.
Henk van Dijken, Christl Vermeij-Keers, Elize Haasdijk, Lennard Boshart, Bas Koekkoek, Arjan van Alphen, Moshe Godschalk –mijn eeuwige vraagbaak-, Joan Holstege, Dick Jaarsma, Jan Velkers, Cees Entius, Margriet Slappendel, dank voor de gezelligheid.
Mijn vriendinnen uit de collegebanken: Sonja van der Wereld, Annemiek van Zaal en Janneke Spek, dit was mij niet gelukt zonder jullie nuchtere kijk op mijn soms chaotisch leven.

Mijn ouders en zus, die mij door dik en dun gesteund hebben.
Tenslotte Rob Stornel. Voor alles. Voor niets.

Color figures from the following chapters:

Chapter 3, Figures 3.3 and 3.4, for legends see page 124.

Chapter 4, Figure 4.1, for legend see page 135.

Chapter 5, Figure 5.7, for legend see page 168.

Chapter 6, Figures 6.1 – 6.11, for legends see pages 210 – 211.

Chapter 7, Figure 7.2, for legend see page 230.

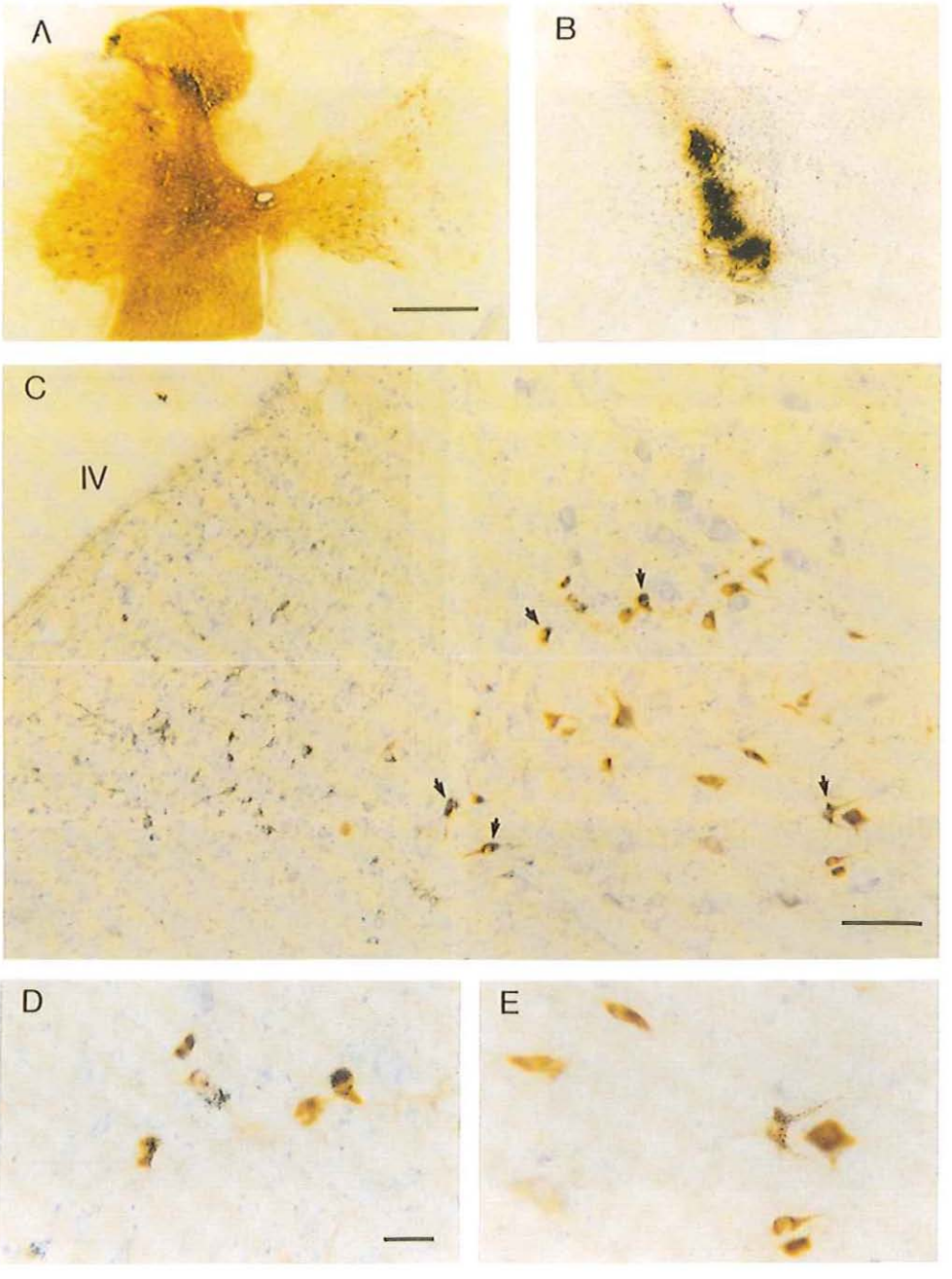

Fig. 3.3

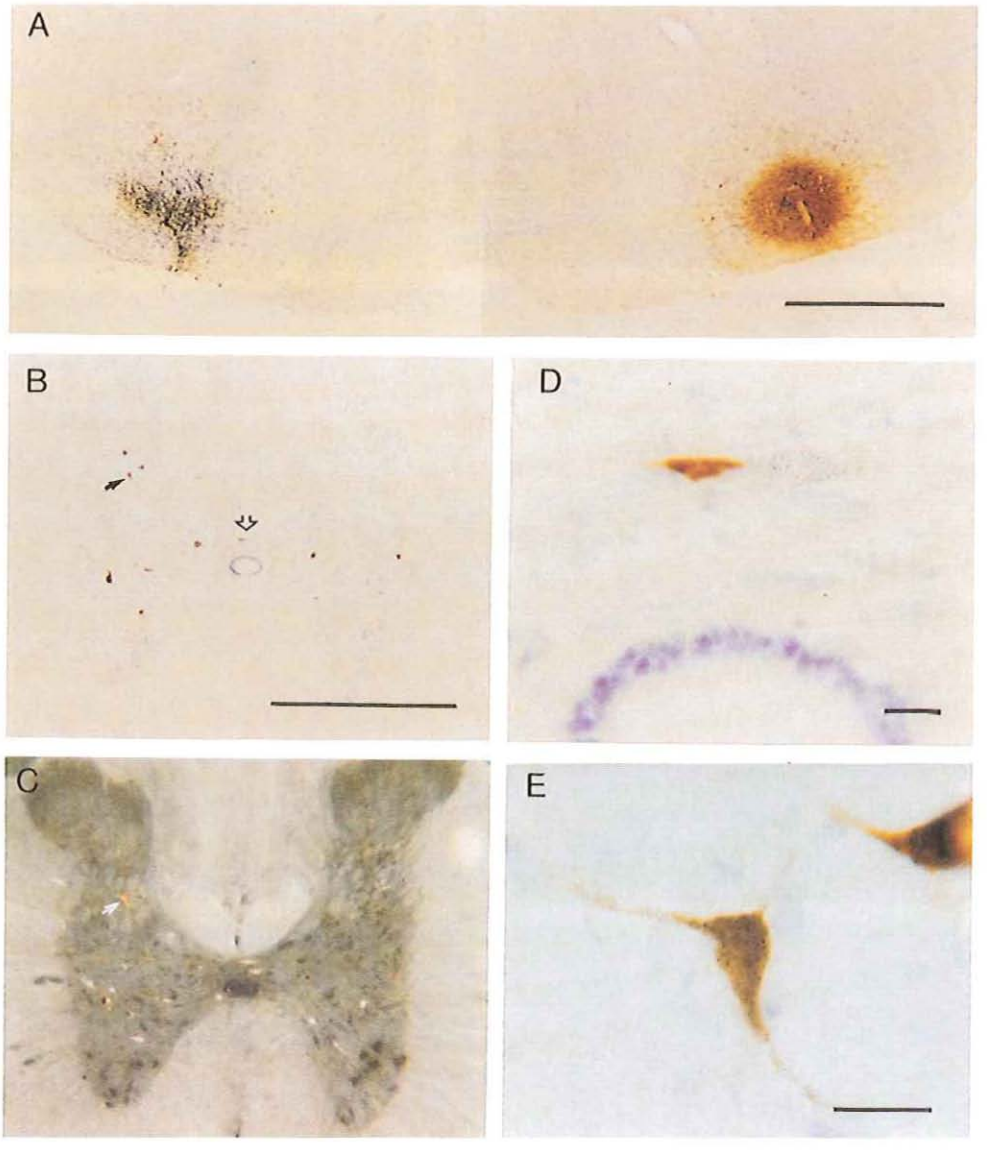

Fig. 3.4

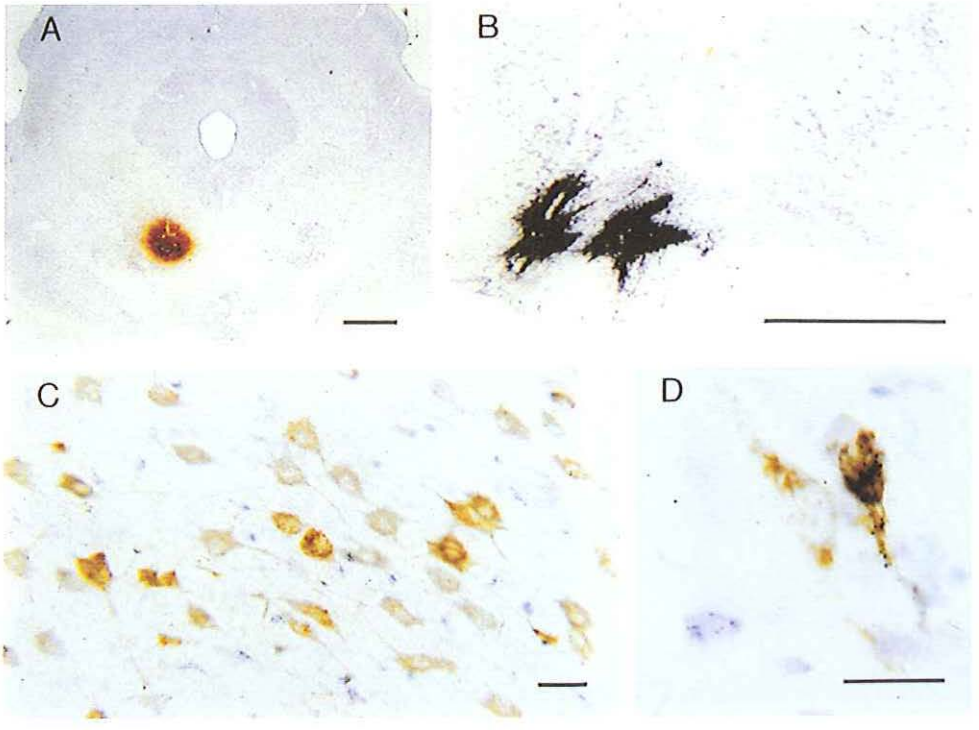

Fig.4.1

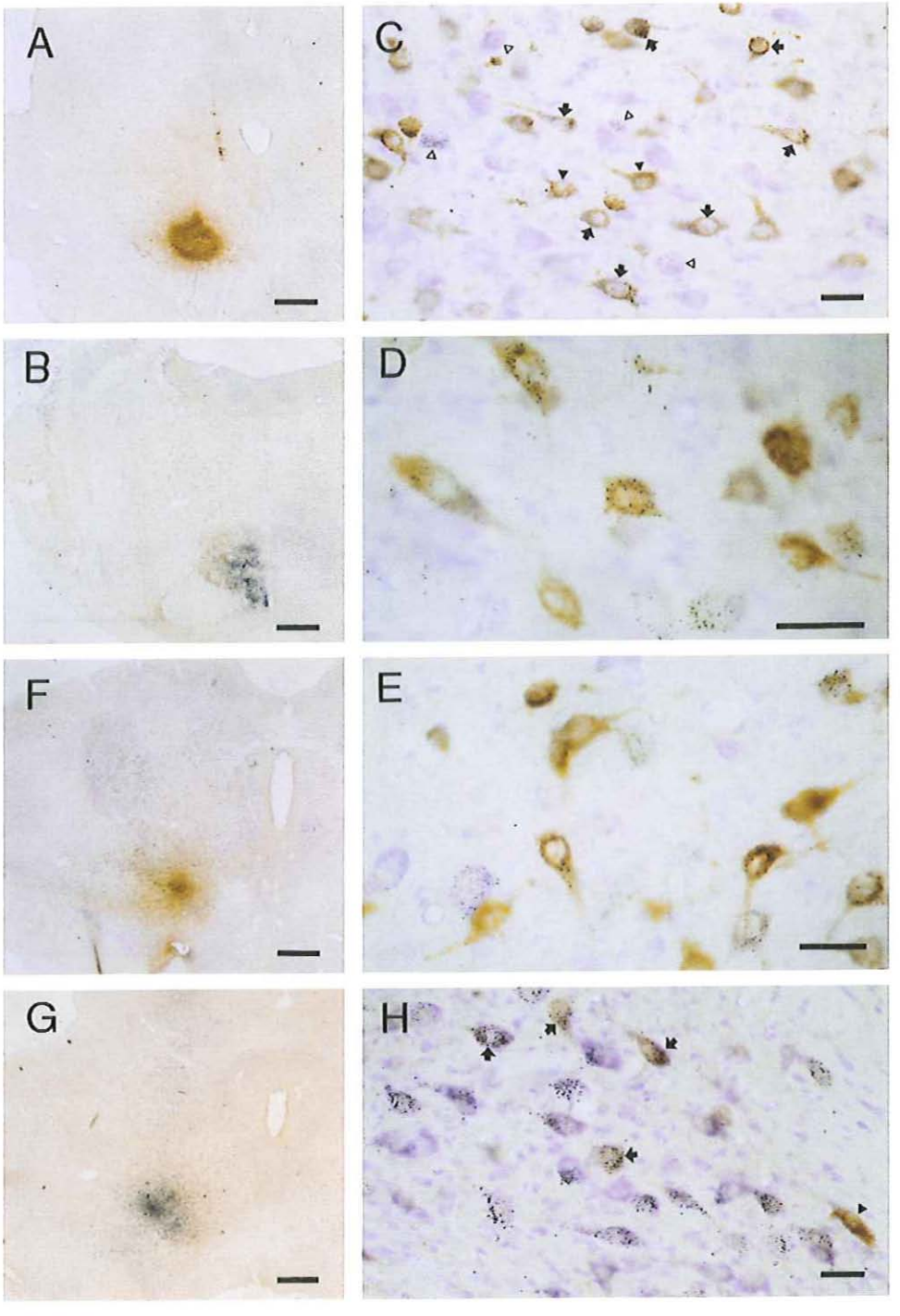

Fig. 5.7

A
B1
DAO
PO
MAO
B2
DM
MAO
DAO
C
RNm
D
E1
DAO
PO
MAO
E2
DM
PO
MAO
DAO
F
G1
G2
H
DM
MAO
I
3V
rDk
fr

Fig. 6.1

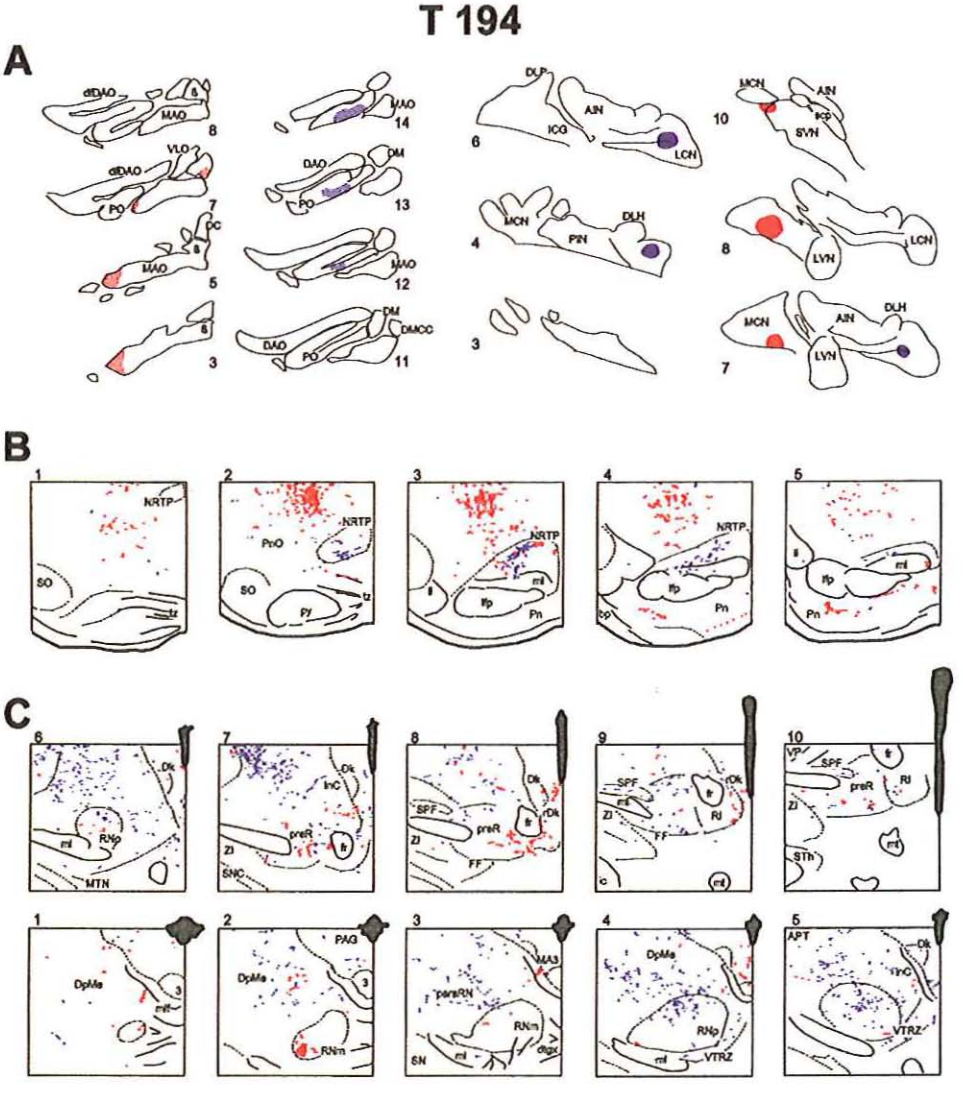
T 194
A
dlDAO
MAO
VLO
PO
DAO
DM
DMCC
DLP
ICG
AIN
LCN
MCN
DLH
PIN
SVN
LVN
B
NRTP
PrO
SO
Py
ll
ml
lfp
Pn
C
Dk
rDk
InC
SNC
MTN
RNp
SPF
preR
RI
FF
ZI
STh
VP
DpMe
PAG
RNm
paraRN
MA3
SN
dscp
APT
VTRZ

Fig. 6.2

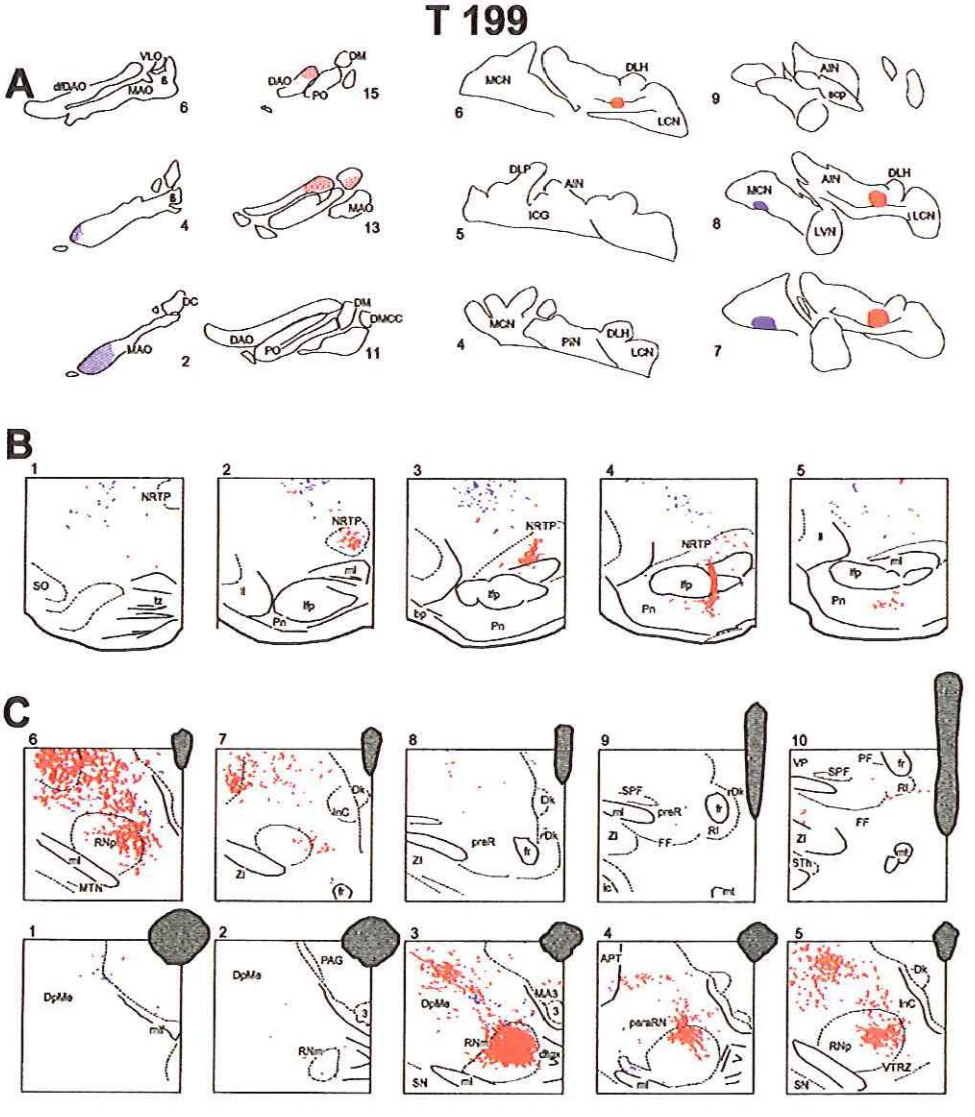
T 199
A
VLO
dlDAO
MAO
6
DM
DAO
PO
15
MCN
DLH
LCN
9
AIN
scp
4
13
DLP
AIN
ICG
5
MCN
AIN
DLH
LVN
LCN
8
DC
MAO
2
DM
DMCC
DAO
PO
11
MCN
PiN
DLH
LCN
4
7
B
1
NRTP
SO
tz
2
NRTP
ml
Pn
3
NRTP
bp
Pn
4
NRTP
Pn
5
ml
Pn
C
6
RNp
ml
MTN
7
Dk
InC
ZI
8
Dk
preR
ZI
9
SPF
preR
ZI
FF
RI
10
VP
PF
SPF
RI
FF
ZI
STh
1
DpMe
ml
2
DpMe
PAG
RNm
3
DpMe
MA3
RN
SN
4
APT
paraRN
ml
5
Dk
InC
RNp
VTRZ
SN

Fig. 6.3

T 96

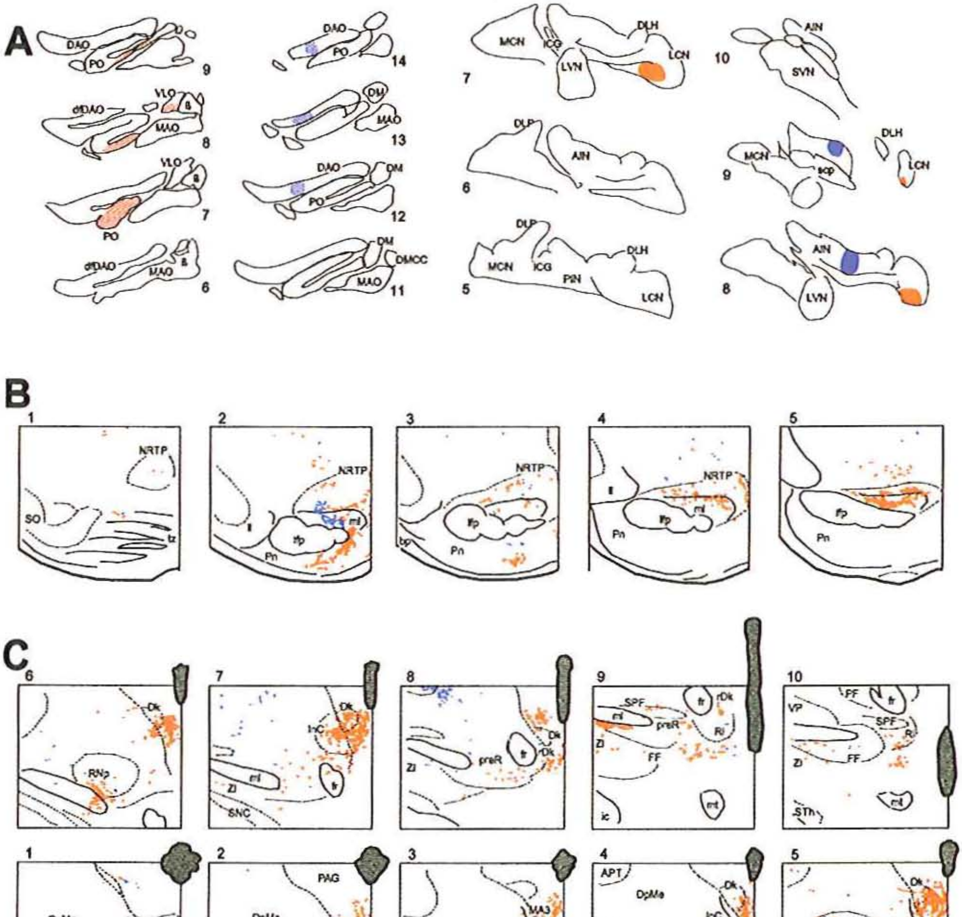

A
DAO
PO
dfDAO
VLO
MAO
DM
DMCC
MCN
ICG
DLH
LCN
LVN
DLP
AIN
PIN
SVN
B
NRTP
SO
tz
tfp
ml
Pn
bp
C
Dk
RNp
InC
ZI
SNC
fr
preR
SPF
RI
FF
ic
mt
VP
PF
STh
DpMe
mlf
PAG
RNm
MA3
paraRN
SN
APT
VTRZ
MTN

Fig. 6.4

T 92

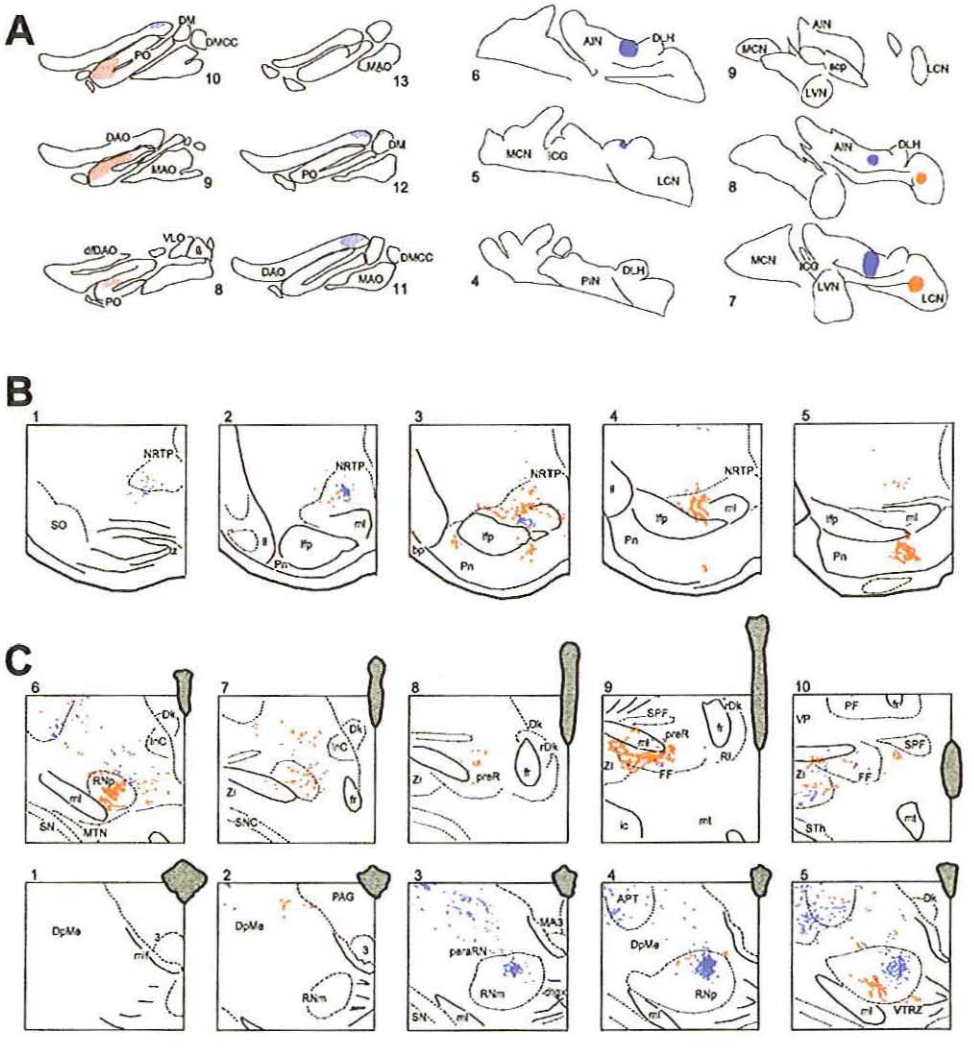
A
DM
DMCC
PO
10
MAO
13
6
AIN
DLH
9
AIN
MCN
scp
LCN
LVN
DAO
MAO
9
DM
PO
12
5
MCN
ICG
LCN
8
AIN
DLH
dlDAO
VLO
IL
PO
8
DAO
MAO
DMCC
11
4
PrN
DLH
MCN
ICG
LVN
LCN
7
B
1
NRTP
SO
2
NRTP
rtp
Pn
3
NRTP
rtp
Pn
4
NRTP
rtp
Pn
5
rtp
Pn
C
6
Dk
rtC
RNp
SN
MTN
7
Dk
rtC
Zi
SNC
8
Dk
rDk
preR
Zi
9
SPF
Dk
preR
Zi
FF
RI
ic
10
PF
VP
SPF
Zi
FF
STh
1
DpMe
3
2
PAG
DpMe
3
RNm
3
MA3
paraRN
RNm
SN
4
APT
DpMe
RNp
5
Dk
VTRZ

Fig. 6.5

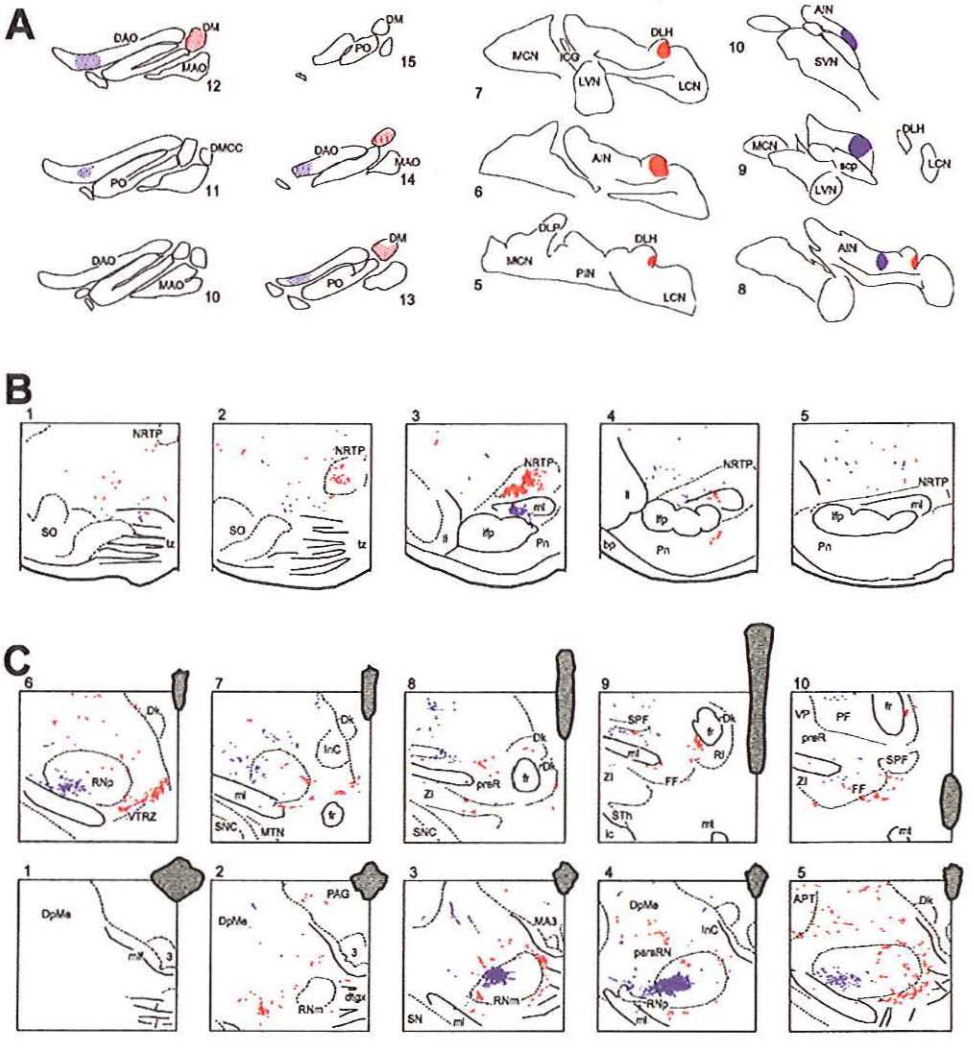
T 84
A
DAO
DM
MAO
12
PO
15
DMCC
11
14
10
13
MCN
ICG
DLH
LVN
LCN
7
AIN
6
DLP
PiN
5
SVN
10
9
scp
8
B
1
NRTP
SO
tz
2
3
ml
lfp
Pn
4
bp
5
C
6
Dk
RNp
VTRZ
7
lnC
SNC
MTN
fr
8
preR
ZI
9
SPF
rDk
Rt
FF
STh
ic
10
VP
PF
1
DpMe
2
PAG
RNm
3
MA3
SN
4
parsRN
5
APT

Fig. 6.6

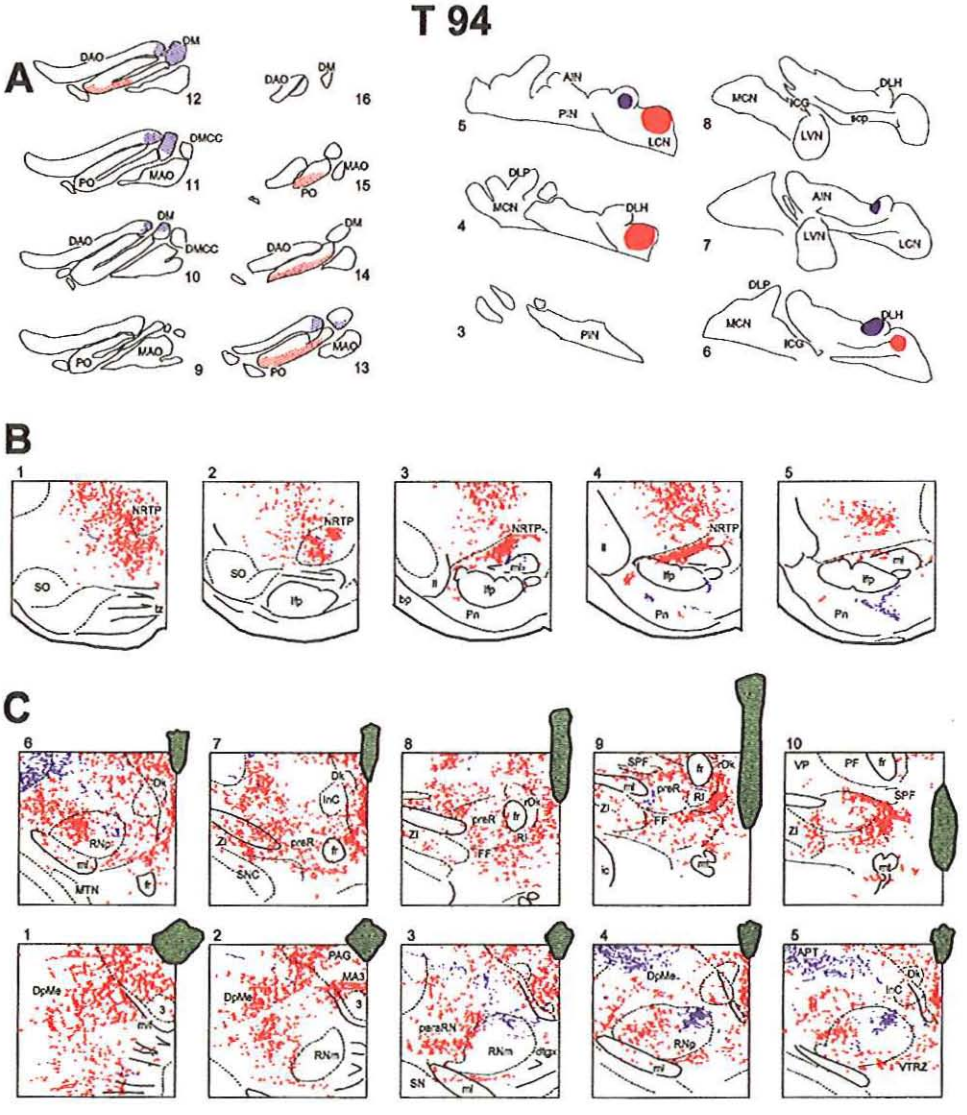
T 94
A
DAO
DM
12
16
DMCC
PO
MAO
11
15
10
14
9
13
AIN
PrN
LCN
5
8
DLH
MCN
ICG
scp
LVN
DLP
4
7
3
6
B
1
2
3
4
5
NRTP
SO
tz
lfp
mlf
bp
II
Pn
C
6
7
8
9
10
Dk
InC
RNp
ml
MTN
fr
ZI
SNC
preR
rDk
RI
FF
SPF
ic
VP
PF
SPF
1
2
3
4
5
DpMe
PAG
MA3
RNm
paraRN
SN
APT
VTRZ

Fig. 6.7

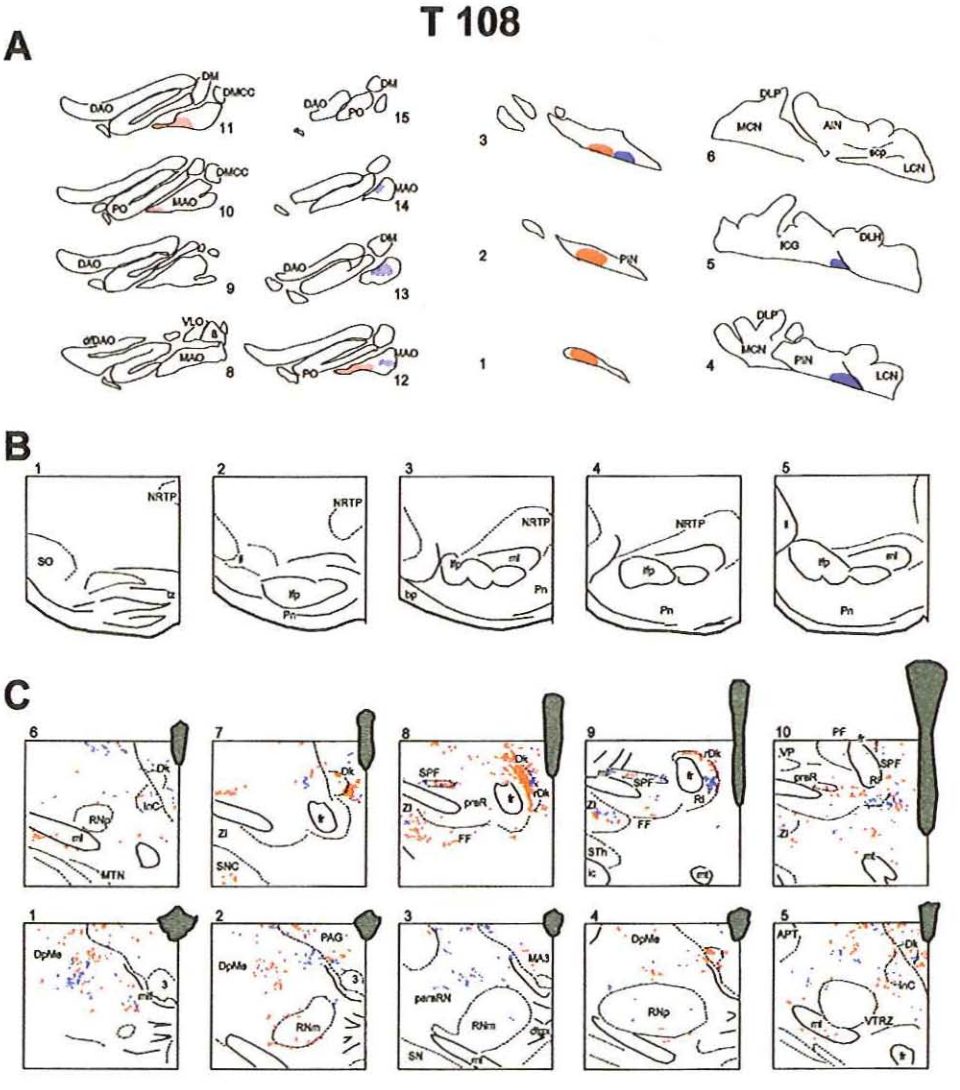
T 108
A
DM
DMCC
DAO
11
DAO
PO
15
DMCC
PO
MAO
10
MAO
14
DAO
9
DM
DAO
13
VLO
dDAO
MAO
8
MAO
PO
12
3
DLP
MCN
AIN
6
scp
LCN
2
PIN
ICG
DLH
5
1
DLP
MCN
PIN
4
LCN
B
1
NRTP
SO
cz
2
NRTP
ll
lfp
Pn
3
NRTP
lfp
ml
Pn
bp
4
NRTP
lfp
Pn
5
ll
lfp
ml
Pn
C
6
Dk
lnC
RNp
ml
MTN
7
Dk
ll
ZI
SNC
8
SPF
Dk
ZI
preR
rDk
ll
FF
9
rDk
SPF
ll
ZI
Rt
FF
STh
ml
10
PF
VP
preR
SPF
Rt
ZI
ml
1
DpMe
3
ml
2
PAG
DpMe
3
RNm
3
MA3
paraRN
RNm
SN
ml
4
DpMe
RNp
5
APT
Dk
lnC
ml
VTRZ

Fig. 6.8

T 98

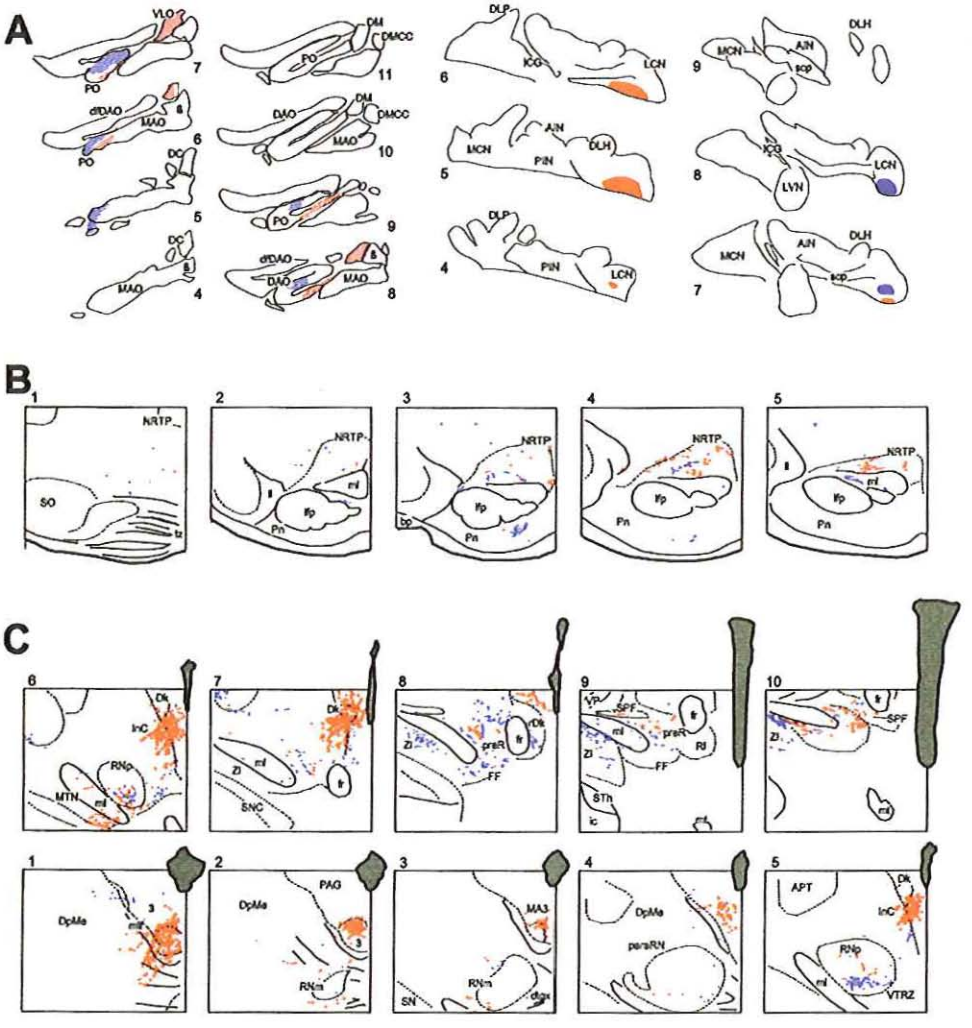
A
VLO
PO
DM
DMCC
dDAO
MAO
DC
DAO
DLP
ICG
LCN
AIN
MCN
PIN
DLH
scp
LVN
B
NRTP
SO
mt
Pn
lfp
bp
C
Dk
InC
RNp
MTN
SNC
ZI
preR
FF
RI
SPF
STh
ic
PAG
DpMe
MA3
RNm
SN
dscp
paraRN
APT
VTRZ

Fig. 6.9

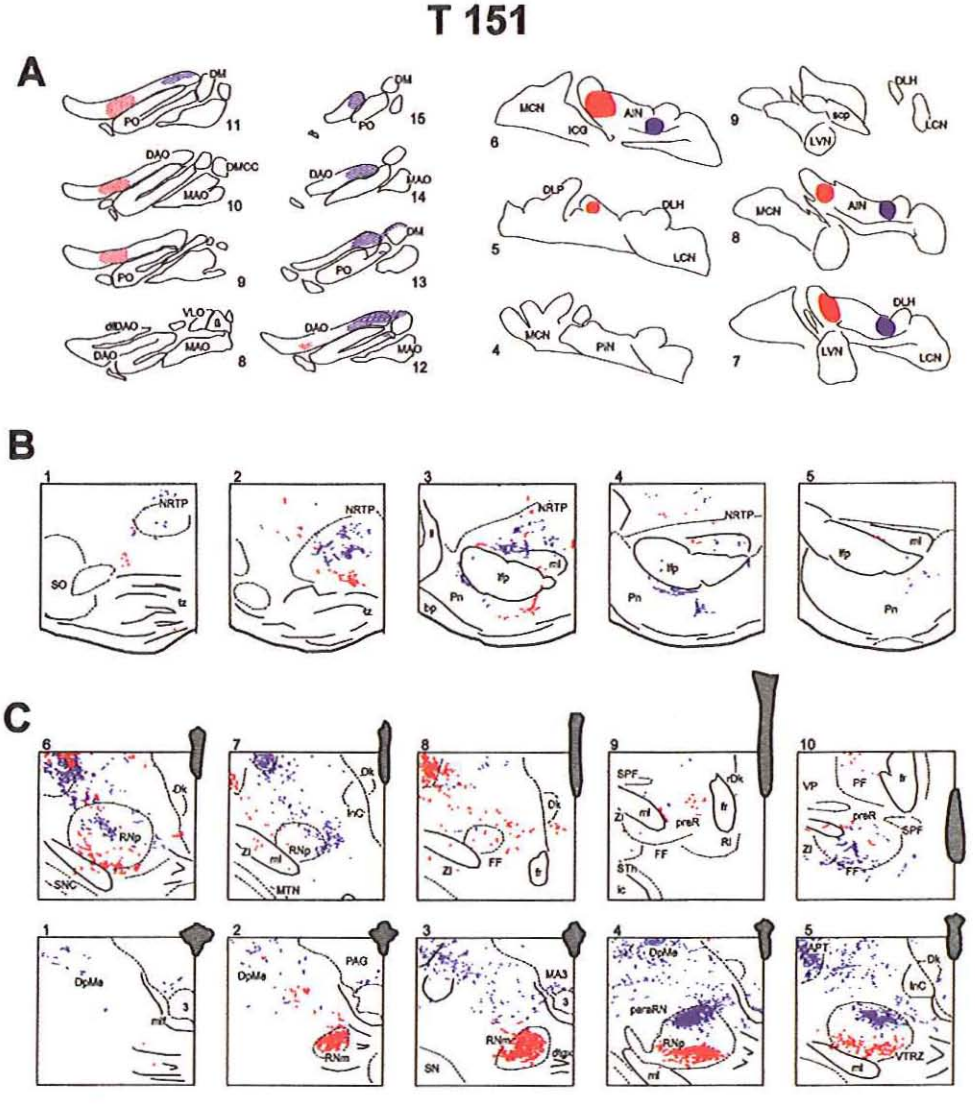
T 151
A
DM
PO
11
15
DAO
DMCC
MAO
10
14
9
13
VLO
dlDAO
8
12
MCN
ICG
AIN
6
9
scp
LVN
DLH
LCN
DLP
5
8
4
PrN
7
B
1
2
3
4
5
NRTP
SO
tz
lfp
Pn
tcp
ml
C
6
7
8
9
10
Dk
RNp
SNC
InC
MTN
ZI
FF
SPF
rDk
STh
ic
preR
RI
VP
PF
1
2
3
4
5
DpMe
PAG
RNm
MA3
SN
paraRN
APT
VTRZ

Fig. 6.10

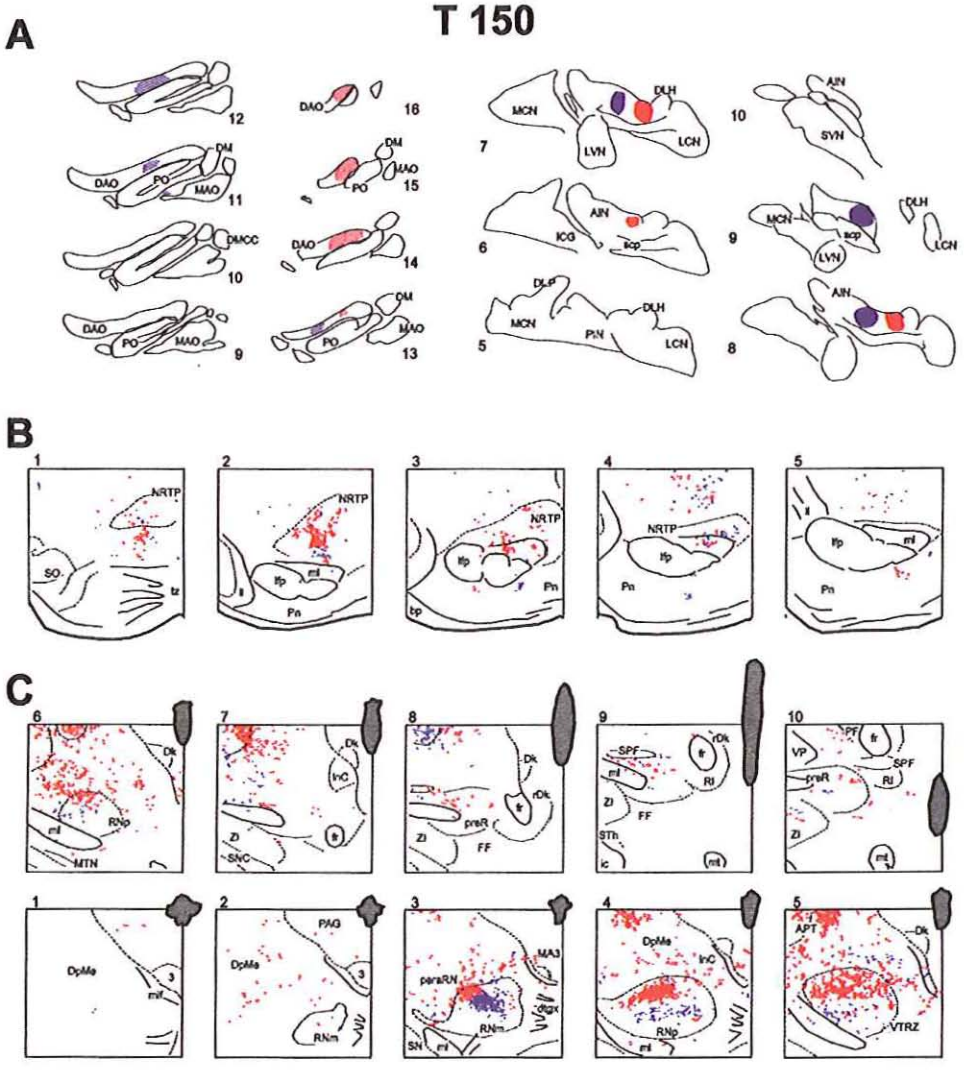
A
T 150
12
DAO
16
DM
DAO
PO
MAO
11
DM
PO
MAO
15
DMCC
DAO
10
DAO
14
DAO
PO
MAO
9
DM
PO
MAO
13
7
MCN
DLH
LVN
LCN
10
AIN
SVN
6
AIN
ICG
icp
9
MCN
DLH
icp
LVN
LCN
5
DLH
MCN
PrN
DLH
LCN
8
AIN
B
1
NRTP
SO
tz
2
NRTP
ltp
ml
Pn
3
NRTP
ltp
Pn
tzp
4
NRTP
ltp
Pn
5
ltp
ml
Pn
C
6
Dk
ml
RNp
MTN
7
Dk
InC
SNC
8
Dk
rDk
preR
ZI
FF
9
SPF
rDk
ml
RI
ZI
FF
STh
10
PF
VP
SPF
preR
RI
ZI
1
DpMe
3
ml
2
PAG
DpMe
3
RNm
3
MA3
paraRN
RNm
SN
ml
4
DpMe
InC
RNp
ml
5
APT
Dk
VTRZ

Fig. 6.11

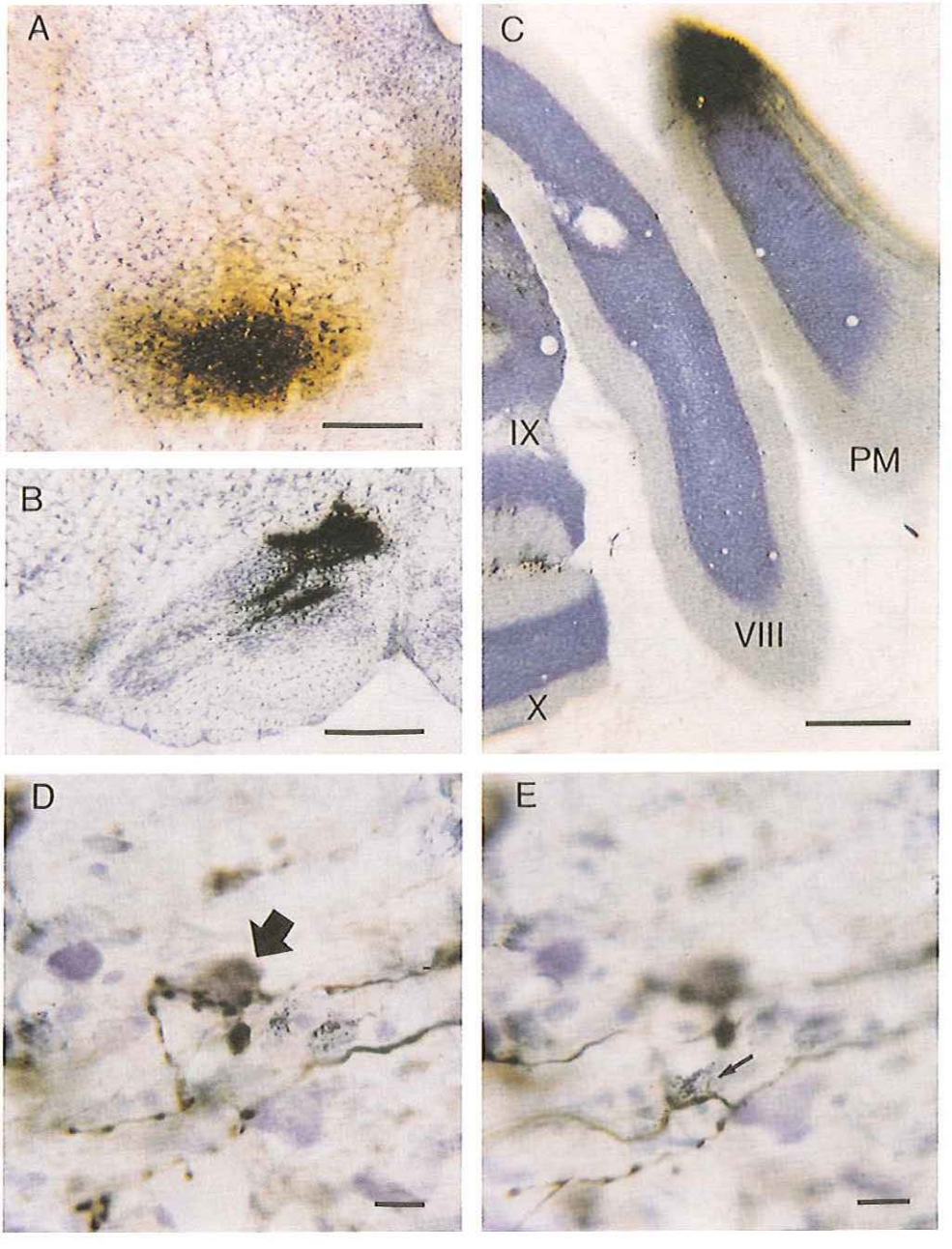

Fig. 7.2